Modeling Spatiotemporal Influences on the Hydrothermal Environment of the Seedling Recruitment Microsite

by

William John Bullied

A Thesis Submitted to the Faculty of Graduate Studies of the University of Manitoba
in Partial Fulfillment of the Requirements for the Degree of

DOCTOR OF PHILOSOPHY

Department of Plant Science
University of Manitoba
Winnipeg, Manitoba

THE UNIVERSITY OF MANITOBA

FACULTY OF GRADUATE STUDIES

*****

COPYRIGHT PERMISSION

Modeling Spatiotemporal Influences on the Hydrothermal Environment of the Seedling Recruitment Microsite

by William John Bullied

A Thesis/Practicum submitted to the Faculty of Graduate Studies of the University of Manitoba in partial fulfillment of the requirement of the degree of

Doctor of Philosophy

Acknowledgments

Funding for this research project was provided by a Natural Sciences and Engineering Research Council NSERC PGS-B scholarship; a Manitoba Rural Adaptation Council, Agriculture and Agri-Food Canada research grant; and a Canadian Wheat Board research fellowship.

I express sincere gratitude to my supervisor, Dr. Rene Van Acker for his support and encouragement during my research study. As well, much appreciation is extended to my advisory committee members, Dr. Paul Bullock and Dr. Martin Entz for their guidance and encouragement throughout the research project. I also extend appreciation to Dr. Paul Bullock for in-depth review of the manuscripts contained in this thesis, and for providing materials and laboratory support. I thank my external thesis examiner, Dr. Frank Forcella for review and helpful suggestions for the thesis.

I thank Dr. Pieter Groenevelt also for manuscript review and Dr. Gerald Flerchinger for modeling guidance. Many thanks to Rufus Oree, Andrea Bartlinski, Ian Brown, Rob Ellis, Jim Griffiths, Alvin Iverson, and Wilfred Mutcher for technical support; Dr. Gary Crow, Dr. Norman Kenkel, Dr. Arthur Lembo and Lyle Friesen for statistical advice; and the many summer students and my nephew Steven for assistance in field sampling.

I extend appreciation to Dr. Antonio DiTommaso and Dr. Arthur Lembo of the Department of Crop and Soil Sciences at Cornell University for their instruction and support during my study sabbatical at Cornell.

Deep gratitude is extended to my parents who instilled in me an appreciation for agriculture in early childhood, and taught me the value and meaning of farming as a way of life. These values are the foundation of all my agricultural research.

I express heartfelt gratitude to my wife, Andrea, and daughter, Amanda for their love and inspiration throughout my study period. I thank Andrea for her support in accompanying me with our baby daughter on my study sabbatical to Cornell University and for her encouragement and reminder of better things to come through this degree. Amanda's quest to learn new and wonderful things in this world has been a tremendous source of inspiration to me.

Table of Contents

List of Tables

List of Figures

List of Abbreviations

AIC: Akaike information criterion

BD: Bulk density

Bias: Model bias

DAE: Days after emergence

DAP: Days after planting

d_g: Geometric mean particle diameter

DOY: Day of year

DTM: Days to maturity

GDD_{air}: Air growing degree days

GDD_{soil}: Soil growing degree days

GPS: Global positioning system

IME: Integral mean error

IRMSE: Integral root mean square error

K_s: Saturated hydraulic conductivity

LAI: Leaf area index

LCS: Lack of correlation weighted by standard deviations

MBE: Mean bias error

ME: Model efficiency

n: Dimensionless curve fitting parameter of the van Genuchten soil water retention equation

OM: Organic matter

PAR: Photosynthetically active radiation

PC: Principal component

PCA: Principal components analysis

PCR: Principal components regression

PTF: Pedotransfer function

r: Pearson correlation coefficient

RMSD: Root mean square deviation

S: Electrical conductivity

SB: Squared bias

SDS: Squared difference between standard deviations

SHAW model: Simultaneous heat and water model

SWRC: Soil water retention characteristic

T: Temperature

VG: van Genuchten soil water retention equation

α: Curve fitting parameter representing capillary pressure at the inflection point of the van Genuchten soil water retention equation

θ: Volumetric water content

$\theta(\psi)$: Water content – water potential function

$\theta_{r(E)}$: Estimated residual volumetric water content

$\theta_{r(M)}$: Modified residual volumetric water content

$\theta_{r(W)}$: Wilting point residual volumetric water content

θ_r: Residual volumetric water content

θ_s: Saturated volumetric water content

$\theta_{v(g)}$: Volumetric water content measured gravimetrically

$\theta_{v(p)}$: Volumetric water content measured by the ThetaProbe^{TM} soil water sensor

ρ_b: Bulk density (dry)

σ_g: Geometric standard deviation

ψ: Matric (water) potential

Abstract

Bullied, William John. Ph.D. The University of Manitoba, 2009. **Modeling Spatiotemporal Influences on the Hydrothermal Environment of the Seedling Recruitment Microsite.** Major Professor; Dr. Rene Van Acker.

Modeling the seedling recruitment microsite involves characterization of the soil environment of the shallow profile from which weed seedlings recruit. Understanding the environment of the seedling recruitment microsite is the prelude to weed emergence studies. Because of spatial and temporal heterogeneity of the recruitment microsite, sufficient measurements are often not feasible. An experiment was established in 2003 and 2004 across topography within an annually cropped field in south-central Manitoba to determine the effect that hillslope aspect and position, and soil residue and depth would have on microsite environment within the shallow seedling recruitment zone. Microclimatic, topographic, soil surface and soil properties were assessed in the context of the weed recruitment microsite. The soil water retention characteristic was measured by pressure plate to determine water availability to germinating seeds at the various topographic positions. The soil water characteristic was evaluated across topography and soil depth. Evaluation of the soil water characteristic by pedotransfer function indicated that a single soil water characteristic is representative of the recruitment zone. Field and laboratory experimental measurements were used as parameterization for the simultaneous heat and water (SHAW) model to generate continuous water and temperature profiles for the recruitment zone. Soil temperature and temperature fluctuation decreased with depth in the recruitment zone. Despite differences of texture, bulk density, and organic matter across topography and soil depth, the soil water characteristic differed only across topography. Soil water potential fluctuated considerably at the soil surface due to numerous precipitation events and direct evaporation. Implications for germinating seeds is that the seedling recruitment zone is influenced by spatial effects of topography and the vertical location of the seed microsite. Physical process based modeling used in this study to predict temperature and water within the seedling recruitment zone enables better understanding of interactions between above-ground microclimate and the recruitment microsite. Such interactions enable

linkage between atmospheric models and recruitment models that can enhance our ability to evaluate crop management decisions.

Forward

Manuscripts contained within the thesis are formatted in accordance with the American Society of Agronomy (ASA) – Crop Science Society of America (CSSA) – Soil Science Society of America (SSSA) Publications Handbook and Style Manual (677 South Segoe Rd., Madison, WI 53711).

1.0 Introduction

There is a need to considerably improve the way we manage weeds in annual agricultural cropping systems. Weed ecology is increasingly becoming more important for weed control due to a number of factors including herbicide resistance in weeds (Mortimer and Maxwell, 1994; Légère et al., 2000; Beckie, 2004), herbicide residues in the environment (Eason et al., 2004; Hildebrandt et al., 2007), and the annual fluctuating economic status of crop producers (Statistics Canada, 2005). The introduction of new weed management technology such as genetically engineered crops has simplified weed control in some systems but has not necessarily solved the problems associated with herbicide intensive weed management (Benbrook, 2004; Nazarko et al., 2005). In some regions, reliance on herbicide tolerant crops has triggered changes in weed communities, most notably resistance to herbicides, thus forcing crop producers to increase rates of herbicide application and/or apply additional herbicides (Benbrook, 2004). The ecological adaptations of selection for herbicide resistant weed biotypes are accelerating due to increased use of select herbicides.

One of the most critical aspects of weed control is knowing the timing and extent of weed seedling emergence, which provides information for integrated weed control decision-making strategies. Weed management systems with a reduced reliance on herbicides pose new challenges for modeling weed–crop interactions (Bastiaans et al., 2000). Because weeds often emerge over a period of time, it is difficult to apply a descriptive model that accounts for the effects of both weed density and the relative time of weed emergence (Bastiaans et al., 2000). Weed emergence models have become an important part of bioeconomic weed and crop management decision aid programs by predicting accurate densities of weeds on a daily basis (Forcella et al., 1995). The inclusion of such models in decision aid programs has resulted in reductions in herbicide use and weed control costs compared to standard farming practices (Forcella et al., 1995). Weed control measures implemented prior to the emergence of a large percentage of weed seedlings may require additional herbicide applications, whereas control measures implemented too late may be ineffective in preventing crop yield loss due to weed interference. The timing and extent of weed seed germination is difficult to predict due to

interactions of environment, soil properties, and management practices that impact weed recruitment. A greater understanding of the relationship between recruitment of weed seedlings and their physical environment, including microclimate, soil, topography, and ground cover may offer the key to understanding the onset and timing of seedling recruitment.

Weed seeds sense their immediate environment to establish whether conditions are suitable for germination. Weed seed germination depends on the temperature and water content in microsites within the relatively shallow recruitment zone for common weeds in typical cropping systems on the northern Great Plains of North America (du Croix Sissons et al., 2000). Field topography greatly influences the soil environment, and weed recruitment patterns are spatially and temporally heterogeneous within a field due to the influence of the varying soil environment on the seedling microsite across the topography of a field. Because of the influence of topography on the seedling recruitment microsite, seedling recruitment in artificial environments often differs from that of natural environments (Leon and Owen, 2004). Weed seed germination is influenced by the spatial and temporal soil microsite, which occurs as a result of environment, soil, and management. Knowledge of environmental and management factors that contribute to microsite conditions will facilitate more effective weed management, and will allow precise manipulation of the processes known to contribute to favorable microsite conditions. Changes in management practices could reduce weed interference in crops by rendering soil microsite conditions less favorable to weed seedling recruitment. Management practices such as tillage influence the vertical placement of weed seeds into diverse microsites within the seedbank (Van Acker et al., 2004). Manipulation of crop residue level influences microsite conditions affecting weed recruitment. The interaction of management practices with topography and environment produce diverse microsite conditions controlling recruitment of weeds within a field.

Identifying weed recruitment and emergence across topography requires a comprehensive understanding of the nature of the soil environmental properties associated with field topography. Characterizing a seedling microsite requires identification of the soil processes associated with the spatial (depth and topographic) and temporal (diurnal and seasonal) soil environment. The spatial and temporal sources of

variability in the soil environment can be the result of either natural or management related processes (Cassel, 1983). Sources of variability in soil properties across topography need to be considered in recruitment studies because results may be biased if generalizations are made over fields with heterogeneous topography. Determining the extent of variability in microsites across field topography can be used to develop weed recruitment models to support weed management decisions.

Research on microsite conditions will assist with the identification and characterization of environmental events such as a wetting front from rainfall, drying due to drainage or evapotranspiration (constant or falling rate), and interactions between water and temperature on weed seedling recruitment. This research project identifies characteristics of the seedling recruitment microsite including soil water, soil temperature, and soil temperature fluctuation that account for hillslope scale complexity and heterogeneity. The profile of the seedling recruitment zone was modeled to obtain a detailed spatial and temporal description of soil temperature and water. Simulated soil temperature and water profiles can be used to develop thermal and hydrothermal time emergence models for prediction of the onset and duration of spring wheat grown in the experiment as a model weed, as well as naturalized annual weeds.

1.1 Objectives

The objectives of this research are to 1) establish the relationship between microclimate and the seedling recruitment microsite across field topography, 2) characterize the environmental properties of the seedling recruitment microsite during the spring and early summer according to topographical aspect and position, residue cover, and soil depth, 3) measure the soil water retention characteristic across field topography, and model the soil water retention characteristic across soil depth by pedotransfer function, and 4) model temperature and water profiles for the seedling recruitment microsite on an hourly time step according to topographical aspect and position, residue cover, and soil depth.

1.2 References

Bastiaans, L., M.J. Kropff, J. Goudriaan, and H.H. van Laar. 2000. Design of weed management systems with a reduced reliance on herbicides poses new challenges and prerequisites for modeling crop–weed interactions. Field Crops Res. 67:161–179.

Beckie, H.J. 2004. Manitoba weed survey of herbicide-resistant weeds in 2002. Weed Survey Series. Pub. 04-2. Agriculture and Agri-Food Canada, Saskatoon Research Centre, Saskatoon, SK.

Benbrook, C.M. 2004. Genetically engineered crops and pesticide use in the United States: The first nine years. [Online]. Available at www.biotech-info.net/Full_version_first_nine.pdf. Ag BioTech InfoNet. Technical Paper No. 7., Sandpoint, ID.

Cassel, D.K. 1983. Spatial and temporal variability of soil physical properties following tillage of Norfolk loamy sand. Soil Sci. Soc. Am. J. 47:196–201.

du Croix Sissons, M.J., R.C. Van Acker, D.A. Derksen, and A.G. Thomas. 2000. Depth of seedling recruitment of five weed species measured in situ in conventional- and zero-tillage fields. Weed Sci. 48:327–332.

Eason, A., U.S.Tim, and X. Wang. 2004. Integrated modeling environment for statewide assessment of groundwater vulnerability from pesticide use in agriculture. Pest. Manage. Sci. 60:739–745.

Forcella, F., J.C. Barbour, C.A. Oriade, R.P. King, and D.D. Buhler. 1995. Weed emergence modeling for a bioeconomic weed. p. 73–76. Clean water, clean environment, 21st century: Team agriculture, working to protect water resources, Kansas City, Missouri 5–8 March 1995. St. Joseph, MI.

Hildebrandt, A., S. Lacorte, and D. Barceló. 2007. Assessment of priority pesticides, degradation products, and pesticide adjuvants in groundwaters and top soils from agricultural areas of the Ebro river basin. Anal. Bioanal. Chem. 387:1459–1468.

Légère, A., H.J. Beckie, F.C. Stevenson, and G. Thomas. 2000. Survey of management practices affecting the occurrence of wild oat (*Avena fatua*) resistance to acetyl-CoA carboxylase inhibitors. Weed Technol. 14:366–376.

Leon, R.G. and M.D.K. Owen. 2004. Artificial and natural seed banks differ in seedling emergence patterns. Weed Sci. 52:531–537.

Mortimer, A.M. and B.D. Maxwell. 1994. Selection for herbicide resistance. p. 1–25. In S.B. Powles and J.A.M. Hotum ed. Herbicide resistance in plants: Biology and biochemistry. CRC Press, Boca Raton, FL.

Nazarko, O.M., R.C. Van Acker, and M.H. Entz. 2005. Strategies and tactics for herbicide use reduction in field crops in Canada: A review. Can. J. Plant Sci. 85:457–479.

Statistics Canada. 2005. Income of farm operators from farming operations, annual (dollars). Record No. 3473. Ottawa ON.

Van Acker, R.C., W.J. Bullied, and M.J. du Croix Sissons. 2004. Tillage index predicts weed seedling recruitment depth. Can. J. Plant Sci. 84:319–326.

2.0 Literature Review

2.1 Microclimate

A field microclimate is defined by the atmospheric conditions that exist locally and is differentiated from the state of the surrounding atmosphere. Microclimates can exist as a result of irregularities in topography and soil surface characteristics within the field. Microclimate may be consistent across a homogeneous field or varied across a non-uniform field. A field microclimate has influence on the spatial and temporal recruitment microsite properties near the soil surface where a recruitment microsite includes the conditions around a seed which determine the germination of that seed and the emergence of a viable seedling according to species specific requirements. The influence of microclimate on properties of the recruitment microsite can be varied across field topography or heterogeneous soil surfaces.

A microclimate can present conditions for recruitment of a species in a unique growing region within a field that may not exist in the broader field. Microclimate conditions acting on a seedling recruitment microsite can enable prediction of the onset and rate at which a weed population will recruit. Microclimate information can be used in weed management decision software programs such as Weedcast^{TM} that predict emergence timing and emergence potential of annual weed species (Forcella, 1998). The main factors affecting the microclimate of seedling recruitment microsites are described below.

2.1.1 Solar Radiation

Solar radiation that reaches the earth's surface is either reflected or absorbed. Solar radiation is the greatest source of energy for soil heat (Baver, 1940; Geiger, 1965; Rosenberg et al., 1983). Solar radiation drives the processes of water evaporation, heating of the soil and heating of the air. Radiant energy is partitioned into sensible and latent heat losses. The portion of absorbed solar radiation that is used for evaporation is returned to the atmosphere with water vapor. The soil surface warms by conversion of intercepted shortwave radiation energy to heat (Geiger, 1965). A temperature gradient is

formed during periods of adequate incoming solar radiation and heat is forced downward from the soil surface into the seedling recruitment zone by thermal conduction.

Shortwave reflection (shortwave albedo) is the portion of the incoming solar radiation (0.3–4.0 μm) that is reflected upward to space. The albedo determines how much of the radiation that reaches the soil surface will be available to heat the soil. Shortwave albedo varies with the season, the type of ground cover, and the time of day (Rosenberg et al., 1983). Most field crops reflect about 20–30% of the incident solar radiation (Davies and Buttimor, 1969; Kalma and Badham, 1972; Oguntoyinbo, 1974). Bare soil reflects 10–40% of the incident radiation (Kung et al., 1964). Dark soils have lower albedo than light colored soils. Crop residues generally reflect more shortwave radiation compared to bare soil (Horton et al., 1996). Maximizing the amount of crop residue cover on the soil surface would reduce the amount of energy available for evaporating water as well as delay heating of the soil. Shortwave albedo is further influenced by the water content of a surface soil with dry soils having greater albedo than corresponding wet soils (Ångström, 1925; Geiger, 1965; Cipra et al., 1971; Idso et al., 1975). Shortwave albedo has been measured as a linear function of water content in the top 0.02 m of a soil (Idso et al., 1975). The state of a soil surface undergoes daily and seasonal changes with resultant variation in albedo. The proportion of incident solar radiation reflected in the morning and evening is greater than that reflected at solar noon (Kalma and Badham, 1972).

2.1.2 Precipitation

Most precipitation on the eastern Canadian Prairies is received in the form of short duration and intense thundershowers. The amount and duration of precipitation influence the degree of wetting of microsites throughout the seedling recruitment zone. Precipitation events interact with wind and solar radiation to control the rate of evaporative loss from the soil surface and drying of near-surface located microsites. The moist upper soil surface is exposed to winds and evaporation begins immediately. Soil surface conditions control the partitioning of precipitation into surface runoff, infiltration, and evaporative losses. Retention of precipitation within the seedling recruitment zone is

affected by soil texture and other physical properties influencing losses from wetting below the zone and evaporation from the soil surface.

2.1.3 Wind

Air flow accelerates heat and water vapor transfer from the soil surface to the atmosphere. The transfer of heat from soil to atmosphere is not limited to molecular conduction, but is greatly increased by the transfer of quantities of air away from the soil surface and replaced by quantities of air at a different temperature (Cochran, 1969). Heat and water vapor are transferred to the atmosphere by convection and turbulent transport (Oke, 1987). Greater turbulence during the day increases sensible and latent heat flux density. The net transport of heat from the soil surface is generally upward during the day and downward at night.

Wind flowing along a rigid surface is slowed due to the drag exerted on the flow by the underlying surface. The aerodynamic roughness of the ground surface over which the wind speed profile is measured is the result of protuberances from the ground surface (Oke, 1987). Soil with crop residue and plant canopies generally has greater protuberances compared to bare soil.

Topography creates perturbations in the pattern of air flow (Oke, 1987). Separation of air flow from the surface occurs as air flow passes over irregularities in a surface. Surface discontinuity causing air turbulence occurs at scales from pebbles to topographical features. Moderate topographical features such as hillslopes usually allow the boundary layer wind flow to adjust without separation (Oke, 1987). Thus, a rise in topography causes the wind flow to constrict vertically, resulting in acceleration of the wind speed, whereas a drop in topography results in a slowing of the wind speed (Oke, 1987; Wood, 2000).

2.1.4 Relative Humidity

Relative humidity is a measure of the amount of water vapor in the atmosphere. Relative humidity is expressed as a percentage of the maximum amount of water vapor that can be held in the air at a given temperature. Water and heat are linked in the transition of water to different states. Evaporation of water at 20ºC requires 2.45 MJ kg^{-1}

whereas condensation releases an equivalent amount of heat (Rosenberg et al., 1983). Water state changes require energy consumption and release that provide the means for the transportation of heat to and from the soil surface (Rosenberg et al., 1983).

Microsite alterations occur within the recruitment zone as a field crop (or weeds) emerges and covers the bare ground. Ground that is shaded by plant cover can be expected to have different microsite environments compared to microsites in soil with no cover (Aguilera and Lauenroth, 1995; Boyd and Van Acker, 2004a). During the day, relative humidity increases and temperature decreases in the still air within the canopy of a transpiring plant cover (Waterhouse, 1950). An increase in the density of a growing crop increases relative humidity within the plant canopy. Surface relative humidity can be characterized by a sigmoidal curve with very few occurrences near 0 or 100% (Yao, 1974). Filzer (1939) measured relative humidity ranging from 40% above open ground to 73% within the canopy of a dense corn stand. Relative humidity at ground level has been shown to be greater at both sunrise and midday under a millet crop compared to bare land (Ramdas et al., 1934).

2.2 Topography

2.2.1 Hillslope Aspect

Hillslope aspect is the direction of exposure to the sun. The angle between the slope surface and the solar beam primarily controls the amount of direct solar radiation received by a surface (Rosenberg et al., 1983; Tian et al., 2001). The effect of topography changes the slope aspect and slope angle, thus altering the angle of incidence (zenith angle). The aspect of a hillslope can accentuate or reduce the angle of incidence and the resultant intensity of exposure, depending on the slope orientation relative to the sun. In the northern hemisphere, south-facing hillslopes receive more direct insolation from the sun than north-facing hillslopes because a smaller angle of incidence increases the amount of intercepted radiation that can be converted to heat at the soil surface.

Hillslope aspect has been shown to influence soil temperature, soil water, and vegetative cover (Ruhe, 1975). Hillslope aspect influences the amount of solar radiation received at the soil surface, thus affecting the amount of evapotranspiration and soil water content (Reid, 1973). South-facing slopes have been shown to have a 2ºC greater average

annual temperature, lower organic matter content, and lower water content compared to north-facing slopes (Franzmeier et al., 1969). Cremeans (1992) also measured greater organic matter in the A horizon and more water in northeast than southwest facing slopes. Soils with a north-facing aspect were found to have 20% greater available water in the 150 cm depth at planting time compared to soils with a south-facing aspect (Hanna et al., 1982). Sharratt (1996) measured greater barley yields (25 g m^{-1} more grain and 20 g m^{-1} more straw) on southern ridge aspects compared to northern ridges. The increased grain yield was attributed to a 2ºC higher temperature on slopes with a southern exposure, despite soil water on northern ridge aspects being greater than on southern aspects. The southern aspects inclined 20 to 40 degrees had 10% greater radiation absorption compared to a horizontal surface (Sharratt et al., 1992).

Exposure can be of greater importance in heat accumulation earlier in the spring season compared to later in the season. Accumulated soil temperature measured at a 5 cm depth on south-facing aspects represented 64% more degree hours in early spring and only 8% more degree hours in late spring compared to the horizontal (Ludwig et al., 1957). Ludwig et al. (1957) found an aspect by seeding date interaction that was most prominent during early seeding, and the later the maize was sown, the less difference existed for the time to emergence between the different aspects. The diminishing advantage of heat accumulation by the south-facing aspect on weed seedling germination would therefore be expected to show less dependence on aspect as the season progresses. Although the south-facing aspect received greater accumulation of degree hours than other aspects or horizontal every week during the experiment, the advantage was reduced with decreasing gradient (Ludwig et al., 1957). Maize emergence was earlier on south-facing slopes and later on north-facing slopes compared to the horizontal, with the degree of gradient strongly influencing the effect of aspect (Ludwig et al., 1957). The differences between slopes and aspects become less significant as the spring season progresses since the air temperature rises increasingly over the period, and direct solar radiation has a diminishing role in maintaining soil temperature. The interaction of aspect and gradient with time during the spring can have different temperature accumulation progressions for different gradient and aspect combinations that lead to different distributions of accumulated temperature (Ludwig et al., 1957).

2.2.2 Hillslope Position

Topography across a field often varies in elevation and slope gradient. A hillslope position is defined as a specific elevation on a gradient relative to the elevation difference in the overall slope (Ruhe, 1960). The relationship between soil properties and hillslope position has led to the partitioning of the hillslope according to geomorphic positions (Fig. 2.1).

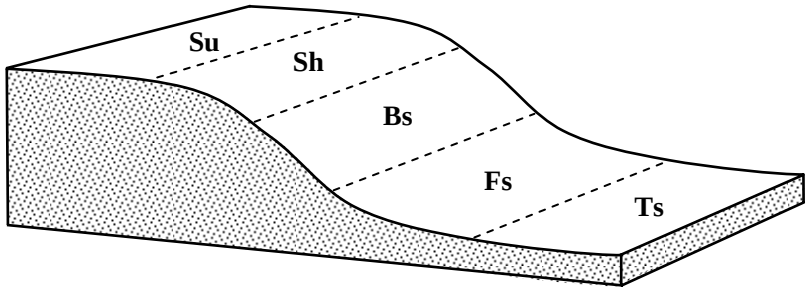

Fig. 2.1. Hillslope positions (Su – summit; Sh – shoulder; Bs – backslope; Fs – footslope; Ts – toeslope) of a hillslope model along a slope gradient (redrawn after Ruhe, 1975).

The amount of solar radiation received by a surface increases as slope gradient increases from 0 to 30 degrees in south, southeast or southwest aspects, whereas solar radiation received by north, northeast or northwest aspects decreases with the same increase in gradient (Garnier and Ohmura, 1968; Monteith, 1990). The gradient of a hillslope influences the receipt of solar radiation per unit area of absorbing surface due to the angle of incidence of the sun's rays to the ground surface (Rosenberg et al., 1983). The angle of incidence for south-facing hillslopes decreases with an increase in gradient resulting in greater flux density of radiation received at the surface (Rosenberg et al., 1983). Solar radiation received by east or west-facing aspects is similar to that received by surfaces with no gradient (Garnier and Ohmura, 1968; Tian et al., 2001). Spatial variability of received solar radiation across different hillslope aspects and gradients causes differences in energy balance and variability in microclimate across topography (Oke, 1987).

Hillslope position influences dynamics of near-surface soil water along the gradient. The spatial and temporal dynamics of near-surface soil water content along a

hillslope exhibit a high degree of variability resulting from interactions of microclimate, soil, vegetation, and hillslope geometry (Famiglietti et al., 1998; Honeycutt et al., 1990; Ridolfi et al., 2003; Tromp-van Meerveld and McDonnell, 2006). Along a hillslope, precipitation is partitioned into a number of components, including runoff, infiltration, drainage, and evapotranspiration (Dingman, 1994; Bronstert, 1999). The water content of surface soils influences control over mass and energy exchanges between the atmosphere and soil along the hillslope by partitioning net radiation into latent and sensible heat (Brubaker and Entekhabi, 1996). The position along the hillslope and exposure to sun and winds strongly affect the rate of evapotranspiration (Hanna et al., 1982; Casanova et al., 2000).

Topography is more important than soil cover or soil properties in controlling the distribution of surface soil water within low-slope cropland watersheds (Hawley et al., 1983). Topographic and soil properties interactively redistribute soil water following precipitation events. Soil water is redistributed across topography according to the variability of surface and subsurface conditions. Changes in gradient, slope pattern, hillslope position, and soil physical properties influence soil hydrology by redistribution of precipitation into vertical and lateral flow (Bathke and Cassel, 1991; Daniels and Hammer, 1992). Effective precipitation may increase from summit to toeslope and also reflects hillslope erosion and subsurface lateral flow (Honeycutt et al., 1990). Under wet conditions, variability in surface water content is most strongly influenced by porosity and hydraulic conductivity, whereas under dry conditions, variability in surface water content is related to elevation, aspect and clay content (Famiglietti et al., 1998). As the hillslope dries following rain events, the dominant influence on soil water variability progressively changes from soil heterogeneity to combined influence by topographic and soil properties (Famiglietti et al., 1998). Variations in soil water content along a hillslope are related to differences in soil texture (Henninger et al., 1976; Crave and Gascuel-Odoux, 1997), with variations in soil water due to differences in soil texture being more pronounced in wet than dry conditions (Hawley et al., 1983; Timm et al., 2006).

The slope gradient affects infiltration, drainage and runoff with steeper gradients being generally drier due to lower infiltration and greater runoff (Hills and Reynolds, 1969; Moore et al., 1988; Brubaker et al., 1994; Nyberg, 1996). Soil water content has

been found to be inversely proportional to elevation (Henninger et al., 1976; Hawley et al., 1983; Schroeder, 1995; Tomer et al., 2006). Soil water content is generally greater in lower hillslope positions and drier in higher hillslope positions due to convergent water flow towards concave hillslope positions (Hanna et al., 1982; Daniels et al., 1987; Cremeans, 1992). Soil hydrological sequences evolve from well-drained at upper hillslope positions to poorly-drained at lower hillslope positions (Crave and Gascuel-Odoux, 1997; Famiglietti et al., 1998). Lateral transport of subsurface water and surface runoff downslope causes plant available water to be greatest in the footslope and depressions, and lowest in the backslope and summit positions (Afyuni et al., 1993). The lowest soil water pressures generally occur at the backslope, followed by the summit being the second most water stressed hillslope position (Afyuni et al., 1993).

Areas of negative profile curvature (depressions) and negative plan curvature (convergent) along the hillslope gradient are generally wetter than areas with positive profile curvature (summits) and positive plan curvature (divergent), resulting in a significant correlation of profile curvature and soil water content (Moore et al., 1988). The relationships between soil physical properties, surface curvature, and precipitation catch on the distribution of soil water in the 0–15 cm soil depth indicated less precipitation catch and lower available water at the backslope than summit and shoulder hillslope positions (Boyer et al., 1990). This was attributed to higher clay content and lower infiltration capacity on the backslope position (Boyer et al., 1990). Greater soil water levels in the lower hillslope positions vary with soil depth as well as surface curvature (Sinai et al., 1981). Topographically derived landform element complexes, which compile relative elevation, slope gradient, aspect, and profile curvature information were determined to be better descriptors of soil water content in a field than using soil series information (Manning et al., 2001a).

The position along the hillslope affects additional physical properties of the soil including organic matter, texture, pH, and fertility (Walker et al., 1968; Carson and Kirkby, 1972; Brubaker et al., 1994; Young and Hammer, 2000). Topographical parameters of elevation and slope gradient were found to be most strongly related to soil properties (Walker et al., 1968). The processes that exist on a hillslope affect distribution of soil properties along the hillslope. The degree of textural variations in hillslope

elements is attributed to erosional and sedimentational activity rather than pedological activity (Kleiss, 1970; Malo et al., 1974; Changere and Lal, 1997; Brubaker et al., 1993). The hillslope gradient results in sorting of soil particles by hydrologic processes, and over time, result in smaller soil particles, predominantly clay, to accumulate downslope (Malo et al., 1974; Young and Hammer, 2000). Hillslope sedimentation also influences accumulation of organic matter, bulk density, and cation exchange capacity in soils formed at different positions on a hillslope (Kleiss, 1970; Young and Hammer, 2000). Organic production at the toeslope is also greater than the upper components of the hillslope due to greater wetness and clay content (Ruhe, 1975). Values of pH tended to be lower within upper hillslope positions with more strongly leached soil horizons (Manning et al., 2001b). Organic carbon contained within the A soil horizon increased downslope (Woods and Schuman, 1988; Elliott and Efetha, 1999; Manning et al., 2001b). Tomer et al. (2006) measured spatial patterns of organic carbon across field topography with the least organic carbon at backslope positions. Slope gradient was considered to be the best characteristic that predicted organic carbon (Tomer et al., 2006). The content of organic carbon in the soil affects soil structure and adsorption properties including bulk density and water retention (Rawls et al., 2004). Bulk density has been shown to increase more rapidly with depth at upper compared to lower hillslope positions (McConkey et al., 1997). Because bulk density is a dynamic property that varies with particle density, organic matter and compaction of a soil (Campbell and Henshall, 1991), it would be expected to vary with topography.

2.3 Soil Cover

2.3.1 Crop Residue

Crop residue cover on a field can alter the physical properties of the soil within the seedling recruitment zone (Teasdale and Mohler, 1993). Crop residues shade portions of the soil surface and have insulating properties due to reduced solar transmittance and greater shortwave albedo that increase resistance to heat and vapor transfer from soil to air (Teasdale and Mohler, 1993; Horton et al., 1996). Crop residues reduce the quantity of energy consumed in evaporation by blocking the transport of vapor out of the soil (Rosenberg et al., 1983). Crop residues have a cooling effect by reducing the amount of

heat penetrating into the soil. Soil is usually cold and wet during spring in temperate climates, and crop residue can delay warming compared to bare soil, thus prolonging cold and wet microclimate springtime conditions in the recruitment zone (Unger, 1978; Johnson and Lowery, 1985; Bristow, 1988; Horton et al., 1996). Incoming solar radiation levels at the onset of spring are fairly low, sustaining soil wetness. Crop residues impact seedling recruitment microsites mainly through effects on the surface energy balance (Horton et al., 1994). In a Manitoba study, the soil temperatures at a 5 cm depth on 23 April were 1–2ºC lower in fall tillage treatments that retained surface residue than tillage treatments that maintained a bare soil surface (Friesen and Bonnefoy, 1972). The effect of crop residue can decrease evaporation, increase the amount of available soil water, maintain cooler soil temperature during the spring, and reduce diurnal fluctuations of soil temperature (Horton et al., 1994).

Soil water has a dominant role in regulating soil temperature. When soils are wet, residue covered and bare soils have similar maximum diurnal soil temperatures at a depth of 2.5 cm. Bristow (1988) found a rapid increase in the maximum diurnal temperature of the bare soil occurred once it began to dry. However, a 6 mm rain caused the maximum diurnal temperature at the 2.5 cm depth to converge in the treatments, and later diverge again as the bare soil dried more quickly compared to the residue covered soil (Bristow, 1988). In contrast, minimum temperatures of the residue covered and bare soils converged with drying (Bristow, 1988). Residue on a soil surface not only decreases diurnal maximum temperature, but also affects how long temperatures remain above a certain critical temperature during the day. Under wet conditions, the duration of temperatures above a critical threshold at a depth of 2.5 cm were similar for residue covered and bare soils, but under dry conditions, the bare soil exceeded the critical threshold by a greater amount (Bristow, 1988).

During conditions where soil water is limiting, residue on the soil surface can reduce evaporative water losses and provide a soil environment with more favorable water conditions for germination (Teasdale and Mohler, 1993). Evaporation at the soil surface is characterized by stages with different rates of water loss. Following a precipitation event, crop residue cover on a field slows first stage drying, and allows water additional time to move deeper into the soil where it will be less susceptible to

evaporative loss (Bond and Willis, 1970; Unger et al., 1971; Unger et al., 1988). First stage evaporation is defined as a constant rate of water evaporation, which is dependent on water flow through the soil and is influenced by soil surface wetness, wind speed, temperature, solar radiation, and relative humidity (Idso et al., 1974). Second stage evaporation, or falling rate evaporation, depends on the drying soil to regulate water flow to the surface, and is less dependent on atmospheric conditions (Idso et al., 1974). Unger and Parker (1976) report cumulative evaporation to be most strongly influenced, in order of importance, by residue thickness, surface coverage, residue application rate, and residue specific gravity. Crop residue has been shown to decrease the soil surface temperature (Gauer et al., 1982), which decreases vapor pressure of the soil water. Residues also reduce water vapor transport from the soil surface by increasing the thickness of the nonturbulent air layer above the soil surface (Bond and Willis, 1969; Smika and Unger, 1986). Evaporation losses are reduced in a linear manner by surface application of wheat straw up to 90% soil cover (Greb, 1966). The ability of crop residue to reduce evaporation is generally limited to a few days after precipitation (Brun et al., 1986; Greb, 1966; Russel, 1939). After this time, the evaporation rate from soil covered with surface mulch is analogous to that of a bare soil (Adams et al., 1976; Brun et al., 1986). Aase and Tanaka (1987) determined that drying rates are greater from bare soils compared to straw covered plots following rain amounts greater than 3 mm. However, differences in drying rates diminished 10 days after rainfall. Similarly, Brun et al. (1986) report evaporation of 0.168 cm day^{-1} the day after rainfall from a bare soil surface, compared to 0.134 cm day^{-1} from a wheat stubble covered surface.

Maintaining a crop residue cover on the soil surface has been shown to not only reduce water evaporation by shading the soil from solar radiation, but also insulate the soil from heat conduction via air (Bond and Willis, 1969). Surface wheat residue lowered maximum soil temperatures 1 to 5°C at 2.5 and 5.0 cm depths during the first 30 days of spring wheat growth under no-till compared to conventional tillage systems (Carter and Rennie, 1985). A crop residue treatment in the northern Corn Belt of the USA with 0 cm stubble and no residue was warmer because of a smaller albedo (0.03) and greater net radiation (0.5 MJ m^{-2} day^{-1}) compared to treatments with stubble and/or residue (Sharratt, 2002). Potter et al. (1985) concluded that thermal diffusivity and thermal

conductivity were greater with a no-tillage system than under conventional tillage. The influence on soil temperature and heat flux differences were attributed primarily to surface residue cover, and to a lesser extent to soil thermal properties.

2.4 Soil Heat

2.4.1 Temperature

Soil temperature is a measure of the heat content (heat energy) contained in the soil medium. Solar radiation is the primary influence on soil temperature. The greatest accumulation of soil heat from solar radiation during the spring occurs at the soil surface and decreases with depth into the soil profile (Rosenberg et al., 1983). Soil temperatures in the Northern Great Plains and Midwest regions are low during early spring, and temperature gradients form across shallow soil depths that direct heat from the surface into the soil profile (Stoller and Wax, 1973b; Reid and Van Acker, 2005). Environmental factors in addition to solar radiation that affect soil temperature are rainfall, condensation, insulation, evaporation, transpiration, and air convection (Scott, 2000). Soil factors that influence soil temperature are mineralogical composition, soil water content, soil color, heat capacity, thermal conductivity, and thermal diffusivity (Scott, 2000).

Soil temperature fluctuations within a field usually display high temporal variability with diurnal and annual fluctuations and generally low spatial variability across the field (Warrick and van Es, 2002). Soil temperature at the soil surface fluctuates diurnally with a wave-like pattern, primarily as a result of changing intensity of shortwave radiation (Van Wijk and De Vries, 1963; Stoller and Wax, 1973b; Schieldge et al., 1982). Temperature in the near-surface soil layers fluctuate due to alternating intervals of storage and release of heat (Van Wijk and De Vries, 1963). The diurnal temperature range displays a pattern of amplitude reduction with depth in the profile below the soil surface (Oke and Hannell, 1966; Stoller and Wax, 1973b; Bruce et al., 1977; Rosenberg et al., 1983; Sauer et al., 1996). There is a time lag in maximum and minimum temperature with depth from the soil surface (Oke and Hannell, 1966; Sauer et al., 1996). The soil surface is coldest at sunrise, and warms by conversion of intercepted shortwave radiation into heat. During the morning, the temperature of the soil surface becomes higher and forms a gradient with depth. The soil surface reaches a maximum

during mid-afternoon as the amount of intercepted radiation decreases when the angle of the sun decreases. By late afternoon, the surface of the soil becomes cooler than the soil below, with heat transfer toward the surface following the upward temperature gradient. The soil surface continues to cool as energy is lost by longwave radiation. The soil surface becomes progressively cooler during the night since heat moving upward does not fully replace the amount of energy lost from the soil surface.

In a silty clay loam soil, Stoller and Wax (1973b) determined that during the summer when soils were heating, the diurnal amplitude to a depth of 5.1 cm was greater than that of the air temperature, however at soil depths of 10.2 cm and deeper, the diurnal amplitude was less than that for air temperature. The diurnal surface temperature wave has been shown to be discernable to a depth of approximately 0.60 m (Bruce et al., 1977) to 0.75 m (Oke, 1987). The diurnal temperature wave is even less in soils with low diffusivity, which indicates that heat movement was extinguished in a thin layer of the soil profile near the surface. Due to the increasing time lag of the wave-like temperature pattern in the soil with depth, the soil can be simultaneously warming in its upper layers while cooling a short depth into the soil profile, with the reverse occurring when the soil surface is cooling.

Crop residue on the surface has a damping influence on the diurnal temperature wave (Bristow, 1988). Hourly soil surface heat flux was higher for bare soil compared to a residue covered soil for the same tillage treatment (Gupta et al., 1984). Daily soil surface heat flux was measured at 69.8, 47.9, and 42.6 W m^{-2} for no-till with no residue, moldboard with surface residue, and no-till with surface residue treatments, respectively (Gupta et al., 1984). Soil temperature amplitude at 0.05 and 0.10 m followed similar trends to the surface temperatures. The differences in soil temperature fluctuations corresponded largely with differences in surface residue cover and to a lesser extent with the difference in soil disturbance by tillage (Gupta et al., 1984).

The annual temperature wave amplitude decreases less rapidly with depth, and the depth of heat influence is greater compared to the diurnal wave pattern. Whereas diurnal temperature wave patterns range to 0.75 m, annual wave patterns penetrate to about 14 m (Oke, 1987). When soils are warming during the spring, a temperature gradient exists in

the soil profile. Temperatures decrease with depth and the associated downward heat flux increases the storage of heat within the soil profile.

2.4.2 Thermal Capacity

The thermal capacity of a soil is the ability of the soil to store heat within its profile, and is expressed as the temperature change due to heat gain or loss. Thermal capacity is expressed as J m^{-3} K^{-1}, which is the amount of heat required to increase a unit volume of soil by a temperature change of one degree (Oke, 1987). Soil thermal capacity is largely dependent on the volume fraction of water, solids, and air in the soil (Ochsner et al., 2001). Typical values of thermal capacity for dry sandy and clay soils are 1.28 and 1.42 J × 10^6 m^{-3} K^{-1} (van Wijk and de Vries, 1963). Clay soils generally have higher thermal capacity than sandy soils at air dry water content (Ghuman and Lal, 1985). Water and air have thermal capacities of 4.18 and 0.0012 J × 10^6 m^{-3} K^{-1} respectively (van Wijk and de Vries, 1963). Saturated sandy and clay soils with 40% pore space have increased thermal capacities of 2.96 and 3.10 J × 10^6 m^{-3} K^{-1} as a result of water displacing air (van Wijk and de Vries, 1963). Yadav and Saxena (1973) also determined that thermal capacity of soil increased with increased water content. This means that it takes more energy input to cause a similar rise in temperature of water compared to soil or air. Also, water does not cool as rapidly as soil when enduring a loss of energy. Therefore, water is better than soil or air at storing energy, and has an associated conservative thermal influence.

The thermal capacity of a soil is strongly dependant on the soil water content such that adding water to an initially dry soil increases thermal capacity of that soil. The thermal capacity of moist soil is a linear function of water content for both sandy and clay soils (Cochran, 1969; Yadav and Saxena, 1973). The increase in thermal capacity occurs because the addition of water, which has a very high thermal capacity, displaces a proportionate volume of air with low thermal capacity. The greater the thermal heat capacity, the lower the change in temperature with the addition or removal of a given amount of heat (Cochran, 1969). Yadav and Saxena (1973) determined that thermal capacity of soil increased with bulk density. Stoller and Wax (1973b) observed that soil temperature depressions coincided with precipitation events, which they attributed to

increased cloudiness and reduced solar radiation as well as increased soil thermal capacity which delayed subsequent soil warming.

2.4.3 Thermal Conductivity

Thermal conductivity is a measure of the ability of the soil to conduct heat and is expressed as W m^{-1} K^{-1} (Oke, 1987). Thermal conductivity is the amount of heat flowing through a unit cross-sectional area (m^2) of a substance per unit time (s), with a perpendicular temperature gradient of 1 degree m^{-1} (Oke, 1987). The thermal conductivity of a soil is influenced by soil water content, soil texture, soil porosity, organic matter, and salt concentration (Nakshabandi & Kohnke, 1965; Ghuman and Lal, 1985; Abu-Hamdeh and Reeder 2000). Thermal conductivity of dry soils increases with both particle size and bulk density, however, variations in soil water content have been shown to have a much greater influence on thermal conductivity in soil than either particle size or bulk density (Nakshabandi and Kohnke, 1965; Abu-Hamdeh and Reeder, 2000). Thermal conductivity in soil is complex because temperature gradients cause redistribution of water within the soil profile (De Vries, 1963).

Lower thermal conductivity in clay compared to sandy soil can be attributed to lower bulk density in the clay soil (Ghuman and Lal, 1985). Abu-Hamdeh and Reeder (2000) determined that an increase in bulk density at a given water content increased thermal conductivity at soil textures ranging from sand to clay. Clay loam soil was shown to have a decrease in thermal conductivity with increasing organic matter levels (Abu-Hamdeh and Reeder, 2000). Abu-Hamdeh and Reeder (2000) determined that thermal conductivity of sandy and clay loam soils decreased with increasing salt contents at given water content.

Thermal conductivity of soil typically ranges from 0.30 W m^{-1} K^{-1} for dry sandy soil to 0.25 W m^{-1} K^{-1} for dry clay soil (van Wijk and de Vries, 1963). Water and air, which displace one another within soil pore space, have thermal conductivities of 0.57 and 0.025 W m^{-1} K^{-1} (van Wijk and de Vries, 1963). Because water is a much better conductor of heat than air, saturated sandy and clay soils (with 40% pore space) have greater thermal conductivities of 2.20 and 1.58 W m^{-1} K^{-1} (van Wijk and de Vries, 1963). Since air is such a poor conductor of heat, it provides soil with good insulation properties.

At low water contents, the air space controls the thermal conductivity, with most air-dry soils having similar thermal conductivities (Shiozawa and Campbell, 1990). Differences in thermal conductivity between clay and sandy soils were determined to be smaller at lower soil water contents than at high water contents (Ghuman and Lal, 1985). Nakshabandi and Kohnke (1965) determined that soils of different textures, which contain similar water contents, display higher thermal conductivities in coarse than fine textured soils. Thermal conductivity was determined to be similar in different textured soils when compared at the same water potential (Nakshabandi and Kohnke, 1965).

Thermal conductivity is not static in soil, but varies both spatially and temporally. Because thermal conductivity depends on soil particles, water and air content, a change in the water and air content of the soil alters its thermal conductivity. Dry soil will exhibit an increase in thermal conductivity with the addition of water because the thermal contact between soil particles is increased by coating the soil particles with water, which increases conduction of heat from one soil particle to the next, and since pore space is finite, water having a high thermal conductivity displaces air volume which has a much lower thermal conductivity. Therefore, thermal conductivity of a soil initially increases dramatically with an increase in water content, but increases at a decreasing rate until a plateau is reached at greater water contents (Nakshabandi and Kohnke, 1965; Oke, 1987). The transition from low to high thermal conductivity occurs at low water contents in sandy soils and at higher water contents in clay soils (Campbell, 1985). Hiraiwa and Kasubuchi (2000) determined that thermal conductivity in soil increased with increasing temperature, as well as increasing water content, thus implying a temperature dependence of thermal conductivity of soil with coupled heat and water vapor transfer.

The amount of organic material on the soil surface influences thermal conductivity of the soil. A surface mulch generally has lower thermal conductivity compared to bare soil. A mulched soil will cause an increase in surface temperature variation of the mulch because heat is not transferred to or from as great a depth in the soil (Cochran, 1969). Conversely, when mulches are wet, surface temperature variation can be reduced even though their thermal conductivity is lower than the underlying soil (Cochran, 1969).

2.4.4 Thermal Diffusivity

The property of thermal diffusivity in a soil is the ability of a soil to diffuse thermal influences. Thermal diffusivity is the speed at which temperature waves are transmitted into the soil, and the depth of thermal influence of the soil surface (Oke, 1987). Soil thermal diffusivity is expressed as a measure of time required for temperature changes to travel ($m^2\ s^{-1}$). Thermal influences are directly proportional to the soil's ability to conduct heat, but inversely proportional to a soil's thermal capacity.

Typical values of a thermal diffusivity for dry sandy and clay soil are 0.24 and $0.18 \times 10^{-6}\ m^2\ s^{-1}$ (van Wijk and de Vries, 1963). Water and air have thermal diffusivities of 0.14 and $21.50 \times 10^{-6}\ m^2\ s^{-1}$ (van Wijk and de Vries, 1963). Saturated sandy and clay soil with 40% pore space have increased thermal diffusivities of 0.74 and $0.51 \times 10^{-6}\ m^2\ s^{-1}$ (van Wijk and de Vries, 1963), due to the greater increase in thermal conductivity compared to that of thermal capacity.

The thermal diffusivity of most soils increases to a high and then decreases with increasing soil water content (Cochran, 1969). An increase in water content of a dry soil will initially increase thermal diffusivity due to the increased thermal contact between soil particles, as a result of water displacing air volume. As volumetric water content continues to increase beyond approximately 20%, thermal diffusivity generally begins to decline because thermal conductivity levels off and thermal capacity continues to increase (Oke, 1987). Ghuman and Lal (1985) determined that thermal diffusivity of sandy and loam soils increases with water content to a peak, and then decreases with increasing water content. However, finer textured soils did not exhibit a distinct peak in thermal diffusivity with increasing water content (Ghuman and Lal, 1985).

Soils with low thermal diffusivities have poor heat movement into the soil profile and therefore concentrate thermal exchanges only in the uppermost soil layers. Alternatively, soils with high thermal diffusivities permit heat to penetrate readily into the soil layers enabling surface temperature changes to spread over a thick profile of soil (Oke, 1987). Wet soils have lower thermal diffusivity and less soil temperature change at high water contents compared to dry soils because the higher water content prohibits a large temperature increase with heat absorption (Cochran, 1969).

Soils with high diffusivities allow surface heating during the day to warm a thick layer of soil, and to draw heat from deeper in the soil profile during surface cooling at night. High diffusivity, therefore, results in less extreme temperature regimes in the soil profile due to greater dispersion of the heat deeper into the soil profile. Lower diurnal temperature amplitude in the surface soil layer is also characteristic of high diffusivity soils. The larger the thermal diffusivity of a soil, the easier it is for heat to be transported to or from the soil surface, and therefore the diurnal surface temperature variation will be smaller (Oke, 1987). Soils with low diffusivity have higher diurnal amplitude in the surface soil layer due to slower heat movement in the soil profile.

2.5 Soil Water

2.5.1 Water Content

Soil water content is a measure of the mass of water stored in a soil, and is expressed on a weight basis as gravimetric soil water content (kg kg^{-1}). Soil water content can also be expressed as a measure of the volume of water content in the soil, which is the percentage of soil volume that is occupied by water or volumetric water content (cm^3 cm^{-3}). Soil water content is important where changes in mass or volume occur in water balance studies, which measure addition or loss of water from the soil. Soil water gradients develop during periods of drying following a precipitation event due to daily radiation inputs and evaporation at the soil surface (Bruce et al., 1977; Schieldge et al., 1982; Allen et al., 1993; Reid and Van Acker, 2005). Changes in soil water content can be utilized to estimate percolating rain and evapotranspiration losses to the atmosphere by measuring the area between successive profiles in the soil depth over time. Soil water affects the soil surface energy balance and therefore affects soil surface temperature. Solar radiation received at the soil surface will not begin heating soils considerably until the evaporative demand is fulfilled (Bristow, 1988).

Diurnal fluctuations of soil water content can develop during periods of soil drying. Soil water content under a bare soil at a depth less than 2 cm displayed diurnal variation in a tilled plow layer following a rainfall event (Bruce et al., 1977). The amplitude of the sinusoidal water content relationship decreases with depth as drying

proceeded with the maximum for the 0.5 cm soil depth at dawn and minimum at noon (Bruce et al., 1977).

2.5.2 Water Potential

Soil water potential is an indirect measure of water content, and is considered to be the energy necessary to extract water from the soil matrix (Hillel, 1982; Oke, 1987). Values of water potential are negative when the soil is unsaturated, indicating that work is required to bring the potential of the water to a zero potential state. Water potential as a function of soil water content varies with soil texture. Soil water potential is expressed in units of energy per unit mass (J kg^{-1}), energy per unit volume (Pa), or energy per unit weight (m). Total water potential is a summation of matric, osmotic, pressure, and gravitational potentials (Hillel, 1982; Penning de Vries et al., 1989). Water potential is a valuable measure in estimating the availability of water for seed imbibition, as well as determining water movement within the soil profile.

The forces determining water potential by binding soil water are related to the soil porosity and the soil water content. Forces acting on water potential are weakest in wet soils with low bulk density and greatest in compacted dry soils. Therefore, at given water content, water potential is lowest in clay soils and greatest in sandy soils. Water potential decreases (becomes more negative) in a sigmoidal fashion as water content decreases. As such, it is relatively easy to extract water from a wet soil, but as the soil dries, water potential decreases and it becomes increasingly more difficult to extract additional water from the soil (Hillel, 1982; Oke, 1987). Water potential is also reduced by the presence of soil solutes (Hillel, 1982).

Within the range of water potentials that permit plants to extract water from the soil, coarse sand has the least available water, and silt loam has the most available water (Brady and Weil, 2002). The upper limit of soil water storage capacity that can be held in the soil against the force of gravity is termed field capacity at a soil water potential at −0.033 MPa. The lower limit of plant available soil water storage capacity at −1.5 MPa is termed the permanent wilting point, which is the water content in the soil after a plant has extracted all the water it can.

The effect of temperature on the soil water potential of sand, sandy loam and muck soils at a constant volumetric water was investigated by Gardner (1955). He determined that within a range of 0 to 50ºC, water potential decreased at about 0.0008 MPa per degree rise in temperature. Campbell and Gardner (1971) determined that the change in soil water potential with temperature becomes greater as soils become drier. Finer textured soils display a greater change in water potential with temperature compared to coarser textured soils at similar water potentials (Campbell and Gardner, 1971). Moore (1940) measured water retention in clay, fine sand, and loam soils, and determined that the amount of water retained decreased with increasing temperatures, with approximately 10% more water retained at 10ºC compared to 45ºC.

2.5.3 Hydraulic Conductivity

Hydraulic conductivity is a measure of the ease with which water flows through a soil in response to a particular water potential gradient. Water flows across a gradient from areas of higher water potential to areas of lower water potential, that is, from wetter to drier regions in the soil. The movement of water at a field scale is a dynamic process, with alternate sequences of wetting and drying. Water movement occurs under water potential and temperature gradients (Philip and de Vries, 1957; Bach, 1992). Within the soil profile, the volumetric water content is constantly fluctuating in response to additions and losses of water due to precipitation, evapotranspiration, and percolation. Additions of water to the soil profile move within the soil profile due to the influence of forces, which result from the attraction of the soil solid matrix for water, as well as from the presence of solutes, atmospheric pressure and gravitational forces (Hillel, 1982). Evapotranspiration of water creates a water potential gradient that becomes greater than the opposing gravitational gradient, which causes upward water movement from high to low water potential.

Hydraulic conductivity can vary with depth in the soil according to a number of factors. Depending on the depth and intensity of tillage, and subsequent settling and compaction, the seedling recruitment zone may not contain uniform soil properties (Cassel, 1983). Slower water flow with depth across hillslope positions was associated with increases in bulk density, total porosity, and clay content, and decreases in

macroporosity and sand content (Bathke and Cassel, 1991). Another hillslope experiment indicated that for given water content, hydraulic conductivity decreased with downslope position in the 0–15 cm depth due to an increase in clay content in the lower slope positions (Matzdorf et al., 1975).

Saturated hydraulic conductivity occurs at saturation when soil porosity is completely water filled. At water levels less than saturation, movement of water is determined by unsaturated hydraulic conductivity which varies with water content. The rate of water vapor transfer within the soil is directly proportional to the diffusion coefficient of water vapor (Cary, 1966). Soil water vapor flow is important relative to liquid water flux during dry soil conditions whereas liquid water flow dominates at high water content (Nassar et al., 1997; Schelde et al., 1998). Hydraulic conductivity is dependent on water content with low levels of hydraulic conductivity occurring at low water levels, and exponentially increasing levels of hydraulic conductivity with increases in water content to the point of saturation (Hillel, 1982). Cary (1966) noted that if the soil contained a compacted layer at or immediately below seeding depth, the rate of vapor transfer at that level would be reduced according to the amount of compaction.

Thermal gradients within the soil profile cause water to redistribute by either vapor pressure gradients or liquid water flow (De Vries, 1963; Hopmans and Dane, 1985; Bach, 1992; Nassar et al., 1997). Liquid water flow is the principal means for water flow under temperature gradients (Cary, 1965), however most liquid water moves as capillary water due to a decrease in surface tension with an increase in temperature (Philip and de Vries, 1957). Movement of water in the vapor phase is from warmer to cooler areas. The temperature dependence of soil hydraulic properties is further due to variation in water viscosity with changing temperature (Constantz, 1982; Hopmans and Dane, 1986a). As temperature increases, the viscosity of water decreases and as a result, hydraulic conductivity is enhanced.

Air is often saturated in the pore spaces of wet soils in close proximity to soil water. Since higher soil temperatures increase saturation vapor pressure, a water vapor concentration gradient exists from high to low soil temperatures (Nassar et al., 1997). As a result of the diurnal heat gradients in the soil, vapor tends to flow downward into the soil during the day, and upwards toward the surface at night. Soil water moves upward in

the soil profile as a result of the temperature gradient and water condenses on the cold soil surface. Changes in water viscosity in response to the diurnal temperature fluctuations alter the hydraulic conductivity of water in the soil surface layer causing water movement to vary throughout the day (Jaynes, 1990). Although the temperature dependence of soil hydraulic properties is well documented, the temperature effect is considered to be small compared to the spatial and temporal variability encountered in the field (Vieira et al., 1981).

2.5.4 Water Retention

The relationships among capillary (pore) size, water content and water potential within a soil describes a capacity factor, soil water content, to a pressure factor, the energy state of the water (Dane and Hopmans, 2002). This relationship describing the amount of water that can be held in a soil at different soil water potentials is called the soil water characteristic curve or soil water retention (release) curve. As the water content of the soil decreases, progressively smaller capillaries lose water and thus the water potential of the soil decreases (becomes more negative). The relation between water potential and volumetric water content is not proportional and is often expressed as a logarithmic function (Penning de Vries et al., 1989). The soil water retention curve has been described by nonlinear equations (Brooks and Corey, 1964; Campbell, 1974; van Genuchten, 1980; Tani, 1982).

The water retention curve is dependent upon the soil texture or particle size distribution (Salter and Williams, 1965; Haverkamp et al., 2005), as well as the arrangement of the solid particles or the soil structure (Croney and Coleman, 1954). Consequently, the soil water characteristic can be estimated from the soil physical properties (Rawls et al., 1991). Organic matter content influences the soil water retention curve due to the ability of organic matter to absorb water and indirectly due to its effect on soil structure (Dane and Hopmans, 2002). Soils containing clay have adsorptive forces that include osmotic pressure due to the presence of a high concentration of cations (Dane and Hopmans, 2002). Spatial variability in the soil water retention curve across a field results from dependence on soil properties that often vary spatially (Greminger et al., 1985; Nielsen et al., 1973; Burden and Selim, 1989).

The temperature effect on soil water retention is attributed to changes in surface tension, the volume of entrapped air, and water flow from isolated packets to continuous water phase (Hopmans and Dane, 1986b; Liu and Dane, 1993). An increase in temperature decreases surface tension of water causing the amount of water held in the soil to decrease. However, the effect of temperature on the soil water retention relationship is generally not important in agricultural soils (Hopmans and Dane, 1986b).

The soil contained within the seedling recruitment zone is a composite of capillaries (pore spaces) of different sizes. Clay soils have smaller capillaries than sandy soils. The smaller the capillary, the greater the suction on a given amount of water. This equates to less (more negative) water potential in the soil. Soils with smaller capillaries retain more water than soils with larger capillaries because the water is held with greater suction and it requires more energy to remove the water. The result is a soil water retention curve that is generally more gradual for clay soils (Hillel, 1982).

In a drying soil, water is initially released from large pores that cannot retain water against the force of suction. A gradual increase in suction results in water being drawn out of progressively smaller pores. At very high suction forces, only very small pores retain water at great tension. It is more difficult for a seed to imbibe water from a soil containing smaller capillaries with lower water potential than from a soil having larger capillaries and greater water potential. The phenomenon by which water is held by the soil at a given time controls the rate of water movement within the soil as well as the availability of water to germinating seeds.

2.6 Recruitment Microsite

A microsite refers to the soil environment immediately surrounding the seed that has a direct influence on seedling recruitment (germination and emergence) (Harper, 1977; Pareja and Staniforth, 1985; Eriksson and Ehrlén, 1992). Heterogeneity within the seedzone creates a wide range of microsites with different environmental conditions that regulate seed germination (Harper et al., 1965; Harper and Benton, 1966; Battaglia and Reid, 1993). Specific requirements of the microsite environment exist for germination and emergence of each species. A microsite is referred to as a safe site which enables germination and establishment of a plant to occur (Harper et al., 1961). A favorable

microsite includes environmental conditions necessary for dormancy breaking, germination and emergence of a particular weed seed (Bibby, 1935; Fowler, 1986). Environmental factors of a microsite that impact recruitment include water, heat and oxygen (Bibbey, 1935; Harper, 1977; Pareja and Staniforth, 1985; Eriksson and Ehrlén, 1992). A favorable microsite for many germinating seeds is one that prevents desiccation (Fowler, 1986; Walters et al., 2001). Detailed knowledge of the microsite environment forms the basis for modeling weed recruitment in the field.

Microsite conditions can vary both spatially and temporally within the soil profile. At the size scale of a seed, the seedling recruitment zone in the soil seedbed represents a high degree of microtopographic heterogeneity (Harper et al., 1965). Soil heterogeneity creates a variety of microsite conditions that regulate seedling recruitment. Soil microtopography further influences seedling recruitment by variation in microsite size (Harper et al., 1965). The size of a microsite can range from partial contact to complete envelopment of a seed (Harper et al., 1965; Harper, 1977). Microtopography of the soil surface has the greatest influence on surface located seeds and can determine recruitment success for surface located seeds due to contact between seed and substrate (Harper et al., 1965).

The abundance of suitable microsites across a field for a given species can vary due to soil texture, soil cover, and topography (Mohler and Galford, 1997). The variability of the soil surface influences the shallow weed seedling recruitment zone to regulate seed germination and seedling emergence by creating microsites with varying temperature and water regimes (Pareja and Staniforth, 1985; Pareja et al., 1985). Additionally, microsites favorable to recruitment vary diurnally as well as temporally throughout the growing season. The spatial and temporal microsite environment controls the occurrence, timing, and proportion of seedling recruitment (Fowler, 1988; Forcella et al., 1997). Microsite influences are more important for germination, emergence, and early establishment than seedling survival (Wood and Morris, 1990; Aguilera and Lauenroth, 1995).

Microsites must have an existence that is temporally sufficient to enable the processes of germination and emergence to occur. Microsites favorable for recruitment often exist for only a limited period of time enabling a temporary window of opportunity

for germination to occur (Johnstone, 1986; Fowler, 1988). Microsites can be short lived due to the nature of diurnal temperature fluxes and hydration fronts in the constantly evolving soil environment. The frequency of microsites along a temperature or water gradient that are conducive to recruitment of a given species exist in response to the level of suitability of the environmental gradient to provide adequate conditions for recruitment. A microsite must provide the minimum temperature and water conditions necessary for germination, however a microsite containing optimal conditions will provide a more suitable environment for germination (Fowler, 1988).

Specific spatial and temporal attributes of the microsite environment are often lengthy and difficult to measure. Generalizations have often been used to describe the microsite conditions using coarse measurements in space or time. A single depth measurement in the soil profile has commonly been used to describe microsite conditions in the seedling recruitment zone (Leguizamón et al., 2005; Rinaldi et al., 2005; Page et al., 2006). Coarse temporal measurements of the water status in the recruitment zone are generally made due to limitations in equipment or labor. Coarse or aggregate measurements limit the description of microsite conditions that can be used for predictive purposes, especially since the size of a microsite is comparable to that of a seed (Harper, 1977). A review of the literature on soil water content in small scale field topography revealed a common feature in each study was low spatial or temporal sampling frequency resulting in no consistent description of soil water variability along a hillslope (Famiglietti et al., 1988).

The seedling recruitment microsite is subject to temporal dynamics of soil water heterogeneity. The variance of soil water content increases with increasing soil water content (Hills and Reynolds, 1969; Henninger et al., 1976; Bell et al., 1980). Variability in soil water content is considered to be largest following a rainfall event since the effects of soil heterogeneity would be at a maximum (Reynolds, 1970). Conversely, the variance would be lowest after an extended dry period, when the effects of soil heterogeneity would be reduced (Reynolds, 1970). Other studies have shown that soil water variability is normally distributed with greatest variance in the mid-range of mean water content when small areas of rapid drying co-exist with wet areas, resulting in more diverse soil water conditions (Hills and Reynolds, 1969; Bell et al., 1980; Hawley et al., 1983;

Loague, 1992). High soil water conditions can contribute to anoxic microsites (Pareja and Staniforth, 1985; Renault and Stengal, 1994).

Although occurrence of some weeds can be influenced by specific attributes of the soil environment, in general, weed seedling emergence can be predicted reliably using the soil processes of soil water and soil heat transfer as the two most important predictors of recruitment and emergence timing. To obtain a better understanding of the soil processes associated with weed recruitment, soil physical properties associated with each process are either measured directly or estimated with the use of predictive models. The condition of the soil microsite at a given time and space are represented by state variables (water content and temperature) resulting from one or more soil processes, as governed by the soil properties associated with each process. Furthermore, water content and temperature are often a result of interactions between soil properties that influence the processes of soil water and soil heat transfer.

2.6.1 Depth of Recruitment Microsite

The depth at which weed seeds originate from the soil profile has a direct effect on successful germination and emergence. The depth of weed seedling recruitment has implications for the onset and duration of weed recruitment, as well as the competitive ability of weeds. The location of a weed seed in the soil profile affects the likelihood of germination, successful emergence and relative time of emergence (Chancellor, 1964; Mohler, 1993; Grundy et al., 2003). The onset and duration of weed seedling recruitment is difficult to predict due to interactions of microclimate, soil properties, and management practices that create diverse microsite conditions at shallow depths within the vertical soil profile that drive the recruitment process (Buhler, 1995; du Croix Sissons et al., 2000; Bàrberi and Lo Cascio, 2001). Weed seeds near the soil surface are exposed to greater variability in environmental conditions. Within the shallow profile of the seedling recruitment zone, differences exist with temperature, water content, aeration, and light availability (Stoller and Wax, 1973b; Reid and Van Acker, 2005).

Soil disturbance during tillage operations is the main cause of burial and vertical movement of weed seeds into unique microsites within the recruitment zone (Pareja et al., 1985; Cousens and Moss, 1990; Buhler and Mester, 1991; Staricka et al., 1990;

Mohler and Galford, 1997; Reid and Van Acker, 2005). Tillage usually causes a vertical gradient of seed numbers with soil depth such that seed numbers are highest in the upper soil layer and decrease with depth in the soil profile (Pareja et al., 1985; Staricka et al., 1990; Yenish et al., 1992). The vertical distribution of seeds in the soil profile can be manipulated with different types of tillage (Staricka et al., 1990; Hoffman et al., 1998; Colbach et al., 2000; O'Donovan and McAndrew, 2000; Swanton et al., 2000; Mohler et al., 2006). Weed seeds are also relocated horizontally into different microsites as a result of tillage (Lindquist and Maxwell, 1991). In addition to the redistribution of weed seeds during tillage operations, changes also occur in the soil microsite physical properties due to the tillage operation (Cassel, 1983; Mohler and Galford, 1997). Tillage systems subject weed seeds to microsites with different soil physical properties as a result of differences in bulk density, soil aeration and porosity, and soil surface conditions (Cassel, 1983; Lal et al., 1994). In essence, weed seeds may be either relocated to microsites having different properties, or the properties of the local microsites may be altered by the tillage process.

The depth at which the recruitment microsite is located in the soil profile affects the soil environmental properties that influence seed germination. Germination cues such as water, temperature, fluctuating temperature, and light often form gradients and different diurnal patterns that are influenced by depth in the seedling recruitment zone (Bruce et al., 1977; Rosenberg et al., 1983; Baskin and Baskin, 1987; Sauer et al., 1996). Seeds located near the soil surface are exposed to greater extremes of temperature and water compared to more moderate changes with depth in the soil profile. Greater exposure to the atmosphere causes drying to occur more readily at the soil surface. Even slight burial reduces seed drying by maintaining an environment with high relative humidity.

2.7 Seedling Recruitment Models

Weed seed germination and emergence models are used to predict the timing and rate of germination of a proportion of a particular weed population from the seedbank. Germination models based on a daily time step can be used to optimize control by establishing when application of a control method will reach the highest proportion of a

weed population. The two approaches used to model seed germination and emergence are empirical and mechanistic modeling. The empirical approach provides information under a given set of conditions. Because empirical models tell us little about the underlying biological process of recruitment, the mechanistic approach enables a better understanding of the factors governing germination and emergence (Bradford, 1990; Forcella et al., 2000). The empirical model often requires additional empirical variables to adequately describe the recruitment process (Brown and Mayer, 1988). Models that use calendar days as the time variable in emergence models have prediction limitations since the passage of time does not directly account for thermal accumulation (Cussans et al., 1996; Gan et al., 1996; Vleeshouwers, 1997).

The predictive performance of a mechanistically based seedling recruitment model generally has greater applicability spatially and temporally compared to an empirically based model. A mechanistic model often involves greater complexity, but is usually able to better describe the recruitment process (Forcella et al., 2000). Mechanistic models involve an understanding of the processes that regulate growth by establishing functional relationships between environmental factors and rates of the processes (Ghersa et al., 2000). Seedling emergence models that are based on mechanistic interpretations of biological significance include environmental factors that directly influence the recruitment process. Mechanistic models that simulate germination and seedling elongation in response to measured or estimated environmental factors are better able to describe the recruitment process than empirical models because they are based on identifiable and quantifiable environmental effects on each of the components of seedling recruitment (Forcella et al., 2000). Although most models involve elements of both empirical and mechanistic phenomena, as a greater number of pertinent environmental variables are integrated into a model, the model becomes more mechanistic in nature.

Seed germination is mainly controlled by temperature (Baskin and Baskin, 1989; Egley, 1995; Grundy and Mead, 2000), temperature fluctuation (Egley, 1986; Baskin and Baskin, 1990), and water potential (Hadas and Russo, 1974; Bradford, 1990), whereas seedling emergence is additionally controlled by recruitment depth (Mohler, 1993; Grundy and Mead, 1998). The seedling recruitment zone is a highly variable environment containing fluxes of temperature and water stratified at depth that is not easily modeled in

controlled environments. Controlled environment studies are often inadequate in simulating field conditions and seldom allow the study of conditions involving physical interactions in the soil environment. Despite variability in the field, seedling recruitment modeling is best suited to field conditions that represent the recruitment zone environment to accurately predict the timing and rate of seedling emergence under field conditions.

2.7.1 Thermal Time

Temperature is the principal environmental regulator of the timing of many plant processes including dormancy and germination of weed species (Garcia-Huidobro et al., 1982; Baskin and Baskin, 1987; Roberts, 1988; Egley, 1995; Grundy and Mead, 2000; Probert, 2000). Temperature is a recognized developmental principle for seedling recruitment because heat is required for the occurrence of biochemical reactions in germination and emergence. Temperature has a critical influence on seedling elongation and therefore determines seedling emergence in most species (Angus et al., 1981; Ellis et al., 1986; Roman et al., 1999). Thermal time is used to form the basis for seed germination models that predict the occurrence of seedling emergence during specific periods of time in the field.

Thermal time refers to the accumulation of heat above a minimum threshold (base) temperature as a function of time. The threshold temperature is the temperature below which germination does not occur. Thermal time emergence models can be represented by a continuous cumulative sigmoidal curve with soil thermal time as the independent variable (Brown and Mayer, 1988; Benech-Arnold et al., 1990; Forcella, 1998; Bullied et al., 2003). The percentage and rate of recruitment of a weed species increases as temperature rises above the minimum threshold required for germination for that species until the optimum germination temperature is reached (McGinnies, 1960; Garcia-Huidobro et al., 1982; Roché et al., 1997; Kruk and Benech-Arnold, 1998). Because germination of seeds occur within a species-specific temperature range, germination rate is temperature dependent.

Thermal time assumes that temperatures below the threshold temperature for a particular weed species are not adequate for the growth of that species. Threshold

temperatures for thermal time models have been developed for a number of weed species (Oryokot et al., 1997; Roché et al., 1997; Hardegree et al., 2002). Minimum threshold temperatures for shoot elongation are generally higher than for seed germination (Oryokot et al., 1997). Cardinal temperatures in germination thermal time models account for variability in the population response to temperature (Hardegree, 2006a). Cardinal temperatures can be assigned a constant value, or derived from normal distributions of cardinal values. Other methods in addition to cardinal temperature models are regression based models and statistical gridding that have been used to predict cumulative germination response to thermal time (Benech-Arnold et al., 1990; Roché et al., 1997; Hardegree, 2006a; Hardegree, 2006b). Under variable temperature conditions in the field, assumptions are often made regarding the relative germination rate of subpopulations despite current and prior temperature conditions (Garcia-Huidobro et al., 1982; Benech-Arnold et al., 1990; Hardegree, 2006b). Germination models may need to account for the response of seeds to temperature variability encountered under diurnal field conditions to have greater predictive accuracy (Hardegree et al., 1999; McDonald, 2002a; McDonald, 2002b; Hardegree, 2006b).

Soil temperatures during the early spring on the Canadian Prairies are generally lower than the optimum for germination of most species, with the onset and rate of recruitment of annual weed species being controlled by the accumulation of soil temperature. Because soil thermal accumulation during the spring is a major limitation to emergence timing, temperatures above the optimal for most species seldom occur.

Temperature was determined to be the dominant factor in predicting the emergence of five weed species in a long-term historical weed emergence study (Grundy and Mead, 2000). When water is not limiting, a thermal time model is used as a reasonable description of the relationship between thermal time and seedling emergence (Bullied et al. 2003; Leblanc et al., 2003; Lawson et al., 2006).

2.7.2 Hydrothermal Time

In addition to temperature, water is a critical factor that determines seed germination and seedling emergence because low water availability often limits seed germination in the field (Bradford, 1995; Kebreab and Murdoch, 1999; Finch-Savage et

al., 2000). Seeds are often subjected to fluctuations in the soil water and are closely attuned to the immediate hydric environment (Bradford, 1995). The concept of hydrotime is analogous to thermal time such that it expresses the rate of progress toward germination as a function of water potential (Gummerson, 1986; Bradford, 1990). At lower water potentials, advancement toward germination is progressively restricted. The progression to germination occurs due to the accumulation of time and reflects the differing lag periods from the start of imbibition until radicle emergence (Bradford, 1995).

The rate of germination as a function of water potential is a linear relationship with values having a similar slope but different intercepts on the water potential axis (Gummerson, 1986; Bradford, 1990). The hydrotime to germination is similar for all seeds of a population despite individual seeds having different lower threshold water potentials (Bradford, 2002). The threshold water potential values vary among seeds in a population in a Gaussian distribution, resulting in a relative frequency forming a normal bell curve (Gummerson, 1986; Bradford, 1990). When water potential approaches the threshold water potential, the germination percentage of seeds remains constant rather than increasing gradually over time as it does with low temperature (Bradford, 2002). As water potential decreases, the spread in time to germination between the first and last seeds of a population will progressively increase (Bradford, 1995). As water potential is reduced, final percentages of seed germination become progressively lower even with extended incubation. The effect of low water potential on percent germination differs from that of suboptimal temperatures above their base temperature in that viable seeds will eventually germinate after sufficient time (Bradford, 1995).

Hydrothermal time models predict seed germination by considering the effects of temperature and water potential simultaneously. Models that consider thermal time alone often underestimate time to germination and emergence because water potential inhibition on the progress to germination is omitted (Finch-Savage et al., 2000). Hydrothermal time describes the progress toward germination by integrating the interactions of temperature above a lower threshold temperature and water potential above a minimum threshold water potential into a single time function (Gummerson, 1986; Forcella et al., 1997; Bauer et al., 1998; Allen et al., 2000; Finch-Savage et al.,

2000; Bradford, 2002). Hydrothermal time curves for a given species can be generated for any temperature and water potential condition from known temperature and water potential minimum thresholds, standard deviation of the water potential threshold, and the hydrothermal time requirement for that species (Allen et al., 2000; Bradford, 2002). Hydrothermal time models enable prediction of both rate and percentage of germination (Gummerson, 1986; Dahal and Bradford, 1994; Grundy et al., 2000). The concept of hydrothermal time allows for a quantitative assessment of water availability and the rate and extent of germination beyond that which temperature alone may not be able to adequately quantify, especially in dry soil conditions. The hydrothermal time concept quantifies concurrent thermal and hydric environmental effects on seed dormancy, germination and seedling emergence (Gummerson, 1986; Bradford, 2002).

During the germination process, water availability is necessary for seed imbibition whereas temperature is related to embryo development (Bewley and Black, 1994). When water is limiting in the soil, the rate of seedling emergence is reduced and thermal time alone cannot adequately predict the process of seedling emergence (Bradford, 1990; Roman et al., 1999; Leguizamón et al., 2005). In the field, hydrothermal time models of seedling recruitment are based on all the processes that begin with microclimate and soil related inputs, and result in predictions of establishment and survival (Allen, 2003). Species-specific parameters for hydrothermal time modeling of germination enable emergence models to be constructed for variable environments such as fields with fluctuating temperatures and water potentials (Finch-Savage et al., 2000; Bradford, 2002). These types of emergence models allow seeds to accumulate hydrothermal time enabling progression toward germination and emergence according to the specified minimum temperature and water potential thresholds for a given species. Germination and emergence in black-grass was modeled with germination triggered by rain or tillage and driven by hydrothermal time, and pre-emergent shoot elongation increases occurred with thermal time (Colbach et al., 2006).

Hydrothermal time utilizes temperature and water potential thresholds that set limits below which seedling emergence does not occur, thus restricting the range of temperatures accumulated and increasing accuracy of the model. The application of hydrothermal time utilizes a threshold soil water potential to stop the temperature

accumulation when soil water potential is less than the soil water potential threshold and allows temperature accumulation to proceed when soil water potential is greater than the soil water potential threshold (Finch-Savage and Phelps, 1993; Forcella, 1998). The punctuated hydrothermal time approach predicts germination and emergence according to thermal time that is started and stopped depending on the water status of the soil. This approach of hydrothermal time enables an integrated representation of both soil water and soil temperature effects on emergence. A threshold model that allowed progress toward germination to be unaffected by soil water potentials above the base water potential was more accurate than laboratory experiments using thermal time or hydrothermal time (Finch-Savage et al., 2000). Thermal time alone underestimated the time to germination whereas hydrothermal time overestimated the time to germination. This suggested that seeds progressed towards germination faster in variable field conditions compared to laboratory experiments in constant temperature and water potential conditions (Finch-Savage et al., 2000).

Predictions of seedling emergence according to hydrothermal time in the field need to describe the reduction in germination rate that occurs at temperatures above the optimal temperature. Hydrothermal models that utilize all accumulated temperature above a minimum threshold are less accurate when temperatures are above the optimum for germination due to progressive inhibition of germination at increasingly supra-optimal temperatures (Alvarado and Bradford, 2002; Rowse and Finch-Savage, 2003). The interactive effect of temperature and water potential on the germinating seed results in a change in the threshold water potential as temperature varies. The upward shift in threshold water potential that occurs at temperatures above the optimum temperature accounts for the reduction in percentage and rate of germination (Rowse and Finch-Savage, 2003). Several studies have shown that temperatures above the optimum cause a shift in the distribution of the threshold water potential increasingly towards and above 0 MPa that causes progressive inhibition of germination (Kebreab and Murdoch, 1999; Bradford, 2002). Hydrothermal time models that utilize progressive thresholds have the potential to more accurately predict seed germination under variable field environments (Rowse et al., 1999; Rowse and Finch-Savage, 2003). Because errors in hydrothermal time models utilizing thresholds have the greatest impact in optimal environments during

rapid germination, the model requires accurate data fit near the optimum (Rowse and Finch-Savage, 2003). Germination rates in hydrothermal time generally have a positive linear relationship in suboptimal temperatures and a negative linear relationship in supra-optimal temperatures, with the convergence point defined as the optimal temperature (Covell et al., 1986; Bradford, 2002).

Soils during early spring can become too wet to allow seed germination to proceed. High soil water content levels during saturated or flooded conditions can also adversely affect seed germination and seedling emergence. The quality of soil air in saturated conditions results in rates of low oxygen and high carbon dioxide. Regulation of germination can occur as a result of oxygen taken into hydrated seed over time. Germination of wheat decreased to between 40 and 80% with duration of soaking in water for 7 days (Ueno and Takahashi, 1997). Relative emergence decreased to approximately 20% after 7 days flooding in *Bidens pilosa* (Reddy and Singh, 1992), *Diodia virginiana* (Baird and Dickens, 1991), and a flood-sensitive *Zea mays* inbred (Khosravi and Anderson, 1990). Dekker and Hargrove (2002) revealed an asymmetrical response of giant foxtail seed germination to incremental changes in oxygen concentration above and below that normally found in agricultural soils. Seed germination and the time to germination decreased with oxygen levels below 10% (Dekker and Hargrove, 2002). Currently, there are no emergence models that incorporate the effects of high soil water content (Forcella et al., 2000).

2.7.3 Recruitment Depth

The depth of burial of a seed in the soil profile influences both the probability of seedling emergence and the timing of emergence of that species (Roberts and Feast, 1972; Mohler, 1993; Grundy and Mead, 1998; Bullied et al., 2003; Grundy et al., 2003). Seeds are distributed throughout the soil profile by tillage leading to a characteristic vertical distribution of seeds in the seedling recruitment zone (Van Acker et al., 2004). The differential response of seeds depending on their vertical location in the soil profile requires modeling the depth of seed placement in order to quantify the recruitment process. The effect of burial depth on seedling emergence can be described by a quadratic model (Grundy et al., 2003).

Modeling the influence of depth of weed seed in the soil profile on seedling emergence requires either precision of placement of weed seeds into the soil (Wiese and Davis, 1967; Stoller and Wax, 1973a; Dawson and Bruns, 1962; Alm et al., 1993; Mohler and Galford, 1997; Grundy and Mead, 1998), or accurate measurement of seedling recruitment depth of natural seed populations in the field (Chancellor, 1964; Buhler and Mester, 1991; du Croix Sissons et al., 2000). Seedling recruitment depth is assessed by measuring the distance between the seed (if present), or the point of attachment to the seed, and the point along the hypocotyl located at the soil surface, which is usually marked by chlorophyll coloration (Chancellor, 1964).

The seedling emergence of downy brome, johnsongrass, and round-leaved mallow as influenced by burial depth, was adequately described by a Fermi-Dirac distribution function (Prostko et al., 1997). The Fermi-Dirac function serves as a mechanistic model containing parameters that are related to abiotic factors including soil texture, temperature and water content. The theoretical maximum emergence at the soil surface is controlled by soil temperature and water, which increases as temperature and water increases to an optimum. The depth at which the modeled emergence is 50% of the theoretical maximum is regulated by soil texture (Prostko et al., 1997). As soil clay content increased, model parameter values decreased, suggesting that less weed emergence occurs from deeper depths in fine textured soils. The emergence from different soil depths for large crabgrass, common lambsquarters (*Chenopodium album* L.), and redroot pigweed (*Amaranthus retroflexus* L.) were adequately characterized using the Fermi-Dirac distribution (Fu and Ashley, 1998).

2.8 Seedling Recruitment

2.8.1 Annual Weeds

A seed must undergo several steps in the recruitment process. Firstly, germination occurs as a result of suitable environmental conditions resulting in rapid metabolic activity within the seed embryo, with the radicle and aerial parts emerging from the testa. Secondly, elongation of the seedling from the soil depth, relying on stored energy reserves, and thirdly, emergence of the aerial parts through the soil surface. Soil environmental properties of temperature, water, compaction, soil texture, and soil

atmosphere composition may considerably modify the percentage and timing of seedling emergence from the soil. The interaction of these soil properties as well as the interaction of these soil properties with the depth of recruitment further influences the recruitment process.

Differences in environmental and soil properties relative to a hillslope position across field topography can result in numerous unique microclimates, which in turn influences weed recruitment in an uneven manner across a field. A close relationship exists between recruitment of a species and the immediate physical environment, including microclimate, soil, topography, and ground cover (Whitney, 1991; Dieleman et al., 2000a). The distribution and abundance of weed species may be selected according to suitable microsite characteristics such as temperature, water and nutrient status. Furthermore, germination of weed seeds is influenced by temperature, water, oxygen, and dormancy (Bibbey, 1935; Blackshaw et al., 2002). In a field situation, environmental factors of light, soil temperature, and soil water are often interrelated in their effect on seed germination (Egley, 1986). Weed species persevere by sensing their immediate environment, to break dormancy at the appropriate time, and to germinate in a preferred window of opportunity. Weed species can germinate over a period of several weeks if the proper soil stimulus for germination allows. Agricultural weeds that have a longer emergence period tend to be more formidable and often escape control.

2.8.1.1 Temperature Effects. All weed species have a range of temperatures over which germination can occur. Correct temperature conditions in the soil must occur for germination to begin (King, 1966; Stoller and Wax, 1973a). A relationship exists between accumulated heat units in the seedzone and the date of initial emergence for weeds (Stoller and Wax, 1973a). Each species of weed emerges in distinct flushes during periods of time during the season defined by thermal accumulation. Within a specific temperature range, the rates of germination and emergence of a species will increase with increasing temperature above a minimum threshold temperature. Temperature influences the timing of germination of weeds in the seedbank (Baskin and Baskin, 1989) and the time to emergence for many species can be shown to have a good relationship with accumulated soil temperature (Benech-Arnold et al., 1990; Oryokot et al., 1997; Roman et al., 2000; Bullied et al., 2003; Leguizamon et al., 2005).

During the early spring, soil temperatures are generally lower than the minimum temperature requirements for germination of most summer annual species. In temperate regions, evaporation from the seedbed is often desired to promote springtime soil warming for the planted crop. Germination of sorghum was delayed 2 to 5 days by early spring application of straw mulch at rates of 8 and 12 t ha^{-1} due to delays in temperature increases (Unger, 1978).

2.8.1.2 Fluctuating Temperature Effects. Fluctuating temperature effects on recruitment are influenced by the average daily temperature, the magnitude of the diurnal temperature fluctuation, and the species (Probert et al., 1986; Baskin and Baskin, 1990; Alm et al., 1993). Weed seed germination is often stimulated or enhanced by temperature fluctuations (Steinbauer and Grigsby, 1957; Probert et al., 1986; Benech-Arnold et al., 1990; Kegode et al., 1998; Chachalis and Reddy, 2000). The number of temperature fluctuations can also affect seed germination (Probert et al., 1986; Ekstam et al., 1999). A study of 85 weed species indicated that 80% had increased germination when exposed to alternating rather than constant temperatures (Steinbauer and Grigsby, 1957).

Reduced soil temperature fluctuation with depth in the soil profile may have partly caused the decrease in final emergence of velvetleaf seedlings with depth in the soil (Alm et al., 1993). Temperature fluctuation in the seedzone may be necessary to overcome seed dormancy in some species, but may not be optimal for seed germination and emergence, since large temperature fluctuations can expose seedlings to desiccation, freezing, or heat damage (Sheldon, 1974).

2.8.1.3 Water Potential Effects. A seed must imbibe water from the surrounding soil before germination can occur. Water uptake by a seed is influenced by seed properties, soil structure, soil water potential and seed–soil contact (Hadas and Russo, 1974; Hadas, 1982; Egley and Duke, 1985; Bewley and Black, 1994). Seed germination is influenced by soil water potential by the amount of aeration, hydraulic conductivity, and the area of seed–water contact (Dasberg and Mendel, 1971; Ward and Shaykewich, 1972). Soil water potential affects the tissue water potential of weed seeds thus also causing changes in their dormancy status (Khan and Karssen, 1980).

The rate of seed germination is often limited by low soil water potential (Bibbey, 1935; Bradford, 1990; Bewley and Black, 1994; Benech-Arnold and Sanchez, 1995).

After a rain, soil water potential reaches a maximum pressure, and then declines with time. Therefore, the maximum water potential that a seed reaches depends on the rate of water movement from the soil to the seed (Egley and Duke, 1985). Seed germination is not uniform over the range from field capacity to the wilting point for all species (Hunter and Erickson, 1952). Despite many species capable of germinating at very low water potentials, the rate and uniformity of germination is often compromised (Hunter and Erickson, 1952). When water potential of the soil is lower than that of the seed, water stress occurs due to water movement in the direction of decreasing water potential (Egley, 1986). The difference in water potential between seed and soil determines the rate of imbibition of water by germinating seeds (Egley, 1986).

Water uptake by dry seeds is a triphasic process. The first phase engages a rapid initial uptake (imbibition) of water, followed by the second phase that forms a plateau or lag period (Hegarty, 1978; Roberts and Ellis, 1989). The first phase is a physical process, whereas during the second phase, metabolic activity occurs within the seed (Bewley and Black, 1994). The third phase involves a further increase in water uptake after the embryo axis (radicle) elongates to complete the germination process. Low soil water potential reduces both the rate of imbibition and the final seed water content during the first phase, extends the length of the second phase, and delays the initiation of the third phase (Bradford, 1986; Bewley and Black, 1994). Imbibition characteristics also vary among species and can affect rates and levels of germination (Hunter and Erickson, 1952; Fan et al., 1961; Phillips, 1968; Shaykewich and Williams, 1971; Boyd and Van Acker, 2004b). Low soil water potential can delay seed germination and emergence, resulting in emergence occurring in flushes (Hegarty, 1977). Water level that is sufficient for seed imbibition but too low for radicle emergence from the testa was found to reduce emergence in soybean (Helms et al., 1996a). The duration of the second phase in water uptake can also be lengthened by low or high temperatures (Bradford, 1990).

Some soil properties can influence weed recruitment by means of influencing the water status of the soil. Soil types with high organic matter content are generally moist and poorly drained. Organic matter was determined to be indirectly linked to weed occurrence through its relation to soil water holding capacity (Andreasen et al., 1991; Hudson, 1994).

Disturbances can create favorable microsite conditions for recruitment. Aguileara and Lauenroth (1995) determined that the positive effect of bare soil microsites on the emergence of *Bouteloua gracilis* was associated with higher soil water levels in the upper 5 cm. The influences of microsite are often greater on seed germination and emergence than on seedling survival (Wood and Morris, 1990).

Soil humidity has biological importance since water vapor affects the internal water potential of seeds by influencing the rate at which water is imbibed by seeds (Bruckler, 2003). The soil atmosphere is close to 100% relative humidity at soil water potentials between field capacity and −1.0 MPa (Papendick and Campbell, 1981). At this range of normal water potential variation, vapor flux is influenced to a lesser extent compared to liquid flux. The importance of vapor transport for germinating seeds was affirmed in a study of soil contact area with seed in different soil textures, water potentials, and bulk densities (Rogers and Dubetz, 1980). Wheat seed was shown to germinate at greater than 70% when surrounding relative humidity was 98.5% (Owen, 1952). Seed–soil contact is attributed to soil packing of field implements in different field conditions at seeding time resulting in differences in vapor loss from the seed zone (Choudhary and Baker, 1982). Water vapor transport from soil to seed is critical in the germination process, contributing to 85% of water absorbed by seed in seed–soil contact (Wuest, 2002). In a closely packed soil, the wetted area of seed in a very moist soil at −0.05 MPa water potential was estimated to be only 13.2%, exposing most of the seed surface to the soil atmosphere (Collis-George and Hector, 1966).

Water absorption by seeds is related to seed size. Because diffusivity does not vary greatly among seeds (Becker, 1960; Fan et al., 1961; Phillips, 1968), larger seeds will have a lower water content compared to small seeds. The rate of germination will therefore be slower for larger seeds since it takes longer for larger seeds to imbibe sufficient water for germination to occur.

Excessive water levels in the soil can reduce seedling emergence (Heydecker, 1962; Forcella et al., 2000; Boyd and Van Acker, 2004b). At high soil water contents, the oxygen concentration in soil is reduced since water displaces air, and the ratio of carbon dioxide to oxygen increases due to continued respiration of soil organisms (Wild, 1988). In saturated soils, lower oxygen diffusion rates can inhibit seed germination and seedling

emergence due to a lack of the oxygen required to produce energy for seedling development (Dasberg and Mendel, 1971; Egley and Duke, 1985). The duration of flooding in a soil is closely related to reduced germination and emergence of seedlings (Martin et al., 1991; Begum et al., 2006). Anoxic conditions in saturated soil can prolong seed dormancy, or induce secondary dormancy in some weed seeds (Murdoch and Ellis, 1992; Qi and Upadhyaya, 1993).

High water content in a soil was found to have a large impact on wild oat seed mortality due to the existence of greater pathogenic soil microorganism activity. As water content increased from 6 to 24%, wild oat seedling mortality increased from 36 and 15% in each of two years to 55% (Mickelson and Grey, 2006). Possibly for similar reasons, Harker et al. (2005) and DeCorby et al. (2007) found that volunteer wheat seeds persisted longer in the less humid regions of western Canada.

2.8.1.4 Temperature and Water Interaction Effects. Seedling recruitment is often influenced by the interaction of environmental factors. The interaction of properties of the soil environment on seedling recruitment is complex when coupled with the diverse characteristics of seeds under field conditions (Dieleman et al., 2000b; Vleeshouwers and Kropff, 2000). Germination of weed seeds can be influenced by magnitude and fluctuations in soil temperature and soil water (Baskin and Baskin, 1985; Egley, 1986). Both water and temperature are essential elements for germination and emergence and need to be considered concurrently (Wilson and Hottes, 1927; Sharma, 1976). Soil environmental conditions that are appropriate for seed germination are generally short lived, and therefore germination is often limited by one or more factors (Egley and Williams, 1991; Mulugenta and Boerboom, 1999).

Seed germination is driven by both temperature and water potential, whereas radicle and shoot elongation are driven primarily by temperature (Angus et al., 1981; Gummerson, 1986; Fyfield and Gregory, 1989; Dahal and Bradford, 1994; Roman et al., 1999). Fluctuation of diurnal temperatures and availability of soil water are the primary environmental factors that stimulate and drive the germination of many weed seeds (Hadas, 1982; Ghersa et al., 1992).

The interaction of soil temperature and soil water has been noted in the literature (Sharma, 1976; Helms et al., 1996b; Roman et al., 1999; Shrestha et al., 1999). Soil water

content was found to interact with temperature to decrease seedling development and emergence of soybean when soil temperature increased and water was sufficient for imbibition but insufficient to allow the radicle to emerge from the testa (Helms et al., 1996b). At temperatures optimum for germination, *Orobanches aegyptiaca* seeds will germinate at lower water potential (Kebreab and Murdoch, 1999). The thermal time to germination is modified by the water potential status (Kebreab and Murdoch, 1999). Alternating wetting and drying of soil during alternating temperatures resulted in dormancy breaking of *Rumex crispus* seeds whereas the same treatments at constant temperatures did not (Vincent and Cavers, 1978). Dormancy breaking of redroot pigweed and barnyardgrass (*Echinochloa crus-galli* L.) by alternating temperatures occurred only when soil water content was sufficiently high for germination to occur (Martinez-Ghersa et al., 1997). Environmental stresses such as extreme soil temperature and low soil water can restrict the germination and emergence of many weed species. Although fluctuating soil temperatures are often a requirement for dormancy breaking and germination to begin, microsites with the greatest temperature fluctuation are located at the soil surface where the evaporation and soil drying occurrence is greatest. Modeling seedling emergence in hydrothermal time takes into account the interactive effect of soil temperature and soil water by simultaneously accounting for the effect of each soil property as influenced by the other.

2.8.1.5 Recruitment Depth Effects. Soil disturbance is the primary cause for the vertical movement of weed seeds (including volunteer wheat) within a soil profile (Pareja et al., 1985; Cousens and Moss, 1990; Staricka et al., 1990; Mohler and Galford, 1997). Burial and dispersal of seeds into favorable microsites occurs within the soil profile during tillage operations (Van Acker et al., 2004; Reid and Van Acker 2005). Differences in the depth of seedling recruitment occur due to soil disturbance events affecting the competitive ability of a species (du Croix Sissons et al., 2000). Egley and Williams (1990) determined that when weed seeds were added to soil, the majority of seeds remained at or near the soil surface and germinated during the first year in no-tillage plots, whereas many weed seeds in tilled plots were moved to locations at depth that were unfavorable for germination. Similarly, Reid and Van Acker (2005) found that a single

tillage pass was sufficient to significantly increase the recruitment of *Galium* species by placing seeds into a favorable microsite of moist soil and darkness.

Information on the depth of weed seedling recruitment and the potential emergence of a species from a given depth in the soil profile is critical to predict the probability of seedling emergence. Sample collection of soil cores from the vertical seedling recruitment zone are frequently bulked and important spatial information is lost when averaging of the vertical seed distribution occurs (Dessaint et al., 1991). Many seedling recruitment models do not include the distribution of seed depth in the soil profile as a component of the recruitment model (Harvey and Forcella, 1993; King and Oliver, 1994; Myers et al., 2004; Leguizamón et al., 2005; Rinaldi et al., 2005; Page et al., 2006).

The ability of weed seeds to germinate and the rate of emergence of weed seedlings from the soil is a function of depth of seed burial within the vertical seed bank (Mohler, 1993). The percentage of weed seedling emergence has been shown to decrease continuously with depth of seed burial (Roberts and Feast, 1972; Froud-Williams et al., 1983; Dyer, 1995; Grundy et al., 1996; Boyd and Van Acker, 2003; Mennan and Zandstra, 2006). Others have found that weed seedling emergence increased with shallow burial and then decreased with greater depth in the soil profile (Wiese and Davis, 1967; Wicks et al., 1971; Grundy et al., 1996; Mohler and Galford, 1997; Ghorbani et al., 1999). Webster et al. (1998) determined that cumulative emergence of velvetleaf decreased with soil depth in a no-till environment whereas emergence was not influenced by depth in a tilled system. The emergence rate of weeds, in addition to emergence percentages, also decreases with increasing depth of burial in the soil (Benvenuti et al., 2001; Cussans et al., 1996; Vleeshouwers, 1997). Weed seedling emergence of several species formed a sigmoidal relationship that declined with soil depth (Benvenuti et al., 2001). Generally, weed emergence decreased exponentially with increasing burial depth below an optimum burial depth (Benvenuti et al., 2001; Grundy et al., 1996; Mohler and Galford, 1997).

The decrease in emergence for seeds located on the soil surface may be due to reduced seed–soil contact and lower soil water potential adjacent to the seed. Seeds located at the soil surface may not germinate during dry years, or may be slower to

germinate during dry periods. Seeds on the soil surface may not imbibe sufficient water to complete the germination process and the onset of desiccation after initiation of embryo growth can cause seedling mortality (Hegarty, 1978; McKersie and Tomes, 1980; Senaratna and McKersie, 1983; Debaene-Gill et al., 1994). Exposure and slow germination may render seeds vulnerable to loss of viability and mortality due to attack by microorganisms and predators (Brenchley and Warrington 1930; Taylorson, 1970; Lund and Turpin, 1977; Pitty et al., 1987; Westerman et al., 2003; Greenfield, 2000; DeCorby et al., 2007). Microbial community composition and weed seed mortality have been shown to be correlated (Kremer, 1993; Davis et al., 2006). Microsites favoring seed germination may not be optimal for seedling survival since the environmental conditions that promote seed germination can also support microbial attack and seed predation (Sheldon, 1974; Schupp, 1995).

The environment across field topography is dynamically influenced by climatic factors according to underlying soil physical and chemical properties (Sheldon, 1974). Conditions may become more or less conducive to germination for seeds located at or near the soil surface. Seeds located near the soil surface undergo greater changes in relative dormancy and decreased duration of viability than deeper placed seeds, whereas burial provides protection for seeds, which retain viability longer (Roberts, 1964; Taylorson, 1987).

Many weed species favor alternating rather than constant temperatures for germination (Probert et al., 1986; Kegode et al., 1998; Chachalis and Reddy, 2000). Greater extremes of temperature and water fluctuations encountered near the soil surface affect changes in relative dormancy and initiation of germination. Weed species requiring greater amplitudes of temperature fluctuation are generally more responsive near the soil surface where temperature fluctuations are greater than at microsites deeper within the seedling recruitment zone (Thompson and Grime, 1983; Kegode et al., 1998). Ghorbani et al. (1999) observed a significant interaction between soil type and planting depth of *A. retroflexus* seed emergence, with a greater emergence in sandier soils compared to clay soils. The decrease in emergence of *A. retroflexus* in clay soils was attributed to poor gas exchange, less light, and lower temperatures (Ghorbani et al., 1999). Emergence of *Bromus tectorum* was greater, and occurred from deeper depths, in coarse textured soils

compared to fine textured soils when water was not limiting (Wicks et al., 1971). Others have observed soil texture influences on the depth of seed burial, with the rate and extent of emergence being greater in coarser textured and well aggregated soils than in fine textured and poorly aggregated soils (Benvenuti 2003; Buhler and Mester 1991; Mohler and Galford 1997).

Most small seeded weed species germinate within a few centimeters of the soil surface (Chancellor, 1964; Wiese and Davis, 1967; Wicks et al., 1971; Froud-Williams et al., 1984; du Croix Sissons et al., 2000). The optimum depth of sixteen arable weed species was determined to be from 0–70 mm (Froud-Williams et al., 1984). Chancellor (1964) determined that 98% of seedlings of 18 common weed species measured originated from less than 5 cm depth. The maximum mean recruitment depth for five annual weed species measured across species, tillage and time was 42 mm (du Croix Sissons et al., 2000). Seeds of *Chenopodium album* and *Amaranthus retroflexus* had greater emergence with shallow burial, but emergence decreased exponentially with depth (Mohler and Galford, 1997). There is often an absence of germination from lower depths in the soil profile caused by the lack of appropriate microsite properties. Microsites at depth lack light, appropriate temperature and water regimes, and sufficient oxygen for germination of seeds (Murdoch and Ellis, 1992; Pareja and Staniforth, 1985; Reuss et al., 2001; Boyd and Van Acker, 2003). Seeds that do germinate at depth may not emerge or establish successfully due to resource exhaustion and may be competitively weak or succumb to fungal attack. Small seeded vegetable crops were found to have optimal emergence from shallow sowing depths of 15–25 mm, however emergence rates declined with increased or reduced depths (Heydecker, 1956).

After seeds germinate, the seedlings must elongate to reach the surface of the soil utilizing stored reserves in the seed to provide the only available energy source. The deeper a seed is located within the seedling recruitment zone, the greater the reserves that are required for emergence since sufficient stored food reserves are required to enable the seedling to reach the soil surface. If the seed is too deep, that is, if the energy reserves are insufficient for the seedling coleoptile or hypocotyl elongation, pre-emergence mortality occurs. Pre-emergence seedling mortality has been shown to increase with soil dryness, clod size and seed depth in the soil (Prostko et al., 1998; Grundy et al., 2003; Colbach et

al., 2006). Generally, weed species with small seeds have better emergence from very shallow soil depths compared to species with larger seeds. Large seeds located at the soil surface are exposed to greater risk of dehydration since greater time is required to imbibe water for germination to occur compared to buried or smaller seeds (Buhler, 1995; Boyd and Van Acker, 2004a). Emergence patterns of large seeded species tend to exhibit parabolic relationships with depth of burial in the soil whereas small seeded species often exhibit logarithmic decreases in emergence with depth (Buhler, 1995; Forcella et al., 1996; Grundy et al., 1996; Forcella et al., 2000; Grundy et al., 2003). Benvenuti et al. (2001) observed a close inverse relationship between seed weight and depth-mediated inhibition to emergence. The number of weed seedlings and rate of seedling emergence decreased with an increase in the depth of seed burial (Benvenuti et al., 2001).

2.8.1.6 Other Soil Properties Effects. Properties of the soil such as soil texture can impose physical limitations to seedling emergence by creating resistance for the seedling as it penetrates the soil. More likely, soil type influences germination and emergence by affecting thermal and water conductivity and holding capacity.

The distribution of 37 common weed species in response to seven edaphic factors was evaluated in Danish fields to determine explanatory variables that influenced the occurrence of the weed species (Andreasen et al., 1991). Clay content generally had the greatest influence on the occurrence of the weed species investigated, however all edaphic factors including organic matter, pH, P, K, Mg, and Mn were associated with the occurrence of specific weed species (Andreasen et al., 1991). Site properties such as topography, soil texture, and soil fertility have been shown to affect weed species abundance (Dieleman et al., 2000a; Dieleman et al., 2000b). A hypothesized mechanism for weed patchiness included the variability in available soil water that affected weed seed germination and emergence (Dieleman et al., 2000b).

2.8.2 Volunteer Wheat

The emergence of volunteer wheat can be difficult to predict due to the influence of interactions of soil temperature, water potential, and depth of recruitment. The emergence rate of wheat is generally reduced with a decrease in temperature below 25ºC (Peterson, 1965; Khah et al., 1986; Lafond and Baker, 1986), a decrease in water

potential (Owen, 1952; Hanks and Thorp, 1956; Gan et al., 1996), or an increase in recruitment depth (Lindstrom et al., 1976; Gan et al., 1992; Kirby, 1993; Gan and Stobbe, 1995).

The rate of germination of wheat has been shown to be linearly related to temperature (Lindstrom et al., 1976; Khah et al., 1986; Lafond and Baker, 1986; Addae and Pearson, 1992). Wilson and Hottes (1927) found little difference in wheat germination between 10ºC and 15ºC, whereas higher temperatures of 20ºC and 30ºC increased the rate but not the completeness of germination. This phenomenon was attributed to higher temperatures that increased germination of wheat but also increased soil microbial activity. Germination percentage was reduced at the higher temperatures due to optimal conditions for fungal activity and susceptibility of the wheat seeds to fungal attack (Wilson and Hottes, 1927). Chopra and Chaudhary (1981) concluded that wheat seedling emergence was earlier at 25ºC compared to 20ºC, however a temperature of 20ºC was more favorable than 25ºC for total emergence. Reducing the temperature from 20ºC to 15ºC caused a 12 hour delay in time to reach 50% germination in wheat (Blackshaw et al., 1981). Similarly, the time of emergence for wheat was delayed by one day when temperature was reduced from 22ºC to 14ºC (Blackshaw et al., 1981).

Temperature effects on wheat emergence are due to influences on the rate of seedling elongation. The rate of coleoptile elongation for wheat increases linearly with temperature between 5 and 25ºC (Addae and Pearson, 1992), with the maximum rate of coleoptile elongation occurring between 15 and 21ºC (Bhatt and Qualset, 1976; Radford, 1987). The rate of wheat seedling emergence is limited outside of the preceding temperature range.

Low soil water potential can delay the initiation of germination, increase the time to germination among seeds, or decrease the final germination percentage (Lindstrom et al., 1976; Naylor and Gurmu, 1990). The effect of water potential on wheat germination percentage can be indicated by a time relation curve. A decrease in soil water potential increases the time to germination and decreases the uniformity of germination (Ward and Shaykewich, 1972; Lindstrom et al., 1976). Wheat seeds initially imbibe water rapidly in saturated conditions by capillary imbibition causing the pericarp to saturate (Becker, 1960; Fan et al., 1961). Subsequent absorption of water by the seed is directly

proportional to the square root of the immersion time (Becker, 1960; Fan et al., 1961). Germination and emergence rates for wheat are progressively delayed as the soil water potential decreases from field capacity, still germination percentage is not affected until soil water potential approaches the threshold (Owen, 1952; Hanks and Thorp, 1956; El-Sharkawi and Springuel, 1977). Wheat germination was shown to have a wide adaptation to varying water conditions, with good results with a water content of 50% saturation (Wilson and Hottes, 1927). Wheat seed must reach a critical water content of approximately 0.27 kg kg^{-1} for germination to occur (Bouaziz and Bruckler, 1989a). The rate of water uptake for eight wheat varieties ranged from 0.11 to 0.16 g h^{-1} $plate^{-1}$ (Clarke, 1980).

The germination and emergence of wheat requires progressively greater heat accumulation as soil water potential is lowered from field capacity (McGinnies, 1960; Lindstrom et al., 1976). Wheat germination was delayed 72 to 82 hours at temperatures of 15, 20 and 25ºC when soil water potential was lowered from 0 to −1.5 MPa (Blackshaw et al., 1981). Wheat germination took approximately twice as long at a soil water potential of −1.5 MPa compared to −0.8 MPa (Pawloski and Shaykewich, 1972). De Jong and Best (1979) determined that the cumulative heat required for wheat to reach 50% emergence did not increase significantly with decreasing soil water potential indicating that there was compensation for adverse soil water conditions by lowering the minimum temperature requirement for emergence. Pawloski and Shaykewich (1972) found little effect on the germination rate with decreasing water potentials to −0.8 MPa. Under conditions of low water potential, optimum temperatures generally produce more rapid germination than temperatures above or below the optimal. The threshold soil water potential for emergence of wheat increases with increasing temperature (Lindstrom et al., 1976; El-Sharkawi and Springuel, 1977). Water potential generally has an increasingly greater effect on germination and emergence as temperature diverges from the optimum (McGinnies, 1960).

Emergence defined by appearance of the plumule is generally more sensitive to water stress compared to germination defined by appearance of the radicle (El-Sharkawi and Springuel, 1977; Naylor and Gurmu; 1990). Plumule emergence is a critical phase in seedling emergence since germination is not complete at the onset of radicle emergence.

Plumule emergence was minimal at −0.9 MPa water potential and was considered to be the lower water potential threshold for wheat germination at temperatures ranging between 15 and 34ºC (El-Sharkawi and Springuel, 1977). The emergence rate index for wheat that accounts for both rate and total emergence decreased when soil water potential was lowered from −0.5 MPa to −1.0 MPa, was attributed to a decrease in emergence rate but not total emergence (Chopra and Chaudhary, 1981). Wheat reached a shoot length of 100 mm in 5 days at soil water potentials of −0.02 to −0.17 MPa, whereas 10 days were required at a soil water potential of −1.31 MPa (Bouaziz and Bruckler, 1989b). The lowest soil water potential that wheat could germinate was determined to be −1.0 MPa (Lindstrom et al., 1976), −1.1 MPa (Wuest et al., 1999), and −1.5 MPa (Owen, 1952). No germination occurred at −2.0 MPa (Lindstrom et al., 1976), −2.3 MPa (Wuest et al., 1999), and −3.0 MPa (Chopra and Chaudhary, 1981). Because germination is not considered the limitation in field emergence, subsurface elongation of wheat is more practically affected by a lower limit of −0.7 MPa (Lindstrom et al., 1976) to −0.9 MPa (El-Sharkawi and Springuel, 1977).

The median germination time for wheat emergence was increased over 50% at both 10ºC and 20ºC when osmotic water potential was lowered from 0 to −0.8 MPa (Lafond and Baker, 1986). Germination time for wheat ranged from 1.1 d at −0.15 MPa at 28ºC to 18.3 d at −1.1 MPa at 3ºC (Wuest et al., 1999). Gan et al. (1996) modeled an increase in median germination time for wheat emergence with durations of 5, 6, and 9 days with water potentials of −0.165, −1.00, and −1.45 MPa, respectively. Wuest et al. (1999) observed a temperature by water interaction for wheat germination where the driest (−1.1 MPa) treatment required 2 days longer than soil water treatments of −0.57, −0.29, and −0.15 MPa at 28ºC, but took 6 days longer than the three wetter treatments at 3ºC. The effect on germination timing by soil water levels greater than −1.1 MPa was determined to be similar at a given temperature (Wuest et al., 1999). Temperature differences ranging from 5 to 30 C have been shown to have a large effect on the rate of water uptake by wheat seed and germination rate (Lafond and Fowler, 1989). An increase in temperature increased the rate of water uptake which decreased germination time from 6.9 d at 5ºC to 0.9 d at 25ºC and 30ºC (Lafond and Fowler, 1989).

Seedling emergence models for wheat generally assume an optimal recruitment depth of 30 to 50 mm with a constant thermal time to seedling emergence (Weir et al., 1984; Reinink et al., 1986). Increasing the planting depth for spring wheat resulted in decreased seedling emergence rate and total emergence (Hadjichristodoulou et al., 1977; Chopra and Chaudhary, 1981; Gan et al., 1992). Chopra and Chaudhary (1981) found that emergence of wheat seedlings were more sensitive to depths of 60 mm and 90 mm than a depth of 30 mm, especially at lower soil water potential of −1.0 MPa compared to −0.5 MPa. A linear response based on 50% wheat seedling emergence to planting depth occurred for wheat, with the highest establishment occurring at the 68 mm depth (Kirby, 1993). Seedling establishment was not affected between 23 and 83 mm depths, but decreased sharply at shallower and deeper depths (Kirby, 1993). An increase in planting depth from 25 mm to 75 mm caused an increase in inflection time, along with corresponding decreases in maximum emergence rate and cumulative percent emergence (Gan et al., 1992). Maximum emergence rate for wheat from a 25 mm depth was reached 1 to 2 days prior to a 50 mm depth and 2 to 3 days prior to a 75 mm depth (Gan et al., 1992). The decrease in emergence of spring wheat planted at greater depths can be attributed to an increase in the heat requirement for emergence (De Jong and Best, 1979). Variability in emergence at increased planting depths was also attributed to greater heat requirement for emergence (De Jong and Best, 1979). Soil type has an influence on wheat emergence as total emergence for wheat was better in medium textured loam soils compared to fine textured clay soil for all recruitment depths (Hadjichristodoulou et al., 1977).

Variation in the time to emergence can be minimized by seedlings emerging through a shallow soil depth from larger seeds containing greater storage reserves. Wheat seedlings from large seeds (45 to 53 mg kernel^{-1}) emerged earlier compared to those from small seeds (22 to 25 mg kernel^{-1}) at identical depths (Hadjichristodoulou et al., 1977). Emergence from the large seeds also provided better establishment than from the small seeds, especially as emergence depth was increased greater than 50 mm (Hadjichristodoulou et al., 1977). Larger wheat seed size averaging 40 mg kernel^{-1} has superior ability to emerge from depths of greater than 50 mm compared to seed size averaging 30 mg kernel^{-1} (Gan et al., 1992; Ueno et al., 1999).

2.9 References

Aase, J.K., and D.L. Tanaka. 1987. Soil water evaporation comparisons among tillage practices in the northern Great Plains. Soil Sci. Soc. Am. J. 51:436–440.

Abu-Hamdeh, N.H. and R.C. Reeder. 2000. Soil thermal conductivity: Effects of density, moisture, salt concentration, and organic matter. Soil Sci. Soc. Am. J. 64:1285–1290.

Adams, J.E., G.F. Arkin, and J.T. Ritchie. 1976. Influence of row spacing and straw mulch on first stage drying. Soil Sci. Soc. Am. J. 40:436–442.

Addae, P.C. and C.J. Pearson. 1992. Thermal requirements for germination and seedling growth of wheat. Aust. J. Agric. Res. 43:585–594.

Afyuni, M.M., D.K. Cassel, and W.P. Robarge. 1993. Effect of landscape position on soil water and corn silage yield. Soil Sci. Soc. Am. J. 57:1573–1580.

Aguilera, M.O. and W.K. Lauenroth. 1995. Influence of gap disturbances and type of microsites on seedling establishment in *Bouteloua gracilis*. J. Ecol. 83:87–97.

Allen, P. 2003. When and how many? Hydrothermal models and the prediction of seed germination. New Phytol. 158:1–9.

Allen, P.S., D.B. White, and A.H. Markhart III. 1993. Germination of perennial ryegrass and annual bluegrass seeds subjected to hydration-dehydration cycles. Crop Sci. 33:1020–1025.

Allen, P.S., S.E. Meyer, and M.A. Khan. 2000. Hydrothermal time as a tool in comparative germination studies. p. 401–410. In M. Black et al. ed. Seed biology: Advances and applications. Proc. 6th Int. workshop on seeds, Mérida, Mexico.

Alm, D.M., E.W. Stoller, and L.M. Wax. 1993. An index model for predicting seed germination and emergence rates. Weed Technol. 7:560–569.

Alvarado, V. and K.J. Bradford. 2002. A hydrothermal time model explains the cardinal temperatures for seed germination. Plant Cell Environ. 25:1061–1069.

Andreasen, C., J.C. Streibig, and H. Haas. 1991. Soil properties affecting the distribution of 37 weed species in Danish fields. Weed Res. 31:181–187.

Ångström, A. 1925. The albedo of various surfaces of ground. Geografiska Annaler. 7:323–342.

Angus, J.F., R.B. Cunningham, M.W. Moncur, and D.H. Mackenzie. 1981. Phasic development in field crops. I. Thermal response in the seedling phase. Field Crops Res. 3:365–378.

Bach, L.B. 1992. Soil water movement in response to temperature gradients: Experimental measurements and model evaluation. Soil Sci. Soc. Am. J. 56:37–46.

Baird, J.H. and R. Dickens. 1991. Germination and emergence of Virginia buttonweed (*Diodia virginiana*). Weed Sci. 39:37–41.

Bàrberi, P. and B. Lo Cascio. 2001. Long-term tillage and crop rotation effects on weed seedbank size and composition. Weed Res. 41:325–340.

Baskin, J.M. and C.C. Baskin. 1985. The annual dormancy cycle in buried weed seeds: A continuum. Bioscience. 35:492–498.

Baskin, J.M. and C.C. Baskin. 1987. Environmentally induced changes in the dormancy states of buried weed seeds. p. 695–706. In Proc. British Crop Protection Conf. – Weeds, 16–19 Nov. 1987. Brighton, UK.

Baskin, J.M. and C.C. Baskin. 1989. Role of temperature in regulating timing of germination in soil seed reserves of *Thlaspi arvense* L. Weed Res. 29:317–326.

Baskin, J.M. and C.C. Baskin. 1990. The role of light and alternating temperatures on germination of *Polygonum aviculare* seeds exhumed on various dates. Weed Res. 30:397–402.

Bathke, G.R. and D.K. Cassel. 1991. Anisotropic variation of profile characteristics and saturated hydraulic conductivity in an Ultisol landscape. Soil Sci. Soc. Am. J. 55:333–339.

Battaglia, M. and J.B. Reid. 1993. The effect of microsite variation on seed germination and seedling survival of *Eucalyptus delegatensis*. Aust. J. Bot. 41:169–181.

Bauer, M.C., S.E. Meyer, and P.S. Allen. 1998. A simulation model to predict seed dormancy loss in the field for *Bromus tectorum* L. J. Exp. Bot. 49:1235–1244.

Baver, L.D. 1940. Soil physics. John Wiley and Sons, Inc., New York.

Becker, H.A. 1960. On the absorption of liquid water by the wheat kernel. Cereal Chem. 37:309–323.

Begum, M., A.S. Juraimi, R. Amartalingam, A. Bin Man, and S.O. Bin Syed Rastans. 2006. The effects of sowing depth and flooding on the emergence, survival, and growth of *Fimbristylis miliacea* (L.) Vahl. Weed Biol. Manage. 6:157–164.

Bell, K.R., B.J. Blanchard, T.J. Schmugge, and M.W. Witczak. 1980. Analysis of surface moisture variations within large field sites. Water Resour. Res. 16:796–810.

Benech-Arnold, R.L. and R.A. Sanchez. 1995. Modelling weed seed germination. p. 545–566. In J. Kigel and G. Galili ed. Seed development and germination. Marcel Dekker, New York.

Benech-Arnold, R.L., C.M. Ghersa, R.A. Sanchez, and P. Insausti. 1990. A mathematical model to predict *Sorghum halepense* (L.) Pers. seedling emergence in relation to soil temperature. Weed Res. 30:91–99.

Benvenuti, S. 2003. Soil texture involvement in germination and emergence of buried weed seed. Agron. J. 95:191–198.

Benvenuti, S., M. Macchia, and S. Miele. 2001. Quantitative analysis of emergence of seedlings from buried weed seeds with increasing soil depth. Weed Sci. 49:528–535.

Bewley, J.D. and M. Black. 1994. Seeds: Physiology of development and germination. 2nd ed. Plenum Press, New York.

Bhatt, G.M. and C.O. Qualset. 1976. Genotype–environment interactions in wheat: Effect of temperature on coleoptile length. Exp. Agric. 12:17–22.

Bibbey, R.O. 1935. The influence of environment upon the germination of weed seeds. Sci. Agric. 15:141–150.

Blackshaw, R.E., R.N. Brandt, and T. Entz. 2002. Soil temperature and soil water effects on henbit emergence. Weed Sci. 50:494–497.

Blackshaw, R.E., E.H. Stobbe, C.F. Shaykewich, and W. Woodbury. 1981. Influence of soil temperature and soil moisture on green foxtail (*Setaria viridis*) establishment in wheat (*Triticum aestivum*). Weed Sci. 29:179–184.

Bond, J.J., and W.O. Willis. 1969. Soil water evaporation: Surface residue rate and placement effects. Soil Sci. Soc. Am. Proc. 33:445–448.

Bond, J.J., and W.O. Willis. 1970. Soil water evaporation: First stage drying as influenced by surface residue and evaporation potential. Soil Sci. Soc. Am. Proc. 34:924–928.

Bouaziz, A. and L. Bruckler. 1989a. Modeling of wheat imbibition and germination as influenced by soil physical properties. Soil Sci. Soc. Am. J. 53:219–227.

Bouaziz, A. and L. Bruckler. 1989b. Modeling wheat seedling growth and emergence: I. Seedling growth affected by soil water potential. Soil Sci. Soc. Am. J. 53:1832–1838.

Boyd, N.S. and R.C. Van Acker. 2003. The effects of depth and fluctuating soil moisture on the emergence of ten annual and five perennial weed species. Weed Sci. 51:725–730.

Boyd, N. and R. Van Acker. 2004a. Seed and microsite limitations to emergence of four annual weed species. Weed Sci. 52:571–577.

Boyd, N.S. and R.C. Van Acker. 2004b. Imbibition response of green foxtail, canola, wild mustard and wild oat to different osmotic potentials. Can. J. Bot. 82:801–806.

Boyer, D.G., R.J. Wright, W.M. Winant, and H.D. Perry. 1990. Soil water relations on a hilltop cornfield in central Appalachia. Soil Sci. 149:383–392.

Bradford, K.J. 1986. Manipulation of seed water relations via osmotic priming to improve germination under stress conditions. HortScience. 21:1105–1112.

Bradford, K.J. 1990. A water relations analysis of seed germination rates. Plant Physiol. 94:840–849.

Bradford, K.J. 1995. Water relations in seed germination. p. 351–396. In J. Kigel and G. Galili ed. Seed development and germination. Marcel Dekker Inc., New York.

Bradford, K.J. 2002. Application of hydrothermal time to quantifying and modeling seed germination and dormancy. Weed Sci. 50:248–260.

Brady, N.C. and R.R. Weil. 2002. The nature and properties of soils. 13th ed. Prentice-Hall, Upper Saddle River, NJ.

Brenchley, W.E. and K. Warrington. 1930. The weed seed population of arable soil. I. Numerical estimation of viable weed seeds and observations on their natural dormancy. J. Ecol. 18:235–272.

Bristow, K.L. 1988. The role of mulch and its architecture in modifying soil temperature. Aust. J. Soil Res. 26:269–280.

Bronstert, A. 1999. Capabilities and limitations of detailed hillslope hydrological modelling. Hydrol. Processes. 13:21–48.

Brooks, R.H. and A.T. Corey. 1964. Hydraulic properties of porous media. Colorado State Univ. Hydrol. Paper 3:1–27.

Brown, R.F. and D.G. Mayer. 1988. Representing cumulative germination. 2. The use of the Weibull function and other empirically derived curves. Ann. Bot. 61:127–138.

Brubaker, K.L., and D. Entekhabi. 1996. Analysis of feedback mechanisms in land–atmosphere interaction. Water Resour. Res. 32:1343–1357.

Brubaker, S.C., A.J. Jones, D.T. Lewis, and K. Frank. 1993. Soil properties associated with landscape position. Soil Sci. Soc. Am. J. 57:235–239.

Brubaker, S.C., A.J. Jones, K. Frank, and D.T. Lewis. 1994. Regression models for estimating soil properties by landscape position. Soil Sci. Soc. Am. J. 58:1763–1767.

Bruce, R.R., A.W. Thomas, L.A. Harper, and R.A. Leonard. 1977. Diurnal soil water regime in the tilled plow layer of a warm humid climate. Soil Sci. Soc. Am. J. 41:455–460.

Bruckler, L. 2003. Role of the physical properties of the seedbed in imbibition and germination. I. A model of the "seed-soil" system. Agronomie. 3:213–222.

Brun, L.J., J.W. Enz, J.K. Larsen, and C. Fanning. 1986. Springtime evaporation from bare and stubble-covered soil. J. Soil Water Conserv. 41:120–122.

Buhler, D.D. 1995. Influence of tillage systems on weed population dynamics and management in corn and soybean in central USA. Crop Sci. 35:1247–1258.

Buhler, D.D. and T.C. Mester. 1991. Effect of tillage systems on the emergence depth of giant (*Setaria faberi*) and green foxtail (*Seteria viridis*). Weed Sci. 39:200–203.

Bullied, W.J., A.M. Marginet, and R.C. Van Acker. 2003. Conventional- and conservation tillage systems influence emergence periodicity of annual weed species in canola. Weed Sci. 51:886–897.

Burden, D.S. and H.M. Selim. 1989. Correlation of spatially variable soil water retention for a surface soil. Soil Sci. 148:436–447.

Campbell, D.J. and J.K. Henshall. 1991. Bulk density. p. 329–366. In K.A. Smith and C.E. Mullins ed. Soil analysis: Physical methods. Marcel Dekker, New York.

Campbell, G.S. 1974. A simple method for determining unsaturated conductivity from moisture retention data. Soil Sci. 117:311–314.

Campbell, G.S. 1985. Soil physics with basic transport models for soil–plant systems. Elsevier, New York.

Campbell, G.S. and W.H. Gardner. 1971. Psychrometric measurements of soil water potential: Temperature and bulk density effects. Soil Sci. Soc. Am. Proc. 35:8–12.

Carson, M.A. and M.J. Kirkby. 1972. Hillslope form and process. Cambridge University Press, Cambridge.

Carter, M.R., and D.A. Rennie. 1985. Soil temperature under zero tillage systems for wheat in Saskatchewan. Can. J. Soil Sci. 65:329–338.

Cary, J.W. 1965. Water flux in moist soil: Thermal versus suction gradients. Soil Sci. 100:168–175.

Cary, J.W. 1966. Soil moisture transport due to thermal gradients: Practical aspects. Soil Sci. Soc. Am. Proc. 30:428–433.

Casanova, M., I. Messing, and A. Joel. 2000. Influence of aspect and slope gradient on hydraulic conductivity measured by tension infiltrometer. Hydrol. Processes. 14:155–164.

Cassel, D.K. 1983. Spatial and temporal variability of soil physical properties following tillage of Norfolk loamy sand. Soil Sci. Soc. Am. J. 47:196–201.

Chachalis, D. and K.N. Reddy. 2000. Factors affecting *Campsis radicans* seed germination and seedling emergence. Weed Sci. 48:212–216.

Chancellor, R.J. 1964. The depth of weed seed germination in the field. p. 607–613. In Proc. 7th British Weed Control Conf., Brighton.

Changere A. and R. Lal. 1997. Slope position and erosional effects on soil properties and corn production on a Miamian soil in central Ohio. J. Sustain. Agric. 11:5–21.

Chopra, U.K. and T.N. Chaudhary. 1981. Seedling emergence of wheat and gram in relation to soil water potential, temperature and seeding depth. J. Indian Soc. Soil Sci. 29:437–440.

Choudhary, M.A., and C.J. Baker. 1982. Effects of drill coulter design and soil moisture status on emergence of wheat seedlings. Tillage Res. 2:131–142.

Cipra, J.E., M.F. Baumgardner, E.R. Stoner, and R.B. MacDonald. 1971. Measuring radiance characteristics of soil with a field spectroradiometer. Soil Sci. Soc. Am. Proc. 35:1014–1017.

Clarke, J.M. 1980. Measurement of relative water uptake rates of wheat seeds using agar media. Can J. Plant Sci. 60:1035–1038.

Cochran, P.H. 1969. Thermal properties and surface temperatures of seedbeds: A guide for foresters. Pacific Northwest Forest and Range Experiment Station, USDA, Portland, OR.

Colbach N., C. Dürr, J. Roger-Estrade, B. Chauvel, and J. Caneill. 2006. AlomySys: Modelling black-grass (*Alopecurus myosuroides* Huds.) germination and emergence, in interaction with seed characteristics, tillage and soil climate I. Construction. Eur. J. Agron. 24:95–112.

Colbach N., J. Roger-Estrade, B. Chauvel, and J. Caneill. 2000. Modelling vertical and lateral seed bank movements during mouldboard ploughing. Eur. J. Agron. 13:111–124.

Collis-George, N. and J.B. Hector. 1966. Germination of seeds as influenced by matric potential and by area of contact between seed and soil water. Aust. J. Soil Res. 4:145–164.

Constantz, J. 1982. Temperature dependence of unsaturated hydraulic conductivity of two soils. Soil Sci. Soc. Am. J. 46:466–470.

Cousens, R. and S.R. Moss. 1990. A model of the effects of cultivation on the vertical distribution of weed seeds within the soil. Weed Res. 30:61–70.

Covell, S., R.H. Ellis, E.H. Roberts, and R.J. Summerfield. 1986. The influence of temperature on seed germination rate in grain legumes. I. A comparison of chickpea, lentil, soybean, and cowpea at constant temperatures. J. Exp. Bot. 37:705–715.

Crave, A., and C. Gascuel-Odoux. 1997. The influence of topography on time and space distribution of soil surface water content. Hydrol. Processes. 11:203–210.

Cremeans, D.W. 1992. Aspect and slope position effects on moisture regime and properties of forest soils in eastern Kentucky. Ph.D. diss. Univ. of Kentucky, Lexington, KY.

Croney, D. and J.D. Coleman. 1954. Soil structure in relation to soil suction (pF). J. Soil Sci. 5:75–84.

Cussans, G.W., S. Raudonius, P. Brain, and S. Cumberworth. 1996. Effects of depth of seed burial and soil aggregate size on seedling emergence of *Alopercurus myosuroides*, *Gallium aparine*, *Stellaria media* and wheat. Weed Res. 36:133–141.

Dahal, P. and K.J. Bradford. 1994. Hydrothermal time analysis of tomato germination at suboptimal temperature and reduced water potential. Seed Sci. Res. 4:71–80.

Dane, J.H. and J.W. Hopmans. 2002. Water retention and storage. p. 671–690. In J.H. Dane and G.C. Topp ed. Methods of soil analysis. Part 4. Physical methods. Soil Sci. Soc. Am., Madison, WI.

Daniels, R.B. and R.D. Hammer. 1992. Soil Geomorphology. John Wiley and Sons, New York.

Daniels, R.B., J.W. Gilliam, D.K. Cassel, and L.A. Nelson. 1987. Quantifying the effects of past soil erosion on present soil productivity. J. Soil Water Cons. 42:183–187.

Dasberg, S. and K. Mendel. 1971. The effects of soil water and aeration on seed germination. J. Exp. Bot. 22:992–998.

Davies, J.A. and P.H. Buttimor. 1969. Reflection coefficients, heating coefficients and net radiation at Simcoe, Southern Ontario. Agric. Meteorol. 6:373–386.

Davis, A.S., K.I. Anderson, S.G. Hallett, and K.A. Renner. 2006. Weed seed mortality in soils with contrasting agricultural management histories. Weed Sci. 54:291–297.

Dawson, J.H. and V.F. Bruns. 1962. Emergence of barnyardgrass, green foxtail, and yellow foxtail seedlings from various soil depths. Weeds. 10:136–139.

De Corby, K.A., R.C. Van Acker, A.L. Brûlé-Babel and L.F. Friesen. 2007. Emergence timing and recruitment of volunteer spring wheat. Weed Sci. 55:60–69.

De Jong, R. and K.F. Best. 1979. The effect of soil water potential, temperature and seeding depth on seedling emergence of wheat. Can. J. Soil Sci. 59:259–264.

De Vries, D.A. 1963. Thermal properties of soils. p. 210–235. In W.R. Van Wijk ed. Physics of plant environment. North-Holland Publ. Co., Amsterdam.

Debaene-Gill, S.B., P.S. Allen, and D.B. White. 1994. Dehydration of germinating perennial ryegrass seeds can alter rate of subsequent radicle emergence. J. Exp. Bot. 43:1301–1307.

Dekker, J. and M. Hargrove. 2002. Weedy adaptation in *Setaria* spp. V. Effects of gaseous environment on giant foxtail (*Setaria faberii*) (Poaceae) seed germination. Am. J. Bot. 89:410–416.

Dessaint, F., R. Chadoeuf, and G. Barralis. 1991. Spatial pattern analysis of weed seeds in the cultivated soil seedbank. J. Appl. Ecol. 28:712–730.

Dieleman, J.A., D.A. Mortensen, D.D. Buhler, C.A. Cambardella, and T.B. Moorman. 2000a. Identifying associations among site properties and weed species abundance. I. Multivariate analysis. Weed Sci. 48:567–575.

Dieleman, J.A., D.A. Mortensen, D.D. Buhler, and R.B. Ferguson. 2000b. Identifying associations among site properties and weed species abundance. II. Hypothesis generation. Weed Sci. 48:576–587.

Dingman, S.L., 1994. Physical hydrology. Prentice-Hall, Englewood Cliffs, NJ.

du Croix Sissons, M.J., R.C. Van Acker, D.A. Derksen, and A.G. Thomas. 2000. Depth of seedling recruitment of five weed species measured in situ in conventional- and zero-tillage fields. Weed Sci. 48:327–332.

Dyer, W. 1995. Exploiting weed seed dormancy and germination requirements through agronomic practices. Weed Sci. 43:498–503.

Egley, G.H. 1986. Stimulation of weed seed germination in soil. Rev. Weed Sci. 2:67 – 89.

Egley, G.H. 1995. Seed germination in soil: Dormancy cycles. p. 529–543. In J. Kiegel and G. Galili ed. Seed development and germination. Marcel Dekker, New York.

Egley, G.H. and S.O. Duke. 1985. Physiology of weed seed dormancy and germination. p. 27–64. In S.O. Duke ed. Weed physiology. Vol. 1. Reproduction and ecophysiology. CRC Press, Boca Raton, FL.

Egley, G.H. and R.D. Williams. 1990. Decline of weed seeds and seedling emergence over five years as affected by soil disturbance. Weed Sci. 38:504–510.

Egley, G.H. and R.D. Williams. 1991. Emergence periodicity of six summer annual weed species. Weed Sci. 39:595–600.

Ekstam, B., R. Johannesson, and P. Milberg. 1999. The effect of light and number of diurnal temperature fluctuations on germination of *Phragmites australis*. Seed Sci. Res. 9:165–170.

Elliott, J.A. and A.A. Efetha. 1999. Influence of tillage and cropping system on soil organic matter, structure, and infiltration in a rolling landscape. Can. J. Soil Sci. 79:457–463.

Ellis, R.H., S. Covell, E.H. Roberts, and R.J. Summerfield. 1986. The influence of temperature on seed germination rate in grain legumes. II. Intraspecific variation in chickpea (*Cicer arietinum* L.) at constant temperatures. J. Exp. Bot. 37:1503–1515.

El-Sharkawi, H.M. and I. Springuel. 1977. Germination of some crop plant seeds under reduced water potential. Seed Sci. Technol. 5:677–688.

Eriksson, O. and J. Ehrlén. 1992. Seed and microsite limitation of recruitment in plant populations. Oecol. 91:360–364.

Famiglietti, J.S., J.W. Rudnicki, and M. Rodell. 1998. Variability in surface moisture content along a hillslope transect: Rattlesnake Hill, Texas. J. Hydrol. 210:259–281.

Fan, L.T., D.S. Chung, and J.A. Shellenberger. 1961. Diffusion coefficients of water in wheat kernels. Cereal Chem. 1961. 38:540–548.

Filzer, P. 1939. Untersuchungen über den wasserumsatz künstlicher pfanzenbestände. Planta. 30:205–223.

Finch-Savage, W.E. and K. Phelps. 1993. Onion (*Allium cepa* L.) seedling emergence patterns can be explained by the influence of soil temperature and water potential on seed germination. J. Exp. Bot. 44:407–414.

Finch-Savage, W.E., K. Phelps, L. Peach, and J.R.A. Steckel. 2000. Use of threshold germination models under variable field conditions. p. 489–497. In M. Black, K.J. Bradford, and J. Vázquez-Ramos ed. Seed biology: Advances and applications. CAB International, Wallingford, UK.

Forcella, F. 1998. Real-time assessment of seed dormancy and seedling growth for weed management. Seed Sci. Res. 8:201–209.

Forcella, F., B.R. Durgan, and D.D. Buhler. 1996. Management of weed seedbanks. p. 21–26. In J. Streibig ed. Proc. Second International Weed Control Congress, Int. Weed Sci. Soc., Copenhagen.

Forcella, F., R.G. Wilson, J. Dekker, R.J. Kremer, J. Cardina, R.L. Anderson, D. Alm, K.A. Renner, G. Harvey, and S. Clay. 1997. Weed seed bank emergence across the Corn Belt. Weed Sci. 45:67–76.

Forcella, F., R.L. Benech Arnold, R. Sanchez, and C.M. Ghersa. 2000. Modeling seedling emergence. Field Crops Res. 67:123–139.

Fowler, N.L. 1986. Microsite requirements for germination and establishment of three grass species. Am. Midl. Nat. 115:131–145.

Fowler, N.L. 1988. What is a safe site?: Neighbor, litter, germination date, and patch effects. Ecology. 69:947–961.

Franzmeier, D.P., E.J. Pedersen, T.J. Longwell, J.G. Byrne, and C.K. Losche. 1969. Properties of some soils in the Cumberland Plateau as related to slope aspect and position. Soil Sci. Soc. Am. Proc. 33:755–761.

Friesen, O. and G. Bonnefoy. 1972. A fall tillage study on Red River clay. p. 11–22. In Proc. MB. Agron. Annu. Conf. Dec. 12–13. Brandon, MB.

Froud-Williams, R.J., R.J. Chancellor, and D.S.H. Drennan. 1983. Influence of cultivation regime upon buried weed seed in arable cropping systems. J. Appl. Ecol. 20:199–208.

Froud-Williams, R.J., R.J. Chancellor, and D.S.H. Drennan. 1984. The effects of seed burial and soil disturbance on emergence and survival of arable weeds in relation to minimal cultivation. J. Appl. Ecol. 21:629–641.

Fu, R. and R.A. Ashley. 1998. Modeling weed emergence from different soil depths. Proc. Northeastern Weed Sci. Soc. 52:77–81.

Fyfield, T.P. and P.J. Gregory. 1989. Effect of temperature and water potential on germination, radicle elongation and emergence of mungbean. J. Exp. Bot. 40:667–674.

Gan, Y. and E.H. Stobbe. 1995. Effect of variations in seed size and planting depth on emergence, infertile plants, and grain yield of spring wheat. Can. J. Plant Sci. 75:565–570.

Gan, Y., E.H. Stobbe, and J. Moes. 1992. Relative date of wheat seedling emergence and its impact on grain yield. Crop Sci. 32:1275–1281.

Gan, Y., E.H. Stobbe, and C. Njue. 1996. Evaluation of selected nonlinear regression models in quantifying seedling emergence rate of spring wheat. Crop Sci. 36:165–168.

Garcia-Huidobro, J., J.L. Monteith, and G.R. Squier. 1982. Time, temperature and germination of pearl millet (*Pennisetum typhoides* S. & H.). I. Constant temperature. J. Exp. Bot. 33:288–296.

Gardner, R. 1955. Relation of temperature to moisture tension of soil. Soil Sci. 79:257–265.

Garnier, B.J. and A. Ohmura. 1968. A method of calculating the direct short wave radiation income of slopes. J. Appl. Meteorol. 7:796–800.

Gauer, E., C.F. Shaykewich, and E.H. Stobbe. 1982. Soil temperature and soil water under zero tillage in Manitoba. Can. J. Soil Sci. 62:311–325.

Geiger, R. 1965. The influence of topography on microclimate. p. 369–467. In R. Geiger ed. The climate near the ground. Oxford University Press, London.

Ghersa, C. M., R. L. Benech-Arnold, E. H. Sattore, and M. A. Martínez-Ghersa. 2000. Advances in weed management strategies. Field Crops Res. 67:95–104.

Ghersa, C.M., R.L. Benech-Arnold, and M.A. Martínez-Ghersa. 1992. The role of fluctuating temperatures in germination and establishment of *Sorghum halepense*. Regulation of germination at increasing depths. Funct. Ecol. 6:460–468.

Ghorbani, R., W. Seel, and C. Leifert. 1999. Effects of environmental factors on germination and emergence of *Amaranthus retroflexus*. Weed Sci. 47:505–510.

Ghuman, B.S. and R. Lal. 1985. Thermal conductivity, thermal diffusivity, and thermal capacity of some Nigerian soils. Soil Sci. 139:74–80.

Greb, B.W. 1966. Effect of surface-applied wheat straw on soil water losses by solar distillation. Soil Sci. Soc. Am. Proc. 30:786–791.

Greenfield, L.G. 2000. The microbial decomposition of seeds. p.47–51. In Agron. Soc. of New Zealand Spec. Publ. 0111-9184. New Zealand.

Greminger, P.J., Y.K. Sud, and D.R. Nielsen. 1985. Spatial variability of field-measured soil-water characteristics. Soil Sci. Soc. Am. J. 49:1075–1082.

Grundy, A.C. and A. Mead. 1998. Modelling the effects of seed depth on weed seedling emergence. Aspects of Appl. Biol. 51:75 –82.

Grundy, A.C. and A. Mead. 2000. Modeling weed emergence as a function of meteorological records. Weed Sci. 48:594–603.

Grundy, A.C., A. Mead, and W. Bond. 1996. Modelling the effect of weed–seed distribution in the soil profile on seedling emergence. Weed Res. 36:375–384.

Grundy, A.C., A. Mead, and S. Burston. 2003. Modelling the emergence response of weed seeds to burial depth: Interactions with seed density, weight and shape. J. Appl. Ecol. 40:757–770.

Grundy, A.C., K. Phelps, R.J. Reader, and S. Burston. 2000. Modelling the germination of *Stellaria media* using the concept of hydrothermal time. New Phytol. 148:433–444.

Gummerson, R.J. 1986. The effect of constant temperatures and osmotic potential on the germination of sugar beet. J. Exp. Bot. 37:729–741.

Gupta, S.C., W.E. Larson, and R.R. Allmaras. 1984. Predicting soil temperature and soil heat flux under different tillage-surface residue conditions. Soil Sci. Soc. Am. J. 48:223–232.

Hadas, A. 1982. Seed soil contact and germination. p. 507–527. In A.A. Khan ed. The physiology and biochemistry of seed development, dormancy and germination. Elsevier, Amsterdam.

Hadas, A. and D. Russo. 1974. Water uptake by seeds as affected by water stress, capillary conductivity and seed soil water contact. I. Experimental study. Agron. J. 66:643–645.

Hadjichristodoulou, A., A. Della, and J. Photiades. 1977. Effect of sowing depth on plant establishment, tillering capacity and other agronomic characters of cereals. J. Agric. Sci. 89:161–167.

Hanks, R.J. and F.C. Thorp. 1956. Seedling emergence of wheat as related to soil moisture content, bulk density, oxygen diffusion rate, and crust strength. Soil Sci. Soc. Am. Proc. 20:307–310.

Hanna, Y.A., P.W. Harlan, and D.T. Lewis. 1982. Soil available water as influenced by landscape position and aspect. Agron. J. 74:999–1004.

Hardegree, S.P. 2006a. Predicting germination response to temperature. I. Cardinal-temperature models and subpopulation-specific regression. Ann. Bot. 97:1115–1125.

Hardegree, S.P. 2006b. Predicting germination response to temperature. III. Model validation under field-variable temperature conditions. Ann. Bot. 98:827–834.

Hardegree, S.P., T.A. Jones, and S.S. Van Vactor. 2002. Variability in thermal response in primed and non-primed seeds of squirreltail [*Elymus elymoides* (Raf.) Swezey and *Elymus multisetus* (J. G. Smith) M. E. Jones]. Ann. Bot. 89:311–319.

Hardegree S.P., S.S. Van Vactor, F.B. Pierson, and D.E. Palmquist. 1999. Predicting variable-temperature response of non-dormant seeds from constant-temperature germination data. J. Range Manage. 52:83–91.

Harker, K.N., G.W. Clayton, R.E. Blackshaw, J.T. O'Donovan, E.N. Johnson, Y. Gan, F.A. Holm, K. Sapsford, R.B. Irvine, and R.C. Van Acker. 2005. Glyphosate-resistant wheat persistence in western Canadian cropping systems. Weed Sci. 53:846–859.

Harper, J.L. 1977. Population biology of plants. Academic Press Inc., London.

Harper, J.L. and R.A. Benton. 1966. The behavior of seeds in the soil. II. The germination of seeds on the surface of a water supplying substrate. J. Ecol. 54:151–166.

Harper, J.L., J.N. Clatworthy, I.H. McNaughton, and G.R. Sager. 1961. The evolution of closely related species living in the same area. Evol. 15:209–227.

Harper, J.L., J.T. Williams, and G.R. Sager. 1965. The behavior of seeds in the soil. I. The heterogeneity of soil surfaces and its role in determining the establishment of plants from seed. J. Ecol. 53:273–286.

Harvey, S.J. and F. Forcella. 1993. Vernal seedling emergence model for common lambsquarters (*Chenopodium album*). Weed Sci. 41:309–316.

Haverkamp, R., F.J. Leij, C. Fuentes, A. Sciortino, and P.J. Ross. 2005. Soil water retention. I. Introduction of a shape index. Soil Sci. Soc. Am. J. 69:1881–1890.

Hawley, M.E., T.J. Jackson, and R.H. McCuen. 1983. Surface soil moisture variation on small agricultural watersheds. J. Hydrol. 62:179–200.

Hegarty, T.W. 1977. Seed and seedling susceptibility to phased moisture stress in soil. J. Exp. Bot. 28:659–668.

Hegarty, T.W. 1978. The physiology of seed hydration and dehydration, and the relation between water stress and the control of germination: A review. Plant Cell Environ. 1:101–119.

Helms, T.C., E.L. Deckard, R.J. Goos, and J.W. Enz. 1996a. Soil moisture, temperature, and drying influence on soybean emergence. Agron J. 88:662–667.

Helms, T.C., E.L. Deckard, R.J. Goos, and J.W. Enz. 1996b. Soybean seedling emergence influenced by days of soil water stress and soil temperature. Agron J. 88:657–661.

Henninger, D.L., G.W. Peterson, and E.T. Engman. 1976. Surface soil moisture within a watershed: Variations, factors influencing, and relationships to surface runoff. Soil Sci. Soc. Am. J. 40:773–776.

Heydecker, W. 1956. Establishment of seedlings in the field. I. Influence of sowing depth on seedling emergence. J. Hort. Sci. 31:76–88.

Heydecker, W. 1962. From seed to seedling: Factors affecting the establishment of vegetable crops. Ann. Appl. Biol. 50:622–627.

Hillel, D. 1982. Introduction to soil physics. Academic Press Inc., London.

Hills, T.C., and S.G. Reynolds. 1969. Illustrations of soil moisture variability in selected areas and plots of different sizes. J. Hydrol. 8:27–47.

Hiraiwa, Y and T. Kasubuchi. 2000. Temperature dependence of thermal conductivity of soil over a wide range of temperature (5–75°C). European J. Soil Sci. 51:211–218.

Hoffman, M.L., M.D.K. Owen, and D.D. Buhler. 1998. Effects of crop and weed management on density and vertical distribution of weed seeds in soil. Agron. J. 90:793–799.

Honeycutt, C.W., R.D. Heil, and C.V. Cole. 1990. Climatic and topographic relations of three Great Plains soils: I. Soil morphology. Soil Sci. Soc. Am. J. 54:469–475.

Hopmans, J.W. and J.H. Dane. 1985. Effect of temperature-dependent hydraulic properties on soil water movement. Soil Sci. Soc. Am. J. 49:51–58.

Hopmans, J.W. and J.H. Dane. 1986a. Temperature dependence of soil hydraulic properties. Soil Sci. Soc. Am. J. 50:4–9.

Hopmans, J.W. and J.H. Dane. 1986b. Temperature dependence of soil water retention curves. Soil Sci. Soc. Am. J. 50:562–567.

Horton, R. K.L. Bristow, G.J. Kluitenberg, and T.J. Sauer. 1996. Crop residue effects on surface radiation and energy balance – review. Theor. Appl. Climatol. 54:27–37.

Horton, R., G.J. Kluitenberg, and K.L. Bristow. 1994. Surface crop residue effects on the soil surface energy balance. p. 143–162. In P.W. Unger ed. Managing agricultural residues. Lewis Publ., Ann Arbor, MI.

Hudson, B.D. 1994. Soil organic matter and available water capacity. J. Soil Water Conserv. 49:189–194.

Hunter, J.R. and A.E. Erickson. 1952. Relation of seed germination to soil moisture tension. Agron J. 44:107–109.

Idso, S.B., R.D. Jackson, R.J. Reginato, B.A. Kimball, and F.S. Nakayama. 1975. The dependence of bare soil albedo on soil water content. J. appl. Meteorol. 14:109–113.

Idso, S.B., R.J. Reginato, R.D. Jackson, B.A. Kimball, and F.S. Nakayama. 1974. The three stages of drying of a field soil. Soil Sci. Soc. Am. Proc. 38:83–837.

Jaynes, D.B. 1990. Temperature variations effect on field-measured infiltration. Soil Sci. Soc. Am. J. 54:305–312.

Johnson, M.D. and B. Lowery. 1985. Effect of three conservation tillage practices on soil temperature and thermal properties. Soil Sci. Soc. Am. J. 49:1547–1552.

Johnstone, I.M. 1986. Plant invasion windows: A time based classification of invasion potential. Biol. Rev. Cambridge Philos. Soc. 61:369–394.

Kalma, J.D. and R. Badham. 1972. The radiation balance of a tropical pasture. I. The reflection of short wave radiation. Agric. Meteorol. 23:217–229.

Kebreab, E. and A.J. Murdoch. 1999. Modelling the effects of water stress and temperature on germination rate of *Orobanche aegyptiaca* seeds. J. Exp. Bot. 50:655–664.

Kegode, G.O., R.B. Pearce, and T.B. Bailey. 1998. Influence of fluctuating temperatures on emergence of shattercane (*Sorghum bicolor*) and giant foxtail (*Setaria faberi*). Weed Sci. 46:330–335.

Khah, E.M., R.H. Ellis, and E.H. Roberts. 1986. Effects of laboratory germination, soil temperature, and moisture content on the emergence of spring wheat. J. Agric. Sci. 107:431–438.

Khan, A.A. and C.M. Karssen. 1980. Induction of secondary dormancy in *Chenopodium bonus-henricus* L. seeds by osmotic and high temperature treatments and its prevention by light and growth regulators. Plant Physiol. 66:175–181.

Khosravi, G.R. and I.C. Anderson. 1990. Pre-emergence flooding and nitrogen atmosphere effects on germinating corn inbreds. Agron. J. 82:495–499.

King, C.A. and L.R. Oliver. 1994. A model for predicting large crabgrass (*Digitaria sanguinalis*) emergence as influenced by temperature and water potential. Weed Sci. 42:561–567.

King, L.J. 1966. Weeds of the world: Biology and control. Interscience Publ., New York.

Kirby, E.J.M. 1993. Effect of sowing depth on seedling emergence, growth and development in barley and wheat. Field Crops Res. 35:101–111.

Kleiss, H.J. 1970. Hillslope sedimentation and soil formation in northeastern Iowa. Soil Sci. Soc. Am. Proc. 34:287–290.

Kremer, R.J. 1993. Management of weed seed banks with microorganisms. Ecol. Appl. 3:42–52.

Kruk, B.C. and R.L. Benech-Arnold. 1998. Functional and quantitative analysis of seed thermal responses in prostrate knotweed (*Polygonum aviculare*) and common purslane (*Portulaca oleracea*). Weed Sci. 46:83–90.

Kung, E.C., R.A. Bryson, and D.H. Lenschow. 1964. Study of a continental surface albedo on the basis of flight measurements and structure of the earth's surface cover over North America. Mon. Weather Rev. 92:543–564.

Lafond, G.P. and D.B. Fowler. 1989. Soil temperature and moisture stress effects on kernel water uptake and germination of winter wheat. Agron. J. 81:447–450.

Lafond, G.P. and R.J. Baker. 1986. Effects of temperature, moisture stress, and seed size on germination of nine spring wheat cultivars. Crop Sci. 26:563–567.

Lal, R., T.J. Logan, D.J. Eckert, and W.A. Dick. 1994. p. 76–113.Convervation tillage in the corn belt of the United States. In M.R. Carter ed. Conservation tillage in temperate agroecosystems. Lewis Publishers, Boca Raton, FL.

Lawson, A.N., R.C. Van Acker, and L.F. Friesen. 2006. Emergence timing of volunteer canola in spring wheat fields in Manitoba. Weed Sci. 54:873–882.

Leblanc, M.L., D.C. Cloutier, K. Stewart, and C. Hamel. 2003. The use of thermal time to model common lambsquarters (*Chenopodium album*) seedling emergence in corn. Weed Sci. 51:718–724.

Leguizamón, E.S., C. Fernandez-Quintanilla, J. Barroso, and J.L. Gonzalez-Andujar. 2005. Using thermal and hydrothermal time to model seedling emergence of Avena sterrilis ssp. Ludoviciana in Spain. Weed Res. 45:149–156.

Lindquist, J.L. and B.D. Maxwell. 1991. The horizontal dispersal pattern of weed seed surrogates by farm machinery. Proc. North Cent. Weed Sci. Soc. 46:108–109.

Lindstrom, M.J., R.I. Papendick, and F.E. Koehler. 1976. A model to predict winter wheat emergence as affected by soil temperature, water potential, and depth of planting. Agron. J. 68:137–141.

Liu, H.H. and J.H. Dane. 1993. Reconciliation between measured and theoretical temperature effects on soil water retention curves. Soil Sci. Soc. Am. J. 57:1202–1207.

Loague, K. 1992. Soil water content at R-5. Part 1. Spatial and temporal variability. J. Hydrol. 139:233–251.

Ludwig, J.W., E.S. Bunting, and J.L. Harper. 1957. The influence of environment on seed and seedling mortality: III. The influence of aspect on maize germination. J. Ecol. 45:205–224.

Lund, R.D. and F.T. Turpin. 1977. Carabid damage to weed seeds found in Indiana corn fields. Environ. Entomol. 6:695–698.

Malo, D.D., B.K. Worchester, D.K. Cassel and K.D. Matzdorf. 1974. Soil–landscape relationships in a closed drainage system. Soil Sci. Soc. Am. Proc. 38:813–818.

Manning G., L.G. Fuller, R.G. Eilers, and I. Florinsky. 2001a. Soil moisture and nutrient variation within an undulating Manitoba landscape. Can. J. Soil Sci. 81:449–458.

Manning G., L.G. Fuller, R.G. Eilers, and I. Florinsky. 2001b. Topographic influence on the variability of soil properties within an undulating Manitoba landscape. Can. J. Soil Sci. 81:439–447.

Martin, B.A., S.F. Cerwick, and L.D. Reding. 1991. Physiological basis for inhibition of maize seed germination by flooding. Crop Sci. 31:1052–1057.

Martinez-Ghersa, M.A., E.H. Satorre, and C.M. Ghersa. 1997. Effect of soil water content and temperature on dormancy breaking and germination of three weeds. Weed Sci. 45:791–797.

Matzdorf, K.D., D.K. Cassel, B.K. Worcester, and D.D. Malo. 1975. In situ hydraulic conductivity at four hillslope locations in a closed drainage system. Soil Sci. Soc. Am. Proc. 39:508–512.

McConkey, B.G., D.J. Ulrich, and F.B. Dyck. 1997. Slope position and subsoiling effects on soil water and spring wheat yield. Can. J. Soil Sci. 77:83–90.

McDonald, C.K. 2002a. Germination response to temperature in tropical and subtropical pasture legumes. 1. Constant temperature. Aust. J. Exp. Agric. 42:407–419.

McDonald, C.K. 2002b. Germination response to temperature in tropical and subtropical pasture legumes. 2. Alternating temperatures. Aust. J. Exp. Agric. 42:421–429.

McGinnies, W.J. 1960. Effects of moisture stress and temperature on germination of six range grasses. Agron. J. 52:159–162.

McKersie, B.D. and D.T. Tomes. 1980. Effects of dehydration treatments on germination, seedling vigor, and cytoplasmic leakage in wild oats and birdsfoot trefoil. Can J. Bot. 58:471–476.

Mennan, H. and B.H. Zandstra. 2006. The effects of depth and duration of seed burial on viability, dormancy, germination, and emergence of ivyleaf speedwell (*Veronica hederifolia*). Weed Technol. 20:438–444.

Mickelson, J.A. and W.E. Grey. 2006. Effect of soil water content on wild oat (*Avena fatua*) seed mortality and seedling emergence. Weed Sci. 54:255–262.

Mohler, C.L. 1993. A model of the effects of tillage on emergence of weed seedlings. Ecol. Applic. 3:53–73.

Mohler, C.L. and A.E. Galford. 1997. Weed seedling emergence and seed survival: Separating the effects of seed position and soil modification by tillage. Weed Res. 37:147–156.

Mohler, C.L., J.C. Frisch, and C.E. McCulloch. 2006. Vertical movement of weed seed surrogates by tillage implements and natural processes. Soil Tillage Res. 86:110–122.

Monteith, J.L. 1990. Principles of environmental physics. 2nd ed. Edward Arnold, New York.

Moore, I.D., G.J. Burch, and D.H. Mackenzie. 1988. Topographic effects on the distribution of surface water and the location of ephemeral gullies. Trans. Am. Soc. Agric. Eng. 31:1098–1107.

Moore, R.E. 1940. The relation of soil temperature to soil moisture: Pressure potential, retention, and infiltration rate. Soil Sci. Soc. Proc. 5:61–64.

Mulugenta, D. and C.M. Boerboom. 1999. Seasonal abundance and spatial pattern of *Setaria faberi*, *Chenopodium album*, and *Abutilon theophrasti* in reduced-tillage soybeans. Weed Sci. 47:95–106.

Murdoch, A.J. and R.H. Ellis. 1992. Longevity, viability, and dormancy. p. 193–229. In M. Fenner ed. Seeds: The ecology of regeneration in plant communities. CAB International, Wallingford, UK.

Myers, M.W., W.S. Curran, M.J. VanGessel, D.D. Calvin, D.A. Mortensen, B.A. Majek, H.D. Karsten, and G.W. Roth. 2004. Predicting weed emergence for eight annual species in the northeastern United States. Weed Sci. 52:913–919.

Nakshabandi, G.A. and H. Kohnke. 1965. Thermal conductivity and diffusivity of soils as related to moisture tension and other physical properties. Agr. Meteorol. 2:271–279.

Nassar, I.N., R. Horton, and A.M. Globus. 1997. Thermally induced water transfer in salinized, unsaturated soil. Soil Sci. Soc. Am. J. 61:1293–1299.

Naylor, R.E.L. and M. Gurmu. 1990. Seed vigour and water relations in wheat. Ann. Appl. Biol. 117:441–450.

Nielsen, D.R., J.W. Biggar, and K.T. Erb. 1973. Spatial variability of field-measured soil-water properties. Hilgardia. 42:215–259.

Nyberg, L. 1996. Spatial variability of water content in the covered catchment at Gardsjon, Sweden. Hydrol. Processes. 10:89–103.

Ochsner, T.E., R. Horton, and T. Ren. 2001. A new perspective on soil thermal properties. Soil Sci. Soc. Am. J. 65:1641–1647.

O'Donovan, J.T. and D.W. McAndrew. 2000. Effect of tillage on weed populations in continuous barley. Weed Technol. 14:726–733.

Oguntoyinbo, J.S. 1974. Land use and reflection coefficient (albedo) map for southern parts of Nigeria. Agric. Meteorol. 13:227–237.

Oke, T.R. 1987. Boundary layer climates. 2nd Edition. Routledge, London.

Oke, T.R. and F.G. Hannell. 1966. Variations of temperature within a soil. Weather. 21:21–28.

Oryokot, J., S.D. Murphy, A.G. Thomas, and C.J. Swanton. 1997. Temperature- and moisture-dependent models of seed germination and shoot elongation in green and redroot pigweed (*Amaranthus powellii, A. retroflexus*). Weed Sci. 45:488–496.

Owen, P.C. 1952. The relation of germination of wheat to water potential. J. Exp. Bot. 3:188–203.

Page, E.R., R.S. Gallagher, A.R. Kemanian, H. Zhang, and E.P. Fuerst. 2006. Modeling site-specific wild oat (Avena fatua) emergence across a variable landscape. Weed Sci. 54:838–846.

Papendick, R.I. and G.S. Campbell. 1981. Theory and measurement of water potential. p. 1–22. In J.F. Parr et al. ed. Water potential relations in soil microbiology. Soil Sci. Soc. Am. Spec. Publ. 13. Madison, WI.

Pareja, M.R. and D.W. Staniforth. 1985. Seed–soil microsite characteristics in relation to weed seed germination. Weed Sci. 33:190–195.

Pareja, M.R., D.W. Staniforth, and G.P. Pareja. 1985. Distribution of weed seed among soil structural units. Weed Sci. 33:182–189.

Pawloski, M.C. and C.F. Shaykewich. 1972. Germination of wheat as affected by soil water stress. Can. J. Plant Sci. 52:619–623.

Penning de Vries, F.W.T., D.M. Jansen, H.F.M. ten Berge, and A. Bakema. 1989. Soil water balance. p. 147–190. In F.W.T. Penning de Vries, D.M. Jansen, H.F.M. ten Berge, and A. Bakema ed. Simulation of ecophysiological processes of growth in several annual crops. Pudoc, Wageningen, Netherlands.

Peterson, R.F. 1965. Wheat: Botany, cultivation, and utilization. Interscience Publ., New York.

Philip, J.R. and D.A. de Vries. 1957. Moisture movement in porous media under temperature gradients. Trans. Am. Geophys. Union. 38:222–232.

Phillips, R.E. 1968. Water diffusivity of germinating soybean, corn and cotton seed. Agron. J. 60:568–571.

Pitty, A., D.W. Staniforth, and L.H. Tiffany. 1987. Fungi associated with caryopses of *Setaria* species from field-harvested seeds and from soil under two tillage systems. Weed Sci. 35:319–323.

Potter, K.N., R.M. Cruise, and R. Horton. 1985. Tillage effects on soil thermal properties. Soil Sci. Soc. Am. J. 49:968–973.

Probert, R.J. 2000 The role of temperature in the regulation of seed dormancy and germination. p. 261–292. In M. Fenner ed. Seeds: The ecology of regeneration in plant communities. 2nd ed. CAB International, Wallingford, UK.

Probert, R.J., R.D. Smith, and P. Birch. 1986. Germination responses to light and alternating temperatures in European populations of *Dactylis glomerata* L. V. The principle components of the alternating temperature requirement. New Phytol. 102:133–142.

Prostko, E.P., H.I. Wu, and J.M. Chandler. 1998. Modeling seedling johnsongrass (*Sorghum halepense*) emergence as influenced by temperature and burial depth. Weed Sci. 46:549–554.

Prostko, E.P., H.I. Wu, J.M. Chandler, and S.A. Senseman. 1997. Modeling weed emergence as influenced by burial depth using the Fermi-Dirac distribution function. Weed Sci. 45:242–248.

Qi, M. and M.K. Upadhyaya. 1993. Seed germination ecophysiology of meadow salsify (*Tragopogon pratensis*) and western salsify (*T. dubius*). Weed Sci. 41:362–368.

Radford, B.J. 1987. Effect of constant and fluctuating temperature regimes and seed source on the coleoptile length of tall and semidwarf wheats. Aust. J. Exp. Agric. 27:313–316.

Ramdas, L.A., R.J. Kalamkar, and K.M. Gadre. 1934. Agricultural studies in microclimatology. Indian J. Agric. Sci. 4:451–467.

Rawls, W.L., T.J. Gish, and D.L. Brakensiek. 1991. Estimating soil water retention from soil physical properties and characteristics. Adv. Soil Sci. 16:213–234.

Rawls, W.L., A. Nemes, and Ya. Pachepsky. 2004. Effect of soil organic carbon on soil hydraulic properties. p. 95–114. In Ya. Pachepsky and W.J. Rawls ed. Development of pedotransfer functions in soil hydrology. Elsevier, Amsterdam, Netherlands.

Reddy, K.N. and M. Singh. 1992. Germination and emergence of hairy beggarticks (*Bidens pilosa*). Weed Sci. 40:195–199.

Reid, D.J. and R.C. Van Acker. 2005. Seed burial by tillage promotes field recruitment of false cleavers (*Galium spurium*) and catchweed bedstraw (*Galium aparine*). Weed Sci. 53:578–585.

Reid, I. 1973. The influence of slope orientation upon the soil moisture regime and its hydrogeomorphological significance, J. Hydrol. 19:309–321.

Reinink, K., I. Jorritsma, and A. Darwinkel. 1986. Adaptation of the AFRC wheat phenology model for Dutch conditions. Neth. J. Agric. Sci. 34:1–13.

Renault, P. and P. Stengel. 1994. Modeling oxygen diffusion in aggregated soils. I. Anaerobiosis inside the aggregates. Soil Sci. Soc. Am. J. 58:1017–1023.

Reuss, S.A., D.A. Buhler, and J.L. Gunsolus. 2001. Effects of soil depth and aggregate size on weed seed distribution and viability in a silt loam soil. Appl. Soil Ecol. 16:209–217.

Reynolds, S.G. 1970. The gravimetric method of soil moisture determination III: An examination of factors influencing soil moisture variability. J. Hydrol. 11:288–300.

Ridolfi, L., P. D'Odoricoc, A. Porporatoa, and I. Rodriguez-Iturbe. 2003. Stochastic soil moisture dynamics along a hillslope. J. Hydrol. 272:264–275.

Rinaldi, M., E. Di Paolo, G.M. Richter, and R.W. Payne. 2005. Modelling the effect of soil moisture on germination and emergence of wheat and sugar beet with the minimum number of parameters. Ann. Appl. Biol. 147:69–80.

Roberts, E.H. 1988. Temperature and seed germination. p. 109–132. In S.P. Long and F.I. Woodward ed. Plants and temperature. Soc. Exp. Biol., Cambridge, UK.

Roberts, E.H. and R.H. Ellis. 1989. Water and seed survival. Ann. Bot. 63:39–52.

Roberts, H.A. 1964. Emergence and longevity in cultivated soil of seeds of some annual weeds. Weed Res. 4:296–307.

Roberts, H.A. and P.M. Feast. 1972. Fate of seeds of some annual weeds in different depths of cultivated and undisturbed soil. Weed Res. 12:316–324.

Roché, C.T., D.C. Thill, and B. Shafi. 1997. Estimation of base and optimum temperatures for seed germination in common crupina (*Crupina vulgaris*). Weed Sci. 45:529–533.

Rogers, R.B. and S Dubetz. 1980. Effect of soil–seed contact on seed imbibition. Can. Agric. Eng. 22:89–92.

Roman, E.S., A.G. Thomas, S.D. Murphy, and C.J. Swanton. 1999. Modeling germination and seedling elongation of common lambsquarters (*Chenopodium album*). Weed Sci. 47:149–155.

Roman, E.S., S.D. Murphy, and C.J. Swanton. 2000. Simulation of Chenopodium album seedling emergence. Weed Sci. 48:217–224.

Rosenberg, N.J., B.L. Blad, and S.B. Verma. 1983. Microclimate: The biological environment. 2nd ed. John Wiley and Sons, New York.

Rowse, H.R. and W.E. Finch-Savage. 2003. Hydrothermal threshold models can describe the germination response of carrot (*Daucus carota*) and onion (*Allium cepa*) seed populations across both sub- and supra-optimal temperatures. New Phytol. 158:101–108.

Rowse, H.R., J.M.T. McKee and E.C. Higgs. 1999. A model of the effects of water stress on seed advancement and germination. New Phytol. 143:273–279.

Ruhe R.V. 1975. Hillslopes. p. 99–123. In R.V. Ruhe ed. Geomorphology: Geomorphic processes and surficial geology. Houghton Mifflin, Boston, MA.

Ruhe, R.V. 1960. Elements of the soil landscape. 7th Trans. Int. Congr. Soil Sci. 4:165–170.

Russel, J.C. 1939. The effect of surface cover on soil moisture losses by evaporation. Soil Sci. Soc. Am. Proc. 4:65–70.

Salter, P.J. and J.B. Williams. 1965. The influence of texture on the moisture characteristics of soils. Part I. A critical comparison of techniques for determining the available water capacity and moisture characteristic curve of a soil. J. Soil Sci. 16:1–15.

Sauer, T.J., J.L. Hatfield, and J.H. Prueger. 1996. Corn residue age and placement effects on evaporation and soil thermal regime. Soil Sci. Soc. Am. J. 60:1558–1564.

Schelde, K., A. Thomsen, T. Heidmann, P. Schjønning, and P.E. Jansson. 1998. Diurnal fluctuations of water and heat flows in a bare soil. Water Resour. Res. 34:2919–2929.

Schieldge, J.P., A.B. Kahle, and R.E. Alley. 1982. A numerical simulation of soil temperature and moisture variations for a bare field. Soil Sci. 133:197–207.

Schroeder, S.A. 1995. Topographic influences on soil water and spring wheat yields on reclaimed mineland. J. Environ. Qual. 24:467–471.

Schupp, E.W. 1995. Seed-seedling conflicts, habitat choice, and patterns of plant recruitment. Am. J. Bot. 82:399–409.

Scott, H.D. 2000. Soil temperature. p. 108–139. In H.D. Scott ed. Soil Physics: Agricultural and environmental applications. Iowa State Univ. Press, Ames, IA.

Senaratna, T. and B.D. McKersie. 1983. Dehydration injury in germinating soybean (*Glycine max* L. Merr.) seeds. Plant Physiol. 72:620–624.

Sharma, M.L. 1976. Interaction of water potential and temperature effects on germination of three semi-arid plant species. Agron. J. 68:390–394.

Sharratt, B.S. 1996. Soil temperature, water content, and barley development of level vs. ridged subarctic seedbeds. Soil Sci. Soc. Am. J. 60:258–263.

Sharratt, B.S. 2002. Corn stubble height and residue placement in the northern US corn belt. II. Spring microclimate and wheat development. Soil Tillage Res. 64:253–261.

Sharratt, B.S., M.J. Schwarzer, G.S. Campbell, and R.I. Papendick. 1992. Radiation balance of ridge-tillage with modeling strategies for slope and aspect in the subarctic. Soil Sci. Soc. Am. J. 56:1379–1384.

Shaykewich, C.F. and J. Williams. 1971. Resistance to water absorption in germinating rapeseed (*Brassica napus* L.) J. Exp. Bot. 22:19–24.

Sheldon, J.C. 1974. The behavior of seeds in the soil: III. The influence of seed morphology and the behavior of seedlings on the establishment of plants from surface-lying seeds. J. Ecol. 62:47–66.

Shiozawa, S. and G.S. Campbell. 1990. Soil thermal conductivity. Remote Sens. Rev. 5:301–310.

Shrestha, A., A.G. Thomas, and C.J. Swanton. 1999. Modeling germination and shoot-radicle elongation of *Ambrosia artemisiifolia*. Weed Sci. 47:557–562.

Sinai, G., D. Zaslavsky, and P. Golany. 1981. The effect of soil surface curvature on moisture and yield–Beer Sheba observation. Soil Sci. 132:367–375.

Smika, D.E., and P.W. Unger. 1986. Effect of surface residues on soil water storage. Adv. Soil Sci. 5:111–138.

Staricka, J.A., P.M. Burford, R.R. Allmaras, and W.W. Nelson. 1990. Tracing the vertical distribution of simulated shattered seeds as related to tillage. Agron. J. 82:1131–1134.

Steinbauer, G.P. and B. Grigsby. 1957. Interaction of temperature, light and moistening agent in the germination of weed seeds. Weeds. 5:175–182.

Stoller, E.W. and L.M. Wax. 1973a. Periodicity of germination and emergence of some annual weeds. Weed Sci. 21:574–580.

Stoller, E.W. and L.M. Wax. 1973b. Temperature variations in the surface layers of an agricultural soil. Weed Res. 13:273–282.

Swanton, C.J., A. Shrestha, S.Z. Knezevic, R.C. Roy, and B.R. Ball-Coelho. 2000. Influence of tillage type on vertical weed seedbank distribution in a sandy soil. Can. J. Plant Sci. 80:455–457.

Tani, M. 1982. The properties of water-table rise produced by a one-dimensional, vertical, unsaturated flow. J. Jpn. For. Soc. 64:409–418.

Taylorson, R.B. 1970. Changes in dormancy and viability of weed seeds in soils. Weed Sci. 18:265–269.

Taylorson, R.B. 1987. Environmental and chemical manipulation of weed seed dormancy. Rev. Weed Sci. 3:135–154.

Teasdale, J.R. and C.L. Mohler. 1993. Light transmittance, soil temperature, and soil moisture under residue of hairy vetch and rye. Agron. J. 85:673–680.

Thompson, K. and J.P. Grime. 1983. A comparative study of germination responses to diurnally-fluctuating temperatures. J. Appl. Eco. 20:141–156.

Tian, Y.Q., R. J. Davies-Colley, P. Gonga, and B.W. Thorrold. 2001. Estimating solar radiation on slopes of arbitrary aspect. Agric. For. Meteorol. 109:67–74.

Timm, L.C., L.F. Pires, R. Roveratti, R.C.J. Arthur, K. Reichardt, J.C.M. de Oliveira, and O.O.S. Bacchi. 2006. Field spatial and temporal patterns of soil water content and bulk density changes. Sci. Agric. 63:55–64.

Tomer, M.D., C.A. Cambardella, D.E. James, and T.B. Moorman. 2006. Surface-soil properties and water contents across two watersheds with contrasting tillage histories. Soil Sci. Soc. Am. J. 70:620–630.

Tromp-van Meerveld, H.J. and J.J. McDonnell. 2006. On the interrelations between topography, soil depth, soil moisture, transpiration rates and species distribution at the hillslope scale. Adv. Water Resour. 29:293–310.

Ueno, K. and H. Takahashi. 1997. Varietal variation and physiological basis for inhibition of wheat seed germination after excessive water treatment. Euphytica. 94:169–173.

Ueno, K. R. Fujita, and K. Yamazaki. 1999. Factors relating to seedling emergence in spring wheat. Plant Prod. 2:235–240.

Unger, P.W. 1978. Straw mulch effects on soil temperatures and sorghum germination and growth. Agron. J. 70:858–864.

Unger, P.W., and J.J. Parker. 1976. Evaporation reduction from soil with wheat, sorghum, and cotton residues. Soil Sci. Soc. Am. J. 40:938–942.

Unger, P.W., R.R. Allen, and A.F. Wiese. 1971. Tillage and herbicides for surface residue maintenance, weed control, and water conservation. J. Soil Water Conserv. 26:147–150.

Unger, P.W., G.W. Langdale, and R.I. Papendick. 1988. Role of crop residues – improving water conservation and use. p. 69–100. In W.L. Hargrove ed. Cropping strategies for efficient use of water and nitrogen. ASA Agron. no. 51. Am. Soc. Agron., Madison, WI.

Van Acker, R.C., W.J. Bullied, and M.J. du Croix Sissons. 2004. Tillage index predicts weed seedling recruitment depth. Can. J. Plant Sci. 84:319–326.

van Genuchten, M.T. 1980. A closed-form equation for predicting the hydraulic conductivity of unsaturated soils. Soil Sci. Soc. Am. J. 44:892–898.

Van Wijk, W.R. and D.A. De Vries. 1963. Periodic temperature variations in a homogeneous soil. p. 102–143. In W.R. Van Wijk ed. Physics of plant environment. North-Holland Publ. Co., Amsterdam.

Vieira, S.R., D.R. Nielsen, and J.W. Biggar. 1981. Spatial variability of field-measured infiltration rate. Soil Sci. Soc. Am. J. 45:1040–1048.

Vincent, E.M. and P.B. Cavers. 1978. The effects of wetting and drying on the subsequent germination of *Rumex crispus*. Can. J. Bot. 56:2207–2217.

Vleeshouwers, L.M. 1997. Modelling the effect of temperature, soil penetration resistance, burial depth and seed weight on pre-emergence growth of weeds. Ann. Bot. 79:553–563.

Vleeshouwers, L.M. and M.J. Kropff. 2000. Modelling field emergence patterns in arable weeds. New Phytol. 148:445–457.

Walker, P.H., G.F. Hall, and R. Protz. 1968. Relation between landform parameters and soil properties. Soil Sci Soc. Am. Proc. 32:101–104.

Walters, C., N.W. Pammenter, P. Berjak, and J. Crane. 2001. Desiccation damage, accelerated ageing and respiration in desiccation tolerant and sensitive seeds. Seed Sci. Res. 11:135–148.

Ward, J. and C.F. Shaykewich. 1972. Water absorption by wheat seeds as influenced by hydraulic properties of soil. Can. J. Soil Sci. 52:99–105.

Warrick, A.W. and H.M. van Es. 2002. Soil sampling and statistical procedures. p 1–13. In J.H. Dane and G.C. Topp ed. Methods of soil analysis. Part 4. Physical methods. Soil Sci. Soc. Am. Madison, WI.

Waterhouse, F.L. 1950. Humidity and temperature in grass microclimates with reference to insolation. Nature (London). 166:232–233.

Webster, T.M., J. Cardina, and H.M. Norquay. 1998. Tillage and seed depth effects on velvetleaf (Abutilon theophrasti) emergence. Weed Sci. 46:76–82.

Weir, A.H., P.L. Bragg, J.R. Porter, and J.H. Rayner. 1984. A winter wheat crop simulation model without water or nutrient limitations. J. Agric. Sci. 102:371–382.

Westerman, P.R., A. Hofmann, L.E.M. Vet, and W. van der Werft. 2003. Relative importance of vertebrates and invertebrates in epigeaic weed seed predation in organic cereal fields. Agric. Ecosyst. Environ. 95:417–425.

Whitney, G.G. 1991. Relation of plant species to substrate, landscape position, and aspect in north central Massachusetts. Can. J. For. Res. 21:1245–1252.

Wicks, G.A., O.C. Burnside, and C.R. Fenster. 1971. Influence of soil type and depth of planting on downy brome seed. Weed Sci. 19:82–86.

Wiese, A.F. and R.G. Davis. 1967. Weed emergence from two soils at various moistures, temperatures and depths. Weeds. 15:118–121.

Wild, A. 1988. Russell's soil conditions and plant growth. 11th ed. John Wiley and Sons, New York.

Wilson, H.K. and C.F. Hottes. 1927. Wheat germination studies with particular reference to temperature and moisture relationships. J. Am. Soc. Agron. 19:181–190.

Wood, D.M. and W.F. Morris. 1990. Ecological constraints to seedling establishment on the Pumice Plains, Mount St. Helens, Washington. Am. J. Bot. 77:1411–1418.

Wood, N. 2000. Wind flow over complex terrain: A historical perspective and the prospect for large-eddy modelling. Boundary-Layer Meteorol. 96:11–32.

Woods, L.E., and G.E. Schuman. 1988. Cultivation and slope position effects on soil organic matter. Soil Sci. Soc. Am. J. 52:1371–1376.

Wuest, S.B. 2002. Water transfer from soil to seed: The role of vapor transport. Soil Sci. Soc. Am. J. 66:1760–1763.

Wuest, S.B., S.L. Albrecht, and K.W. Skirvin. 1999. Vapor transport vs. seed–soil contact in wheat germination. Agron. J. 91:783–787.

Yadav, M.R. and G.S. Saxena. 1973. Effect of compaction and moisture content on specific heat and thermal capacity of soils. J. Indian Soc. Soil Sci. 21:129–132.

Yao, A.Y.M. 1974. A statistical model for the surface relative humidity. J. Appl. Meteorol. 13:17–21.

Yenish, J.P., J.D. Doll, and D.D. Buhler. 1992. Effects of tillage on vertical distribution and viability of weed seed in soil. Weed Sci. 40:429–433.

Young, F.J. and R.D. Hammer. 2000. Soil–landform relationships on a loess-mantled upland landscape in Missouri. Soil Sci. Soc. Am. J. 64:1443–1454.

3.0 Field Calibration of an Impedance Soil Water Probe for the Shallow Seedbed across Field Topography

3.1 ABSTRACT

Impedance soil water probes enable frequent and non-destructive determination of soil water status in situations where gravimetric soil sampling is too demanding of time and sampling space. The ThetaProbe is an impedance soil water probe requiring calibration for local soil conditions, because measurement accuracy can be affected by properties of the soil. Often, only a single calibration is performed for an experimental site. An experiment investigating the seedbed to 75 mm depth across a field topography with variable soil properties was examined to determine which soil properties affected the calibration of the ThetaProbe, and if soil-specific calibration was required to derive suitable estimates of the water status in the experiment. Experimental factors examined included hillslope aspect, hillslope position, crop residue, and soil depth. Soil properties, other than volumetric water content, significantly affecting the probe measurements were bulk density, electrical conductivity, and temperature. The probe underestimated soil water at very low water contents, and overestimated soil water at contents greater than 0.11 m^3 m^{-3}, compared to gravimetric measurements. A single calibration, not corrected for hillslope position at water content of 0.20 m^3 m^{-3}, overestimated water content by 0.02 m^3 m^{-3} in the summit hillslope position and underestimated water content by 0.04 m^3 m^{-3} in the toeslope position. A single calibration, not corrected for soil depth at a water content of 0.20 m^3 m^{-3}, overestimated water content by 0.02 m^3 m^{-3} in the 0–25 mm soil layer and underestimated water content by 0.03 m^3 m^{-3} in the 50–75 mm layer. The complexity of microsites in a shallow seedbed requires soil-specific calibration in field experiments containing heterogeneous soil properties.

3.2 INTRODUCTION

Soil water is an essential component for modeling seedling emergence of weeds (Forcella et al., 2000; Bradford, 2002). Weed seedlings germinate and emerge from a shallow soil layer over a prolonged period of time (Wiese & Davis, 1967; Forcella et al., 2000). Environmental conditions in the seedbed, including soil water, usually vary

temporally and spatially (Stoller & Wax, 1973; Oke, 1987). Heterogeneity in the seedbed environment is also influenced by variation of soil properties according to hillslope position (Brubaker et al., 1993; Ridolfia et al., 2003). To monitor the heterogeneous environment of a shallow seedbed requires frequent and incremental measurements of soil water across field topography. This requires time and resources beyond the scope of gravimetric soil sampling.

The ThetaProbe is an impedance soil water probe that provides a rapid method of estimating volumetric soil water content with minimal soil disturbance. The probe measures volumetric water by responding to changes in the relative permittivity or dielectric constant of soils (Gaskin & Miller, 1996). The relative permittivity of water has a value of 78.5 at 25°C, whereas air has a value of 1, and soil minerals range from 4.5 to 10 (Hoekstra & Delaney, 1974; Keller, 1989; Robinson & Friedman, 2003). Relative permittivity is approximately proportional to the soil water content over a wide range of field conditions (Topp et al., 1980; Gaskin & Miller, 1996). Measurements made with impedance probes are also influenced by the electrical conductivity of the soil (Sun et al., 2000; Robinson et al., 2003). The apparent permittivity as measured by the ThetaProbe can therefore be affected by the variability in several properties of the soil environment (Delta-T Devices Ltd., 1999). Consequently, calibration of the probe with gravimetric water measurements provides reassurance of accuracy.

The objectives of this study were to develop a calibration of the ThetaProbe for measurement of volumetric water content in seedbeds across field topography with variable soil properties. Physical and chemical soil properties that influence ThetaProbe measurement were identified. Site topographical and soil factors were separated by factor level to investigate their effect on probe readings of water content.

3.3 MATERIALS AND METHODS

3.3.1 Field Experiment Description

An experiment in a field containing a wide range of soil textures and soil water contents was conducted in a 64 ha annually cropped field at Graysville, MB during 2003. The experiment included four factors (hillslope aspect, hillslope position, soil residue, and soil depth). Two opposing hillslope aspects (southwest and northeast) were located at

north and south ends of the field, respectively. Each aspect contained three positions (summit, backslope and toeslope) along the hillslope gradient (Fig. 3.1) as outlined by Ruhe (1975). Each aspect covered an area approximately 60 m wide by 100 m along the hillslope gradient with an elevation rise of approximately 4 m from toeslope to summit. Six replications were randomized within each hillslope position, and two types of crop residue were applied (resident soybean residue and added oat straw at a rate of 6000 kg ha^{-1}) to each of these replicates. Three soil depths (0–25 mm, 25–50 mm and 50–75 mm) representing the range of typical weed seedling rooting depths (du Croix Sissons et al., 2000), were included within each residue plot. Individual plot size was 2 m by 4 m. The experiment was arranged as a split-plot with the whole plot factor (soil residue) arranged in a randomized complete block design on each hillslope position. Individual plots were arranged within each hillslope position in a block of two rows containing three replicates each. Blocks were arranged on the hillslope to maximize homogeneous conditions within each hillslope position.

3.3.2 Soil Physical And Chemical Properties

Soil physical and chemical properties were measured in three of the six replicates (soil water was measured in all six replicates) to characterize topography and soil factors (Table 3.1). Soil pH and electrical conductivity were measured in a 1:2 deionised water suspension with a pH and conductivity electrode, respectively (McKeague, 1978b). Organic matter content was determined by the loss on ignition (McKeague, 1978a). Particle size analysis was determined by the hydrometer method (Gee & Or, 2002). Bulk density was determined by averaging determinations on soil samples of known volume taken for gravimetric water measurement.

Soil water and soil temperature data were separated into four growth phases to represent a typical spring sigmoidal emergence curve based on cumulative degree days (GDD) using a soil temperature of base 0°C (Table 3.1). Soil temperature was recorded hourly with Stowaway Tidbit^{TM} temperature loggers (Onset Computer Corporation, 536 MacArthur Boulevard, Pocassat, MA, 02559-3450). The temperature loggers were centered within each of the three soil depths at the time of seeding in three replicates

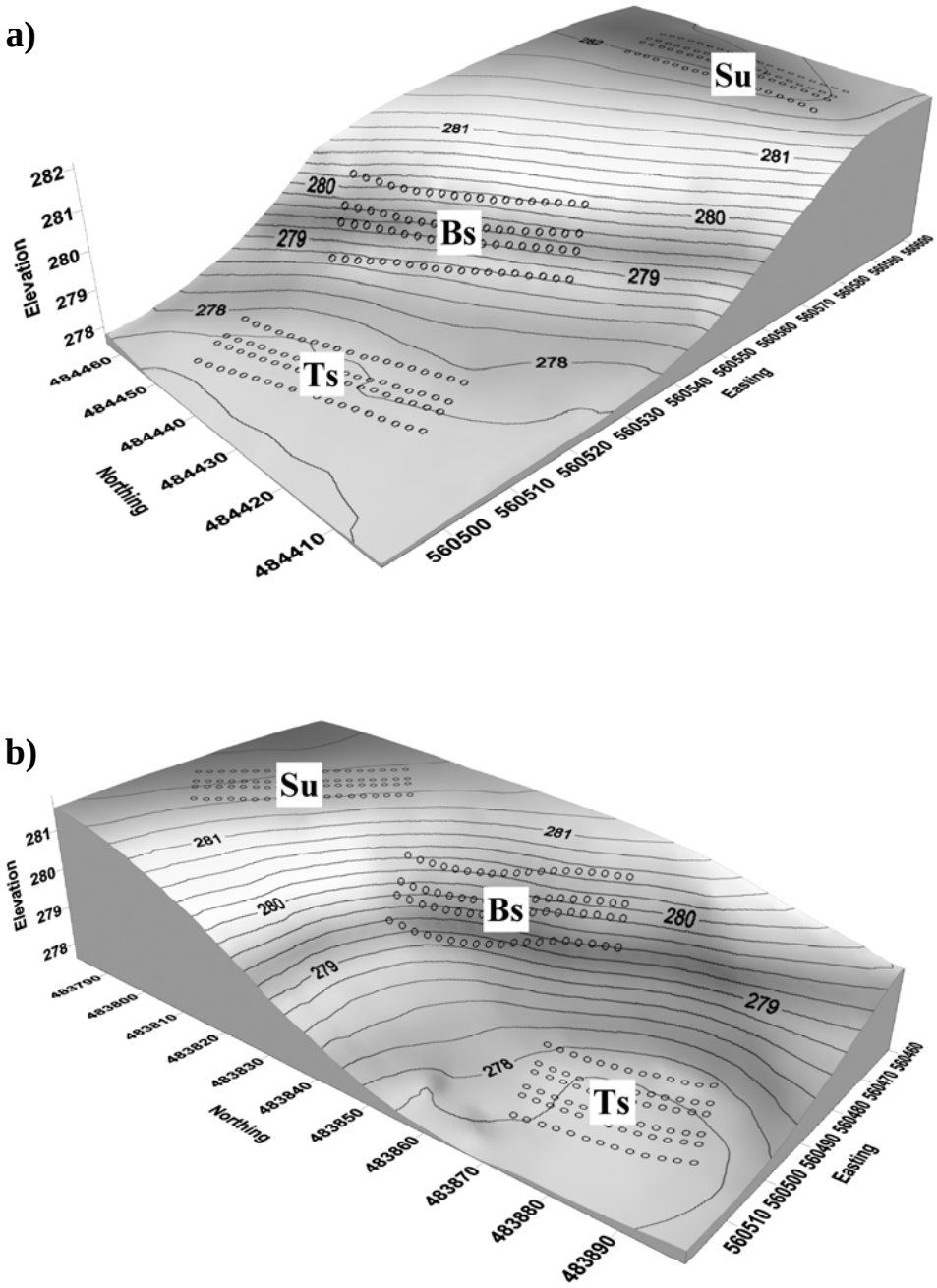

Fig. 3.1. Physiographic view of the experiment showing a) southwest and b) northeast facing hillslope aspects. Hillslope positions (Su – summit; Bs – backslope; Ts – toeslope) along the hillslope gradient are shown by blocks of small circles identifying corners of individual plots. Northing, easting, and elevation (units: m; UTM Zone 14).

Table 3.1. Soil properties of microsites across topographical and soil factors in the experimental field.

	Hillslope aspect		Hillslope position			Soil residue		Soil depth (mm)		
Soil property	SW	NE	Summit	Backslope	Toeslope	Native	Added	0–25	25–50	50–75
Water (m^3 m^{-3})†										
0–300 GDD	0.18*b*#	0.29*a*	0.19*c*	0.24*b*	0.27*a*	0.24	0.23	0.22*b*	0.23*b*	0.25*a*
300–600 GDD	0.21*a*	0.20*b*	0.16*c*	0.20*b*	0.25*a*	0.21*a*	0.20*b*	0.15*c*	0.22*b*	0.25*a*
600–900 GDD	0.15*b*	0.19*a*	0.13*c*	0.17*b*	0.21*a*	0.17	0.17	0.10*c*	0.18*b*	0.23*a*
> 900 GDD	0.17*b*	0.18*a*	0.14*c*	0.17*b*	0.21*a*	0.18	0.18	0.13*c*	0.18*b*	0.21*a*
Clay (g kg^{-1})§	147*a*	116*b*	71c	102*b*	222*a*	133	130	128*b*	128*b*	139*a*
Silt (g kg^{-1})	564*b*	598*a*	717*a*	632*b*	395*c*	580	582	585*a*	581*b*	578*c*
Sand (g kg^{-1})	289	285	212*c*	266*b*	383*a*	286	288	286*b*	291*a*	284*b*
Bulk density (g cm^{-3})	0.99*b*	1.07*a*	1.08*a*	1.08*a*	0.92*b*	1.06*a*	1.00*b*	0.96*c*	1.00*b*	1.12*a*
Temperature (°C)‡										
0–300 GDD	13.1	13.2	13.1	13.0	13.3	13.1	13.1	13.1	13.1	13.1
300–600 GDD	13.8	13.8	13.9	13.7	13.7	13.8	13.8	14.5*a*	13.6*b*	13.2*c*
600–900 GDD	18.4	18.0	18.1	18.3	18.2	17.8*b*	18.6*a*	19.2*a*	17.9*b*	17.5*c*
> 900 GDD	19.0*a*	18.5*b*	18.8	18.7	18.7	18.4*b*	19.2*a*	19.3*a*	18.6*b*	18.4*c*
Organic matter (g kg^{-1})	45*a*	41*b*	39*b*	37*b*	52*a*	43	43	44*a*	43*b*	41*c*
pH ($-\log[H^+]$)	7.8*a*	7.3*b*	7.0*c*	8.0*a*	7.8*b*	7.6	7.6	7.6	7.6	7.6
EC (dS m^{-1})	1.12	1.00	0.74*c*	1.13*b*	1.32*a*	1.05	1.07	1.01	1.07	1.09

†‡ Mean volumetric water and soil temperature for time periods based on cumulative daily soil growing degree days (GDD) using base 0°C. Time periods represent a typical sigmoidal emergence curve separated into phases of lag (0–300 GDD), exponential (300–600 GDD), stationary (600–900 GDD) and late stationary (>900 GDD). Seeding occurred at 271 GDD.

§ Particle size of clay (<0.002mm), silt (0.002–0.05mm), and sand (0.05–2.0mm).

Within topographical or soil factor, means of each soil property followed by different letters are significantly different at $P \leq 0.05$ according to Fisher's protected LSD.

across all factors. Mean soil temperature measurements for each emergence phase were calculated by averaging measurements within each phase.

Soil water measurements with a ThetaProbe^{TM} type ML2x (Delta-T Devices Ltd., 1999), and gravimetric water of soil cores of a known volume, were taken on 16 occasions from six replicates during the early growing season from May 6 until July 20 (271–1590 GDD). Mean water contents for each emergence phase were derived by averaging all the individual values. The probe is influenced by a cylindrical soil volume approximately 60 mm long by 40 mm diameter (Delta-T Devices Ltd., 1999). Instantaneous readouts were taken from the probe with a ThetaMeter^{TM} type HH1 (Delta-T Devices Ltd., 1997) using the manufacturer's integrated calibration.

To measure shallow increments in the soil profile, a hole was dug to expose a vertical face of soil into which a guide was placed to position the probe horizontally at each 25 mm increment of depth. Soil cores for gravimetric measurements were taken by pressing a metal ring with a tapered edge (to reduce soil compaction) into the soil profile. A vertical face was cut in the soil profile beside the ring to enable a trowel to cut the soil level at the bottom of the ring before extraction for each 25 mm increment of depth. Gravimetric water was determined (48 h drying at 80ºC) and volumetric water was then calculated from the bulk density of the soil sample. Subsequent measurements taken during the season were from undisturbed locations within each plot to avoid artifacts caused by the previous soil excavations. A total of 3,456 paired (probe and gravimetric) measurements were taken (2 hillslope aspects × 3 hillslope positions × 6 replicates × 2 soil residues × 3 soil depths on each of 16 occasions).

3.3.3 Data Analyses

Multiple regression with stepwise selection was used to model the relationship between a set of soil physical and chemical variables and probe readings of volumetric water content by fitting a linear regression equation to observed data. The variables selected were volumetric soil water content, clay, silt and sand content, bulk density, organic matter content, cation exchange capacity, pH, electrical conductivity, soil temperature, nitrogen, phosphorous, potassium, sulfur, calcium, magnesium, and sodium. Multicollinearity was identified and autocorrelated terms were removed from the model.

Linear and quadratic equations were investigated for the stepwise regression, however the quadratic terms did not improve model performance. The coefficient of multiple determination (R^2) was used to explain the proportion of variance of deviation between probe readings and volumetric soil water content. All soil properties meeting the 0.05 significance level in the full model were included in the reduced model (Table 3.2).

Table 3.2. Summary of factors influencing readings taken with the ThetaProbe meeting the 0.05 significance level for entry into the model.

Soil property	Partial R^2	Model R^2	Mallow's C(p)	$P > F$
Volumetric water	0.457	0.457	51.14	<.001
Temperature	0.009	0.466	26.70	<.001
Bulk density	0.005	0.471	13.00	<.001
Electrical conductivity	0.004	0.475	3.97	<.001

Linear regression analysis (SAS Institute, 2004) was used to determine significance of intercepts and slopes for model calibrations of soil water content measured by the probe across the topographical and soil factors. Analysis of covariance (SAS Institute, 2004) was used to determine model selection based on significance ($P \leq 0.05$) of intercepts and slopes. All model slopes were significantly different from 0 ($P \leq 0.001$). The data were examined to establish if they conformed to general (different intercepts, different slopes), parallel (different intercepts, common slope), concurrent (common intercept, different slopes), or coincident (common intercept, common slope) models (Weisberg, 2005).

3.4 RESULTS AND DISCUSSION

3.4.1 Soil Physical And Chemical Properties

The significance of soil properties influencing the deviation of probe reading from volumetric soil water content is shown in Table 3.2. The appropriate reduced model included four soil properties analyzed by contribution to model R^2 and Mallow's (C)p statistic (Table 3.2). The regression model giving the best prediction was:

$$\theta_{v(p)} = -0.235 + 1.459\ \theta_{v(g)} + 0.147\ \rho_b + 0.042\ S + 0.006\ T \qquad [1]$$

where $\theta_{v(p)}$ is the volumetric water content measured by the Thetaprobe (units: $m^3\ m^{-3}$), $\theta_{v(g)}$ is the volumetric water content measured gravimetrically (units: $m^3\ m^{-3}$), ρ_b is the dry bulk density (units: g cm^{-3}), S is the electrical conductivity (units: dS m^{-1}), and T is the soil temperature (units: ºC).

The regression model indicated that the probe overestimated soil water. Using a ThetaProbe, Robinson et al. (1999) measured an overestimation of apparent permittivity of the soil by 1.5 compared to a time domain reflectometry (TDR) probe. Overestimation of soil water with the ThetaProbe may have been the result of compaction of the soil close to the electrodes (Rothe et al., 1997; Robinson et al., 1999). In our experiment, greater water contents occurred in soil with greater clay content (toeslope position), which may have compacted more readily compared to the sandier soil in the summit position (Table 3.1). Robinson et al. (1999) also suggested that a strong bias in the sensitivity of the probe to the region close to the central electrode may have contributed to overestimation of water content. In contrast, results of an experiment with soil in pots by Blanc and Dick (2003) showed that the ThetaProbe underestimated soil water by 12.2 to 21.8% of the total soil water content, for peat and brown soils, respectively. The authors suggested that repeat measurements in the same locations may have compacted soil around the insertion rods, causing a reduction of the soil pore volume or air gaps around the rods, both of which can result in an underestimation of water content. Soil compaction was avoided during our experiment by ensuring that repeat measurements were taken at different locations within each plot.

Bulk density positively affected the probe measurements of soil water content. Bulk density varied with topography and with soil residue and depth (Table 3.1). Soil compaction caused by insertion of the electrodes into the soil may have accounted for unmeasured additional bulk density resulting in overestimation of water (Robinson et al., 1999). Whalley et al. (2004) concluded that including bulk density did not improve the calibration for an impedance probe, possibly as a result of spatial variation between bulk density and water measurements. Inclusion of bulk density in the calibration equation has been shown to improve the calibration of TDR soil moisture sensors (Topp et al., 1980; Malicki et al., 1996). Soil bulk density has also been used to obtain a consistent set of calibration curves of relative permittivity as a function of gravimetric water content and

bulk density (Perdok et al., 1996). Bulk density impact on apparent permittivity is confounded by the fact that bulk density is also used in the calculation of volumetric soil water.

Electrical conductivity of the soil positively influenced the probe water content readings. Electrical conductivity has been shown to increase the apparent permittivity of the soil (Robinson et al., 1999; Topp et al., 2000). The signal frequency used by the ThetaProbe minimizes the effect of ionic conductivity but only for salinities below 250 mS m^{-1} (Delta-T Devices Ltd., 1999; Robinson et al., 1999). Electrical conductivity values across the topography in our study ranged from 74 mS m^{-1} in the summit to 132 mS m^{-1} in the toeslope (Table 3.1) suggesting that the effect of electrical conductivity would be limited. Baumhardt et al. (2000) found that the effect of adding 1130 mS m^{-1} saline water to soil increased predicted water content by 0.10 m^3 m^{-3} more than tap water as measured by a capacitance probe.

A small but significant temperature effect increased the probe water content readings. Temperatures differed by 1.7°C across depths in the seedbed (Table 3.1). Field studies by Kaleita et al. (2005) also indicated a small positive effect of temperature, but laboratory studies by the same authors showed a small negative effect of temperature. Seyfried and Murdock (2004) also showed a small positive temperature effect on the measurement ability of an impedance probe with oven dried soils, and variable response (0.03 m^3 m^{-3} at 25°C) with saturated soils.

3.4.2 Topographical And Soil Experimental Factors

A single calibration for the probe measurements pooled across all experimental factors indicated a linear relationship with gravimetric water content having an R^2 of 0.46 (Table 3.3; Fig. 3.2). Using the manufacturer's built in calibration, the probe underestimated soil water at contents less than 0.11 m^3 m^{-3}, and overestimated water at contents greater than 0.11 m^3 m^{-3} (Fig. 3.2).

The water measurements were separated by experimental factor levels (Fig. 3.3), to determine if differences existed among levels of a factor, whereby separate calibrations of each level could improve model fit. The effects of site topography and soil factors on probe readings were included because data on soil properties that influence the probe

Table 3.3. Parameter estimates for linear models for the relationship between ThetaProbe soil water measurements and volumetric soil water content for combined and individual levels of hillslope aspect, hillslope position, soil residue, and soil depth.

Factor	No	Intercept	Slope	R^2
Combined factors				
All measurements	3456	0.074 (0.002)†	0.322 (0.006)	0.46
Hillslope aspect				
Southwest	1728	0.071 (0.003)	0.319 (0.009)	0.43
Northeast	1728	0.079 (0.003)	0.324 (0.009)	0.49
P > *F*‡		0.071	0.683	0.46§
Hillslope position				
Summit (Su)	1152	0.051 (0.003)	0.337 (0.011)	0.48
Backslope (Bs)	1152	0.073 (0.004)	0.312 (0.010)	0.46
Toeslope (Ts)	1152	0.124 (0.005)	0.255 (0.011)	0.35
P > *F*				
All		<.001	<.001	0.51
Su vs Bs		<.001	<.001	0.50
Su vs Ts		<.001	<.001	0.53
Bs vs Ts		<.001	<.001	0.44
Soil residue				
Native	1728	0.080 (0.003)	0.311 (0.009)	0.45
Added	1728	0.069 (0.003)	0.334 (0.009)	0.46
P > *F*		0.015	0.069	0.46
Soil depth (mm)				
0–25	1152	0.060 (0.004)	0.301 (0.015)	0.28
25–50	1152	0.099 (0.004)	0.260 (0.012)	0.33
50–75	1152	0.115 (0.005)	0.266 (0.010)	0.40
P > *F*				
All		<.001	<.001	0.50
0–25 vs 25–50		<.001	0.030	0.42
0–25 vs 50–75		<.001	0.048	0.55
25–50 vs 50–75		0.014	0.718	0.40

† Linear regression parameter estimates ($P \leq 0.001$) are followed by standard errors in parentheses.
‡ Significance of ANCOVA for difference among or between parameter estimates ($P \leq 0.05$).
§ One R^2 value is determined for the model fit among or between levels of a factor.

readings may not be available to researchers. Hence, calibration of the probe can be accomplished by separating individual levels of an experimental factor.

Hillslope aspect conformed to the coincident model (Table 3.3; Fig. 3.3). Differences between aspects for a number of soil properties, including soil water, bulk density, and temperature (only in the late stationary phase) (Table 3.1) were insufficient to affect model calibration.

The soil water measurements for hillslope position conformed to the general model (Table 3.3; Fig. 3.3). A single calibration, not corrected for hillslope position at

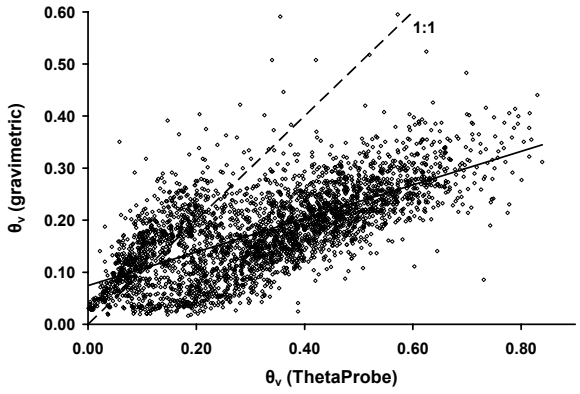

Fig. 3.2. Single calibration of volumetric water content measured by the ThetaProbe with volumetric water content measured gravimetrically.

water content of 0.20 m^3 m^{-3}, overestimated water content by 0.02 m^3 m^{-3} in the summit hillslope position and underestimated water content by 0.04 m^3 m^{-3} in the toeslope position (Fig. 3.4). Differences in bulk density between the upper two hillslope positions and the toeslope position may have necessitated a separate calibration for levels of hillslope position. In addition to bulk density, there were significant differences in texture and organic matter among the hillslope positions (Table 3.1). The greatest difference in soil texture existed among hillslope positions compared to other factor levels in the experiment (Table 3.1). The soil in the toeslope positions had greater content of clay that becomes sticky when wet and hard when dry, and may have caused variability in the soil due to localized compaction of soil when inserting the probe. Electrical conductivity exhibited the greatest range among hillslope positions compared to the other experimental factors (Table 3.1). Although soil temperature did not differ among hillslope positions, soil water had a maximum range of 0.09 m^3 m^{-3} among positions, with value in toeslopes greater than those in summit positions (Table 3.1).

Soil residue conformed to the parallel model (Table 3.3; Fig. 3.3). A reduction in bulk density in the added soil residue treatment required a separate calibration for each residue level. A single calibration not corrected for soil residue overestimated water content by less than 0.01 m^3 m^{-3} in the added residue treatment and underestimated water content by less than 0.01 m^3 m^{-3} in the native residue treatment (Fig. 3.4).

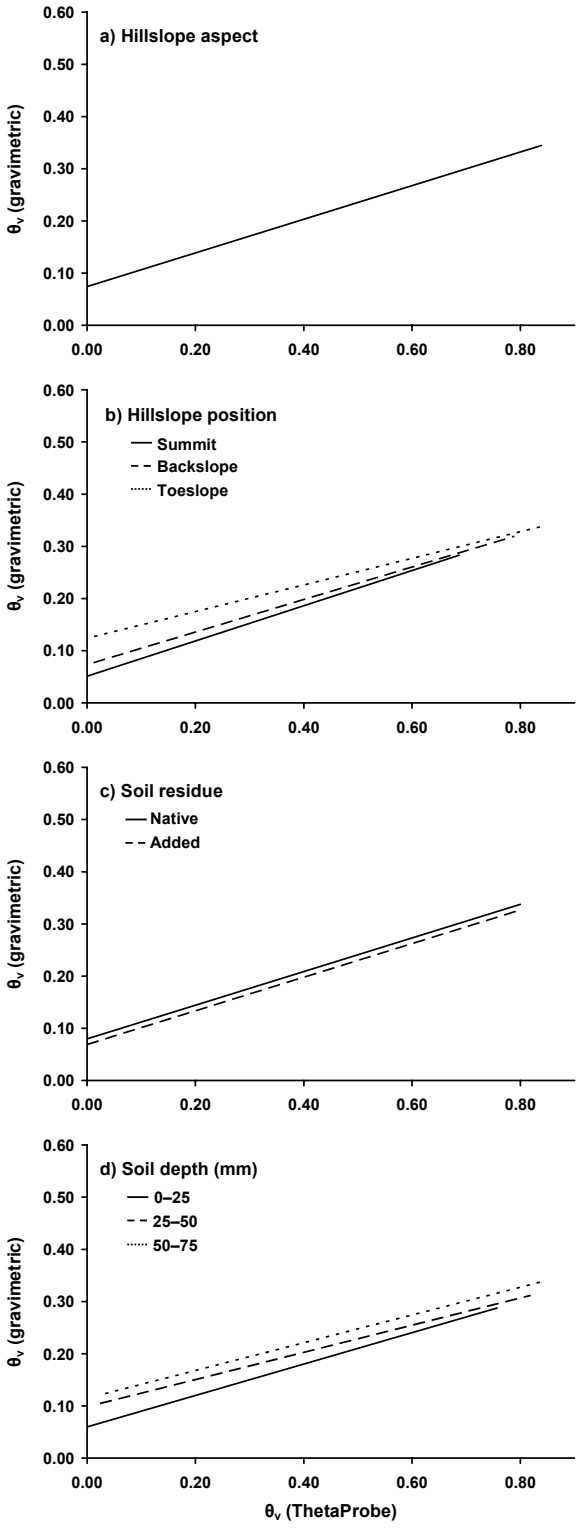

Fig. 3.3. Field calibration of volumetric water content measured by the ThetaProbe with volumetric water content measured gravimetrically, corrected for a) hillslope aspect, b) hillslope position, c) soil residue, and d) soil depth.

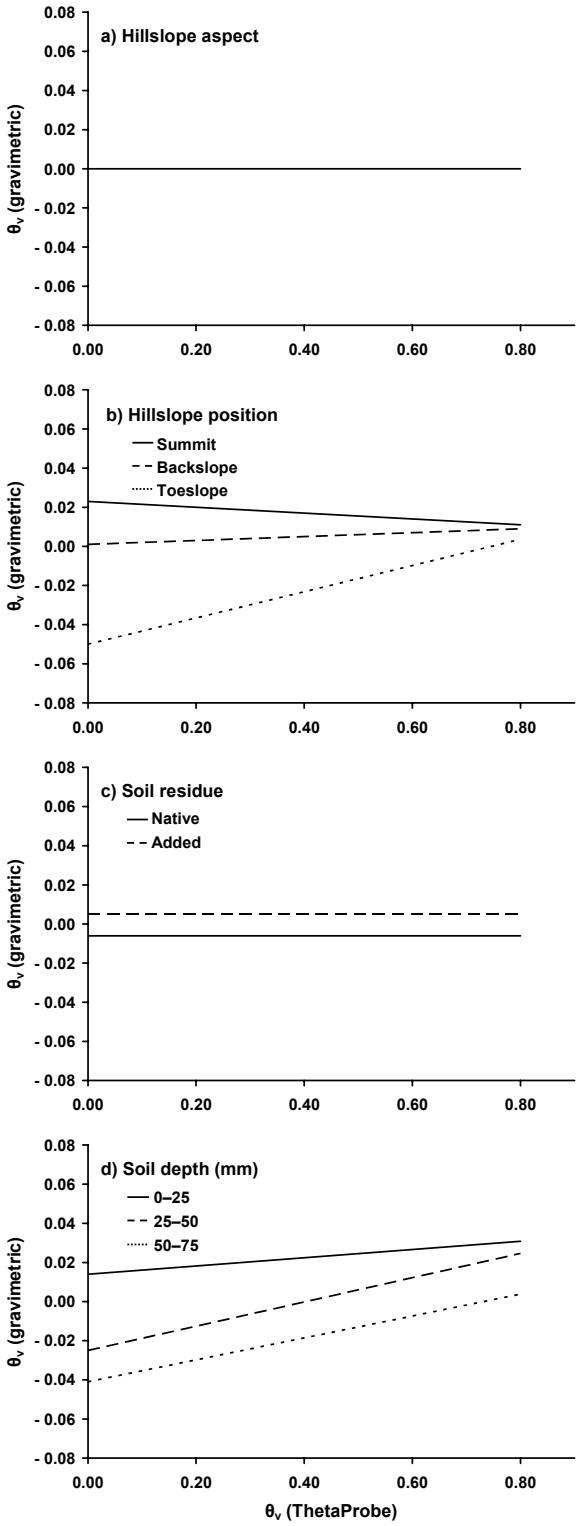

Fig. 3.4. Deviation of a single calibration of volumetric water content measured by the ThetaProbe not having a calibration corrected for a) hillslope aspect, b) hillslope position, c) soil residue, and d) soil depth.

Soil depth was separated significantly by increment in the seedbed and conformed to the general model (Table 3.3; Fig. 3.3). A single calibration, not corrected for soil depth at water content of 0.20 m^3 m^{-3}, overestimated water content by 0.02 m^3 m^{-3} in the 0–25 mm soil layer and underestimated water content by 0.03 m^3 m^{-3} in the 50–75 mm layer (Fig. 3.4). Water content increased with depth, with a maximum range of 0.13 m^3 m^{-3} (Table 3.1). Soil temperature decreased with depth, with a maximum range of 1.7°C. Bulk density increased 0.16 g cm^{-3} with soil depth (Table 3.1).

3.5 CONCLUSIONS

Soil properties influencing the deviation of Thetaprobe water content readings from gravimetric water content were bulk density, electrical conductivity and temperature. The probe underestimated soil water at very low water contents, perhaps because of air pockets in the loose, dry soil, but it overestimated water at contents greater than 0.11 m^3 m^{-3}. Separate calibrations were required to take account of variation in soil bulk density, electrical conductivity and temperature. Separating the soil water measurements by hillslope position, soil residue, and soil depth, also produced significantly different calibrations due to differences in the underlying soil properties. This study emphasizes the need to investigate multiple calibrations for an impedance soil water probe in situations where factors vary across field topography and/or with soil depth. The narrow range of values for soil properties influencing the probe readings in our study may limit the application of the multiple regression model for other sites. Field experimenters lacking measurements for the soil properties that influence probe readings can consider calibration using the same approach as used in our work. To avoid misleading soil water content results because of inadequate calibration, separate calibration of topographical and/or soil depth levels can account for variation in underlying soil properties influencing the probe readings.

3.6 REFERENCES

Baumhardt, R.L., R.J. Lascano, and S.R. Evett. 2000. Soil material, temperature, and salinity effects on calibration of multisensor capacitance probes. Soil Sci. Soc. Am. J. 64:1940–1946.

Blanc, L. and J.M. Dick. 2003. Errors in repeated measurements of soil water content in pots using a ThetaProbe. Soil Use Manage. 19:87–88.

Bradford, K.J. 2002. Applications of hydrothermal time to quantifying and modeling seed germination and dormancy. Weed Sci. 50:248–260.

Brubaker, S.C., A.J. Jones, D.T. Lewis, and K. Frank. 1993. Soil properties associated with landscape position. Soil Sci. Soc. Am. J. 57:235–239.

Delta-T Devices Ltd. 1997. ThetaMeter™ hand-held readout unit for ThetaProbe type HH1 user manual. HH1-UM-2. Cambridge, CB5 0EJ, England.

Delta-T Devices Ltd. 1999. ThetaProbe™ soil water sensor type ML2x user manual. v1.21. Cambridge, CB5 0EJ, England.

du Croix Sissons, M.J., R.C. Van Acker, D.A. Derksen, and A.G. Thomas. 2000. Depth of seedling recruitment of five weed species measured in situ in conventional- and zero-tillage fields. Weed Sci. 48:327–332.

Forcella, F., R.L. Benech-Arnold, R. Sanchez, and C.M. Ghersa. 2000. Modeling weed emergence. Field Crops Res. 67:123–139.

Gaskin, G.J. and J.D. Miller. 1996. Measurement of soil water content using a simplified impedance measuring technique. J. Agric. Eng. Res. 63:153–160.

Gee, G.W. and D. Or. 2002. Particle size analysis. p. 255–293. In J.H. Dane and G.C. Topp ed. Methods of soil analysis. Soil Sci. Soc. Am., Madison, WI.

Hoekstra, P. and A. Delaney. 1974. Dielectric properties of soils at UHF and microwave frequencies. J. Geophys. Res. 79:1699–1708.

Kaleita, A.L., J.L. Heitman, and S.D. Logsdon. 2005. Field calibration of the Theta Probe for Des Moines lobe soils. Appl. Eng. Agric. 21:865–870.

Keller, G.V. 1989. Electrical properties. p. 359–427. In R.S. Carmichael ed. CRC practical handbook of physical properties of rocks and minerals. CRC Press, Boca Raton, FL.

Malicki, M.A., R. Plagge, and C.H. Roth. 1996. Improving the calibration of dielectric TDR soil moisture determination taking into account the soil solid. Eur. J. Soil Sci. 47:357–366.

McKeague, J.A. 1978a. Manual on soil sampling and methods of analysis. Method 3.8, loss on ignition. Can. Soc. Soil Sci., Ottawa, ON, Canada.

McKeague, J.A. 1978b. Manual on soil sampling and methods of analysis. Method 4.12, 1:2 soil:water ratio. Can. Soc. Soil Sci., Ottawa, ON, Canada.

Oke, T.R. 1987. Climates of non-uniform terrain. p. 158–189. In T.R. Oke ed. Boundary layer climates. Routledge Press, New York.

Perdok, U.D., B. Kroesbergen, and M.A. Hilhorst. 1996. Influence of gravimetric water content and bulk density on the dielectric properties of soil. Eur. J. Soil Sci. 47:367–371.

Ridolfia, L., P. D'Odoricoc, A. Porporatoa, and I. Rodriguez-Iturbe. 2003. Stochastic soil moisture dynamics along a hillslope. J. Hydrol. 272:264–275.

Robinson, D.A., C.M.K. Gardner, and J.D. Cooper. 1999. Measurement of relative permittivity in sandy soils using TDR, capacitance and theta probes: comparison, including the effects of bulk soil electrical conductivity. J. Hydrol. 223:198–211.

Robinson D.A. and S.P. Friedman. 2003. A method for measuring the solid particle permittivity or electrical conductivity of rocks, sediments, and granular materials. J. Geophys. Res. 5:1–9.

Robinson, D.A., S.B. Jones, J.M. Wraith, D. Or, and S.P. Friedman. 2003. A review of advances in dielectric and electrical conductivity measurement in soils using time domain reflectometry. Vadose Zone J. 2:444–475.

Rothe, A., W. Weis, K. Kreutzer, D. Matthies, U. Hess, and B. Ansorge. 1997. Changes in soil structure caused by the installation of time domain reflectometry probes and their influence on the measurement of soil moisture. Water Resour. Res. 33:1585–1593.

Ruhe R.V. 1975. Hillslopes. p. 99–123. In R.V. Ruhe ed. Geomorphology: Geomorphic processes and surficial geology. Houghton Mifflin, Boston, MA.

SAS Institute, Inc. 2004. SAS/STAT® user's guide. Version 9. SAS Institute, Inc., Cary, NC.

Seyfried, M.S. and M.D. Murdock. 2004. Measurement of soil water content with a 50-MHz soil dielectric sensor. Soil Sci. Soc. Am. J. 68:394–403.

Stoller, E.W. and L.M. Wax. 1973. Temperature variations in the surface layers of an agricultural soil. Weed Res. 13:273–282.

Sun, Z.J., G.D. Young, R.A. McFarlane, and B.M. Chambers. 2000. The effect of soil electrical conductivity on moisture determination using time-domain reflectometry in sandy soil. Can. J. Soil Sci. 80:13–22.

Topp, G.C., J.L. Davis, and A.P. Annan. 1980. Electromagnetic determination of soil water content: Measurements in coaxial transmission lines. Water Resour. Res. 16:574–582.

Topp, G.C., S. Zegelin, and I. White. 2000. Impacts of the real and imaginary components of relative permittivity on time domain reflectometry measurements in soils. Soil Sci. Soc. Am. J. 64:1244–1252.

Weisberg, S. 2005. Applied linear regression. Wiley-Interscience, New York.

Whalley, W.R., R.E. Cope, C.J. Nicholl, and A.P. Whitmore. 2004. In-field calibration of a dielectric soil moisture meter designed for use in an access tube. Soil Use Manage. 20:203–206.

Wiese, A.F. and R.G. Davis. 1967. Weed emergence from two soils at various moistures, temperatures and depths. Weeds. 15:118–121.

4.0 Microclimatic and Topographic Influences on the Hydrothermal Environment of the Seedling Recruitment Microsite

4.1 ABSTRACT

Predictive modeling of factors of the soil environment is essential to determine microsite conditions conducive to weed recruitment. An experiment was established in 2003 and 2004 across topography within an annually cropped field in south-central Manitoba to determine the effects that hillslope aspect and position, and soil residue and depth would have on the microsite environment within the shallow seedling recruitment zone. Microclimatic, topographic, soil surface and soil properties were assessed in the context of the weed recruitment microsite. Solar radiation received on the southwest backslope was greater compared to the northeast aspect, but did not result in higher soil temperatures within the recruitment zone. Soil temperature was uniform between years and decreased with depth in the seedling recruitment zone. Soil temperature fluctuation decreased with soil depth and lower hillslope position. Soil water potential varied between years, as well as with topography and soil depth. Soil texture varied across the topography and soil depth, whereas soil bulk density differed across all experimental factors. Soil chemical properties differed primarily across the topography, and to a lesser extent, with soil depth. The soil residue treatment had little influence on the soil environment. The seedling recruitment microsite is subject to diverse spatial and temporal influences from microclimate, topographic, soil surface, and edaphic properties. The variability of the recruitment zone environment would be expected to have a diverse effect on weed recruitment from heterogeneous seedling microsites within the recruitment zone. The results of this study indicate that topography influences microsite properties within the shallow profile of the seedling recruitment zone. Microsite properties were shown to vary with depth in the recruitment zone. Weed recruitment would therefore be influenced by both topographic effects on microsite conditions and vertical location of the microsite in the recruitment zone. This study indicated that hillslope position and depth of recruitment are important factors influencing the weed recruitment microsite accounting for hillslope scale complexity and heterogeneity. Site-specific weed recruitment models need to include topographic and soil depth as factors

that affect weed recruitment to generate robust models that reflect the spatial and temporal dynamics of the recruitment zone environment.

4.2 ABBREVIATIONS

DOY, day of year; GDD_{air}, air growing degree days; GDD_{soil}, soil growing degree days.

4.3 INTRODUCTION

Weed seedling recruitment (germination and emergence) is a primary factor determining the level of weed interference in crops. Successful weed seedling recruitment occurs as a result of dormancy breaking, germination and emergence. Since not all seeds of a weed species recruit from the seedbank in a given season (Roberts, 1986; Cousens and Mortimer, 1995), weed recruitment studies focus on predictive modeling of factors influencing the incidence of weeds in the current season. The underlying factors governing whether a seed will recruit to germinate and emerge are the conditions of the soil environment in which a seed resides (recruitment microsite). The influence of properties of the seed microsite on the ability of weed seeds to germinate result in seedling recruitment across field topography that is always patchy in nature. Considering the importance of weed seedling recruitment to the success of a weed species, greater understanding is required of the characteristics of the recruitment microsite from which a weed seedling originates.

Determining the environmental conditions that affect timing and extent of weed seedling recruitment is relevant for modeling an integrated weed control decision-making strategy. Timing and extent of weed seedling recruitment is difficult to predict due to interactions of microclimate, soil properties, and management practices that create microsite conditions that influence the dormancy state of weed seeds and the recruitment of weed seedlings from a shallow zone in the upper soil profile (Buhler, 1995; du Croix Sissons et al., 2000; Bàrberi and Lo Cascio, 2001). Soil disturbance is the primary cause of vertical movement of weed seeds (Pareja et al., 1985; Cousens and Moss, 1990; Staricka et al., 1990; Mohler and Galford, 1997), therefore, burial and movement of seeds into unique microsites occurs within the recruitment zone during tillage operations. Weeds generally occur in irregular patches across fields (Cardina et al., 1997), due in part

to heterogeneous recruitment, which is restricted by microsite limitations through the influence of the non-uniform soil environment across the vertical and horizontal topography of a field (Brubaker et al., 1993; Ridolfia et al., 2003).

Weed recruitment is influenced by both temporal and spatial dimensions in the field topography. Identifying weed recruitment across topography requires an understanding of the varying nature of the soil environment associated with a particular time and location in the topography (Fenner and Thompson, 2005). Sources of variability in soil properties across topography need to be considered in recruitment studies because germination modeling may be biased if generalizations are made over a heterogeneous topography. The sources of spatial and temporal variability in the soil environment may be the result of either natural (topographic, edaphic) or management (tillage, residue cover) related processes. Edaphic characteristics have been shown to vary with depth in the soil (Reuss et al., 2001; Reid and Van Acker, 2005) and position in the topography (Ross and Van Acker, 2005). Solar radiation received by the soil surface is a major determinant of its environment (Oke, 1987). Hillslope aspect and gradient can affect the energy and water balance of the recruitment zone due to spatial discontinuity and gradients of microclimate. Spatial variation of soil surface character and topography affect the way radiation is received and retained at the soil surface (Geiger, 1965; Oke, 1987). The amount and type of residue cover on the surface of a field can further affect the energy and water balance of the soil environment through reflective and insulation properties of the residue (Horton et al., 1994; Lowery and Stoltenberg, 1998).

A microsite refers to the soil environment immediately surrounding the seed that has a direct influence on seed germination and emergence (Harper 1977; Eriksson and Ehrlén 1992). Microsite conditions in the recruitment zone can vary temporally (Stoller and Wax, 1973; Egley, 1986; Bullied et al., 2003) and spatially (Boyd and Van Acker, 2004; Reid and Van Acker, 2005) within the soil profile. A favorable microsite for seedling recruitment includes all of the environmental conditions necessary for recruitment of a particular weed (Bibbey 1935). Although occurrence of some weeds are influenced by specific physical (Pareja and Staniforth, 1985; Reuss et al., 2001) or chemical (Egley, 1986; Hurtt and Taylorson, 1986; Andreasen and Streibig, 1991; Medlin et al., 2001) properties of the soil environment, in general, weed seedling emergence has

been predicted reliably using the soil processes of soil water and soil heat transfer as the two most important predictors of recruitment (Forcella et al., 2000; Bradford, 2002; Leguizamón et al., 2005). In addition to seasonal accumulations of soil heat, diurnal fluctuation of soil heat can affect recruitment of many weed species (Probert et al., 1986; Kegode et al., 1998; Chachalis and Reddy, 2000). To obtain a better understanding of the soil processes associated with weed recruitment, soil physical properties associated with the soil processes of soil water and soil heat transfer are either measured directly or modeled. The condition of the soil microsite at a given time and space are represented by state variables (water content and temperature) resulting from one or more soil processes, as governed by the soil properties associated with each process. Soil water and soil temperature are often a result of interactions between soil properties across topography that influence the processes of soil water (Hanna et al., 1982; Ridofia et al., 2003) and soil heat (Hares and Novak, 1992) transfer. The objectives of this study were to identify 1) influences of above-ground microclimate on the seedling recruitment zone environment across field topography, 2) influences of hillslope aspect and position, and soil residue and depth on the recruitment zone environment, and 3) effects of topographical, soil cover and soil depth interactions on the recruitment zone environment.

4.4 MATERIALS AND METHODS

4.4.1 Field Experiment

The experiment was established in 2003 and 2004 across a topography within an annually cropped farmer's field near Graysville in south-central Manitoba, Canada (49º30´ N, 98º09´ W). Three positions along the vertical hillslope (summit, backslope and toeslope) were established at each of two locations within the field having opposing aspects (southwest and northeast). Each aspect covered an area of approximately one hectare. Soil types occurring within the plot areas are described in detail in Table 4.1.

The experiment was organized as a split-plot design with the whole plot factor arranged in a randomized complete block design on each hillslope position. The experiment included five factors (hillslope aspect, hillslope position, year, soil residue, soil depth). Blocks of six replications were randomized and arranged perpendicular to the gradient to maximize homogeneous conditions at each hillslope position. The two years

(2003 and 2004) were randomized within replication, enabling the exact same topography to be overlaid by the experiment in each year of the study. Soil residue level (native and added) was randomized within year. Soil depth in three 25-mm increments was sampled within each plot. Individual plot size was 2 m by 4 m.

Table 4.1. Classification of soil types occurring within the hillslope aspects and positions of the experiment.

	Soil series (soil symbol)		
	Almissipi (ALS)	Gervais(GVS)	Willowbend (WWB)
Hillslope			
Aspect	northeast	southwest	southwest
Position(s)	summit, backslope, toeslope	summit	backslope, toeslope
Soil classification			
Canadian†	Gleyed Rego Black Chernozem	Gleyed Cumulic Regosol	Rego Humic Gleysol
US‡	Udic Boroll	Mollic Udifluvent	Typic Agriaquoll
Family particle size	sandy	loamy	loamy
Surface texture	loamy fine sand	silty clay	loam
Soil drainage	imperfect	imperfect	poor
Mode of deposition	lacustrine	fluvial	fluvial

† Soil Classification Working Group (1998).
‡ Soil Survey Staff (1999).

The experiment was established on previous soybean (*Glycine max* [L.] Merr.) residue. Residue treatments included the presence or absence of 6000 kg ha^{-1} finely chopped oat (*Avena sativa* L.) straw on a dry weight basis in addition to native soybean residue. In treatments with high residue, the oat straw was manually spread evenly over the entire plot. Plots were then fertilized by broadcasting a blend of 10.4 kg ha^{-1} actual N, 8.7 kg ha^{-1} actual P, 8.3 kg ha^{-1} actual K and 3.3 kg ha^{-1} actual S on 1 May [Day of Year (DOY) 121] in 2003 and 30 April (DOY 121) in 2004 to mimic normal farming practices and facilitate the accompanying biotic section of the experiment. Plots were rototilled to a depth of 75 mm to incorporate and distribute the oat straw and fertilizer throughout the seedling recruitment zone.

4.4.2 Microclimate

Microclimate data were recorded at each hillslope position by a HOBO™ Weather Station with environmental sensors (Onset Computer Corporation, 536 MacArthur Boulevard, Pocassat, MA, 02559-3450). Air temperature was logged hourly

at a height of 1.5 m above the soil surface with HOBO^{TM} temperature data loggers fitted with a solar radiation shield beginning 9 May in 2003 and 2 May in 2004. Accumulated air growing degree days (GDD_{air}) using a base of 0 C was derived from the mean of daily maximum and daily minimum air temperatures. Precipitation was measured with tipping bucket rain gauges at a height of 1.5 m above the soil surface beginning 9 May in 2003 and 2 May 2004. HOBO^{TM} Weather Station data loggers were installed 26 May in 2003 and 2 May in 2004 with hygrometers fitted with a solar radiation shield to monitor hourly relative humidity, silicon pyranometers to monitor hourly total incoming solar radiation (300–1100 nm), and 3 cup anemometers to monitor hourly wind speed. Relative humidity sensors and anemometers were mounted at 1.5 m above the soil surface. Pyranometers were mounted 15 cm above the soil surface on a leveled base at each summit position and on a base parallel to the soil surface at each backslope position. Shortwave incoming solar radiation and albedo were measured instantaneously on all plots with a LI-COR model LI-200 pyranometer and model LI-1000 handheld logger (LI-COR Biosciences, 4421 Superior Street, Lincoln, NE, 68504-0425) as close as possible to solar noon. Instantaneous shortwave radiation was measured by placing the pyranometer on a base parallel to the soil surface. Albedo was measured by facing the pyranometer downwards 20 cm from the soil surface supported on a wire U-shaped frame. Albedo was expressed as a percentage of total incoming shortwave solar radiation. Environmental data from the beginning of the year until installation of the field environment loggers just after planting in the experiment were obtained from other weather stations. Temperature and precipitation data were obtained from the University of Manitoba weather station at Carman MB, which was 10 km from the experiment site. Solar radiation data were obtained from the University of Manitoba weather station at Winnipeg, MB (90 km distance). Wind data were obtained from the North Dakota Agricultural Weather Network (NDAWN) station at Walhalla (70 km distance). Wind data were equilibrated to the Graysville dataset to account for height (3 m at Walhalla), surface drag, and topographic differences (Oke, 1987).

4.4.3 Topography

Topographic properties of the microsite experiment were determined by utilizing global positioning system technology (GPS). A GPS coordinate was determined with a Trimble TSC1 Surveyor Controller™ (Trimble Navigation Ltd., 935 Stewart Drive, Sunnyvale, CA 94085) by averaging coordinates over a four hour period at a single location adjacent to the summit hillslope position at each hillslope aspect in the field. A Sokkia SET4110 Total Station™ (Sokkia Co. Ltd., 260-63, Hase, Atsugi, Kanagawa, 243-0036, Japan) was positioned over the GPS coordinate adjacent to the summit at each hillslope aspect. The Total Station™ was used to map easting, northing and elevation coordinates for the corners of every plot, areas between hillslope position blocks, and a buffer of 10 m surrounding each experimental area.

Hillslope gradient and aspect were derived from analyzing the GPS coordinates for plot corners and areas between and around hillslope position blocks with ArcView Spatial Analyst™ (Environmental Systems Research Institute Inc. (ESRI), 380 New York Street, Redlands, CA, 92373-8100). Gradient and aspect for each plot were derived by averaging values of the four corners for each plot. Slope aspect was further processed by changing the scale from 360° clockwise with a starting point at due north to a scale of 180° clockwise and counterclockwise from due south. Converting the slope aspect scale to due south provided a relative measure of maximum sun exposure between aspects.

4.4.4 Soil Cover

Soil surface cover by crop residue was determined after planting and before any plant emergence by digital photography taken at an angle perpendicular to the ground surface. Gap Light Analyzer™ (Institute of Ecosystem Studies, Simon Fraser University, Burnaby, BC, V5A 1S6) was used to determine the percentage of ground covered with residue by contrasting crop residue against the soil background in the images. Soil cover for each plot was expressed as a percentage of total ground area.

4.4.5 Soil Microsite

4.4.5.1 Physical Properties

Soil physical properties were determined after time of planting on 14 May (DOY 134) in 2003 in three replications from three 25-mm increments to a depth of 75 mm. Soil temperature was logged hourly with Stowaway Tidbit™ temperature loggers (Onset Computer Corporation, 536 MacArthur Boulevard., Pocassat, MA, 02559-3450), which were installed at the time of planting in three replications across all factors. Four temperature dataloggers were placed in each plot at 1, 13, 38, and 63 mm depths to record soil temperature at the soil surface and within each of the three 25-mm increments to a depth of 75 mm. Daily average soil temperature and diurnal soil temperature fluctuation were derived from daily maximum and daily minimum soil temperatures.

Soil water content was measured approximately twice weekly (16 occasions) from 6 May until 20 July in six replications by excavating gravimetric soil samples of a known volume from three 25-mm increments to a depth of 75 mm in 2003. Soil water content was also simultaneously measured with a ThetaProbe™ ML2x impedance soil water sensor (Delta-T Devices Ltd., 128 Low Road, Burwell, Cambridge, CB5 0EJ, UK). In 2004, soil water was measured on 17 occasions from 6 May until 20 July with the impedance soil water sensor only. Subsequent measurements taken during the season were from undisturbed locations within each plot to avoid artifacts caused by the previous soil excavations. Soil water content results from the impedance soil water sensor were calibrated with the volumetric soil water measurements. Mean water contents for each emergence phase were derived by averaging all the individual values. Soil water retention was determined for three replications in each hillslope position with a Model 1600 5-bar pressure plate extractor with a 1-bar ceramic pressure plate, and a model 1500, 15-bar pressure plate extractor with 5-bar and 15-bar ceramic pressure plates (Soil Moisture Equipment Corp., P.O. Box 30025, Santa Barbara, CA, 93130). Soil water retention was determined at 0.10, 0.33, 0.50, 1.0, 5.0, and 15.0 bar pressures by determining the amount of volumetric water at each matric pressure (Dane and Hopmans, 2002). Soil water retention relationships were then determined for each hillslope position. Volumetric soil water content was then converted to water potential by using the water

retention relationships indicating the volumetric water content at corresponding osmotic suction.

Soil temperature and soil water for each factor level in the experiment were grouped into four time periods (emergence phases) to approximate the phases in a typical spring annual sigmoidal emergence curve typical of southern Manitoba conditions (e.g. Avena fatua L., Polygonum convolvulus L.) (Bullied et al., 2003). The time periods were based on cumulative daily soil growing degree days (GDD_{soil}) using base 0°C for that factor level. Phases in the emergence curve were lag (0–300 GDD_{soil}), exponential (300–600 GDD_{soil}), stationary (600–900 GDD_{soil}), and late stationary (> 900 GDD_{soil}). The lag phase was represented only from the time since planting which occurred at 270.8 GDD_{air} in 2003, and 176.6 GDD_{air} in 2004.

Particle size analysis was determined by the hydrometer method (Gee and Or, 2002). Analysis of sand separates was determined by wet sieve to remove silt, clay and organic particle portions, and dry sieve to separate sand fractions. Organic matter (OM) content was determined by the loss on ignition procedure (McKeague, 1978). Bulk density (BD) was determined by averaging all gravimetric soil water samples of a known volume in six replications from three 25-mm increments in 2003.

4.4.5.2 Chemical Properties

Soil samples were removed to determine chemical properties 14 May (DOY 134) in 2003 and 18 May (DOY 139) in 2004 from three 25-mm increments to a depth of 75 mm in three replications. Soil nitrate-N analysis was determined by the automated cadmium reduction method (American Public Health Association, 1998b). Soil sulfate-S was extracted in 0.1M $CaCl_2$ (Kowalenko, 1993), with sulfate-S analysis based on the turbidimetric method (American Public Health Association, 1998d). Soil P and K were extracted using a modified Kelowna extraction (Ashworth and Mrazek, 1995). Soil P analysis was based on the stannous chloride method (American Public Health Association, 1998c), and K analysis was based on the automated flame photometry method (Alberta Research Council, 1996). The Ca, Mg and Na content was determined using ammonium acetate extraction (McKeague, 1978d) and inductively coupled plasma analysis (American Public Health Association, 1998a). Soil pH and electrical

conductivity were measured in a 1:2 deionised water suspension with a pH and conductivity electrode, respectively (McKeague, 1978c). Cation exchange capacity (CEC) was determined by ammonium acetate saturation and displacement of exchangeable cations (McKeague, 1978a).

4.4.6 Data Analyses

Microclimate data that were logged with weather stations were analyzed using the repeated measures design in Proc Mixed procedure of Statistical Analysis Systems (SAS) (Littell et al. 1996). Hillslope aspect and position were analyzed as fixed effects and year was considered as a random effect. Daily averages of hourly recorded air temperature, dew point temperature, relative humidity, wind run, wind gust and incoming solar radiation, and daily total precipitation, were analyzed using daily data as a repeated measure for 76 d. Instantaneous albedo data were analyzed as a repeated measures design using 10 measurements in 2003 and 4 measurements in 2004 occurring from planting until late June. The albedo data were analyzed with hillslope aspect, position and residue as fixed effects, whereas year and replication were considered as random effects. Where treatment separation of microclimate properties occurred according to the repeated measures analysis, cumulative data trends of that microclimate property were investigated with linear regression analysis.

Statistical analysis of topographic, soil physical and chemical properties utilized Proc Mixed procedure using Statistical Analysis Systems (SAS) (Littell et al. 1996). The linear mixed-effects model was used to specify year as a random factor thus enabling interpretation of results from the analysis such that the years from which the data were collected were a random sample from a population of possible years where the microsite experiment could have been assessed. The mixed effects structure accounts for random variation in time due to year and random variation in space due to replication. This enabled estimation of the fixed effects of interest, namely hillslope aspect, hillslope position, soil residue, and soil depth. Data met assumptions of normality. The optimal model structure for common or heterogeneous variance by year, where measurements were taken in both years, was determined by Akaike's Information Criterion (AIC) (Table 4.2), where AIC = 2 L + 2 n_p, where L is the negative log likelihood and n_p is

Table 4.2. Comparison of linear mixed-effects models performance for microclimate, soil surface, and soil microsite properties within the weed recruitment zone for common or heterogeneous variance by year.

	$Year_c$		$Year_{he}$		
Property	n_p†	*AIC*‡	n_p	*AIC*	*p*§
Microclimate¶					
Air temperature, °C	8	581	–	–	–
Dew point, °C	7	430	–	–	–
Precipitation, mm d^{-1}	5	2109	–	–	–
Relative humidity, %	8	1143	–	–	–
Wind speed, m s^{-1}	7	509	–	–	–
Wind gust, m s^{-1}	8	516	–	–	–
Solar radiation, w m^{-2}	5	2069	–	–	–
Albedo, %	11	−4708	–	–	–
Soil Surface					
Slope gradient, °	3	−996	4	−998	0.040
Slope aspect, °	5	33	6	35	0.655
Cover, %	8	592	8	585	<.001
Soil microsite (physical)					
Soil texture, g kg^{-1}#					
Clay	3	571	–	–	–
Silt	3	624	–	–	–
Sand	3	630	–	–	–
Very fine sand	2	358	–	–	–
Fine sand	2	340	–	–	–
Medium sand	2	169	–	–	–
Coarse sand	2	100	–	–	–
Very coarse sand	2	34	–	–	–
Organic matter, g kg^{-1}	7	928	8	927	0.094
Bulk density, g cm^{-3}#	2	−182	–	–	–
Temperature, °C††					
Lag	9	−106	11	−101	0.741
Exponential	10	340	12	334	0.007
Stationary	10	624	11	626	1.000
Late stationary	12	399	13	401	0.655
Season	11	377	12	378	0.317
Fluctuation, °C‡‡					
Lag	14	384	15	383	0.074
Exponential	10	1003	11	977	<.001
Stationary	10	1092	11	1086	0.008
Late stationary	12	891	13	890	0.114
Season	8	867	9	865	0.038
Water content, m^3 m^{-3}††					
Lag	12	−2656	13	−2670	<.001
Exponential	14	−2627	15	−2627	0.157
Stationary	13	−2601	14	−2636	<.001
Late stationary	11	−2769	12	−2776	0.003
Season	14	−2970	15	−2988	<.001
Water potential, MPa††					
Lag	12	−764	13	−764	0.138
Exponential	6	−912	7	−917	0.016
Stationary	12	−608	13	−670	<.001
Late stationary	15	−781	15	−960	<.001
Season	12	−1105	11	−1211	<.001

Table 4.2. Continued.

Soil microsite (chemical)					
N, mg kg^{-1}	10	1310	11	1249	<.001
P, mg kg^{-1}	8	1317	9	1319	0.655
K, mg kg^{-1}	12	1984	13	1985	0.237
S, mg kg^{-1}	11	1466	12	1334	<.001
Ca, mg kg^{-1}	10	2594	12	2762	<.001
Mg, mg kg^{-1}	5	1982	6	1984	1.000
Na, mg kg^{-1}	8	1136	9	1136	0.129
CEC, $cmol_c$ kg^{-1}	8	749	9	750	0.584
pH, $-\log[H^+]$	8	−135	9	−136	0.078
EC, dS m^{-1}	10	−200	12	−236	<.001

† Number of parameters.

‡ Within a row, the model with a smaller Akaike's Information Criterion where $AIC = 2$ (negative log likelihood) + 2 n_p is considered superior.

§ A nonsignificant log likelihood ratio χ^2 test ($p > 0.05$) indicates that the lower parameter model is superior.

¶ Repeated measures analysis.

Single year model.

††Mean soil temperature, soil water content, and soil water potential for time periods based on cumulative daily soil growing degree days (GDD_{soil}) using base 0°C. Time periods represent a typical sigmoidal emergence curve separated into phases of lag (0–300 GDD_{soil}), exponential (300–600 GDD_{soil}), stationary (600–900 GDD_{soil}) and late stationary (>900 GDD_{soil}). Lag phase is represented from time of planting only (270.8 GDD_{air} in 2003 and 176.6 GDD_{air} in 2004).

‡‡Diurnal soil temperature fluctuation is the difference between daily high and daily low temperature.

the number of parameters (Littell et al. 1996). Main fixed effects were analyzed and the source of variation for fixed effects was determined. Where two-way and three-way interactions of fixed effects were significant ($p \leq 0.05$), individual levels of each interaction factor were investigated for significance of one factor across all levels of the other factor(s) with mean separations to determine how the effect of one factor changed with the level of the other factors(s). Orthogonal contrasts were used to determine differences between backslope positions in each hillslope aspect, which represented the greatest degree of gradient difference in opposing aspects. Soil residue and soil depth treatments within each backslope position were also contrasted between backslope positions in each hillslope aspect.

4.5 RESULTS AND DISCUSSION

4.5.1 Microclimate

Wind and solar radiation were the only microclimate effects to display treatment separation according to the repeated measures analysis (Table 4.3; Fig. 4.1). Wind run and wind gust diminished with lower position in the hillslope (Table 4.3). Wind run interactions of hillslope aspect by hillslope position showed the southwest aspect having greater wind speed compared to the northeast aspect, with the differential increasing with lower hillslope position (Fig. 4.2a). Because wind direction was predominantly from the south for the duration of the experiment, an increase in ground elevation in the direction of the wind, as in the southwest aspect, can cause the wind flow to constrict vertically, resulting in acceleration of the wind (Oke, 1987). Conversely, a drop in surface elevation, as in the northeast aspect, can result in a slowing of the wind speed (Oke, 1987).

Incoming solar radiation received at the soil surface was less at the northeast aspect compared to the southwest aspect (Table 4.3). Solar radiation interactions of hillslope aspect by hillslope position indicated that between the opposing hillslope aspects, the summit hillslope positions did not differ, whereas the backslopes did, with the southwest facing backslope receiving a greater amount of solar radiation compared to the northeast facing backslope (Fig. 4.2b). Since the angle between the slope surface and the solar beam primarily controls the amount of direct solar radiation received by a surface (Tian et al., 2001), it is not unexpected that the northeast facing backslope would

Table 4.3. Microclimate properties response to repeated measures analysis of hillslope aspect, hillslope position and soil residue.†

Main fixed effect	Air temperature	Dew point temperature	Precipitation	Relative humidity	Wind run	Wind gust	Solar radiation	Albedo‡
	°C		mm d^{-1}	%	m s^{-1}		w m^{-2}	%
Hillslope aspect								
Southwest	15.6	9.1	2.5	70.9	2.01	4.25	206.3*a*	13.3
Northeast	15.6	9.2	2.6	70.7	1.34	3.67	200.4*b*	13.8
Hillslope position								
Summit	15.6	9.1	2.6	70.8	1.96*a*	4.31*a*	203.4	13.4
Backslope	15.5	–	2.3	–	1.63*b*	3.87*b*	203.4	13.9
Toeslope	15.6	9.2	2.7	70.9	1.43*c*	3.70*c*	–	13.3
Residue								
Native	–	–	–	–	–	–	–	12.4
Added	–	–	–	–	–	–	–	14.7
Source of variation					*p > F*			
Aspect (A)	0.966	0.549	0.590	0.591	0.264	0.216	0.004	0.539
Position (P)	0.997	0.504	0.149	0.859	<.001	<.001	0.984	0.780
A × P	0.996	0.457	0.177	0.117	0.041	0.066	0.001	0.525
Residue (R)	–	–	–	–	–	–	–	0.094
A × R	–	–	–	–	–	–	–	0.865
P × R	–	–	–	–	–	–	–	0.829
A × P × R	–	–	–	–	–	–	–	0.312
Time (T)	<.001	<.001	0.387	0.017	0.223	0.363	0.150	0.174
A × T	0.126	0.659	0.585	0.480	0.189	0.481	0.442	<.001
P × T	0.679	0.047	0.039	0.323	<.001	<.001	0.403	0.805
R × T	–	–	–	–	–	–	–	0.338
A × P × T	0.993	0.460	0.134	0.693	0.100	0.007	0.278	0.592
A × R × T	–	–	–	–	–	–	–	0.864
P × R × T	–	–	–	–	–	–	–	0.731
A × P × R × T	–	–	–	–	–	–	–	0.050

a–c Within columns and factors, means followed by different letters are significantly different at $p \leq 0.05$ according to Fisher's protected LSD.

† All properties were hourly logged and daily averaged data except for albedo, which were instantaneous measurements of incoming and reflected solar radiation taken as close as possible to solar noon.

‡ Albedo is a percentage of incoming solar radiation.

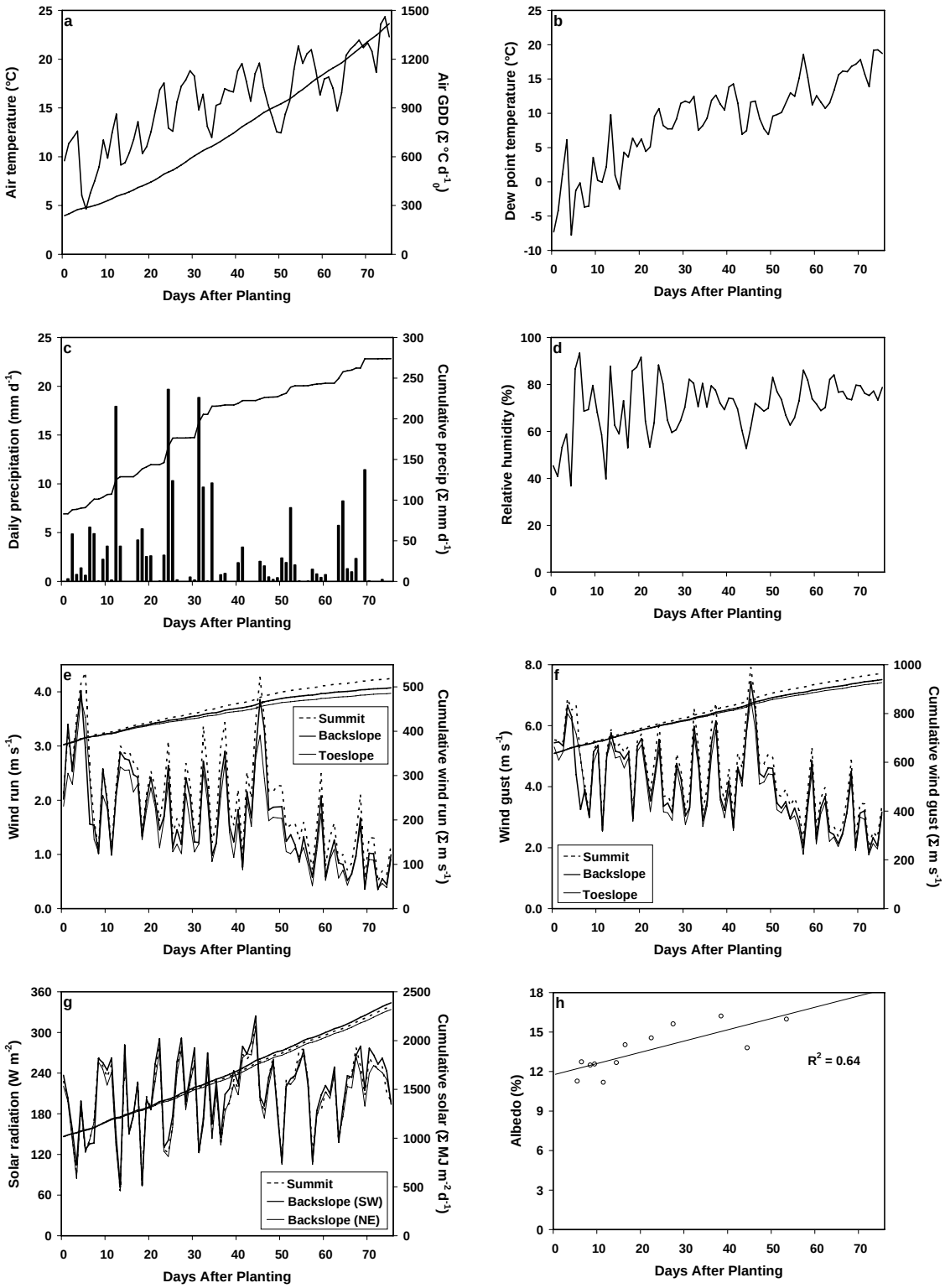

Fig. 4.1. Microclimate properties of (a) air temperature, (b) dew point temperature, (c) precipitation, (d) relative humidity, (e) wind run, (f) wind gust, (g) solar radiation, and (h) albedo daily and yearly cumulative data for 75 d after planting.

receive less solar radiation. Solar radiation received by a surface increases as slope gradient increases in south, southeast or southwest aspects from 0 to 30 degrees, whereas solar radiation received by north, northeast or northwest aspects decreases with the same increase in gradient (Garnier and Ohmura, 1968; Monteith, 1990). Within the range of slope gradients in our experiment (7 degrees), solar radiation received by east or west facing aspects was similar to that received by flat surfaces (Garnier and Ohmura, 1968; Tian et al., 2001)

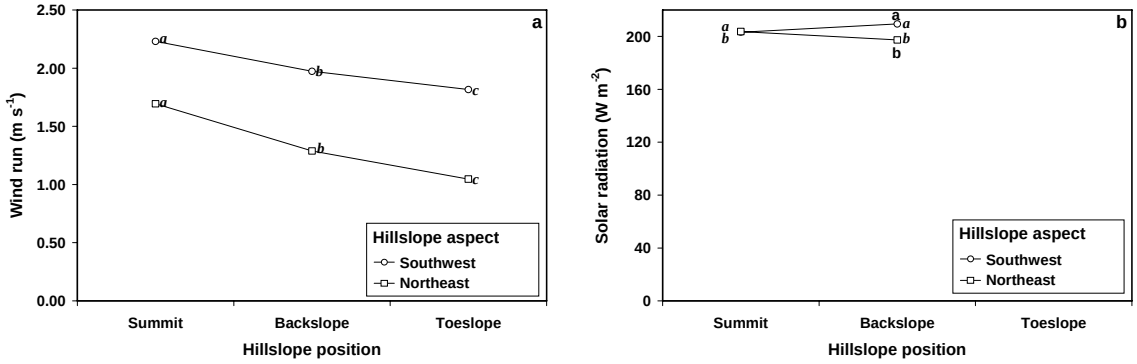

Fig. 4.2. Microclimate response to interactions of hillslope aspect by hillslope position. Lowercase serif letters to the left or right of points designate horizontal separation of simple effects ($p \leq 0.05$), and lowercase non-serif letters above or below points designate vertical separation of simple effects ($p \leq 0.05$).

Albedo did not differ among topographic or residue treatments (Table 4.3), however surface residue (P = 0.094) cannot be overlooked since an increase in surface residue cover has been shown to increase the amount of reflected solar radiation (Sharratt, 2002). Since the oat residue was incorporated in our experiment, differences in surface residue levels between treatments were moderate (P = 0.072).

Cumulative wind speed and wind gust separation of treatments by regression analysis further verified differences among the hillslope positions (Table 4.4; Figs. 4.1e and 4.1f). The magnitude of cumulative wind run and wind gust decreased from the summit to the backslope to the toeslope. Solar radiation accumulated to a greater extent on the southwest facing backslope compared to summit positions (Table 4.4; Fig. 4.1g). Furthermore, the summit positions accumulated greater solar radiation compared to the northeast facing backslope.

Table 4.4. Microclimate properties cumulative response to treatment separation specified by repeated measures analysis of daily data. Linear regression parameter estimates are followed by SEs in parentheses.

	Parameter estimates† (SE)		
Property	a	b	R^2‡
Wind run			
Summit	380 (0.76)	2.0 (0.020)	0.99
Backslope	§	1.7 (0.020)	
$p > F$	0.647	<0.001	
Wind run			
Backslope	380 (0.76)	1.7 (0.020)	0.98
Toeslope	§	1.6 (0.020)	
$p > F$	0.778	<0.001	
Wind gust			
Summit	648 (1.08)	4.5 (0.028)	0.99
Backslope	§	4.1 (0.028)	
$p > F$	0.863	<0.001	
Wind gust			
Backslope	649 (1.09)	4.1 (0.028)	0.99
Toeslope	§	3.9 (0.028)	
$p > F$	0.2832	<0.001	
Solar radiation			
Summit	977 (2.47)	18.0 (0.064)	0.99
SW Backslope	§	18.4 (0.064)	
$p > F$	0.792	<0.001	
Solar radiation			
Summit	977 (2.43)	18.0 (0.063)	0.99
NE Backslope	§	17.6 (0.063)	
$p > F$	1.000	<0.001	

† Parameters constrained to indicated values. Significance between parameter estimates were determined by lack-of-fit F test ($p \leq 0.05$).

‡ One R^2 value is determined for the model fit for hillslope position comparisons.

§ Parameter estimates for paired hillslope positions are constrained to the same value.

4.5.2 Topography

Average slope gradients on the two aspects were similar (Table 4.5). As expected, the backslope had a greater gradient than that of the summit or toeslope positions. A hillslope aspect by hillslope position interaction indicated that the southwest facing backslope was steeper compared to the northeast facing backslope, whereas other positions were similar (Fig. 4.3a).

The two aspects were separated by over 60 degrees, as measured from due south (Table 4.5). This difference in orientation of the two opposing aspects accounts for an increase in received solar radiation at the soil surface by the backslope of the southwest aspect (Fig 4.2b) (Monteith, 1990). Spatial variability of energy distribution across different aspects and gradients of the topography would therefore culminate into variations of microclimate across the topography (Oke, 1987). Interaction of hillslope aspect by hillslope position showed that, although all positions of the southwest aspect were closer to due south compared to corresponding positions of the northeast aspect, the magnitude between summits was greater compared to backslopes or toeslopes (Fig 4.3b). Although there was a difference in aspect between the summit positions, the gradient of these positions was ≤ 1 degree (Table 4.5), and therefore did not translate into differences in solar radiation received (Fig. 4.2b). With the southwest aspect, the summit was closer to due south than the toeslope, but would not be expected to receive more solar radiation because the magnitude of difference was less than that of the two opposing summits (Fig. 4.3b). Aspect differences associated with the summit and toeslope positions would therefore have a minimal effect on the amount of solar radiation received.

4.5.3 Soil Cover

Soil cover did not differ across hillslope aspect or hillslope position (Table 4.5). The addition of chopped oat straw at 6000 kg ha^{-1} more than doubled the soil cover compared to the native soybean residue cover (Table 4.5). Residue treatment was not significant (P = 0.072), with percent cover being low as a result of additional residue being incorporated to the depth of the measured recruitment zone. Although the residue treatment was not significant at $p \leq 0.05$ level, the added residue could influence the recruitment zone climate due to the cumulative effect of additional surface cover and

Table 4.5. Topographic and soil cover properties response to hillslope aspect, hillslope position, and soil residue.

Main fixed effect	Slope gradient†	Slope aspect‡	Soil cover
	°		%
Hillslope aspect			
Southwest	3	67*b*	12.3
Northeast	3	128*a*	11.6
Hillslope position			
Summit	1*b*	101*ab*	11.0
Backslope	7*a*	86*b*	11.7
Toeslope	1*b*	104*a*	13.1
Soil residue			
Native	3	98	7.5
Added	3	97	16.3
Source of variation		*p* > *F*	
Aspect (A)	0.877	<.001	0.756
Position (P)	<.001	0.063	0.168
A × P	0.016	0.029	0.190
Residue (R)	0.208	0.770	0.072
A × R	0.324	0.359	0.535
P × R	0.983	0.757	0.696
A × P × R	0.887	0.285	0.496

a–c Within columns and factors, means followed by different letters are significantly different at $p \leq 0.05$ according to Fisher's protected LSD.
† Degrees from horizontal.
‡ Degrees from due south.

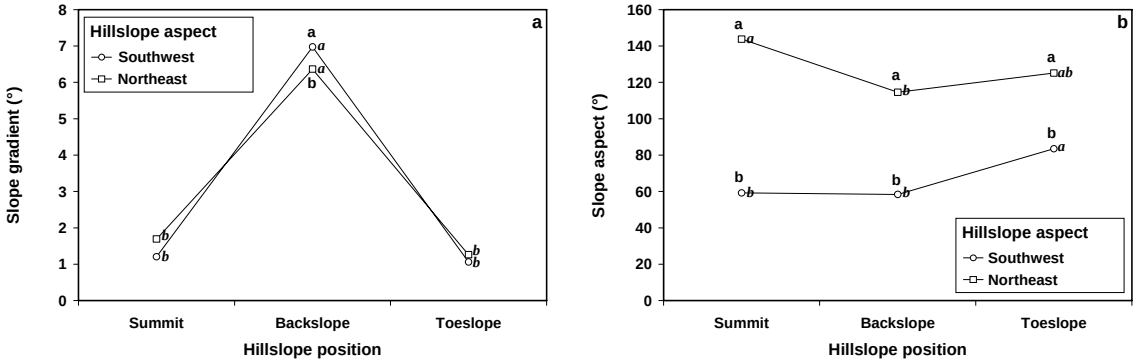

Fig. 4.3. Soil surface properties response to interactions of hillslope aspect by hillslope position. Lowercase serif letters to the right of points designate horizontal separation of simple effects ($p \leq 0.05$), and lowercase non-serif letters above or below points designate vertical separation of simple effects ($p \leq 0.05$).

incorporated residue. The additional residue covering the soil surface (Table 4.5) increased albedo by 2.3% (Table 4.3).

4.5.4 Soil Microsite

4.5.4.1 Physical Properties

4.5.4.1.1 Soil Texture. Soil texture differed across hillslope aspect and hillslope position, as well as soil depth, indicating a considerable range of soil particle size heterogeneity across both the topography and soil depth in the experiment (Table 4.6). Clay content was 27% greater in the southwest aspect compared to the northeast aspect, which was accounted for by different soil series. Clay content varied the greatest with hillslope position, increasing 43% and 212% from the summit position to the backslope and toeslope positions, respectively (Table 4.6). Since the backslope gradient had an average slope of 7° (Table 4.5), sorting of soil particles by hydrologic processes would, over time, result in smaller soil particles, predominantly clay, to accumulate downslope (Malo et al., 1974; Young and Hammer, 2000). A hillslope aspect by hillslope position interaction for clay content indicated that clay content was greater in the southwest toeslope, and less in the southwest summit, compared to corresponding hillslope positions in the northeast aspect (Fig. 4.4a). This would have been a result of aspects being located on different soil series, as well as particle sorting over the gradient due to hydrologic processes. Silt and fine sand contents also displayed interactions of hillslope aspect by hillslope position, also attributed to geomorphic processes and hydrological sorting of soil particles down the gradient (Figs. 4.4b and 4.4c). A hillslope position by soil depth interaction for clay content indicated that clay content was greater in the 50–75 mm increment compared to the upper soil increments for the backslope and toeslope, but these were only greater than the uppermost soil increment for the summit position (Fig. 4.4e). Less difference in clay content with depth in the recruitment zone for the summit position could have resulted from reduced hydrological sorting of soil particles on the summit. As well, less horizontal sorting of clay particles on the summit would occur due to the initially lower clay content.

4.5.4.1.2 Organic Matter. Organic matter content was greater downslope, which could be attributed to downhill transport and accumulation of OM downslope. Production of

Table 4.6. Soil physical properties of microsites within the weed recruitment zone response to hillslope aspect, hillslope position, soil residue and soil depth.

Main fixed effect	Soil texture			Sand separates					Organic matter	Bulk density
	Clay	Silt	Sand	VF	F	M	C	VC		
	g kg^{-1}									g cm^{-3}
Hillslope aspect										
Southwest	147*a*	564*b*	289	233	44*b*	7	2*a*	0	46	0.99*b*
Northeast	116*b*	598*a*	285	225	53*a*	7	1*b*	0	39	1.07*a*
Hillslope position										
Summit	71*c*	717*a*	212*c*	145*c*	60*a*	4*b*	1*b*	0	37*b*	1.08*a*
Backslope	102*b*	632*b*	266*b*	223*b*	39*b*	6*b*	1*b*	0	34*b*	1.08*a*
Toeslope	222*a*	395*c*	383*a*	320*a*	46*ab*	10*a*	3*a*	0	56*a*	0.92*b*
Residue										
Native	133	580	286	–	–	–	–	–	42	1.06*a*
Added	130	582	288	–	–	–	–	–	43	1.00*b*
Soil depth										
0–25mm	128*b*	585*a*	286*b*	226	50	7	2	0	43	0.96*c*
25–50mm	128*b*	581*b*	291*a*	228	53	7	2	0	43	1.00*b*
50–75mm	139*a*	578*c*	284*b*	233	42	7	2	0	41	1.12*a*
Source of variation					$p > F$					
Aspect (A)	<.001	0.033	0.682	0.533	0.213	0.673	0.008	0.131	0.073	<.001
Position (P)	<.001	<.001	<.001	<.001	0.078	<.001	<.001	0.611	0.019	<.001
A × P	<.001	<.001	0.058	0.346	0.002	0.067	0.109	0.702	0.036	<.001
Residue (R)	0.504	0.795	0.818	–	–	–	–	–	0.373	<.001
A × R	0.457	0.943	0.405	–	–	–	–	–	0.108	0.710
P × R	0.579	0.937	0.525	–	–	–	–	–	0.719	0.508
A × P × R	0.714	0.913	0.823	–	–	–	–	–	0.284	0.995
Depth (D)	<.001	<.001	0.007	0.586	0.140	0.430	0.316	0.257	0.132	<.001
A × D	0.211	0.782	0.617	0.783	0.722	0.482	0.475	0.427	0.470	0.185
P × D	0.006	0.334	0.351	0.698	0.840	0.321	0.146	0.108	0.217	0.747
R × D	0.796	0.721	0.737	–	–	–	–	–	0.114	<.001
A × P × D	0.461	0.870	0.928	0.244	0.327	0.662	0.644	0.070	0.644	0.731
A × R × D	0.306	0.782	0.442	–	–	–	–	–	0.470	0.921
P × R × D	0.279	0.857	0.520	–	–	–	–	–	0.859	0.547
A × P × R × D	0.970	0.740	0.744	–	–	–	–	–	0.651	0.820

a–c Within columns and factors, means followed by different letters are significantly different at $p \leq 0.05$ according to Fisher's protected LSD.

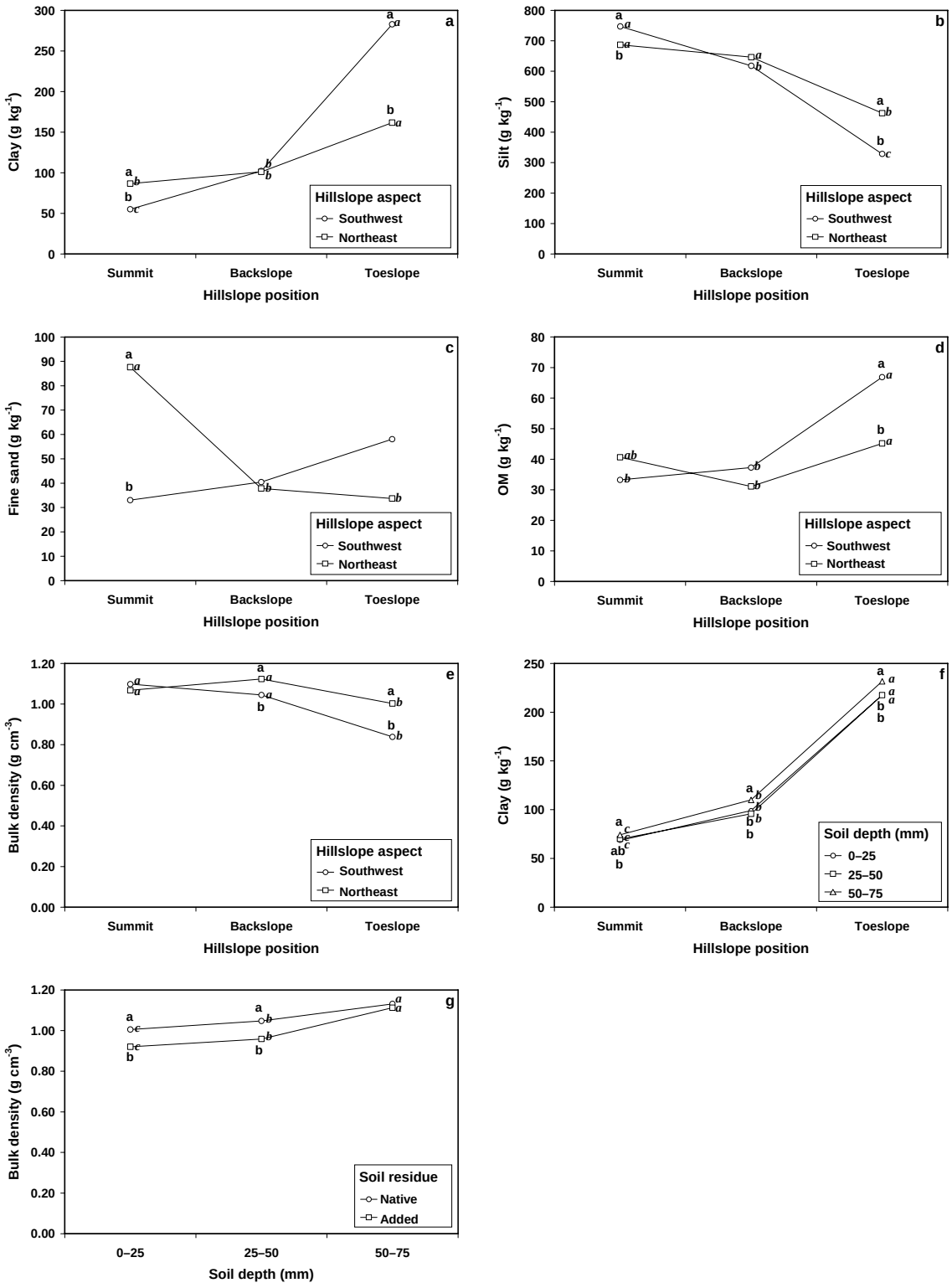

Fig. 4.4. Soil physical properties of microsites within the weed recruitment zone response to interactions of (a–e) hillslope aspect by hillslope position, (f) hillslope position by soil depth, and (g) soil residue by soil depth. Lowercase serif letters to the right of points designate horizontal separation of simple effects ($p \leq 0.05$), and lowercase non-serif letters above or below points designate vertical separation of simple effects ($p \leq 0.05$).

organic matter at the toeslope was likely greater than the upper components of the hillslope due to greater wetness and clay content in the toeslope (Ruhe, 1975). Although there was no difference in OM content with depth in the recruitment zone, this is probably a reflection of the shallow measured increments (Table 4.6).

A hillslope aspect by hillslope position interaction for OM indicated that the southwest toeslope had greater OM concentration compared to the northeast toeslope, while no differences occurred in the summit or backslope (Fig. 4.4d). This can be attributed to diverse soil types across the topography. The Willowbend soil in the toeslope of the southwest aspect had greater clay content and poor drainage, which would account for retention of OM.

4.5.4.1.3 Bulk Density. Significant differences in BD existed between levels of all factors in the experiment (Table 4.6). Because BD is a dynamic property, which varies with particle density, OM and compaction of a soil (Campbell and Henshall, 1991), it is not unexpected that it would vary across both topographic and soil factors. Greater BD in the northeast aspect and toeslope position may reflect differences in soil series. The applied oat straw residue treatment decreased BD by 6% over that of the native residue (Table 4.6). Bulk density increased 4% and 16% from the 0–25 mm increment to the 25–50 mm and 50–75 mm increments, respectively (Table 4.6), despite all increments in the recruitment zone being completely rotary tilled. Because BD affects air and water movement within the seedling recruitment zone, it would be expected that BD differences across the topography, residue level, or recruitment zone depth could have an influence on seedling recruitment. A hillslope aspect by hillslope position interaction for BD showed a greater difference in bulk density between backslope and toeslope positions across the two aspects compared to the summit position (Fig. 4.4d), which could be attributed to spatial variability of soil series across the experiment. A soil residue by soil depth interaction for BD indicated that the added oat straw residue reduced bulk density for the 0–25 mm and 25– 50 mm recruitment zone increments, but not the 50–75 mm increment (Fig. 4.4f). Bulk density may be higher at lower depths in the recruitment zone due to the weight of the soil above the measured soil depth increment. Higher BD at lower depths could also be attributed to variable mixing of the straw throughout the

recruitment zone, and because straw is less dense compared to soil particles, would tend to accumulate to a greater extent in the upper portion of the soil profile being tilled.

4.5.4.1.4 Soil Temperature. Soil temperature did not differ across the topographic main effects (Table 4.7). Temperature was higher in the added residue treatment in the late stationary phase, possibly as a result of reduced thermal diffusivity resulting in less conduction of heat from the soil surface (Cochran, 1969). Temperature decreased with soil depth in the exponential, stationary, and late stationary phases (Table 4.7). The deeper the soil increment, the longer it takes heat from the surface to reach it, therefore a declining temperature gradient with soil depth occurs in the spring as soils warm (Miller and Gardiner, 2001). A hillslope aspect by hillslope position by soil depth interaction for temperature in the exponential phase indicated that temperature declined from the summit to toeslope position, but only in the southwest aspect (Fig. 4.5a). Furthermore, the three-way interaction indicated that temperature in the toeslope position was lower for the southwest aspect compared to the northeast aspect for all soil depths, except the surface (Fig. 4.5a). Lower temperature in the southwest toeslope could be attributed to reduced thermal conductivity due to greater clay content with BD and greater OM level (Abu-Hamdeh and Reeder, 2000). A hillslope aspect by soil depth interaction for temperature during the late stationary phase indicated that the southwest aspect displayed a greater soil temperature decline with depth compared to the northeast aspect (Fig. 4.5b). This may have been due to increased heating of the soil surface in the southerly facing aspect, as indicated by greater solar radiation received by that aspect (Table 4.3). A hillslope aspect by hillslope position by soil depth interaction for temperature in the late stationary phase displayed a greater temperature for all soil depths of the summit position (but not other positions) in the southwest aspect compared to the northeast aspect (Fig. 4.5c). The three-way interaction also showed that summit and toeslope hillslope positions in the southwest aspect displayed steeper temperature declines with depth in the recruitment zone compared to corresponding hillslope positions in the northeast aspect (Fig. 4.5c).

The greatest diurnal soil temperature fluctuation (difference between daily high and daily low) occurred with hillslope position and soil depth (Table 4.7). Soil temperature fluctuation varied more between years than soil temperature (Table 4.3). Soil temperature fluctuation decreased downslope with hillslope position, but only when the

Table 4.7. Mean soil temperature and diurnal soil temperature fluctuation during emergence phases and season of microsites within the weed recruitment zone response to hillslope aspect, hillslope position, soil residue and soil depth.

	Soil temperature Emergence phase					Soil temperature fluctuation‡ Emergence phase				
Main fixed effect	Lag†	Exponential	Stationary	Late stationary	Season§	Lag	Exponential	Stationary	Late stationary	Season
	°C					°C				
Hillslope aspect										
Southwest	11.1	14.0	17.6	19.7	16.6	13.6	12.4	11.9	8.3	11.6
Northeast	11.2	14.3	17.8	18.7	16.4	13.0	12.9	11.4	6.9	11.0
Hillslope position										
Summit	11.2	14.4	17.9	19.4	16.7	13.6	13.1	12.1	8.1	11.8*a*
Backslope	11.0	14.0	17.7	19.4	16.5	13.4	12.4	11.7	7.7	11.2*ab*
Toeslope	11.2	14.0	17.5	18.8	16.3	12.9	12.4	11.1	7.0	10.9*b*
Residue										
Native	11.1	14.2	17.4	18.8*b*	16.3	13.4	12.6	10.7	6.8*b*	10.9
Added	11.2	14.0	18.1	19.6*a*	16.7	13.2	12.7	12.6	8.4*a*	11.7
Soil depth										
Surface	11.3	15.0*a*	19.0*a*	19.8*a*	17.4*a*	14.0	16.8*a*	16.0*a*	10.3*a*	14.2*a*
0–25mm	11.1	14.4*a*	18.1*b*	19.4*b*	16.8*b*	13.5	14.4*ab*	13.4*a*	8.7*b*	12.4*b*
25–50mm	11.1	13.7*b*	17.1*c*	18.9*c*	16.1*c*	13.0	10.7*bc*	9.6*b*	6.3*c*	9.9*c*
50–75mm	11.1	13.3*b*	16.7*c*	18.7*d*	15.7*c*	12.7	8.7*c*	7.6*b*	5.1*c*	8.6*d*
Contrast										
A in P(Backslope)	0.403	0.915	0.642	0.304	0.975	0.924	0.467	0.852	0.936	0.808
A in P(B), R(Native)	0.521	0.364	0.806	0.325	0.836	0.565	0.662	0.589	0.288	0.404
A in P(B), R(Added)	0.586	0.437	0.736	0.364	0.868	0.534	0.661	0.519	0.275	0.399
A in P(B), D(surface)	0.509	0.684	0.818	<.001	0.520	0.745	0.717	0.694	0.072	0.517
A in P(B), D(0–25)	0.629	0.871	0.735	0.006	0.675	0.432	0.555	0.561	0.111	0.428
A in P(B), D(25–50)	0.534	0.326	0.862	0.140	0.974	0.513	0.715	0.941	0.350	0.686
A in P(B), D(50–75)	0.540	0.486	0.827	0.247	0.984	0.529	0.716	0.947	0.574	0.740
Source of variation					*p > F*					
Aspect (A)	0.336	0.385	0.824	0.215	0.742	0.770	0.654	0.802	0.182	0.740
Position (P)	0.415	0.336	0.476	0.505	0.336	0.548	0.125	0.202	0.489	0.033
A × P	0.377	0.122	0.145	0.069	0.107	0.487	0.448	0.240	0.145	0.034
Residue (R)	0.931	0.424	0.102	0.016	0.239	0.499	0.916	0.198	0.013	0.315

Table 4.7. Continued.

A × R	0.429	0.778	0.724	0.721	0.908	0.814	0.991	0.785	0.886	0.964
P × R	0.360	0.459	0.492	0.959	0.711	0.580	0.288	0.693	0.938	0.726
A × P × R	0.418	0.516	0.906	0.674	0.912	0.381	0.838	0.662	0.368	0.681
Depth (D)	0.500	0.007	0.001	<.001	<.001	0.502	0.021	0.016	0.003	<.001
A × D	0.685	0.813	0.969	0.022	0.388	0.493	0.824	0.812	0.176	0.794
P × D	0.532	0.642	0.132	0.519	0.288	0.514	0.806	0.611	0.764	0.868
R × D	0.466	0.355	0.141	0.081	0.125	0.492	0.544	0.249	0.110	0.088
A × P × D	0.270	<.001	0.091	<.001	0.002	0.615	0.018	0.001	0.015	0.062
A × R × D	0.991	0.754	0.817	0.575	0.641	0.960	0.672	0.433	0.421	0.826
P × R × D	0.767	0.418	0.624	0.975	0.865	0.727	0.406	0.667	0.889	0.765
A × P × R × D	0.144	0.866	0.964	0.197	0.772	0.540	0.864	0.896	0.643	0.869

a–c Within columns and factors, means followed by different letters are significantly different at $p \leq 0.05$ according to Fisher's protected LSD.

† Mean daily soil temperature and diurnal soil temperature fluctuation for emergence phases are based on cumulative daily soil growing degree days (GDD_{soil}) using base 0°C. Time periods approximate a sigmoidal emergence curve separated into phases of lag (0–300 GDD_{soil}), exponential (300–600 GDD_{soil}), stationary (600–900 GDD_{soil}) and late stationary (> 900 GDD_{soil}) (e.g. Avena fatua, Polygonum convolvulus) (Bullied et al., 2003). Lag phase is represented only from time of planting (270.8 GDD_{air} in 2003 and 176.6 GDD_{air} in 2004).

‡ Diurnal soil temperature fluctuation is the difference between daily high and daily low temperature.

§ Season is from time of planting to the end of the late stationary phase.

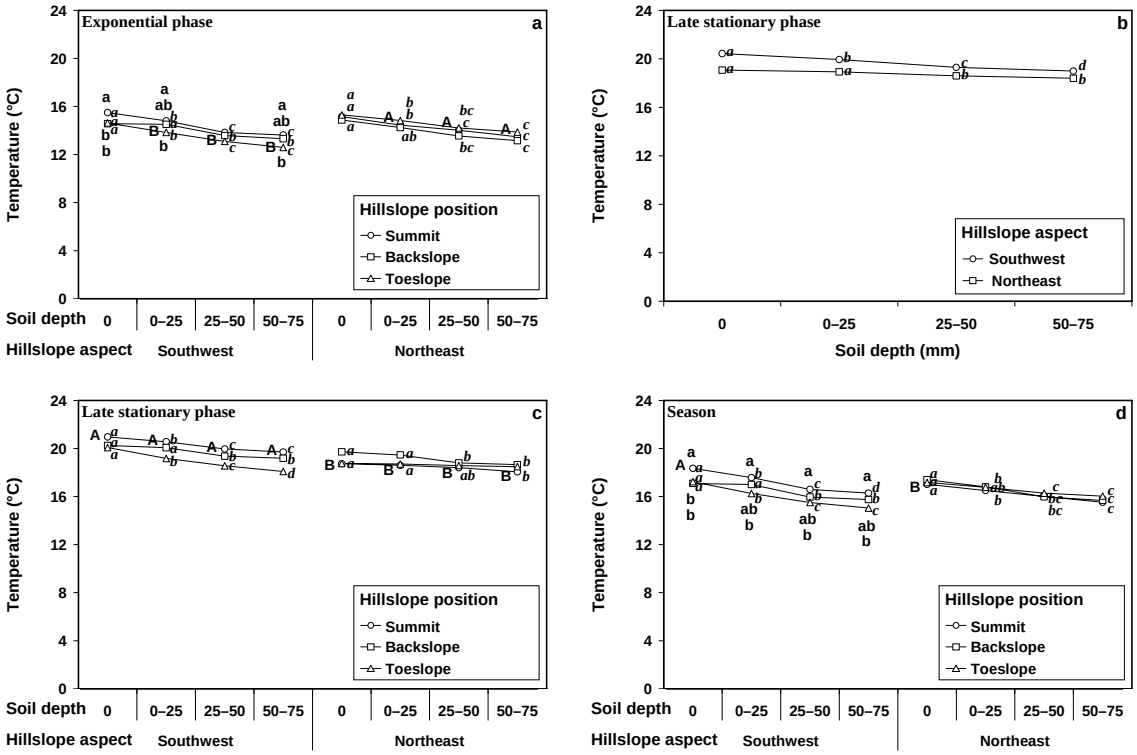

Fig. 4.5. Soil temperature for the exponential phase (300–600 GDD_{soil}) in microsites within the weed recruitment zone response to interactions of (a) hillslope aspect by hillslope position by soil depth. Soil temperature for the late stationary phase (> 900 GDD_{soil}) in microsites within the weed recruitment zone response to interactions of (b) hillslope aspect by soil depth, and (c) hillslope aspect by hillslope position by soil depth. Soil temperature for the season in microsites within the weed recruitment zone response to interactions of (d) hillslope aspect by hillslope position by soil depth. Lowercase serif letters to the right of points designate horizontal separation of simple effects ($p \leq 0.05$), and lowercase non-serif letters above or below points designate vertical separation of simple effects ($p \leq 0.05$). For three-way interactions, uppercase non-serif letters to the left of points designate separation of simple effects between left and right sets of points ($p \leq 0.05$).

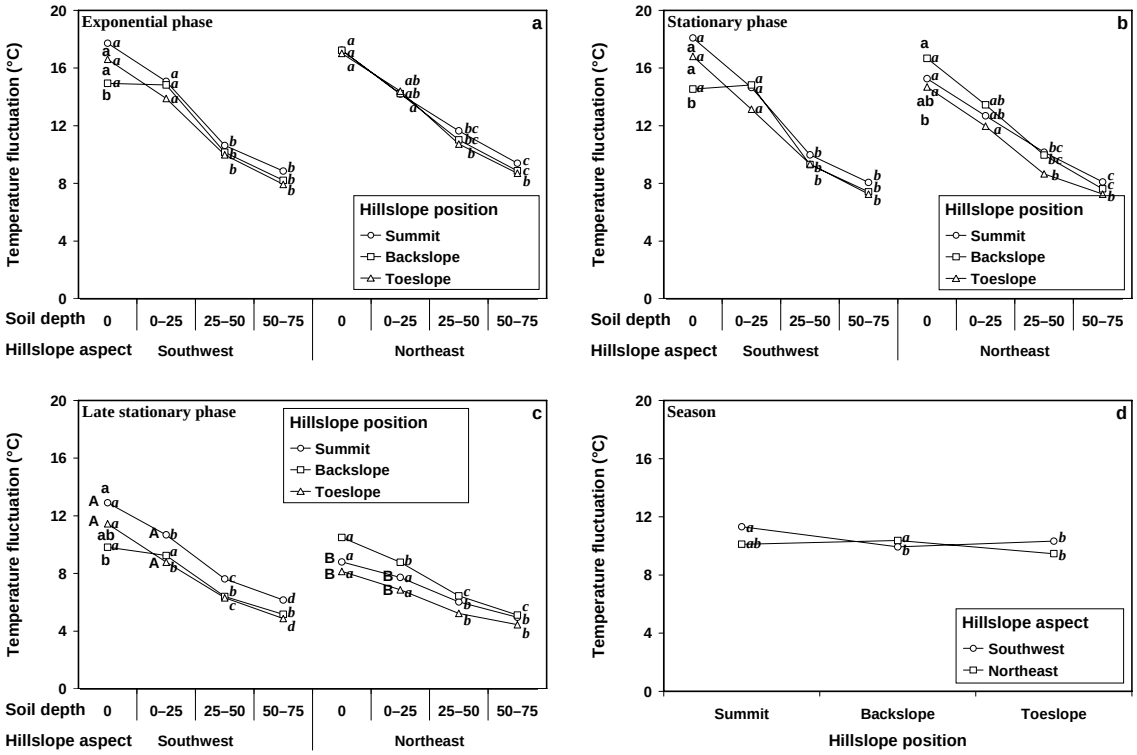

Fig. 4.6. Soil temperature fluctuation for (a) the exponential phase (300–600 GDD_{soil}), (b) the stationary phase (600–900 GDD_{soil}), and (c) the late stationary phase (> 900 GDD_{soil}) in microsites within the weed recruitment zone response to interactions of hillslope aspect by hillslope position by soil depth. Soil temperature fluctuation for the season in microsites within the weed recruitment zone response to interactions of (d) hillslope aspect by hillslope position. Lowercase serif letters to the right of points designate horizontal separation of simple effects ($p \leq 0.05$), and lowercase non-serif letters above or below points designate vertical separation of simple effects ($p \leq 0.05$). For three-way interactions, uppercase non-serif letters to the left of points designate separation of simple effects between left and right sets of points ($p \leq 0.05$).

entire season was considered (Table 4.7). This may have been due to increased thermal capacity from greater soil water content in the lower hillslope positions. Soil temperature fluctuation was greatest on the soil surface and decreased with soil depth (Table 4.7). Soil temperature displays a reduction in amplitude with depth in the profile due to the increased time lag in daily maximum and minimum temperatures with soil depth (Oke and Hannell, 1966; Rosenberg et al., 1983). The greatest temperature differences exist on the soil surface as a result of influences by incoming and outgoing radiation (Stoller and Wax, 1973). Increased soil water content with soil depth increases thermal capacity lower in the soil profile resulting in a decrease in temperature extremes. Soil temperature fluctuation was greater for the added residue only for the late stationary phase (Table 4.7), possibly due to lower thermal diffusivity with the addition of straw (Cochran, 1969). Soil temperature fluctuation interactions of hillslope aspect by hillslope position by soil depth occurred for the exponential, stationary, and late stationary phases (Figs. 4.6a, 4.6b, and 4.6c). The soil surface of the backslope position in the southwest aspect had lower temperature fluctuation compared to the other hillslope positions possibly due to greater soil water content. In contrast, on the soil surface in the stationary phase, the backslope position had greater temperature fluctuation than the toeslope position in the northeast aspect (Fig 4.6b). Temperature fluctuation was greater on the soil surface for the summit and toeslope positions in the southwest aspect compared to the corresponding treatments in the northeast aspect (Fig 4.6c). A hillslope aspect by hillslope position interaction for the season indicated that the backslope position had greater temperature fluctuation than the toeslope position on the northeast aspect (Fig. 4.6d). The southwest aspect differed in that the summit had the greatest temperature fluctuation of all hillslope positions (Fig. 4.6d).

4.5.4.1.5 Soil Water. Soil water displayed greater year to year heterogeneity than soil temperature (Table 4.3). Soil water content increased downslope with hillslope position (Table 4.8) likely due to hydrology flow as well as greater clay content at lower hillslope positions. Soil water content increased with depth in soil profile (Table 4.8). Soil water gradients develop during periods of no rain due to daily radiation inputs and evaporation at the soil surface (Bruce et al., 1977; Schieldge et al., 1982). Hillslope position by soil depth interactions for soil water content during the lag and exponential phases indicated a

Table 4.8. Soil water content and soil water potential during emergence phases and season of microsites within the weed recruitment zone response to hillslope aspect, hillslope position, soil residue and soil depth.

	Soil water content Emergence phase					Soil water potential Emergence phase				
Main fixed effect	Lag†	Exponential	Stationary	Late stationary	Season‡	Lag	Exponential	Stationary	Late stationary	Season
	$m^3\ m^{-3}$					MPa				
Hillslope aspect										
Southwest	0.14	0.17	0.17	0.16	0.17	−0.30	−0.19	−0.25	−0.28	−0.25*b*
Northeast	0.16	0.18	0.17	0.17	0.17	−0.21	−0.15	−0.20	−0.22	−0.20*a*
Hillslope position										
Summit	0.12*c*	0.15*c*	0.13*c*	0.13*c*	0.13*c*	−0.28	−0.21*b*	−0.32	−0.31	−0.29
Backslope	0.15*b*	0.17*b*	0.17*b*	0.16*b*	0.17*b*	−0.20	−0.11*a*	−0.14	−0.19	−0.16
Toeslope	0.19*a*	0.21*a*	0.21*a*	0.20*a*	0.21*a*	−0.29	−0.18*ab*	−0.21	−0.25	−0.23
Residue										
Native	0.15	0.18	0.17	0.17	0.17	−0.25	−0.17	−0.23	−0.25	−0.23
Added	0.15	0.18	0.17	0.16	0.17	−0.26	−0.17	−0.23	−0.25	−0.23
Soil depth										
0–25mm	0.11*b*	0.12*c*	0.11*c*	0.12*c*	0.12*c*	−0.60	−0.43*b*	−0.59	−0.62*b*	−0.57*b*
25–50mm	0.16*a*	0.19*b*	0.18*b*	0.17*b*	0.18*b*	−0.11	−0.05*a*	−0.06	−0.09*a*	−0.07*a*
50–75mm	0.18*a*	0.22*a*	0.22*a*	0.20*a*	0.21*a*	−0.05	−0.03*a*	−0.03	−0.04*a*	−0.03*a*
Contrast										
A in P(Backslope)	0.629	0.382	0.905	0.484	0.839	0.560	0.657	0.652	0.628	0.863
A in P(B), R(Native)	0.595	0.683	0.860	0.662	0.559	0.122	0.301	0.401	0.423	0.073
A in P(B), R(Added)	0.600	0.680	0.532	0.506	0.423	0.091	0.259	0.364	0.339	0.052
A in P(B), D(0–25)	0.456	0.551	0.746	0.754	0.910	0.294	0.051	0.320	0.084	0.005
A in P(B), D(25–50)	0.430	0.679	0.931	0.608	0.482	0.755	0.885	0.815	0.831	0.783
A in P(B), D(50–75)	0.839	0.505	0.724	0.230	0.156	0.781	0.890	0.810	0.864	0.913
Source of variation					*p > F*					
Aspect (A)	0.520	0.428	0.937	0.820	0.351	0.316	0.149	0.626	0.252	0.044
Position (P)	0.005	0.005	0.005	<.001	<.001	0.293	0.082	0.349	0.215	0.249
A × P	0.280	0.081	0.052	0.012	0.009	0.238	0.655	0.098	0.068	0.093
Residue (R)	0.929	0.507	0.189	0.670	0.586	0.539	0.145	0.966	0.945	0.871
A × R	0.989	0.958	0.164	0.787	0.803	0.613	0.778	0.666	0.636	0.707
P × R	0.591	0.989	0.719	0.937	0.954	0.063	0.866	0.891	0.966	0.624

Table 4.8. Continued.

A × P × R	0.936	0.963	0.898	0.187	0.704	0.206	0.287	0.947	0.905	0.374
Depth (D)	0.046	0.005	0.069	<.001	0.025	0.390	<.001	0.253	0.155	0.174
A × D	0.174	0.169	0.811	0.385	0.102	0.405	0.074	0.696	0.380	0.031
P × D	0.029	0.039	0.295	0.142	0.111	0.344	0.004	0.284	0.172	0.171
R × D	0.895	0.539	0.115	0.517	0.573	0.519	0.237	0.915	0.992	0.986
A × P × D	0.570	0.338	0.966	0.546	0.634	0.095	0.587	0.078	0.054	0.046
A × R × D	0.247	0.373	0.269	0.139	0.106	0.686	0.900	0.928	0.875	0.939
P × R × D	0.940	0.532	0.153	0.977	0.234	0.071	0.984	0.967	0.876	0.517
A × P × R × D	0.282	0.308	0.578	0.593	0.819	0.099	0.231	0.979	0.973	0.211

a–c Within columns and factors, means followed by different letters are significantly different at $p \leq 0.05$ according to Fisher's protected LSD.

† Mean daily water content and water potential for emergence phases are based on cumulative daily soil growing degree days (GDD_{soil}) using base 0°C. Time periods approximate a sigmoidal emergence curve separated into phases of lag (0–300 GDD_{soil}), exponential (300–600 GDD_{soil}), stationary (600–900 GDD_{soil}) and late stationary (> 900 GDD_{soil}) (e.g. Avena fatua, Polygonum convolvulus) (Bullied et al., 2003). Lag phase is represented only from time of planting (270.8 GDD_{air} in 2003 and 176.6 GDD_{air} in 2004).

‡ Season is from time of planting to the end of the late stationary phase.

gradient of water with both hillslope position and soil depth (Figs. 4.7a and 4.7b). Hillslope aspect by hillslope position interactions for water content during the late stationary phase and season specified greater water content for the northeast aspect, but only for the uppermost soil increment (Figs. 4.7c and 4.7d).

Soil water potential was lower (more negative) in the southwest aspect compared to the northeast aspect when the entire season was considered (Table 4.8). Precipitation was not a contributing factor since precipitation levels were similar at each aspect over the course of the spring emergence period (Table 4.3). Greater solar radiation was received on the southwest backslope compared to the northeast backslope (Fig. 4.2b), which could have resulted in greater evaporation from the southwest backslope, culminating in lower water potential in the southwest backslope (Oke, 1987). Differences in soil water potential could also be attributed to soil type on the southwest aspect having greater clay content (Table 4.6). Soil water content was not different between hillslope aspects for any phase (Table 4.8). Because retention of soil water is mainly determined by clay content, soils with greater clay content would retain a similar amount of water at lower potentials compared to soils with less clay content (Reeve and Carter, 1991).

Soil water potential was lower in the summit than the backslope position during the exponential phase (Table 4.8). Coarser textured soil in the summit positions would have released water more readily to allow water movement deeper into the recruitment zone, as well as enabling more rapid evaporation of water from the soil surface. Because coarser textured soils contain large pores, the majority of water is released at high water potential (Reeve and Carter, 1991). The summit position had lower water content than the backslope, which in turn had lower water content than the toeslope (Table 4.8). The summit position dried more quickly with the remaining water at lower water potential compared to the backslope position.

The oat residue treatment did not influence soil water potential in any of the emergence phases (Table 4.8). Since the surface cover was low in both treatments (7.5 vs. 16.3% for native vs. added residue, respectively), the small amount of surface residue cover had a minimal effect on evaporation of soil water under the weather conditions experienced at the site. Furthermore, the ability of crop residue to reduce evaporation from soil is limited to a few days following precipitation, after which, the evaporation

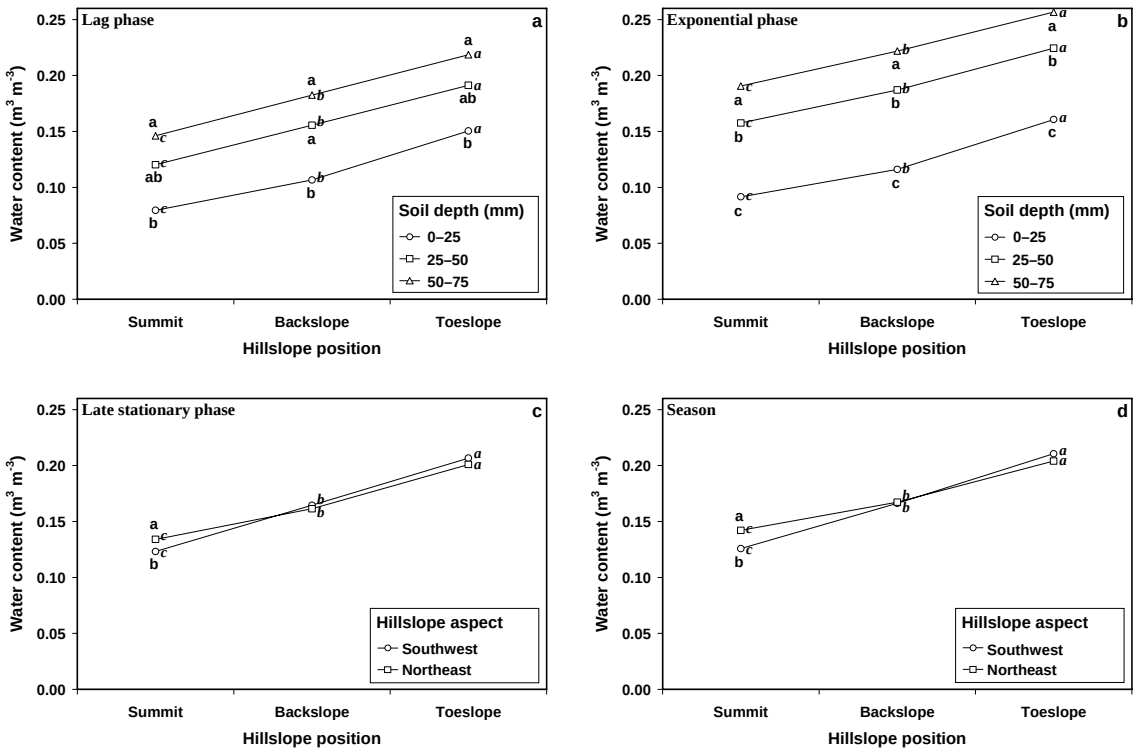

Fig. 4.7. Soil water content in microsites within the weed recruitment zone for (a) the lag phase (0–300 GDD_{soil}), and (b) the exponential phase (300–600 GDD_{soil}) response to interactions of hillslope position by soil depth. Soil water content for (c) the late stationary phase (> 900 GDD_{soil}), and (d) the season in microsites within the weed recruitment zone response to interactions of hillslope aspect by hillslope position. Lowercase serif letters to the right of points designate horizontal separation of simple effects ($p \leq 0.05$), and lowercase non-serif letters above or below points designate vertical separation of simple effects ($p \leq 0.05$).

rate from soil covered with surface mulch is similar to that of a bare soil (Brun et al., 1986).

The greatest differences in soil water potential for the time periods were seen in recruitment depth (Table 4.8). Soil water potential was lower in the 0–25 mm soil increment compared to increments deeper in the recruitment zone during the exponential and late stationary phases, and season (Table 4.8). The gradient of decreasing soil water content toward the soil surface explains the lower potential of sparse tightly bound water in the uppermost soil increment of the recruitment zone (Table 4.8).

A hillslope aspect by soil depth interaction for the season indicated that soil water potential was lower on the southwest aspect compared to the northeast aspect for only the uppermost soil increment of the recruitment zone (Fig. 4.8a). This was also seen in the contrast of the uppermost soil depth in the backslope positions of each aspect for the season (Table 4.8). Because water content was less in the uppermost soil increment, it would be at a lower water potential level, and more readily influenced by differing clay contents of the two aspects.

A hillslope position by soil depth interaction for the exponential phase displayed lower water potential for the summit compared to the backslope position, but only for the uppermost soil increment (Fig. 4.8b). The three-way interaction between hillslope aspect, hillslope position, and soil depth indicated differences in the uppermost soil increment across hillslope positions at each aspect (Fig. 4.8c). This was indicative of the uppermost soil layer in the summit drying more readily than soil layers deeper in the recruitment zone. The uppermost soil increment was different between hillslope positions, with lower water potential in the summit for both aspects and toeslope for the southwest aspect. This may have been due to greater loss of water through evaporation and drainage in the summit, and greater clay content with more small pores in the toeslope, both situations that cause water to be bound tighter.

4.5.4.2 Chemical Properties

The response of soil chemical properties of microsites within the recruitment zone indicated that overall, the greatest effects occurred across hillslope aspect and hillslope position (Table 4.9). Soil chemical properties were not affected by the residue treatment

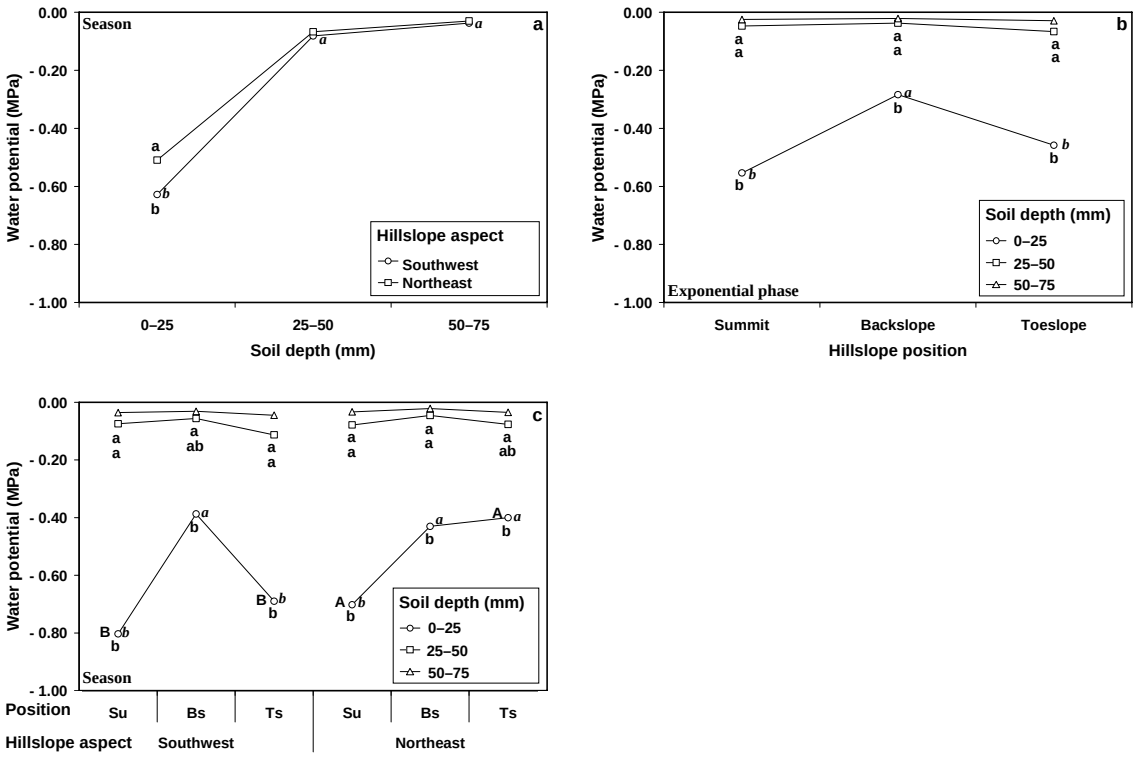

Fig. 4.8. Soil water potential for the season in microsites within the weed recruitment zone response to interactions of (a) hillslope aspect by soil depth, and (c) hillslope aspect by hillslope position by soil depth. Soil water potential for the exponential phase (300–600 GDD_{soil}) in microsites within the weed recruitment zone response to interactions of (b) hillslope position by soil depth. Lowercase serif letters to the right of points designate horizontal separation of simple effects ($p \leq 0.05$), and lowercase non-serif letters above or below points designate vertical separation of simple effects ($p \leq 0.05$). For three-way interactions, uppercase non-serif letters to the left of points designate separation of simple effects between left and right sets of points ($p \leq 0.05$).

Table 4.9. Soil chemical properties of microsites within the weed recruitment zone response to hillslope aspect, hillslope position, soil residue and soil depth.

Main fixed effect	N	P	K	S	Ca	Mg	Na	CEC	pH	EC
	mg kg^{-1}							cmol kg^{-1}	−log[H$^+$]	dS m^{-1}
Hillslope aspect										
Southwest	30	32	368*b*	25	4879*a*	599*a*	24*a*	30*a*	7.9*a*	0.80
Northeast	34	39	445*a*	14	3701*b*	288*b*	16*b*	22*b*	7.4*b*	0.70
Hillslope position										
Summit	28	28*b*	365*b*	9	2304*c*	315*b*	14*b*	16*c*	7.0*b*	0.54
Backslope	31	24*b*	324*b*	23	4616*b*	344*b*	20a*b*	27*b*	8.0*a*	0.81
Toeslope	37	54*a*	530*a*	27	5949*a*	671*a*	27*a*	37*a*	7.9*a*	0.90
Soil residue										
Native	35	36	370	20	4299	443	20	26	7.6	0.75
Added	29	35	442	20	4291	443	20	26	7.7	0.75
Soil depth										
0–25mm	34	37*a*	417*a*	17	4276	446	18	26	7.6	0.75
25–50mm	32	37*a*	422*a*	20	4281	439	20	26	7.6	0.76
50–75mm	31	32*b*	380*b*	22	4313	445	22	26	7.7	0.74
Source of variation	($p > F$)									
Aspect (A)	0.307	0.068	0.045	0.507	0.003	<.001	0.014	<.001	<.001	0.271
Position (P)	0.717	<.001	<.001	0.582	<.001	<.001	0.031	<.001	0.005	0.253
A × P	0.622	0.108	0.049	0.555	0.019	<.001	0.011	<.001	<.001	0.374
Residue (R)	0.072	0.807	0.159	0.805	0.978	0.999	0.715	0.760	0.089	0.682
A × R	0.006	0.774	0.919	0.347	0.902	0.108	0.391	0.795	0.918	0.274
P × R	0.908	0.783	0.787	0.605	0.786	0.026	0.739	0.972	0.322	0.353
A × P × R	0.661	0.293	0.673	0.614	0.978	0.407	0.496	0.888	0.841	0.767
Depth (D)	0.846	0.006	0.018	0.562	0.705	0.314	0.111	0.585	0.365	0.959
A × D	0.395	0.274	0.869	0.834	0.345	0.407	<.001	0.271	0.139	0.496
P × D	0.481	0.412	0.391	0.865	0.782	0.058	0.289	0.696	0.063	0.903
R × D	0.004	0.758	0.242	0.874	0.550	0.141	0.923	0.682	0.077	0.052
A × P × D	0.191	0.528	0.316	0.726	0.850	0.220	0.159	0.229	0.005	0.254
A × R × D	0.925	0.784	0.632	0.883	0.022	0.584	0.254	0.021	0.951	0.756
P × R × D	0.548	0.872	0.068	0.932	0.171	0.129	0.463	0.281	0.197	0.890
A × P × R × D	0.413	0.670	0.461	0.778	0.448	0.194	0.916	0.434	0.615	0.139

a–c Within columns and factors, means followed by different letters are significantly different at $p \leq 0.05$ according to Fisher's protected LSD.

and only to a small extent by soil depth (Table 4.9). Although the residue treatment did not affect any properties, some nitrogen (P = 0.072) may have been immobilized by the addition of the straw, as has been shown in other experiments (Silgram and Chambers, 2002; Shindo and Nishio, 2005). Soil depth was inconsequential for most chemical properties possibly as a result of the small depth increments measured, in addition to the mixing within the recruitment zone in preparation for planting, which may have induced homogeneity of environmental conditions throughout the recruitment zone.

A number of chemical properties differed between hillslope aspects, and this may be due to a site difference rather than an aspect difference *per se*. Management history of fertility inputs prior to and during the experiment were similar for the two aspects, therefore differences between the two aspects for chemical properties such as cation concentrations, CEC, and pH, can be attributed to underlying edaphic properties such as soil type. Because concentrations of cations, CEC and pH are interrelated (Hendershot et al., 1993), greater clay content of the soils in the southwest aspect would be influential on all three chemical properties.

The majority of chemical properties differed across the hillslope positions (Table 4.9). This is reasonable given different soil types, soil movement, and hydrologic flow across the hillslope positions. Cation concentrations, CEC, and pH increased downslope, likely due to the increasing clay content from summit to toeslope (Table 4.9). Although nitrate-N and sulfate-S were not different across the hillslope positions, P increased downslope, likely due to downslope soil movement.

No differences between residue treatments existed for any soil chemical properties (Table 4.9). Although the addition of mature crop straw can influence soil chemical properties, it would have less effect on soil properties compared to green residues (Hulugalle and Weaver, 2005).

Most of the soil chemical properties did not differ with depth in the recruitment zone, which is probably a reflection of the shallow measured increments (Table 4.9). Phosphorus and potassium declined in concentration with depth in the recruitment zone.

The majority of differences in chemical properties involving topographic interactions can be attributed to diverse soil types across the topography. A hillslope aspect by hillslope position interaction for K (Fig. 4.9a), Ca (Fig. 4.9b), Mg (Fig. 4.9c),

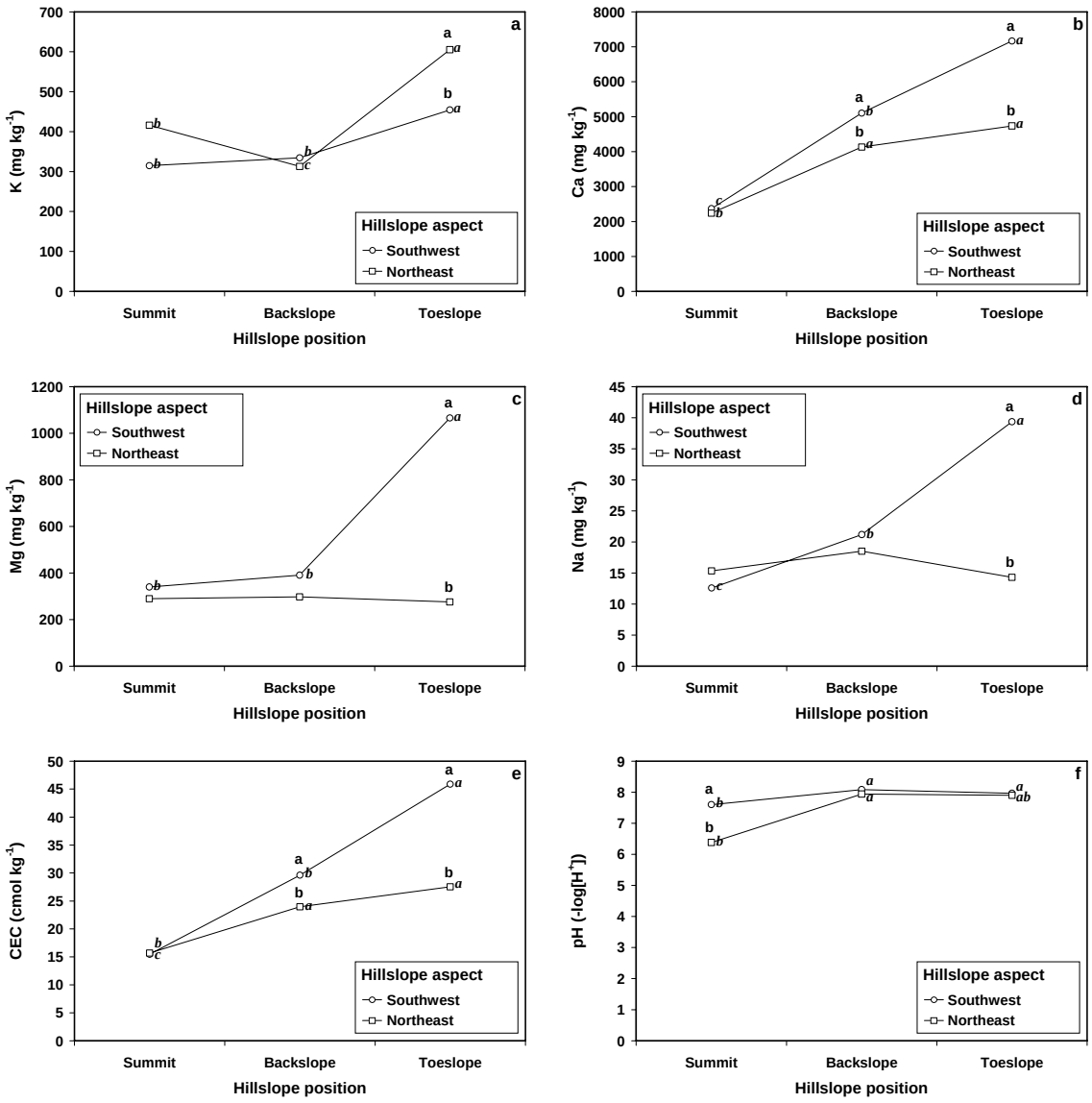

Fig. 4.9. Soil chemical properties of microsites within the weed recruitment zone response to interactions of (a–f) hillslope aspect by hillslope position, (g) hillslope aspect by soil residue, (h) hillslope position by soil residue, (i) hillslope aspect by soil depth, (j) soil residue by soil depth, (k) hillslope aspect by hillslope position by soil depth, and (l–m) hillslope aspect by soil residue by soil depth. Lowercase serif letters to the right of points designate horizontal separation of simple effects ($p \leq 0.05$), and lowercase non-serif letters above or below points designate vertical separation of simple effects ($p \leq 0.05$). For three-way interactions, uppercase non-serif letters to the left of points designate separation of simple effects between left and right sets of points ($p \leq 0.05$).

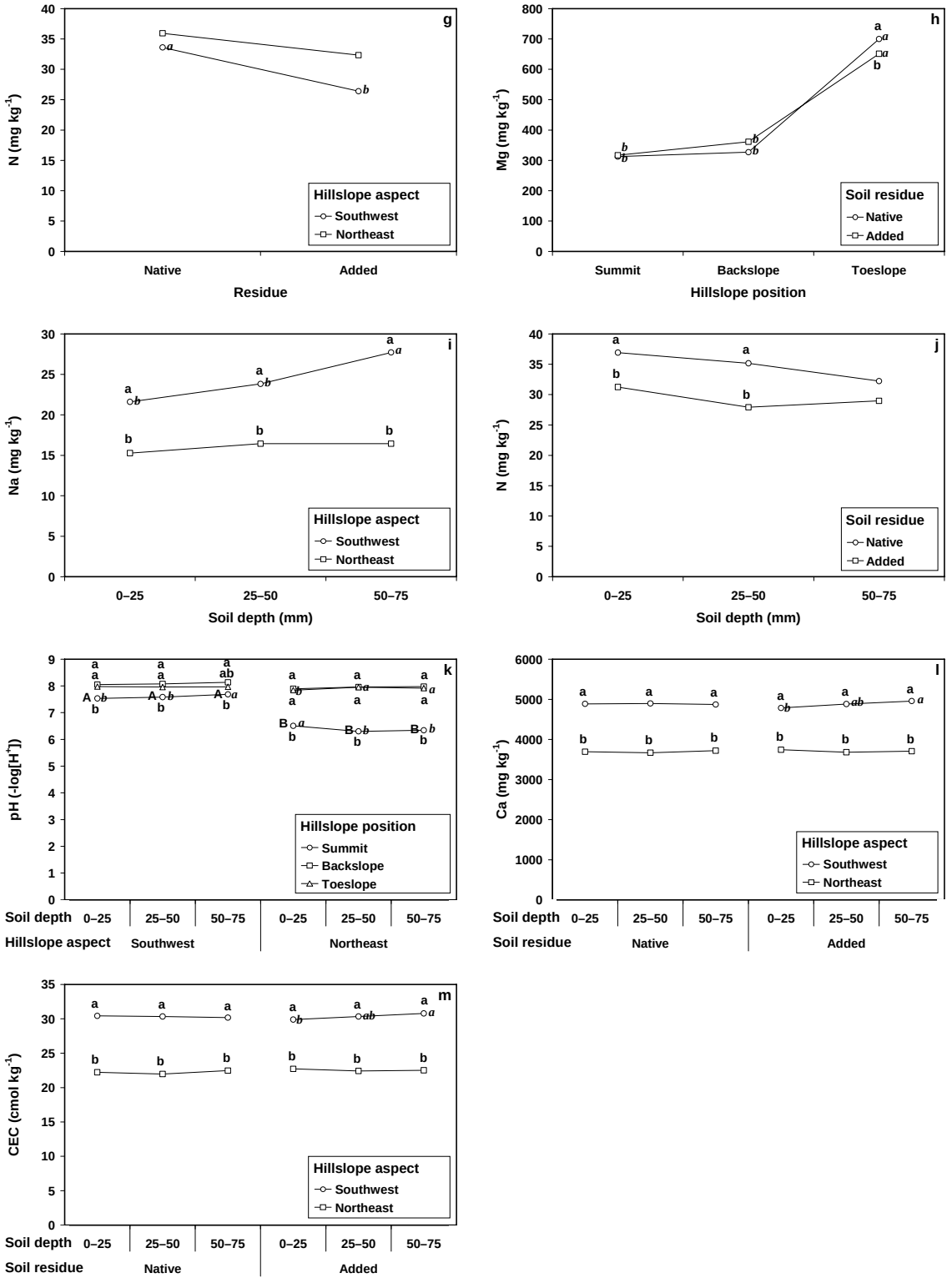

Fig 4.9. Continued.

Na (Fig. 4.9d), and CEC (Fig. 4.9e) indicated that the northeast toeslope had greater concentrations compared to the southwest toeslope, while no differences occurred in the summit, and differences occurred in the backslope for calcium and CEC. The Willowbend soil in the toeslope of the southwest aspect had greater clay content and poor drainage, which would account for retention of many nutrients. A hillslope aspect by hillslope position interaction also occurred for pH, however differences between aspects existed on only the summit (Fig. 4.9f).

Interactions involving residue occurred for nitrate-N (Fig. 4.9g) and Mg (Fig. 4.9h). Nitrate-N level declined with the added straw on the southwest aspect (Fig. 4.9g), possibly as a result of immobilization of nitrogen by the additional crop residue. Magnesium concentration was reduced in the toeslope with added crop straw (Fig. 4.9h). Interactions of soil depth occurred for Na (Fig. 4.9i) and nitrate-N (Fig. 4.9j). Only the southwest aspect had an increase in sodium concentration with depth in the recruitment zone (Fig. 4.9i). Nitrate-N concentration was greater for the native residue treatment in the upper two soil increments (Fig. 4.9j), perhaps reflecting a decreasing gradient of oat straw with soil depth. The nitrate-N concentration may have been higher in the native residue treatment (soybean residue) due to decomposition and mineralization of the higher N-containing soybean residue whereas the low N-containing oat straw residue would not have mineralized as much nitrogen and may actually have immobilized some nitrogen.

A three-way interaction for pH indicated that pH was either greater or similar with depth in the recruitment zone, except for the summit of the northeast aspect, in which pH decreased with depth (Fig. 4.9k). Since the northeast summit had a lower pH compared to the other hillslope positions, it may have been increased in the uppermost soil increment by the addition of the oat straw (Hulugalle and Weaver, 2005). Hillslope aspect by soil residue by soil depth interactions for Ca (Fig. 4.9l) and CEC (Fig. 4.9m) indicated that the addition of oat straw decreased Ca and CEC in the uppermost soil increment of the southwest aspect. Since the southwest aspect had greater levels of Ca (Fig. 4.9b) and CEC (Fig. 4.9e) compared to the northeast aspect, it may have been more subject to decline in Ca and CEC levels from the addition of the oat straw (Hulugalle and Weaver, 2005).

4.6 CONCLUSIONS

Most weeds recruit from a relatively shallow recruitment zone in the soil where spatial and temporal environmental conditions can vary considerably. Wind run and solar radiation differed across topography. Soil temperature and soil temperature fluctuation decreased with depth in the seedling recruitment zone. Soil temperature fluctuation additionally decreased with lower hillslope position when the entire season was considered. Soil water content and water potential varied more between years than soil temperature. Soil water increased with soil depth and lower hillslope position. Physical edaphic properties including texture varied across the topography and soil depth, whereas soil bulk density differed across all experimental factors. Soil chemistry differed mainly across the topography, and to a lesser extent, with soil depth. Soil residue had less influence on the soil environment in general compared to the topographic and soil depth factors.

The seedling recruitment zone represents a heterogeneous environment influencing weed germination and emergence. The recruitment zone becomes even more diverse across field topography, where microclimate conditions act differentially across an uneven soil surface to form a variable environment within the recruitment zone. Edaphic properties additionally create variability within the recruitment zone that regulates weed germination and emergence. The variability of the recruitment zone environment would be expected to have a diverse effect on weed recruitment from various microsites within the recruitment zone. Implications for predictions of weed recruitment across a field topography would therefore be reliant not only on site-specific properties of the topography, but also the vertical location of the microsite within the profile of the recruitment zone as they are affected by hillslope position and related microclimate conditions.

The most important spatial factors in relation to seedling recruitment environment in this study were influences of topographic hillslope position and recruitment zone depth. Temperature and water in the seedling recruitment zone varied mostly with hillslope position and soil depth. Site-specific weed recruitment models therefore need to comprise spatial elements of hillslope position and microsite depth that reflect the spatial

and temporal dynamics of the recruitment zone environment to generate robust seedling recruitment models.

4.7 REFERENCES

Abu-Hamdeh, N.H. and R.C. Reeder. 2000. Soil thermal conductivity: Effects of density, moisture, salt concentration, and organic matter. Soil Sci. Soc. Am. J. 64:1285–1290.

Alberta Research Council. 1996. Methods manual for chemical analysis of water and wastes. Method 19103 565, potassium, dissolved (automated flame photometry method). Alberta Environmental Centre, Vegreville, AB, Canada.

American Public Health Association. 1998a. Standard methods for the examination of water and wastewater, 20th edition. APHA 3120 B, inductively coupled plasma (ICP) method. APHA, Washington, DC.

American Public Health Association. 1998b. Standard methods for the examination of water and wastewater, 20th edition. APHA 4500-NO_3^- F, automated cadmium reduction method. APHA, Washington, DC.

American Public Health Association. 1998c. Standard methods for the examination of water and wastewater, 20th edition. APHA 4500-P D, stannous chloride method. APHA, Washington, DC.

American Public Health Association. 1998d. Standard methods for the examination of water and wastewater, 20th edition. APHA 4500-SO_4^{2-} E, turbidimetric method. APHA, Washington, DC.

Ashworth, J. and K. Mrazek. 1995. “Modified Kelowna” test for available phosphorus and potassium in soil. Commun. Soil Sci. Plant Anal. 26:731–739.

Andreasen, C. and J.C. Streibig. 1991. Soil properties affecting the distribution of 37 weed species in Danish fields. Weed Res. 31:181–187.

Bàrberi, P. and B. Lo Cascio. 2001. Long-term tillage and crop rotation effects on weed seedbank size and composition. Weed Res. 41:325–340.

Bibbey, R.O. 1935. The influence of environment upon the germination of weed seeds. Sci. Agric. 15:141–150.

Boyd, N. and R.C. Van Acker. 2004. Seed and microsite limitations to emergence of four annual weed species. Weed Sci. 52:571–577.

Bradford, K.J. 2002. Applications of hydrothermal time to quantifying and modeling seed germination and dormancy. Weed Sci. 50:248–260.

Brubaker, S.C., A.J. Jones, D.T. Lewis, and K. Frank. 1993. Soil properties associated with landscape position. Soil Sci. Soc. Am. J. 57:235–239.

Bruce, R.R., A.W. Thomas, L.A. Harper, and R.A. Leonard. 1977. Diurnal soil water regime in the tilled plow layer of a warm humid climate. Soil Sci. Soc. Am. J. 41:455–460.

Brun, L.J., J.W. Enz, J.K. Larsen, and C. Fanning. 1986. Springtime evaporation from bare and stubble-covered soil. J. Soil Water Conserv. 41:120–122.

Buhler, D.D. 1995. Influence of tillage systems on weed population dynamics and management in corn and soybean in the central USA. Crop Sci. 35:1247–1258.

Bullied, W.J., A.M. Marginet, and R.C. Van Acker. 2003. Conventional- and conservation-tillage systems influence emergence periodicity of annual weed species in canola. Weed Sci. 51:886–897.

Campbell, D.J. and J.K. Henshall. 1991. Bulk density. p. 329–366. In K.A. Smith and C.E. Mullins ed. Soil analysis: physical methods. Marcel Dekker, Inc., New York.

Cardina, J., G.A. Johnson, and D.H. Sparrow. 1997. The nature and consequences of weed spatial distribution. Weed Sci. 45:364–373.

Chachalis, D. and K.N. Reddy. 2000. Factors affecting *Campsis radicans* seed germination and seedling emergence. Weed Sci. 48:212–216.

Cochran, P. H. 1969. Thermal properties and surface temperatures of seedbeds; a guide for foresters. USDA. Portland OR.

Cousens, R. and M. Mortimer. 1995. Dynamics of weed populations. Cambridge University Press, Cambridge, UK.

Cousens, R. and S.R. Moss. 1990. A model of the effects of cultivation on the vertical distribution of weed seeds within the soil. Weed Res. 30:61–70.

Dane, J.H. and J.W. Hopmans. 2002. Water retention and storage. p. 671–690. In J.H. Dane and G.C. Topp ed. Methods of soil analysis. Soil Sci. Soc. Am., Madison, WI.

du Croix Sissons, M.J., R.C. Van Acker, D.A. Derksen, and A.G. Thomas. 2000. Depth of seedling recruitment of five weed species measured in situ in conventional- and zero-tillage fields. Weed Sci. 48:327–332.

Egley, G.H. 1986. Stimulation of weed seed germination in soil. Rev. Weed Sci. 2:67–89.

Eriksson, O. and J. Ehrlén. 1992. Seed and microsite limitation of recruitment in plant populations. Oecol. 91:360–364.

Fenner, M. and K. Thompson. 2005. The ecology of seeds. Cambridge University Press, Cambridge, UK.

Forcella F., R.L. Benech-Arnold, R. Sanchez, and C.M. Ghersa. 2000. Modeling weed emergence. Field Crops Res. 67:123–139.

Garnier, B.J. and A. Ohmura. 1968. A method of calculating the direct short wave radiation income of slopes. J. Appl. Meteorol. 7:796–800.

Gee, G.W. and D. Or. 2002. Particle size analysis. p. 255–293. In J.H. Dane and G.C. Topp ed. Methods of soil analysis. Soil Sci. Soc. Am., Madison, WI.

Geiger, R. 1965. The influence of topography on microclimate. p. 369–467. In R. Geiger ed. The climate near the ground. Oxford University Press, London.

Hanna, A.Y., P.W. Harlan, and D.T. Lewis. 1982. Soil available water as influenced by landscape position and aspect. Agron. J. 74:999–1004.

Hares, M.A. and M.D. Novak. 1992. Simulation of surface energy balance and soil temperature under strip tillage. II. Field test. Soil Sci. Soc. Am. J. 56:29–36.

Harper, J.L. 1977. The recruitment of seedling populations. p. 111–147. In J.L. Harper ed. Population biology of plants. Academic Press, London.

Hendershot, W.H., H. Lalande and M. Duquette. 1993. Ion exchange and exchangeable cations. p. 167–176. In M.R. Carter ed. Soil sampling and methods of analysis, CRC Press, Boca Raton.

Horton, R., G.J. Kluitenberg, and K.L. Bristow. 1994. Surface crop residue effects on the soil surface energy balance. p. 143–162. In P.W. Unger ed. Managing agricultural residues. Lewis Publ., Ann Arbor, MI.

Hulugalle, N.R. and T.B. Weaver. 2005. Short-term variations in chemical properties of vertisols as affected by amounts, carbon/nitrogen ratio, and nutrient concentration of crop residues. Commun. Soil Sci. Plant Anal. 36:1449–1464.

Hurtt, W. and R.B. Taylorson. 1986. Chemical manipulation of weed emergence. Weed Res. 26:259–267.

Kegode, G.O., R.B. Pearce, and T.B. Bailey. 1998. Influence of fluctuating temperatures on emergence of shattercane (*Sorghum bicolor*) and giant foxtail (*Setaria faberi*). Weed Sci. 46:330–335.

Kowalenko, C.G. 1993. Extraction of available sulfur. p. 65–74. In M.R. Carter ed. Soil sampling and methods of analysis. CRC Press, Boca Raton.

Leguizamón, E.S., C. Fernandez-Quintanilla, J. Barroso, and J.L. Gonzalez-Andujar. 2005. Using thermal and hydrothermal time to model seedling emergence of *Avena sterilis* ssp. ludoviciana in Spain. Weed Res. 45:149–156.

Littell, R.C., G.A. Milliken, W.W. Stroup, and R.D. Wolfinger. 1996. SAS System for mixed models. SAS Institute Inc., Cary, NC.

Lowery, B. and D.E. Stoltenberg. 1998. Tillage systems and crop residue management impacts on soil physical properties: Implications for weed management. p. 87–105. In J.L. Hatfield, D.D. Buhler, and B.A. Stewart ed. Integrated weed and soil management. Ann Arbor Press, Ann Arbor, MI.

Malo, D.D., B.K. Worchester, D.K. Cassel and K.D. Matzdorf. 1974. Soil-landscape relationships in a closed drainage system. Soil Sci. Soc. Am. Proc. 38:813–818.

McKeague, J.A. 1978a. Manual on soil sampling and methods of analysis. Method 3.32, CEC and exchangeable cations by NH_4OAc at pH 7. Canadian Society of Soil Science, Ottawa, ON, Canada.

McKeague, J.A. 1978b. Manual on soil sampling and methods of analysis. Method 3.8, loss on ignition. Canadian Society of Soil Science, Ottawa, ON, Canada.

McKeague, J.A. 1978c. Manual on soil sampling and methods of analysis. Method 4.12, 1:2 soil:water ratio. Canadian Society of Soil Science, Ottawa, ON, Canada.

McKeague, J.A. 1978d. Manual on soil sampling and methods of analysis. Method 4.51, ammonium acetate extractable cations. Canadian Society of Soil Science, Ottawa, ON, Canada.

Medlin, C.R., D.R. Shaw, M.S. Cox, P.D. Gerard, M.J. Abshire, and M.C. Wardlaw III. 2001. Using soil parameters to predict weed infestations in soybean. Weed Sci. 49:367–374.

Miller, R.W. and D.T. Gardiner. 2001. Soils in our environment. 9th ed. Prentice-Hall Inc., Upper Saddle River, NJ.

Mohler, C.L. and A.E. Galford. 1997. Weed seedling emergence and seed survival: separating the effects of seed position and soil modification by tillage. Weed Res. 37:147–155.

Monteith, J.L. 1990. Principles of environmental physics. 2nd ed. Edward Arnold, New York.

Oke, T.R. 1987. Climates of non-uniform terrain. p. 158–189. In T.R. Oke ed. Boundary layer climates. 2nd ed. Routledge, New York.

Oke, T.R. and F.G. Hannell. 1966. Variations of temperature within a soil. Weather. 21:21–28.

Pareja, M.R. and D.W. Staniforth. 1985. Seed-soil microsite characteristics in relation to weed seed germination. Weed Sci. 33:190–195.

Pareja, M.R., D.W. Staniforth, and G.P. Pareja. 1985. Distribution of weed seed among soil structural units. Weed Sci. 33:182–189.

Probert, R.J., R.D. Smith, and P. Birch. 1986. Germination responses to light and alternating temperatures in European populations of *Dactylis glomerata* L. V. The principle components of the alternating temperature requirement. New Phytol. 102:133–142.

Reeve, M.J. and A.D. Carter. 1991. Water release characteristics. p. 111–160. In K.A. Smith and C.E. Mullins ed. Soil analysis: physical methods. Marcel Dekker, Inc., New York.

Reid, D.J. and R.C. Van Acker. 2005. Seed burial by tillage promotes field recruitment of false cleavers (*Galium spurium*) and catchweed bedstraw (*Galium aparine*). Weed Sci. 53:578–585.

Reuss, S.A., D.D. Buhler, and J.L. Gunsolus. 2001. Effects of soil depth and aggregate size on weed seed distribution and viability in a silt loam soil. Appl. Soil Ecol. 16:209–217.

Ridolfia, L., P. D'Odoricoc, A. Porporatoa, and I. Rodriguez-Iturbe. 2003. Stochastic soil moisture dynamics along a hillslope. J. Hydrol. 272:264–275.

Roberts, H.A. 1986. Seed persistence in soil and seasonal emergence in plant species from different habitats. J. Appl. Ecol. 23:639–656.

Rosenberg, N.J., B.L. Blad, and S.B. Verma. 1983. Microclimate: The biological environment. 2nd ed. John Wiley and Sons. New York.

Ross, D.M. and R.C. Van Acker. 2005. Effect of nitrogen fertilizer and landscape position on wild oat (*Avena fatua*) interference in spring wheat. Weed Sci. 53:869–876.

Ruhe R.V. 1975. Hillslopes. p. 99–123. In R.V. Ruhe ed. Geomorphology: Geomorphic processes and surficial geology. Houghton Mifflin, Boston, MA.

Schieldge, J.P., A.B. Kahle, and R.E. Alley. 1982. A numerical simulation of soil temperature and moisture variations for a bare field. Soil Sci. 133:197–207.

Sharratt, B.S. 2002. Corn stubble height and residue placement in the northern US corn belt. II. Spring microclimate and wheat development. Soil Tillage Res. 64:253–261.

Shindo, H. and T. Nishio. 2005. Immobilization and remineralization of N following addition of wheat straw into soil: determination of gross N transformation rates by ^{15}N-ammonium isotope dilution technique. Soil Biol. Biochem. 37:425–432.

Silgram, M., and B.J. Chambers. 2002. Effects of long-term straw management and fertilizer nitrogen additions on soil nitrogen supply and crop yields at two sites in eastern England. J. Agric. Sci. (Cambridge) 139:115–127.

Soil Classification Working Group. 1998. The Canadian system of soil classification, 3rd ed. Agriculture and Agri-Food Canada Publ. 1646. NRC Research Press, Ottawa, ON.

Soil Survey Staff. 1999. Soil taxonomy: A basic system of soil classification for making and interpreting soil surveys. 2nd ed. USDS-NRCS Agric. Handb. 436. U.S. Gov. Print Office, Washington, DC.

Staricka, J.A., P.M. Burford, R.R. Allmaras, and W.W. Nelson. 1990. Tracing the vertical distribution of simulated shattered seeds as related to tillage. Agron. J. 82:1131–1134.

Stoller, E.W. and L.M. Wax. 1973. Temperature variations in the surface layers of an agricultural soil. Weed Res. 13:273–282.

Tian, Y.Q., R. J. Davies-Colley, P. Gonga, and B.W. Thorrold. 2001. Estimating solar radiation on slopes of arbitrary aspect. Agric. For. Meteorol. 109:67–74.

Young, F.J. and R.D. Hammer. 2000. Soil–landform relationships on a loess-mantled upland landscape in Missouri. Soil Sci. Soc. Am. J. 64:1443–1454.

5.0 Spatial Variability of the Soil Water Retention Characteristic for the Shallow Seedling Recruitment Zone across Field Topography

5.1 ABSTRACT

The soil water retention characteristic (SWRC) is important for the study of water availability to germinating seeds. The objective of this study was to determine the SWRC for three increments of the shallow seedling recruitment zone to a depth of 75 mm at three hillslope positions on two hillslope aspects across agricultural field topography. Suction cups and pressure plates were used to determine volumetric water content at matric suctions of 0.0, 0.01, 0.033, 0.05, 0.1, 0.5, and 1.5 MPa for the middle soil increment of the shallow seedling recruitment zone. Analytical models were evaluated to describe the SWRC. The Brooks-Corey, van Genuchten, and Campbell models ranked similarly well in their ability to describe the water retention relationships for the seedling recruitment zone. The continuous form of the van Genuchten model was considered to be superior to model water content at low pressures. Estimating θ_r as an optimized parameter yielded superior fit compared to either measured values of θ_r at −1.5 MPa, or modifying θ_r with a logarithmic equation. Three pedotransfer functions (PTFs) were formulated to estimate the parameters of the SWRC for the van Genuchten model using basic soil physical properties or detailed particle-size distribution. The SWRC in the adjacent soil increments of the seedling recruitment zone were then estimated by PTF using immediate soil physical properties and the best estimated SWRC of the middle soil increment. Soil physical properties varied with incremental depth in the recruitment zone, although this did not translate into differences in water retention with depth. Where direct measurement of soil hydraulic properties is not feasible due to time or resource constraints, estimation of the SWRC by PTF using the SWRC from the adjacent soil increment coupled with more easily measured soil physical properties of the immediate soil increment can predict the SWRC for the entire shallow seedling recruitment profile.

5.2 ABBREVIATIONS

AIC, Akaike Information Criterion; BC, Brooks and Corey (1964); BD, bulk density; CA, Campbell (1974); IME, integral mean error; IRMSE, integral root mean square error; OM, organic matter; PC, principal components; PCR, principal components regression; PTF, pedotransfer function; RU, Russo (1988); SWRC, soil water retention characteristic; TA, Tani (1982); VG_1, van Genuchten (1980) with five free parameters; VG_2, van Genuchten (1980) with four free parameters.

5.3 INTRODUCTION

The soil water retention characteristic (SWRC) is a basic hydrophysical property of the soil that relates the energy state of the soil water to its water content (Hillel, 1982). The water content–potential function $\theta(\psi)$ is fundamental to the characterization of water holding capacity, water retention, and water flow in soil (Bruce and Luxmoore, 1986; Topp et al., 1993). Since the SWRC is necessary for modeling fluxes in soil water, knowledge of the SWRC is essential for germination studies.

Seed germination is a function of soil water potential. As the soil dries, soil water potential is reduced, and it becomes increasingly difficult for seeds to imbibe water. At inadequately low soil water potential, seeds do not imbibe sufficient water to germinate. Therefore, accurate representation of the water status within the seedling recruitment zone is fundamental to seedling recruitment modeling.

One of the greatest challenges in characterizing the SWRC is obtaining the parameters of the soil hydrological property. Determining the SWRC across field topography by direct measurement is time consuming to obtain sufficient representation of the area due to spatial and temporal variability of soil water properties in the field (Greminger et al., 1985; Nielsen et al., 1973; Cassel, 1983; Burden and Selim, 1989; Scheinost et al., 1997; Saito et al., 2008). The ability of the soil to retain and transmit water is affected by soil texture, and soil pore size and arrangement, and is specific to soil type (Hillel, 1982; Penning de Vries et al., 1989; Jauhiainen, 2002). Diverse SWRCs often exist in soils along a hillslope as a result of variability in texture and pore size distribution (Jauhiainen, 2002; Tomer et al., 2006). The SWRC is not proportional and can be expressed as a nonlinear function (Brooks and Corey, 1964; Campbell, 1974; van

Genuchten, 1980). Detailed characterization of the spatial and temporal variability of the SWRC across field topography and seedling recruitment depth is essential for germination and emergence modeling.

Estimation of the SWRC using readily available basic soil physical properties and mathematical equations is an alternative to direct measurement (Rawls et al., 1991; Wösten et al., 2001; Cook and Cresswell, 2008). The transfer of information from basic soil properties to more difficult to obtain SWRC information is termed a pedotransfer function (PTF) (Bouma, 1989). PTFs are frequently derived from field measurements of soil properties using multiple regression analysis (Rawls and Brakensiek, 1982; Vereecken et al., 1989). PTFs provide a means to translate basic soil property information into a form useful in broader applications such as simulation modeling. The soil properties used most frequently to estimate the SWRC are soil particle size, bulk density (BD), and soil organic matter (OM) (De Jong et al., 1983; Rawls et al., 1991; Nemes and Rawls, 2004; Rawls et al., 2004). Additionally, topographic attributes including slope curvature and particle redistribution can improve the ability of PTFs to predict the SWRC over that of texture alone (Pachepsky et al., 2001b; Rawls and Pachepsky, 2002; Romano and Palladino, 2002; Romano and Chirico, 2004). The structure of spatial variability in soil properties across topography used as variables in PTFs was adequate for describing the SWRC (Romano and Santini, 1997).

PTFs using basic soil properties as predictors have been used to estimate specific points on the SWRC (Gupta and Larson, 1979; Rawls and Brakensiek, 1982; Ahuja et al., 1985; Williams et al., 1992b; Shein et al., 2004; Walczak et al., 2006), or to predict parameters of a regression function representing the SWRC (Wösten and van Genuchten, 1988; Vereecken et al., 1989; Scheinost et al., 1997; Wösten et al., 2001). Functional parameter regression intrinsically implies that a closed-form parametric equation predicts the SWRC, with the parameters of the regression equation predicted by specific soil properties.

The performance of PTFs is often influenced by geographical preference of the source data set such that PTFs developed on soils of similar properties to the ones under study generally perform better than those developed on soils of different properties (Cornelis et al., 2001; Nemes et al., 2003; Givi et al., 2004). Numerous PTFs are based

on data from a specific region and intended for local application (De Jong et al., 1983; Wösten and van Genuchten, 1988; Vereecken et al., 1989). PTFs may have limited transferability to other regions or soil types as the performance of a PTF may vary with pedological origin of the soil on which the PTF was developed (Schaap and Leij, 1998a; Schaap and Leij, 1998b). Most PTFs are developed from small sample size which affects average parameter values and their spatial distribution (Pachepsky et al., 2001a). PTFs developed at the sample scale are typically used for regional applications (Wösten et al., 2004). PTFs can however provide accurate and precise estimates of the SWRC at the hillslope scale even at relatively coarse sampling resolution (Chirico et al., 2007).

The purpose of this study was to estimate the SWRC based on PTFs in terms of describing the spatial structure of the SWRC across field topography and depth of seedling recruitment. The objectives of this study were to fit analytical models to the measured data and compare the models to best describe the SWRC for the 25–50 mm increment in the 75 mm vertical profile of the shallow seedling recruitment zone across field topography. A second objective was to estimate and validate the accuracy of the SWRC for the middle increment in the seedling recruitment zone by estimating SWRC parameters with three PTFs using basic soil properties. The best predicting PTFs were then used to locally estimate SWRCs for the adjacent upper (0–25 mm) and lower (50–75 mm) increments of the shallow seedling recruitment zone by using basic soil property information in the immediate soil increments and the SWRC predicted by PTF from the 25–50 mm soil increment.

5.4 MATERIALS AND METHODS

5.4.1 Experimental Methods

SWRCs were created for the shallow seedling recruitment zone from three replicates in each of three hillslope positions on two hillslope aspects across topography in an annually cropped agricultural field. Individual SWRCs were produced for each hillslope position (summit, backslope and toeslope) since soil physical properties have been shown to reflect hillslope position with much greater variability between positions than within a position (Ovalles and Collins, 1986; Kreznor et al., 1989; Brubaker et al., 1993). The seedbed was prepared by rotary tillage and press seeder. Surface soil texture

ranged from loamy fine sand to silty clay. Average soil physical properties in the shallow seedling recruitment zone are indicated in Table 5.1.

Soil samples were extracted from the 25–50 mm soil depth by using 50 mm diameter by 25 mm deep rings. Subsamples of soil weighing 12 g were placed in shallow plexiglass cylinders and saturated for 24 h. The water retention relationship for each hillslope position was determined on desorption from saturation to the permanent wilting point. Volumetric water content was determined at pressures of 0.0, 0.01, 0.033, 0.05, 0.1, 0.5, and 1.5 MPa (0.00, 0.10, 0.33, 0.50, 1.0, 5.0, and 15.0 bar) (Dane and Hopmans, 2002). The soil samples were placed on saturated porous plates in covered ceramic suction cups to equilibrate saturation water content over 48 h by placing the meniscus in the burette level with the top of the ceramic plate. A model 1600 5-bar pressure plate extractor with a 1-bar porous ceramic pressure plate (Soil Moisture Equipment Corp., P.O. Box 30025, Santa Barbara, CA, 93130) with compressed air was used to produce pressures of 0.01 to 1.0 MPa. Compressed nitrogen was used in a model 1500 15-bar pressure plate extractor with 5-bar and 15-bar porous ceramic pressure plates (Soil Moisture Equipment Corp., P.O. Box 30025, Santa Barbara, CA, 93130) to produce pressures of 0.5 and 1.5 MPa. At each pressure increment increase, progressively smaller soil pores lose water and the water content of the soil decreases until equilibrium is achieved. At equilibrium, soils were removed from the ceramic plates, transferred to a beaker, and oven dried at 105 C for 48 h. The pressure plate method of determining the SWRC does not account for the effect of hysteresis since only the desorption curve is obtained. The amount of water at a given pressure is greater on desorption compared to sorption (Hillel, 1982). The desorption curve may be more representative for the shallow recruitment zone since seeds encounter drying over a number of days following rainfall events, whereas sorption generally occurs rapidly following a precipitation event.

5.4.2 Soil Water Retention Models

5.4.2.1 Model Specifications

Of the many models reported in the literature representing the SWRC, several commonly used equations having a low number of parameters were evaluated for their ability to fit the data. SWRC models provide a systematic way of extrapolating the

Table 5.1. Average measured soil physical properties for the shallow seedling recruitment zone of the hillslope positions.

Hillslope position Soil depth (mm)	Textural class	Clay	Silt	Sand	Organic matter	Bulk density
		g kg^{-1}				g cm^{-3}
SW summit	Silt loam					
0–25		53.3*d*	750.0*a*	196.7*d*	34.7*d*	1.08*a* (*b*)
25–50		56.7*d*	746.7*a*	196.7*c*	35.3*d*	1.12*a* (*b*)
50–75		56.7*d*	746.7*a*	196.7*d*	32.7*d*	1.20*ab* (*a*)
SW backslope	Silt loam					
0–25		96.7*c* (*b*)	623.3*c*	280.0*b*	38.7*cd* (*a*)	1.03*ab* (*b*)
25–50		96.7*c* (*b*)	616.7*c*	286.7*b*	38.7*cd* (*a*)	1.04*a* (*b*)
50–75		113.3*c* (*a*)	613.3*c*	273.3*b*	35.3*cd* (*b*)	1.14a*b* (*a*)
SW toeslope	Clay loam					
0–25		290.0*a* (*b*)	333.3*e* (*a*)	376.7*a*	61.3*a* (*a*)	0.84*c* (*b*)
25–50		286.7*a* (*b*)	323.3*e* (*ab*)	390.0*a*	60.6*a* (*a*)	0.86*b* (*b*)
50–75		300.0*a* (*a*)	320.0*e* (*b*)	380.0*a*	57.3*a* (*b*)	0.95*c* (*a*)
NE summit	Silt loam					
0–25		86.7*c*	690.0*b*	223.3*cd*	44.7*bc* (*a*)	1.03*ab* (*b*)
25–50		83.3*cd*	690.0*b*	226.7*c*	44.0*bc* (*ab*)	1.09*a* (*b*)
50–75		90.0*c*	683.3*b*	226.7*cd*	41.3*bc* (*b*)	1.16*ab* (*a*)
NE backslope	Silt loam					
0–25		96.7*c* (*b*)	646.7*bc*	256.7*bc*	36.7*d*	1.07*a* (*b*)
25–50		93.3*c* (*b*)	640.0*bc*	266.7*b*	34.7*d*	1.13*a* (*b*)
50–75		110.0*c* (*a*)	636.7*bc*	253.3*bc*	34.0*d*	1.23*a* (*a*)
NE toeslope	Loam					
0–25		156.7*b* (*b*)	466.7*d*	376.7*a*	47.3*b* (*a*)	0.97*b* (*b*)
25–50		156.7*b* (*b*)	463.3*d*	380.0*a*	46.0*b* (*ab*)	1.05*a* (*a*)
50–75		173.3*b* (*a*)	456.7*d*	370.0*a*	43.3*b* (*b*)	1.11*b* (*a*)

a–*e* Within columns and soil depth, soil property means followed by different letters are significantly different at $p \leq 0.05$ according to Fisher's protected LSD.

(*a*–*b*) Within columns and hillslope position, soil property means followed by different letters are significantly different at $p \leq 0.05$ according to Fisher's protected LSD.

SWRC from a limited number of measurements. The Brooks-Corey (BC) model (Brooks and Corey, 1964) is a four parameter equation in which water content is expressed as a power function of soil water pressure using the expression

$$\theta = \theta_r + (\theta_s - \theta_r)\left[\frac{\psi}{\psi_e}\right]^{-\lambda} \qquad \text{for } \psi < \psi_e$$

$$\theta = \theta_s \qquad \text{for } \psi \geq \psi_e \qquad [1]$$

where θ is volumetric water content, ψ is matric potential, θ_s is saturated volumetric water content, θ_r is residual soil water content when ψ is infinitely small, ψ_e is a curve fitting parameter, known as the air entry matric suction, and λ is a pore size distribution factor. The residual soil water content is the water content at the dry end of the SWRC at which the gradient $(d\theta / d\psi)$ becomes zero and unsaturated hydraulic conductivity ceases (van Genuchten, 1980). The restriction $\theta = \theta_s$ is applied for $\psi \geq \psi_e$ to prevent overestimation of water content at low soil suctions. The Campbell (CA) model (Campbell, 1974) is a three parameter power function to obtain water content from soil water potential

$$\theta = \theta_s\left[\frac{\psi}{\psi_e}\right]^{\lambda} \qquad \text{for } \psi < \psi_e$$

$$\theta = \theta_s \qquad \text{for } \psi \geq \psi_e \qquad [2]$$

where ψ_e is the air entry matric suction, and λ is a curve fitting parameter representing pore size distribution where $\lambda = -1/\beta$, and β is an empirically derived constant. The Campbell equation is similar to the Brooks-Corey model but with $\theta_r = 0$. The van Genuchten (VG_1) model (van Genuchten, 1980) is an expression originally based on five parameters

$$\theta = \theta_r + (\theta_s - \theta_r)\left[1 + (\alpha\psi)^n\right]^{-m} \qquad [3]$$

where α is a curve fitting parameter related to ψ^{-1} and the slope of the curve at inflection, and n and m are dimensionless curve fitting parameters. The parameters all depend on the pore size distribution. The four parameter van Genuchten (VG_2) model is

similar to the VG_1 model except for $m = 1 - 1/n$ (van Genuchten, 1980). The Tani (TA) model (Tani, 1982) is a three parameter model using the expression

$$\theta = \theta_r + (\theta_s - \theta_r)\left[1 + \frac{\psi}{\psi_o}\right] e^{\left(-\frac{\psi}{\psi_o}\right)} \quad [4]$$

where ψ_o is the soil water potential at the inflection point on the curve. The Russo (RU) model (Russo, 1988) is a four parameter model that produces the water conductivity-capillary potential relationship when integrated into Mualem's model (Mualem, 1976) for relative hydraulic conductivity

$$\theta = \theta_r + (\theta_s - \theta_r)\left[e^{-0.5\alpha|\psi|}\left(1 + 0.5\alpha|\psi|\right)\right]^{2/(m+2)} \quad [5]$$

where α is related to the width of the pore size distribution, and is interpreted as the inverse of the air entry matric suction, and m accounts for the dependence of the tortuosity and the correlation factors on the soil water content.

5.4.2.2 Model Evaluation

The SWRC for the 25–50 mm increment of the hillslope positions was determined by nonlinear analysis with the likelihood based Proc NLMIXED using an iterative optimization procedure to compute the parameter estimates (SAS Institute, Inc., 2004). The values for θ_s and θ_r were taken from measurements at saturation and 1.5 MPa, respectively. Values of θ_r derived from measurements at the permanent wilting point are designated $\theta_{r(W)}$. For practical purposes, θ_r can sufficiently be defined as the water content at a large negative value such as the permanent wilting point, despite further desorption of water with increasing suction (van Genuchten, 1980). This is considered suitable for purposes of this study since most agricultural crops and weeds do not germinate at water suction greater than 1.5 MPa (El-Sharkawi and Springuel, 1977; Roman et al., 1999; Page et al., 2006). Even so, the data were re-analyzed with θ_r replaced by a logarithmic equation describing the adsorption of water on soil in the dry range of the retention curve (Campbell and Shiozawa, 1992; Fayer and Simmons, 1995)

$$\theta = \left[1 - \frac{\ln(\psi)}{\ln(\psi_m)}\right]\theta_a \quad [8]$$

where θ_a is a curve fitting parameter representing the volumetric water content when $\psi = 1$, and ψ_m is the matric suction at oven dryness, which is generally accepted to be 10^3 MPa. The modified form of θ_r is assigned $\theta_{r(M)}$. The data were analyzed a third time with θ_r estimated as one of the fitted parameters, referred to $\theta_{r(E)}$, which contained the restriction $\theta_r \geq 0$. In all cases, the optimization results were improved by setting the measured value of θ_s as a constant parameter. Previous SWRC estimates have shown improvement by using known constant rather than optimized values of θ_s (Matula et al., 2007). The BC and CA models were analyzed as segmented models, whereas the VG, TA, and RU models were analyzed as continuous models.

The Akaike Information Criterion (*AIC*) (Akaike, 1974) was used to evaluate the models. The *AIC* was used to select the most parsimonious model (Burnham and Anderson, 2002; Cornelis et al., 2005). The *AIC* is a likelihood-based comparison of the data for model discrimination expressed as

$$AIC = -2\log(likelihood) + 2k \qquad [9]$$

where k is the number of estimable model parameters. The *AIC* selects for a model that fits well and has a low number of parameters. The *AIC* compares the data to a probability index, with a lower value of *AIC* indicating a better model fit. The *AIC* is a relative ranking statistic, therefore values are interpreted in terms of the magnitude of their differences among all models being considered.

Because an individual *AIC* value is not interpretable due to the unknown interval scale, model comparisons were facilitated using delta *AIC* (Δ_i) and Akaike weights (w_i) (Akaike, 1978; Burnham and Anderson, 2002). Delta *AIC* is a measure of the *AIC* differences of each model relative to the best model derived by

$$\Delta_i = AIC_i - AIC_{\min} \qquad [10]$$

where AIC_i is the *AIC* value for model i, and $AIC_{\min}$ is the smallest value of *AIC* in the set of candidate models. The relative likelihood of each SWRC model was realized by relative scaling of the models with w_i (Burnham and Anderson, 2002). Akaike weights

provide an effective way to scale and interpret the Δ_i values. Akaike weights compare the ratio of each model to the best model relative to the entire set of candidate models by

$$w_i = \frac{e^{(-\Delta_i/2)}}{\sum_{r=1}^{R} e^{(-\Delta_r/2)}} \quad [11]$$

given a set of R models being evaluated. Akaike weights compare models on a scale of one (the sum of w_i equals one) indicating the weight of evidence that model i is superior among the set of R models (Burnham and Anderson, 2002).

Model inference was based on evidence ratios that evaluate the relative likelihood of model pairs. Evidence ratios are calculated as the ratio of Akaike weights (w_i / w_j), where i is the estimated best model in the set, and j indexes the remaining models in the set. Evidence ratios provide support about the fitted models as to which one is superior, by comparing models in a pairwise approach that is invariant to all models in the set except the i and j models (Burnham and Anderson, 2002).

5.4.3 Pedotransfer Functions

5.4.3.1 Pedotransfer Function Parameterization

The SWRCs were estimated for the shallow soil profile increments via PTF using multiple regressions with sets of soil properties as predictor variables to estimate the θ_r, θ_s, α, and n parameters of the Van Genuchten (VG_2) model. Three PTFs were evaluated with PTF_1 and PTF_2 having soil particle size data (clay, silt, and sand), OM and BD, while PTF_3 contained greater information on the particle-size distribution of the soil. The textural fractions in PTF_3 included clay (0.00–0.002 mm), silt (0.002–0.05 mm), very fine sand (0.05–0.10 mm), fine sand (0.10–0.25 mm), medium sand (0.25–0.50 mm), coarse sand (0.50–1.00 mm), and very coarse sand (1.00–2.00 mm). Additionally, two distributional parameters in PTF_3, the geometric mean particle size diameter (d_g), calculated as

$$d_g = e\left[\frac{\sum_{i=1}^{n} n_i \ln M_i}{\sum n_i}\right] \quad [6]$$

and the geometric standard deviation (σ_g), calculated as

$$\sigma_g = e\left[\sqrt{\frac{\sum_{i=1}^{n} n_i \left(\ln M_i - \ln d_g\right)^2}{\sum_{i=1}^{n} n_i}}\right] \quad [7]$$

where M_i is the arithmetic mean of two consecutive particle-size limits, and n is the number of soil separate groups, which describe the distribution of the particle-size data (Irani and Callis, 1963; Shirazi and Boersma, 1984; Shiozawa and Campbell, 1991). The d_g and σ_g parameters were calculated from the seven particle-size fractions. PTF_3 also included OM and BD parameters.

The PTF_2 and PTF_3 data sets were formed with variables from principal components regression (PCR), which uses principal components analysis (PCA) to compute regression coefficients (SAS Institute, Inc., 2004; Vereecken and Herbst, 2004). Since, multicollinearity was identified in the original soil variable predictor set, PCR was utilized in PTF_2 and PTF_3 to avoid multicollinearity among predictor variables, and increase stability of the prediction equation (Montgomery et al., 2006). Removing correlated variables from the predictor set may bias the estimates of parameters for variables remaining in the model that are correlated with excluded variables (Quinn and Keough, 2002).

To retain all variables, PCR was used to transform the textural variables in PTF_2 and PTF_3 into principal components, which are orthogonal or uncorrelated (Dunteman, 1989; Quinn and Keough, 2002). Parameters of the VG_2 model were regressed against the principal component scores rather than from a direct regression of the original variables (Quinn and Keough, 2002). The eigenvectors of the PCA decomposition represent textural variations that are common to all of the soil water data. Therefore, using principal component information to calculate a regression equation in place of the original variables can produce a robust PTF for predicting parameters of the VG_2 model.

Variable reduction was used to summarize the patterns in the original data based on a smaller number of principal components (PCs) for a more parsimonious and robust model (Centner et al., 1996). The number of variables to retain in each PTF was based on variance decomposition and component sum of squares.

Stepwise regression was used to select variables for each parameter of the VG_2 model in each PTF at a 0.15 significance level for entry into the model, while a 0.05 significance level was used to retain the variables in the model. The α and n parameters were considered to be lognormally distributed as determined by Carsel and Parrish (1988). Logarithmic transformation of the α and n parameters improved correlations with soil variables. Data in the PTF_2 and PTF_3 sets were logarithmically transformed prior to PCR analysis. Quadratic and cross-product terms of the variables already in the regression equations were added as independent variables to explore higher order and interactive effects between variables. To account for the number of variables in the model, the adjusted coefficient of determination $\left(R_a^2\right)$ was used (Kvålseth, 1985). Regression equations containing PCs were transformed using original soil or detailed particle-size variables to facilitate estimation of the parameters of the VG_2 equation for adjacent soil layers using soil physical property values from each adjacent soil layer.

5.4.3.2 Pedotransfer Function Evaluation

The accuracy of the PTFs was based on correspondence between data predicted by the PTFs and data fitted to the measurements for the data set from which the PTFs were developed (Pachepsky et al., 1999). The functional parameters of the VG_2 model predicted by the PTFs were compared to corresponding parameters fitted to the measured soil water retention data by correlation analysis. Additionally, the mean error was calculated as the difference between the predicted and fitted parameter values, and the standard deviation was calculated as the root of the squared difference between the predicted and fitted parameter values. Common parameters of the VG_2 model predicted by the PTFs and the parameters fitted to the measured data were obtained by iterative optimization to derive the parameter estimates in the Proc NLMIXED procedure (SAS Institute, Inc., 2004). Optimal model fit for the hillslope positions for each PTF were derived by using *AIC* likelihood-based comparisons.

The prediction accuracy of the PTFs was quantified by comparing the PTF predicted retention curves with the curves fitted to the measured data for each hillslope position by calculating the integral mean error (IME), the integral root mean square error (IRMSE), and the Pearson correlation coefficient (*r*) between PTF predicted and measured water content for any given matric potential (Schaap, 2004). The indices were used to compare functions, that is, a number of water content values within a specified matric potential range. Differences between predicted and measured curves were calculated with numerical quadrature of the following integrals (Tietje and Tapkenhinrichs, 1993)

$$IME = \frac{1}{b-a}\int_a^b \left(\theta_p - \theta_m\right) d\log\psi \qquad [8]$$

$$IRMSE = \sqrt{\frac{1}{b-a}\int_a^b \left(\theta_p - \theta_m\right)^2 d\log\psi} \qquad [9]$$

and with the dimensionless Pearson correlation coefficient

$$r = \frac{\int_a^b \left(\theta_p - \bar{\theta}_p\right)\left(\theta_m - \bar{\theta}_m\right) d\log\psi}{\sqrt{\int_a^b \left(\theta_p - \bar{\theta}_p\right)^2 d\log\psi \int_a^b \left(\theta_m - \bar{\theta}_m\right)^2 d\log\psi}} \qquad [10]$$

where

$$\bar{\theta}_p = \frac{1}{b-a}\int_a^b \theta_p d\log\psi \qquad [11]$$

and

$$\bar{\theta}_m = \frac{1}{b-a}\int_a^b \theta_m d\log\psi \qquad [12]$$

where the values θ_p and θ_m are the predicted and measured water contents ($m^3\ m^{-3}$), respectively. The values $\bar{\theta}_p$ and $\bar{\theta}_m$ are the mean water contents of the predicted and measured retention curves for each hillslope position, respectively. The IME, IRMSE and *r* indices are integrated statistics that take into account the entire range of water potentials within the integration interval. The integration boundaries were set to $a = -0.001\log_{10}\psi$ MPa and $b = -1.5\log_{10}\psi$ MPa to define the integration interval for the ψ range over which the curves were compared. The indices were calculated using $\log_{10}\psi$ to account for the log-normal distribution of ψ, and thus avoid over-weighting of more negative

matric potentials. The IME evaluates bias by accounting for positive and negative differences between curves. The IME can only be interpreted to indicate whether water content predicted by a PTF is overestimated (IME >> 0) or underestimated (IME << 0) compared to the measured water content. The IRMSE is always positive and only equals zero if all the predicted water contents equal the measured water contents. The IRMSE can be interpreted as the continuous analog of the standard deviation over the entire retention curve, thus providing an absolute error index (Tietje and Tapkenhinrichs, 1993). The *r* statistic defines the strength of the association between the predicted and measured retention curves, with increasing linearity around the 1:1 line as an *r* value that approaches 1, thus indicating similarity of shape between the predicted and measured curves.

In addition to comparing total water content differences between predicted and fitted models, individual water contents were compared. Mean water contents at matric potentials of 0.01, 0.033, 0.05, 0.1, 0.5, and 1.5 MPa for the PTF predicted models were compared to water contents from the fitted model to determine significant differences ($p \leq 0.05$) using Fisher's protected LSD.

Model parameters were contrasted across soil depth and hillslope position by mean-centered bootstrap resampling of 1×10^5 samples with replacement from the original dataset using Proc Multtest (SAS Institute, Inc., 2004). Bootstrap resampling was used to obtain a more robust nonparametric estimate of the standard errors and confidence intervals (Efron and Tibshirani, 1993). The bootstrap procedure is preferable for small samples and explicitly incorporates all sources of correlation from both the multiple contrasts and the multivariate structure (Efron and Tibshirani, 1993). The bootstrap dataset was resampled on parameter values predicted by all PTFs excluding predictions for the toeslope position by PTF_2.

Mean water contents at matric potentials of 0.01, 0.033, 0.05, 0.1, 0.5, and 1.5 MPa for the average PTFs (excluding the toeslope position by PTF_2) were compared across incremental depths of the seedling recruitment zone using Fisher's protected LSD.

5.5 RESULTS AND DISCUSSION

5.5.1 Soil Water Retention Models

The respective SWRC models (excluding CA) all exhibited better fit with $\theta_{r(M)}$ and $\theta_{r(E)}$ over that of $\theta_{r(W)}$ (Table 5.2). This may be an indication that θ_r was better represented by values smaller than those measured at −1.5 MPa. Estimating or modifying θ_r as a free parameter provided better fit in the dry range of the curve (Figs. 5.1–5.3). Models containing the modified form of θ_r retain the form of the original model in the wet range of the curve and the form of the logarithmic adsorption equation in the dry range (Fayer and Simmons, 1995). The BC and VG models showed the greatest fit when θ_r was estimated rather than modified. The TA and RU models, however, had improved fit with $\theta_{r(M)}$ compared to $\theta_{r(E)}$ (Table 5.3), which occurred mainly in the dry range of the curve (Figs. 5.2 and 5.3).

The evidence ratio provided a discrete comparison of the water retention models in a pairwise manner that is unaffected by the other models in the set. The water retention models were compared to the BC model with $\theta_{r(E)}$, which was deemed to be the best model based on w_i derived from average *AIC* values (Table 5.3). An evidence ratio of 3 or less in relation to another model provides little evidence that model i is superior (Burnham and Anderson, 2002). Accordingly, the BC model with $\theta_{r(E)}$, CA model, and VG_2 model with $\theta_{r(E)}$ would serve nearly equally well in approximating the water retention information (Table 5.3). There is relatively weak support for the best model and is perhaps an indication that the limited dataset is not sufficient to realize a single best model. Additionally, the BC model with $\theta_{r(M)}$, VG_2 model with $\theta_{r(M)}$, and VG_1 model with $\theta_{r(E)}$ would be only slightly less adequate in describing the water retention relationship compared to the aforementioned three models. The TA and RU models consistently had relatively high evidence ratios no matter the derivation of θ_r, indicating low prediction ability compared to the other models (Table 5.3).

The discontinuous nature of the CA and BC models provide poor description of the SWRC near saturation (van Genuchten and Nielsen, 1985; Milly, 1987; Lenhard et

Table 5.2. Fitted parameter values for the water retention models plotted in Figs. 5.1–5.3, and *AIC* values of the curve fittings for the hillslope positions.

Hillslope position		Parameter values (SE)						
θ_r derivation	Model	θ_s †	θ_r	P_1‡	P_2§	P_3¶	P_4#	*AIC*††
		$m^3\ m^{-3}$		MPa		dimensionless		
SW summit		0.370						
Absent	CA		0.000 (–)	−0.0027 (0.0008)	–	3.09 (0.36)	–	−25.9
−1.5 MPa	BC		0.062 (–)	−0.0048 (0.0006)	–	0.63 (0.06)	–	−28.2
	VG_1		0.062 (–)	–	−0.0048 (0.0006)	9.98 (0.32)	0.063 (0.004)	−26.2
	VG_2		0.062 (–)	–	−0.0062 (0.0012)	1.70 (0.08)	–	−27.3
	TA		0.062 (–)	–	−0.0121 (0.0032)	–	–	−14.1
	RU		0.062 (–)	−0.0011 (<.0001)	–	17.50 (4.76)	–	−14.5
Modified	BC		0.068 (0.009)	−0.0052 (0.0008)	–	0.91 (0.23)	–	−28.0
	VG_1		0.068 (0.009)	–	−0.0052 (0.0008)	15.80 (0.06)	0.057 (0.014)	−26.0
	VG_2		0.070 (0.009)	–	−0.0068 (0.0012)	2.07 (0.29)	–	−27.2
	TA		0.085 (0.005)	–	−0.0061 (0.0008)	–	–	−24.7
	RU		0.083 (0.005)	−0.0011 (<.0001)	–	6.61 (1.55)	–	−25.3
Estimated	BC		0.054 (0.014)	−0.0045 (0.0008)	–	0.57 (0.11)	–	−28.5
	VG_1		0.054 (0.014)	–	−0.0045 (0.0008)	13.32 (0.11)	0.043 (0.008)	−26.5
	VG_2		0.059 (0.014)	–	−0.0060 (0.0014)	1.66 (0.15)	–	−27.3
	TA		0.100 (0.014)	–	−0.0079 (0.0021)	–	–	−18.3
	RU		0.093 (0.014)	−0.0011 (<.0001)	–	11.35 (3.89)	–	−17.8
SW backslope		0.392						
Absent	CA		0.000 (–)	−0.0033 (0.0005)	–	3.36 (0.20)	–	−32.1
−1.5 MPa	BC		0.074 (–)	−0.0050 (0.0005)	–	0.55 (0.04)	–	−29.5
	VG_1		0.074 (–)	–	−0.0050 (0.0005)	10.35 (0.39)	0.054 (0.002)	−27.5
	VG_2		0.074 (–)	–	−0.0072 (0.0009)	1.64 (0.05)	–	−30.9
	TA		0.074 (–)	–	−0.0161 (0.0034)	–	–	−13.6
	RU		0.074 (–)	−0.0011 (<.0001)	–	24.84 (5.60)	–	−14.6
Modified	BC		0.066 (0.010)	−0.0046 (0.0005)	–	0.59 (0.09)	–	−33.9
	VG_1		0.066 (0.007)	–	−0.0046 (<.0001)	12.25 (0)	0.048 (0.004)	−31.9
	VG_2		0.072 (0.007)	–	−0.0064 (<.0001)	1.73 (0.07)	–	−32.9
	TA		0.104 (0.008)	–	−0.0069 (0.0015)	–	–	−20.8
	RU		0.099 (0.008)	−0.0011 (<.0001)	–	9.57 (3.05)	–	−22.6
Estimated	BC		0.045 (0.011)	−0.0043 (0.0004)	–	0.42 (0.05)	–	−35.4
	VG_1		0.045 (0.009)	–	−0.0043 (<.0001)	12.11 (0)	0.035 (0.002)	−33.4
	VG_2		0.056 (0.011)	–	−0.0063 (0.0009)	1.52 (0.07)	–	−33.7
	TA		0.111 (0.020)	–	−0.0119 (0.0036)	–	–	−16.3

Table 5.2. Continued.

	RU		0.103 (0.017)	−0.0011 (<.0001)	–	18.11 (5.36)	–	−16.9
SW toeslope		0.423						
Absent	CA		0.000 (–)	−0.0011 (0.0002)	–	6.26 (0.34)	–	−35.0
−1.5 MPa	BC		0.130 (–)	−0.0026 (0.0009)	–	0.39 (0.06)	–	−23.1
	VG_1		0.130 (–)	–	−0.0026 (<.0001)	9.92 (<.01)	0.040 (0.003)	−21.1
	VG_2		0.130 (–)	–	−0.0032 (0.0013)	1.42 (0.07)	–	−23.7
	TA		0.130 (–)	–	−0.0175 (0.0060)	–	–	−9.7
	RU		0.130 (–)	−0.0011 (0.0014)	–	28.57 (45.41)	–	−10.0
Modified	BC		0.092 (0.054)	−0.0009 (0.0003)	–	0.27 (0.13)	–	−32.2
	VG_1		0.092 (0.054)	–	−0.0009 (<.0001)	9.33 (<.01)	0.029 (0.014)	−30.2
	VG_2		0.087 (0.061)	–	−0.0010 (<.0001)	1.26 (0.14)	–	−32.4
	TA		0.157 (0.005)	–	−0.0033 (0.0007)	–	–	−25.3
	RU		0.156 (0.005)	−0.0011 (<.0001)	–	1.45 (0.96)	–	−25.3
Estimated	BC		0.000 (–)	−0.0011 (0.0002)	–	0.16 (0.01)	–	−33.0
	VG_1		0.000 (–)	–	−0.0010 (<.0001)	9.44 (1.49)	0.017 (0.003)	−30.8
	VG_2		0.000 (–)	–	−0.0012 (<.0001)	1.16 (<.01)	–	−33.5
	TA		0.193 (0.019)	–	−0.0057 (0.0025)	–	–	−13.3
	RU		0.177 (0.031)	−0.0011 (<.0001)	–	12.97 (13.13)	–	−12.0
NE summit		0.388						
Absent	CA		0.000 (–)	−0.0018 (0.0005)	–	3.49 (0.31)	–	−29.2
−1.5 MPa	BC		0.067 (–)	−0.0036 (0.0006)	–	0.57 (0.05)	–	−28.5
	VG_1		0.067 (–)	–	−0.0036 (0.0006)	10.15 (0.14)	0.056 (0.005)	−26.5
	VG_2		0.067 (–)	–	−0.0045 (0.0009)	1.61 (0.07)	–	−28.4
	TA		0.067 (–)	–	−0.0108 (0.0041)	–	–	−12.1
	RU		0.067 (–)	−0.0011 (<.0001)	–	15.80 (5.44)	–	−12.4
Modified	BC		0.067 (0.011)	−0.0036 (0.0008)	–	0.70 (0.18)	–	−29.1
	VG_1		0.067 (0.008)	–	−0.0036 (<.0001)	10.15 (<.01)	0.069 (0.008)	−27.1
	VG_2		0.068 (0.008)	–	−0.0043 (<.0001)	1.77 (0.10)	–	−28.6
	TA		0.091 (0.005)	–	−0.0050 (0.0006)	–	–	−23.5
	RU		0.091 (0.005)	−0.0011 (<.0001)	–	4.42 (1.24)	–	−23.8
Estimated	BC		0.047 (0.016)	−0.0030 (0.0007)	–	0.45 (0.09)	–	−30.4
	VG_1		0.047 (0.011)	–	−0.0030 (<.0001)	8.67 (<.01)	0.052 (0.004)	−28.4
	VG_2		0.051 (0.011)	–	−0.0037 (<.0001)	1.49 (0.04)	–	−29.7
	TA		0.110 (0.015)	–	−0.0063 (0.0016)	–	–	−16.9
	RU		0.104 (0.016)	−0.0011 (<.0001)	–	8.32 (4.12)	–	−15.8
NE backslope		0.389						

Table 5.2. Continued.

Absent	CA		0.000 (–)	−0.0014 (0.0004)	–	3.92 (0.31)	–	−31.0
−1.5 MPa	BC		0.073 (–)	−0.0031 (0.0006)	–	0.52 (0.05)	–	−27.3
	VG_1		0.073 (–)	–	−0.0031 (0.0006)	10.06 (0.20)	0.051 (0.004)	−25.3
	VG_2		0.073 (–)	–	−0.0038 (0.0009)	1.55 (0.06)	–	−27.5
	TA		0.073 (–)	–	−0.0112 (0.0047)	–	–	−11.2
	RU		0.073 (–)	−0.0011 (<.0001)	–	16.69 (6.40)	–	−11.3
Modified	BC		0.068 (0.017)	−0.0026 (0.0009)	–	0.57 (0.20)	–	−28.7
	VG_1		0.068 (0.011)	–	−0.0026 (<.0001)	8.01 (<.01)	0.071 (0.010)	−26.7
	VG_2		0.069 (0.010)	–	−0.0031 (<.0001)	1.61 (0.09)	–	−28.4
	TA		0.099 (0.005)	–	−0.0046 (0.0006)	–	–	−23.2
	RU		0.098 (0.006)	−0.0011 (<.0001)	–	3.62 (1.17)	–	−23.3
Estimated	BC		0.038 (0.024)	−0.0022 (0.0007)	–	0.35 (0.09)	–	−30.3
	VG_1		0.038 (0.014)	–	−0.0022 (<.0001)	6.91 (28.4)	0.051 (0.211)	−28.3
	VG_2		0.042 (0.014)	–	−0.0026 (<.0001)	1.38 (0.04)	–	−29.9
	TA		0.120 (0.015)	–	−0.0059 (0.0016)	–	–	−16.2
	RU		0.115 (0.017)	−0.0011 (<.0001)	–	7.37 (4.39)	–	−14.8
NE toeslope		0.411						
Absent	CA		0.000 (–)	−0.0018 (0.0004)	–	5.07 (0.30)	–	−33.0
−1.5 MPa	BC		0.109 (–)	−0.0035 (0.0009)	–	0.43 (0.06)	–	−23.3
	VG_1		0.109 (–)	–	−0.0035 (0.0009)	9.99 (0.33)	0.043 (0.004)	−21.3
	VG_2		0.109 (–)	–	−0.0046 (0.0014)	1.47 (0.07)	–	−24.1
	TA		0.109 (–)	–	−0.0178 (0.0054)	–	–	−10.5
	RU		0.109 (–)	−0.0011 (<.0001)	–	29.45 (9.76)	–	−10.9
Modified	BC		0.042 (0.142)	−0.0019 (0.0005)	–	0.25 (0.24)	–	−29.0
	VG_1		0.042 (0.115)	–	−0.0019 (<.0001)	5.79 (<.01)	0.043 (0.032)	−27.0
	VG_2		0.049 (0.124)	–	−0.0021 (<.0001)	1.27 (0.23)	–	−28.9
	TA		0.141 (0.006)	–	−0.0045 (0.0009)	–	–	−21.8
	RU		0.140 (0.006)	−0.0011 (<.0001)	–	3.37 (1.64)	–	−21.9
Estimated	BC		0.000 (–)	−0.0018 (0.0004)	–	0.20 (0.01)	–	−31.0
	VG_1		0.000 (–)	–	−0.0018 (<.0001)	5.33 (1.39)	0.037 (0.010)	−29.0
	VG_2		0.000 (–)	–	−0.0021 (<.0001)	1.20 (0.01)	–	−30.9
	TA		0.168 (0.024)	–	−0.0077 (0.0053)	–	–	−13.3
	RU		0.150 (0.026)	−0.0011 (<.0001)	–	17.02 (10.03)	–	−12.8

Table 5.2. Continued.

† θ_s are measured values.

‡ P_1 is the air entry matric suction (ψ_e, ψ_e, and α^{-1} of the CA, BC, and RU models, respectively).

§ P_2 is the capillary pressure at the inflection point on the water retention curve (α^{-1}, α^{-1}, and ψ_o of the VG_1, VG_2, and TA models, respectively).

¶ P_3 is a dimensionless parameter (β, λ, n, n, and m of the CA, BC, VG_1, VG_2, and RU models, respectively).

P_4 is a dimensionless parameter (m of the VG_1 model).

††A lower value of *AIC* indicates a better model fit.

Table 5.3. Akaike weights (w_i) and evidence ratios for the respective water retention models.

θ_r derivation Model	SW summit	SW backslope	SW toeslope	NE summit	NE backslope	NE toeslope	Average†	Evidence ratio‡
	w_i							
Absent								
CA	0.046	0.062	0.385	0.117	0.272	0.455	0.189	1.2
−1.5 MPa								
BC	0.147	0.017	0.001	0.082	0.043	0.004	0.021	10.9
VG_1	0.054	0.006	0.000	0.030	0.016	0.001	0.008	29.7
VG_2	0.094	0.034	0.001	0.078	0.047	0.005	0.025	9.2
TA	0.000	0.000	0.000	0.000	0.000	0.000	0.000	17704.5
RU	0.000	0.000	0.000	0.000	0.000	0.000	0.000	14374.9
Modified								
BC	0.133	0.152	0.095	0.111	0.086	0.062	0.121	1.9
VG_1	0.049	0.056	0.035	0.041	0.032	0.023	0.045	5.2
VG_2	0.089	0.092	0.105	0.086	0.074	0.059	0.098	2.3
TA	0.025	0.000	0.003	0.007	0.006	0.002	0.004	60.7
RU	0.034	0.001	0.003	0.008	0.006	0.002	0.005	47.7
Estimated								
BC	0.170	0.323	0.142	0.212	0.192	0.167	0.230	1.0
VG_1	0.063	0.119	0.047	0.078	0.070	0.062	0.083	2.8
VG_2	0.094	0.138	0.182	0.150	0.157	0.159	0.171	1.3
TA	0.001	0.000	0.000	0.000	0.000	0.000	0.000	2582.7
RU	0.001	0.000	0.000	0.000	0.000	0.000	0.000	3665.0

† w_i based on average *AIC* values across all hillslope positions.

‡ Evidence ratios (w_i / w_j) are based on w_i from average *AIC* values where model i is the best fitting model (determined to be the BC model with estimated θ_r), and j indexes the remaining models in the set.

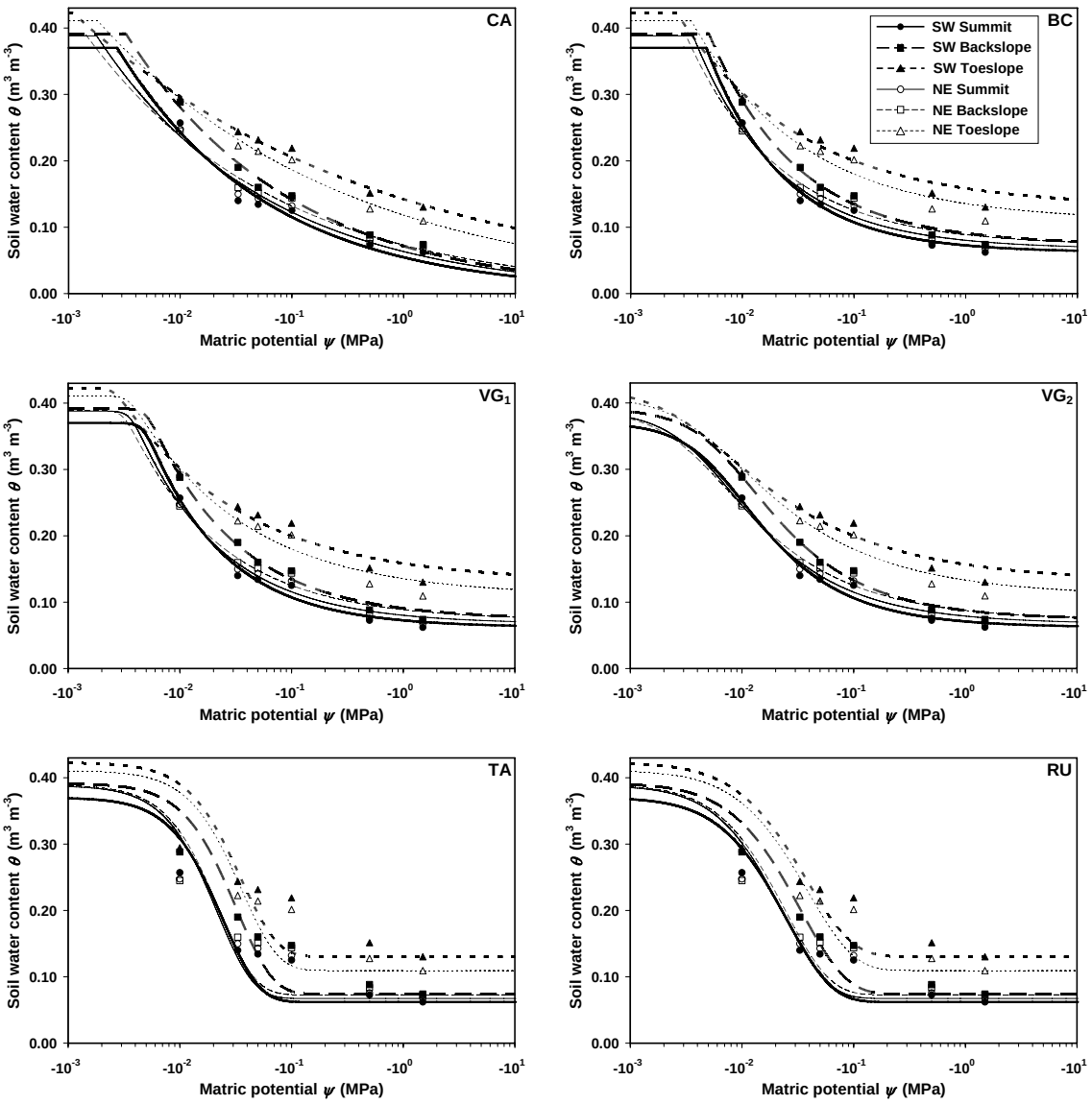

Fig. 5.1. Fitted SWRCs for soil water contents (θ) at soil matric potentials (ψ) among the hillslope positions using the Campbell (CA) model with absent θ_r parameter, and Brooks-Corey (BC), van Genuchten (VG_1 and VG_2), Tani (TA), and Russo (RU) models with θ_r constrained to measured values at −1.5 MPa.

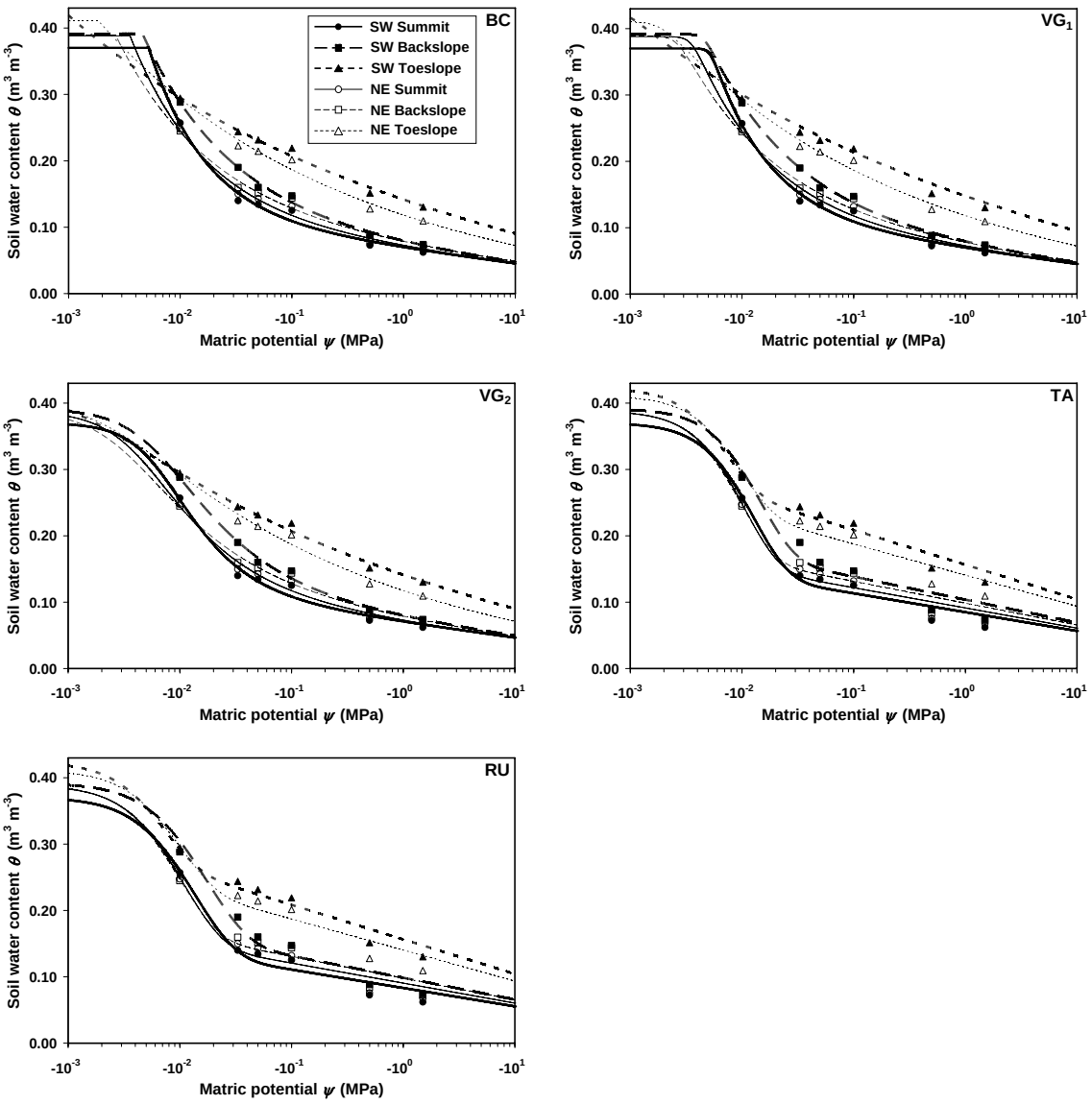

Fig. 5.2. Fitted SWRCs for soil water contents (θ) at soil matric potentials (ψ) among the hillslope positions using the Brooks-Corey (BC), van Genuchten (VG_1 and VG_2), Tani (TA), and Russo (RU) models with θ_r modified by a logarithmic equation describing the adsorption of water on soil in the dry range of the retention curve.

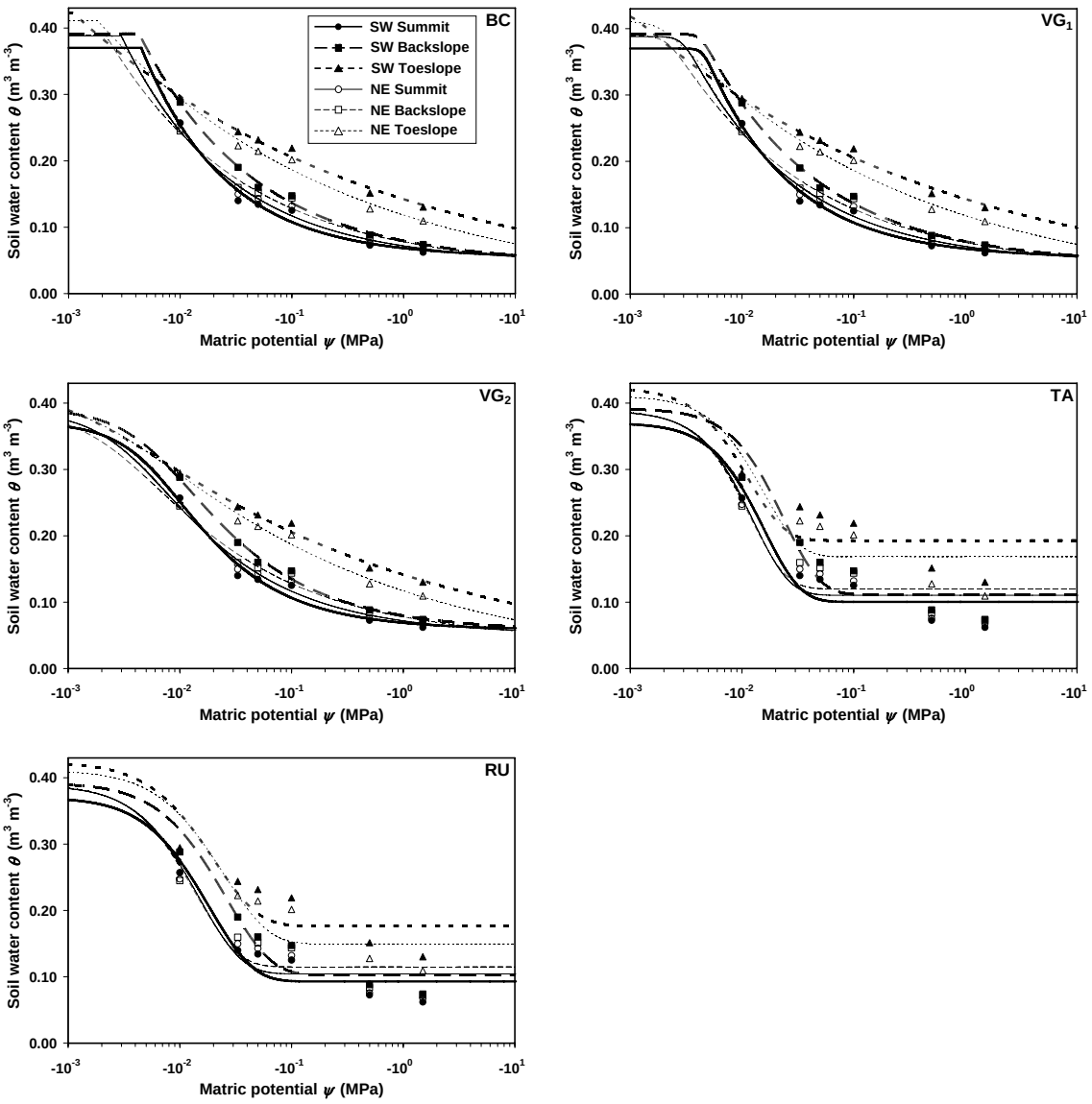

Fig. 5.3. Fitted SWRCs for soil water contents (θ) at soil matric potentials (ψ) among the hillslope positions using the Brooks-Corey (BC), van Genuchten (VG_1 and VG_2), Tani (TA), and Russo (RU) models with θ_r estimated as one of the fitted parameters.

al., 1989). The continuous VG models contain an inflection point enabling better representation of water retention near saturation (van Genuchten and Nielsen, 1985). However, the continuous VG models were not superior to the discontinuous CA and BC models in our study. The absence of measured data above −0.01 MPa (except θ_s) in the wet range of the curve where the discontinuous character occurs, may have provided an apparent advantage for the CA and BC models over that of the continuous VG models that may otherwise not have occurred (Figs. 5.1–5.3).

The VG_2 model was superior to the VG_1 model no matter the derivation of θ_r (Table 5.3). The VG_2 model has one less parameter making it more parsimonious than the VG_1 model. The VG_2 model may also have provided improved estimation of the water retention relationships compared to the VG_1 model due to independence of the n and m parameters in the VG_1 model. The n and m parameter independence can lead to distinctiveness problems in the estimation process resulting in a less accurate description of the SWRC in the dry range (van Genuchten et al., 1991).

The SWRC for the coarse soils in the summit position was best described by the BC model, based on w_i values. The CA model, however, showed the best fit to the data for the soils with greater clay content in the toeslope position (Table 5.3).

5.5.2 Pedotransfer Functions

5.5.2.1 Pedotransfer Function Evaluation

The SWRCs for the 25–50 mm soil increment in the shallow seedling recruitment zone were estimated by PTF for each hillslope position from basic soil physical properties. In general, clay and sand contents increased and silt content decreased downslope in the hillslope (Table 5.1). The textural variations typical of hillslopes were most likely a result of particle separation caused primarily by water erosion (Kreznor et al., 1989) and tillage erosion (Li et al., 2007). Downslope increases in OM and decreases in BD were apparent in the northeast hillslope (Table 5.1).

A high degree of multicollinearity existed among the soil variables used in PTF_1 (Table 5.4). Relationships typically exist among soil physical properties (Shaykewich and Zwarich, 1968; Rawls, 1983). Correlated variables represent redundant information in a regression model, resulting in instability in the estimates of the regression coefficients

(Dunteman, 1989; Quinn and Keough, 2002). PTF_2 and PTF_3 used soil variables in PCR analysis to extract PCs, which were then used as the regressors. The PCs for PTF_2 and PTF_3 were orthogonal which eliminates problems associated with multicollinearity in regression analysis (Dunteman, 1989).

Table 5.4. Pearson correlation matrix of soil variables.

Soil variable	Clay	Silt	Sand	Organic matter	Bulk density
	g kg^{-1}				g cm^{-3}
Clay	1.000	–	–	–	–
Silt	−0.962	1.000	–	–	–
Sand	0.843	−0.958	1.000	–	–
Organic matter	0.865	−0.826	0.717	1.000	–
Bulk density	−0.783	0.742	−0.638	−0.864	1.000

Selection of PCs to retain for PTF_2 and PTF_3 initially was based on variance decomposition (Table 5.5). The number of PCs equals the number of original textural variables, with the first PC accounting for the maximal amount of total variance in the variables (Table 5.5). The first few PCs generally summarize most of the variation in the original variables, with each component accounting for a maximal amount of variance in the measured variables not accounted for by the preceding components (Quinn and Keough, 2002). Selection of PCs to retain for PTF_2 and PTF_3 was further based on contribution of each PC to the regression sum of squares and SSE (Table 5.6). Both variance decomposition and component sum of squares criteria were evaluated because PCs selected according to the magnitudes of their eigenvalues alone do not necessarily contribute monotonically to the SSE (Hadi and Ling, 1998). This is indicated by the 4th or 5th PCs in PTF_2 contributing more to SSE compared to some of the preceding PCs for all the VG_2 parameters (Table 5.6). Retaining the 4th and 5th PC in PTF_2 improved the model fit, therefore all PCs were retained in PTF_2. For PTF_3, the 5th PC had greater contribution to SSE than several of the preceding PCs for the θ_r, θ_s, and n parameters, and was retained because it improved model fit (Table 5.6). PCs beyond the 5th PC for PTF_3 contributing little to the total variance were deleted, and the regression of the model parameters was refitted against the remaining PCs. Despite using less than the full set of PCs for PTF_3, the regression equation will contain all of the variables of particle size

Table 5.5. Variance decomposition for principal components analysis of original soil variables (PTF_2) and particle-size distribution variables (PTF_3).

Pedotransfer function Principal component	Eigenvalue	Proportion	Cumulative proportion
PTF_2†			
PC_1	4.24141619	0.8483	0.8483
PC_2	0.50480790	0.1010	0.9492
PC_3	0.14604547	0.0292	0.9785
PC_4	0.08975728	0.0180	0.9964
PC_5	0.01797316	0.0036	1.0000
PTF_3‡			
PC_1	6.09508114	0.6772	0.6772
PC_2	1.39085844	0.1545	0.8318
PC_3	0.73723112	0.0819	0.9137
PC_4	0.56831510	0.0631	0.9768
PC_5	0.11164253	0.0124	0.9892
PC_6	0.05850203	0.0065	0.9957
PC_7	0.02623815	0.0029	0.9987
PC_8	0.01123381	0.0012	0.9999
PC_9	0.00089769	0.0001	1.0000

† PTF_2 contains clay, silt, sand, organic matter, and bulk density.

‡ PTF_3 contains clay, silt, very fine sand, fine sand, medium sand, coarse sand, very coarse sand, geometric mean particle diameter, and geometric standard deviation.

Table 5.6. Contribution to individual SS and cumulative SSE by principal components of regression models derived from original soil (PTF_2) and particle-size distribution (PTF_3) variables.†

Pedotransfer function Principal component	θ_r		θ_s		$\ln(\alpha)$		$\ln(n)$	
	SS	SSE	SS	SSE	SS	SSE	SS	SSE
PTF_2‡								
PC_1	7.5956	3.3383	4.7831	0.4230	3797.6106	3156.4708	232.7365	125.2270
PC_2	0.2627	3.0756	0.1804	0.2426	7.5495	3148.9211	23.9270	101.2999
PC_3	0.0408	3.0348	0.0075	0.2351	19.0870	3129.8350	5.8890	95.4107
PC_4	0.0983	2.9365	0.0024	0.2327	315.8381	2813.9971	3.6384	91.7724
PC_5	0.0039	2.9326	0.1192	0.1135	92.5372	2721.4599	6.3632	85.4092
PTF_3§								
PC_1	6.7858	4.1481	4.6348	0.5713	3221.4256	3732.6470	203.1199	154.8433
PC_2	0.6630	3.4851	0.0978	0.4735	253.0039	3479.6502	11.4572	143.3863
PC_3	1.2669	2.2182	0.0450	0.4285	449.3267	3030.3265	57.8732	85.5134
PC_4	0.0657	2.1525	0.0090	0.4195	358.6991	2671.6251	0.1197	85.3937
PC_5	0.1159	2.0365	0.1464	0.2731	269.9487	2401.6775	36.5517	48.8421
PC_6	0.0799	1.9566	0.0177	0.2555	0.1512	2401.5265	0.4999	48.3422
PC_7	0.0540	1.9027	0.1007	0.1548	6.3519	2395.1742	0.7673	47.5749
PC_8	0.1119	1.7908	0.0216	0.1331	68.0698	2327.1052	2.0044	45.5705
PC_9	0.0004	1.7904	0.0000	0.1331	52.8839	2274.2213	0.0000	45.5705

† Multiply reported values by 10^{-3} to obtain actual values.

‡ PTF_2 contains clay, silt, sand, organic matter, and bulk density.

§ PTF_3 contains clay, silt, very fine sand, fine sand, medium sand, coarse sand, very coarse sand, geometric mean particle diameter, and geometric standard deviation.

because each PC is a linear combination of the original variables (Dunteman, 1989). The process of PC reduction provides a means to improve parsimonious description of the data and numerical accuracy of the regression estimates (Dunteman, 1989).

The PC loadings (contribution of the original variables to the PCs) for PTF_2 and PTF_3 are shown in Table 5.7. Soil variables in neither data set correlated strongly with PC_1. However in PTF_2, PC_2 correlated most strongly with sand and BD, PC_3 with BD and OM, PC_4 with clay and sand, and PC_5 with clay and silt. In PTF_3, PC_2 correlated most strongly with fine sand, PC_3 with VCS, PC_4 with MS and d_g, and PC_5 with VFS, MS and d_g.

The multiple regression equations for the parameters of the VG_2 model are expressed as a function of original soil variables (PTF_1), transformed soil variables (PTF_2), and transformed particle-size distribution variables (PTF_3) (Table 5.8). The regression for PTF_1 indicated that clay was the most predictive variable for each of the parameters in the VG_2 model (Table 5.8). Bulk density was also an important predictor in PTF_1 for the θ_s parameter. Clay and BD generated a high correlation with the θ_s parameter due to their close relationship to saturated water content. The $\ln(\alpha)$ parameter was generally more sensitive to fitting compared to the other parameters which may be reflected by the lower correlation coefficient. Quadratic terms for clay improved the fit for the θ_r, θ_s, and $\ln(n)$ parameters (Table 5.8). No other soil variables in PTF_1 were significant, which may have resulted from multicollinearity of the original soil predictors.

Using PCR for PTF_2 improved the predictive fit for the θ_s and $\ln(\alpha)$ parameters, but not the θ_r and $\ln(n)$ parameters (Table 5.8). Improvements may have been due to a reduction in multicollinearity in the predictor set. The first principal component was almost exclusively the most important predictor variable for each of the parameters in PTF_2 (Table 5.8).

The fit was improved for all of the parameters in the VG_2 model for PTF_3 compared to either PTF_1 or PTF_2 with the exception of the $\ln(\alpha)$ parameter in PTF_2 (Table 5.8). Logarithmic transformation of the soil variable predictors for the PTFs improved fit of the multiple regression equations in this study as seen previously (Williams et al., 1992a). The greater amount of detailed information on the particle-size

Table 5.7. Principal component loadings for the original soil (PTF_2) and particle-size distribution (PTF_3) variables.

Pedotransfer function	Standardized scores						
Variables†	PC_1	PC_2	PC_3	PC_4	PC_5	Mean‡	SD‡
PTF_2							
Clay	0.4672	0.2750	0.0701	−0.5621	0.6207	128.9	80.0
Silt	−0.4756	−0.1867	0.0140	0.3712	0.7753	580.0	150.3
Sand	0.4342	0.5526	−0.1544	0.6908	0.0714	291.1	76.6
BD	−0.4197	0.6106	0.6621	−0.0672	−0.0902	1.05	0.10
OM	0.4369	−0.4598	0.7298	0.2540	0.0225	43.2	9.6
PTF_3							
Clay	0.3882	0.1155	−0.1967	−0.1150	0.3054	128.9	80.0
Silt	−0.3953	−0.1118	0.1754	0.0613	−0.0577	580.0	150.3
VFS	0.3475	−0.3206	−0.2346	0.2665	0.5387	228.3	76.5
FS	0.0359	0.7802	0.3915	0.2177	0.1614	53.3	23.4
MS	0.3321	−0.0994	0.0592	0.6938	−0.5391	7.3	3.4
CS	0.3677	−0.2080	0.3191	0.0195	−0.1129	1.9	1.4
VCS	0.2626	−0.2780	0.7317	−0.3400	0.0857	0.3	0.4
d_g	−0.3436	−0.1623	0.2806	0.5170	0.5145	0.025	0.004
σ_g	0.3721	0.3255	−0.0526	−0.0059	0.1086	0.052	0.013

† Original soil (PTF_2) and detailed particle-size distribution (PTF_3) variables C, Si, S, VFS, FS, MS, CS, VCS = clay, silt, sand, very fine sand, fine sand, medium sand, coarse sand, very coarse sand content (g kg^{-1}), respectively; BD = bulk density (g cm^{-3}); OM = organic matter (g kg^{-1}); d_g = geometric mean particle diameter (mm); σ_g = geometric standard deviation (mm).

‡ Mean and standard deviation of original non-transformed variables.

Table 5.8. Multiple regression equations for estimating the parameters of the van Genuchten model as a function of soil variables.

Pedotransfer function Model parameter	Multiple regression equation†	R_a^2 ‡
PTF_1§		
θ_r	$0.098 - 0.0007(C) + 0.000001(C)^2$	0.708
θ_s	$0.36177 - 0.0006(C) + 0.000001(C)^2 - 0.0165(BD)^2$	0.952
$\ln(\alpha)$	$-4.9768 - 0.006(C)$	0.539
$\ln(n)$	$0.7745 - 0.0053(C) + 0.00001(C)^2$	0.736
PTF_2¶		
θ_r	$0.0355 - 0.0103(PC_1)$	0.676
θ_s	$0.3954 + 0.0081(PC_1) + 0.0046(PC_2) + 0.0198(PC_5)$	0.971
$\ln(\alpha)$	$-5.9872 - 0.2612(PC_1) + 2.7766(PC_4)^2$	0.695
$\ln(n)$	$0.3383 - 0.0568(PC_1)$	0.628
PTF_3#		
θ_r	$0.0333 - 0.008(PC_1) + 0.0106(PC_3)^2 - 0.0096(PC_4)^2$	0.875
θ_s	$0.3956 + 0.0058(PC_1) + 0.0018(PC_2)^2 - 0.2169(\ln BD)^2 - 0.0049(PC_1PC_5)$ $- 0.0059(PC_2PC_5) - 0.0072(PC_3PC_4)$	0.993
$\ln(\alpha)$	$-5.9653 - 0.2029(PC_1) + 0.3065(PC_3)^2$	0.662
$\ln(n)$	$0.3151 - 0.0462(PC_1) + 0.0219(PC_3) + 0.0602(PC_3)^2 - 0.0349(PC_4)^2$ $- 0.0371(PC_5 \ln OM)$	0.965

† Regression variables C = clay content (g kg^{-1}); BD = bulk density (g cm^{-3}); OM = organic matter (g kg^{-1}); PC_1 to PC_5 = respective principal components.

‡ Adjusted coefficient of determination is used as criterion for model fit by adjusting for the number of variables in the equation.

§ PTF_1 contains original soil variables as regressors.

¶ PTF_2 contains principal components derived from the original soil variables.

PTF_3 contains principal components derived from detailed particle-size distribution variables.

distribution in PTF_3 may have been a factor in improving fit of the parameters for PTF_3. Although water retention in this study is determined by particle-size distribution rather than pore-size distribution, the two distributions are related (Arya and Paris, 1981; Campbell, 1985; Kosugi, 1994; Chan and Govindaraju, 2004). Improvement in model fit has previously been observed using detailed particle-size distribution in PTFs to estimate the SWRC (Haverkamp and Parlange 1986; Vereecken et al., 1989; Rajkai et al., 1996). The first principal component was the most important predictor variable for each of the parameters (Table 5.8). In addition to the particle-size distribution, BD and OM were significant predictors for the θ_s and $\ln(n)$ parameters, respectively. Bulk density and saturation are closely related due to the effect of BD on soil structure and soil pores which have the greatest effect on water content at high water potentials (Hill and Sumner, 1967). The effect of OM on BD further influences soil structure and adsorption properties (Rawls et al., 2004). The inclusion of OM in addition to textural class as a predictor has been shown to improve the water retention estimation (Kern, 1995; Rawls et al., 2003). Cross-product terms of variables already in the equations significantly improved fit for the θ_s and $\ln(n)$ parameters (Table 5.8). The $\ln(\alpha)$ parameter was the most difficult to fit, and although only 66.2% of the variance was explained for the $\ln(\alpha)$ parameter in PTF_3, the model fit was improved compared to using the original soil variables. Derived nonlinear and cross-products of soil variables improved flexibility of linear PTFs and increased prediction accuracy (Rajkai et al., 2004).

Unexplained variability in the estimation of the VG_2 parameters by the PTFs may have been due to the influence of the SWRC by different independent variables at different ranges of soil water potential, with those differences not directly related to the VG_2 parameters. Because the multiple regression equations do not exhibit a conceptual meaning for estimation of the VG_2 parameters in terms of PCs, the PCs were transformed into original soil variables for PTF_2 and into detailed particle-size distribution variables for PTF_3 (Table 5.9).

The VG_2 parameters predicted by the pedotransfer functions correlated well with the parameters fitted to the measured soil water retention data (Table 5.10). The correlation coefficients on average were better for PTF_3 than for the other PTFs. This may have been due to the greater amount of detailed soil textural information used in

Table 5.9. Transformed principal component equations for estimating the parameters of the van Genuchten model as a function of original soil (PTF_2) and detailed particle-size distribution (PTF_3) variables.

Pedotransfer function Principal component	Transformed principal component equations†‡
PTF_2	
PC_1	$-10.8839+0.8625(C)-1.5881(Si)+1.6429(S)-4.1185(BD)+2.075(OM)$
PC_2	$-2.3129+0.5077(C)-0.6234(Si)+2.0909(S)+5.9909(BD)-2.1836(OM)$
PC_4	$-22.1902-1.0376(C)+1.2396(Si)+2.6141(S)-0.6598(BD)+1.2063(OM)$
PC_5	$-23.6562+1.1458(C)+2.5889(Si)+0.2702(S)-0.8851(BD)+0.1068(OM)$
PTF_3	
PC_1	$-3.5151+0.7166(C)-1.3202(Si)+0.977(VFS)+0.0751(FS)+0.7026(MS)+0.5812(CS)$ $+0.2946(VCS)-1.8462(d_g)+1.6587(\sigma_g)$
PC_2	$1.0155-0.2132(C)-0.3733(Si)-0.9012(VFS)+1.6309(FS)-0.2103(MS)-0.3288(CS)$ $-0.3119(VCS)-0.872(d_g)+1.4507(\sigma_g)$
PC_3	$4.1567-0.3632(C)+0.5858(Si)-0.6594(VFS)+0.8184(FS)+0.1253(MS)+0.5045(CS)$ $+0.8208(VCS)+1.5077(d_g)-0.2345(\sigma_g)$
PC_4	$0.6837-0.2124(C)+0.2048(Si)+0.7491(VFS)+0.455(FS)+1.468(MS)+0.0309(CS)$ $-0.3814(VCS)+2.7778(d_g)-0.0262(\sigma_g)$
PC_5	$3.1608+0.5638(C)-0.1928(Si)+1.5143(VFS)+0.3373(FS)-1.1407(MS)-0.1785(CS)$ $+0.0961(VCS)+2.7646(d_g)+0.4839(\sigma_g)$

† Original soil (PTF_2) and detailed particle-size distribution (PTF_3) variables C, Si, S, VFS, FS, MS, CS, VCS = clay, silt, sand, very fine sand, fine sand, medium sand, coarse sand, very coarse sand content (g kg^{-1}), respectively; BD = bulk density (g cm^{-3}); OM = organic matter (g kg^{-1}); d_g = geometric mean particle diameter (mm); σ_g = geometric standard deviation (mm).

‡ Values for original soil (PTF_2) and detailed particle-size distribution (PTF_3) variables are logarithmically transformed.

Table 5.10. Comparison of the van Genuchten parameters predicted by the pedotransfer functions and the parameters fitted to the measured soil water retention data.

Pedotransfer function Model parameter	Mean error†	Standard deviation†	Correlation
PTF_1			
θ_r	0.0002	0.0090	0.8620
θ_s	−0.000005	0.0028	0.9800
$\ln(\alpha)$	0.0004	0.3271	0.7521
$\ln(n)$	−0.0005	0.0402	0.8759
PTF_2			
θ_r	0.0005	0.0086	0.8369
θ_s	0.00000000001	0.0020	0.9881
$\ln(\alpha)$	−0.000001	0.2336	0.8549
$\ln(n)$	0.000002	0.0556	0.8064
PTF_3			
θ_r	0.0004	0.0055	0.9490
θ_s	−0.000009	0.0009	0.9976
$\ln(\alpha)$	−0.000001	0.2757	0.8376
$\ln(n)$	0.0000004	0.0185	0.9875

† Units for θ_r and θ_s are $m^3\ m^{-3}$; units for $\ln(\alpha)$ are MPa^{-1}; units for $\ln(n)$ are dimensionless.

estimation of the parameters in PTF_3. Estimation of the curve fitting parameters $\ln(\alpha)$ and $\ln(n)$ provided somewhat lower correlation coefficients relative to the θ_r and θ_s parameters. Lower correlation of the $\ln(\alpha)$ parameter has occurred in other studies (Tietje and Tapkenhinrichs, 1993), possibly due to the independence of $\ln(\alpha)$ from particle size (Puckett et al., 1985).

Optimal model fit of common parameters between PTF predicted and fitted models were determined with *AIC* (Table 5.11). One-half of the PTF predicted retention curves across the hillslope positions had all VG_2 parameters in common with the fitted models (Table 5.11). The remaining models differed by only one parameter. The parameter that differed most frequently was the α parameter. This may have been due to lower fit of the α parameter relative to the other parameters for the VG_2 function (Table 5.8). The exception was PTF_2 where the n parameter differed for the toeslope positions, attributed to lower fit of the n parameter for PTF_2 shown in Table 5.8. PTF_1 had the most hillslope retention curves containing all common parameters, whereas PTF_2 had the least. Common parameter estimates for the optimal model fit of the VG_2 function for predicted with fitted models are shown in Table 5.12.

The accuracy of the SWRCs predicted by the PTFs compared to the models fitted to the measured data is shown for each hillslope position in Fig. 5.4. The IME and IRMSE validation indices evaluated the accuracy of the PTFs by computing the normalized area between predicted SWRCs and SWRCs fitted to the measured data (Table 5.13). The average deviation between predicted and fitted SWRCs as quantified by mean IME values was generally low with few exceptions. PTF_2 had the greatest systematic errors in the dry range of the SWRC for the toeslope positions. The inability of PTF_2 to accurately predict water content in the lower hillslope positions containing greater clay content could have been due to insufficient information for the particle-size distribution used in PTF_2. No consistent deviations by the PTFs were observed near saturation or dry ranges of the SWRC. Overall, the PTFs all slightly underestimated water content. Because water content for some SWRCs were both overestimated and underestimated along the curve, IRMSE was used to quantify random error. Mean IRMSE ranged from 0.0049 to 0.0319 $m^3\ m^{-3}$ (Table 5.13). The highest IRMSE values

Table 5.11. Common parameters of the van Genuchten model predicted by the pedotransfer functions and the parameters fitted to the measured soil water retention data. Values are *AIC*†.

Common parameters	PTF_1						PTF_2						PTF_3					
	Southwest			Northeast			Southwest			Northeast			Southwest			Northeast		
	Su‡	Bs	Ts	Su	Bs	Ts	Su	Bs	Ts	Su	Bs	Ts	Su	Bs	Ts	Su	Bs	Ts
None	−65.0	−77.7	−77.3	−69.8	−70.1	−71.9	−65.0	−77.7	−76.4	−69.8	−70.1	−72.1	−65.0	−77.7	−77.4	−69.8	−70.1	−72.1
θ_r	−66.9	−78.5	−79.1	−71.8	−72.1	−73.8	−67.0	−78.2	−79.4	−71.7	−72.0	−73.7	−67.0	−79.7	−79.4	−71.8	−72.1	−74.0
θ_s	−67.0	−79.7	−79.3	−71.8	−72.1	−73.9	−67.0	−79.7	−78.7	−71.8	−72.1	−74.1	−67.0	−79.7	−79.4	−71.8	−72.1	−74.1
α	−66.3	−73.5	−79.4	−71.6	−70.4	−73.6	−66.9	−76.3	−79.3	−71.8	−71.1	−73.8	−66.2	−78.2	−79.3	−71.3	−71.5	−74.1
n	−67.0	−78.4	−79.4	−71.8	−71.5	−73.7	−66.7	−78.1	−79.1	−71.8	−70.8	−72.3	−67.0	−79.5	−79.0	−71.7	−72.1	−74.1
θ_r , θ_s	−68.9	−80.6	−81.4	−73.7	−74.1	−75.8	−69.0	−80.3	−81.4	−73.7	−74.0	−75.7	−69.0	−81.7	−81.4	−73.8	−74.1	−75.9
θ_r , α	−67.5	−74.7	−81.4	−73.1	−70.9	−75.6	−68.8	−78.3	−81.3	−73.7	−72.7	−75.7	−67.9	−79.5	−81.3	−73.1	−72.4	−76.0
θ_r , n	−68.7	−80.4	−81.2	−73.4	−71.3	−75.5	−68.1	−80.1	−73.0	−73.5	−69.5	−67.5	−69.0	−80.5	−80.9	−73.6	−73.9	−75.8
θ_s , α	−68.5	−75.7	−81.4	−73.6	−72.5	−75.6	−68.9	−78.8	−81.3	−73.7	−73.1	−75.9	−68.2	−80.2	−81.1	−73.3	−73.5	−76.1
θ_s , n	−69.0	−80.5	−81.4	−73.8	−73.5	−75.7	−68.8	−80.3	−81.1	−73.8	−72.8	−74.4	−69.0	−81.5	−81.0	−73.7	−74.1	−76.1
α , n	−66.2	−70.7	−81.4	−73.0	−71.2	−75.6	−68.7	−77.5	−78.8	−73.7	−72.8	−74.1	−66.0	−73.2	−80.9	−72.7	−68.8	−76.0
θ_r , θ_s , α	−69.7	−77.0	−83.4	−75.2	−73.1	−77.6	−70.8	−80.8	**−83.3**	−75.7	−74.7	**−77.7**	−69.9	−81.4	−83.3	−75.1	−74.4	−78.0
θ_r , θ_s , n	**−70.8**	**−82.5**	−83.2	−75.4	−73.3	−77.5	−70.1	**−82.2**	−75.0	−75.5	−71.5	−69.5	**−71.0**	**−82.6**	−82.9	−75.6	**−75.9**	−77.8
θ_r , α , n	−67.7	−66.8	−82.2	−75.0	−72.9	−77.5	−69.2	−76.3	−54.7	−74.6	−67.8	−52.0	−66.0	−67.3	−81.7	−74.2	−64.3	−76.1
θ_s , α , n	−68.7	−73.2	−83.4	−75.2	−73.4	−77.6	−70.7	−80.2	−80.6	−75.6	**−74.8**	−72.6	−68.0	−75.1	−83.0	−74.6	−70.9	−78.1
θ_r , θ_s , α , n	−70.3	−69.3	**−84.2**	**−77.2**	**−75.0**	**−79.5**	**−71.1**	−79.5	−56.5	**−76.4**	−69.8	−53.4	−68.0	−69.2	**−83.7**	**−76.1**	−66.3	**−78.3**

† A lower value of *AIC* within each column indicates a better model fit with the best model indicated in bold.

‡ Hillslope positions Su, Bs, Ts = summit, backslope, and toeslope, respectively.

Table 5.12. Optimal model fit of common parameter estimates of the van Genuchten model predicted by the pedotransfer functions and the parameters fitted to the measured soil water retention data.†

Pedotransfer function	θ_r		θ_s ‡		α^{-1}		n	
Hillslope position	Est (SE)	*Pr* > *t*	Est (SE)	*Pr* > *t*	Est (SE)	*Pr* > *t*	Est (SE)	*Pr* > *t*
	$m^3\ m^{-3}$		$m^3\ m^{-3}$		MPa		–	
PTF_1								
SW summit								
Predicted	0.061 (0.007)	<.001	0.372 (0)	<.001	−0.0051 (0.0007)	<.001	1.67 (0.08)	<.001
Fitted	§		§		−0.0059 (0.0008)	<.001	§	
SW backslope								
Predicted	0.049 (0.005)	<.001	0.392 (0)	<.001	−0.0043 (0.0001)	<.001	1.48 (0.02)	<.001
Fitted	§		§		−0.0058 (0.0002)	<.001	§	
SW toeslope								
Predicted	0.000 (–)	–	0.423 (0)	<.001	−0.0012 (<.0001)	<.001	1.16 (<.01)	<.001
NE summit								
Predicted	0.049 (0.006)	<.001	0.387 (0)	<.001	−0.0039 (<.0001)	<.001	1.50 (0.02)	<.001
NE backslope								
Predicted	0.044 (0.008)	<.001	0.389 (0)	<.001	−0.0032 (<.0001)	<.001	1.42 (0.02)	<.001
NE toeslope								
Predicted	0.009 (0.016)	0.597	0.410 (0)	<.001	−0.0023 (<.0001)	<.001	1.22 (0.01)	<.001
PTF_2								
SW summit								
Predicted	0.059 (0.008)	<.001	0.371 (0)	<.001	−0.0058 (0.0008)	<.001	1.63 (0.08)	<.001
SW backslope								
Predicted	0.048 (0.005)	<.001	0.393 (0)	<.001	−0.0050 (0.0001)	<.001	1.48 (0.02)	<.001
Fitted	§		§		−0.0057 (0.0002)		§	
SW toeslope								
Predicted	0.000 (–)	–	0.423 (0)	<.001	−0.0012 (<.0001)	<.001	1.13 (<.01)	<.001
Fitted	§		§		§		1.16 (<.01)	<.001
NE summit								
Predicted	0.049 (0.006)	<.001	0.388 (0)	<.001	−0.0036 (<.0001)	<.001	1.49 (0.02)	<.001
NE backslope								
Predicted	0.039 (0.007)	<.001	0.389 (0)	<.001	−0.0031 (<.0001)	<.001	1.44 (0.02)	<.001
Fitted	0.055 (0.007)	<.001	§		§		§	
NE toeslope								
Predicted	0.015 (0.012)	0.234	0.410 (0)	<.001	−0.0023 (<.0001)	<.001	1.28 (0.02)	<.001
Fitted	§		§		§		1.22 (0.01)	<.001

Table 5.12. Continued.

PTF_3								
SW summit								
Predicted	0.058 (0.007)	<.001	0.370 (0)	<.001	−0.0048 (0.0007)	<.001	1.66 (0.08)	<.001
Fitted	§		§		−0.0060 (0.0008)	<.001	§	
SW backslope								
Predicted	0.055 (0.004)	<.001	0.392 (0)	<.001	−0.0049 (0.0001)	<.001	1.53 (0.02)	<.001
Fitted	§		§		−0.0066 (0.0002)	<.001	§	
SW toeslope								
Predicted	0.000 (–)	–	0.423 (0)	<.001	−0.0013 (<.0001)	<.001	1.17 (<.01)	<.001
NE summit								
Predicted	0.052 (0.006)	<.001	0.388 (0)	<.001	−0.0041 (<.0001)	<.001	1.51 (0.02)	<.001
NE backslope								
Predicted	0.041 (0.008)	<.001	0.389 (0)	<.001	−0.0035 (<.0001)	<.001	1.37 (0.02)	<.001
Fitted	§		§		−0.0024 (<.0001)	<.001	§	
NE toeslope								
Predicted	<.001 (0.019)	0.597	0.411 (0)	<.001	−0.0021 (<.0001)	<.001	1.20 (0.02)	<.001

† Where only predicted values are shown, all parameter values are common with the fitted model.

‡ θ_s is constrained to measured values.

§ Model fit for predicted and fitted parameter values are not different according to *AIC* likelihood (Table 5.11).

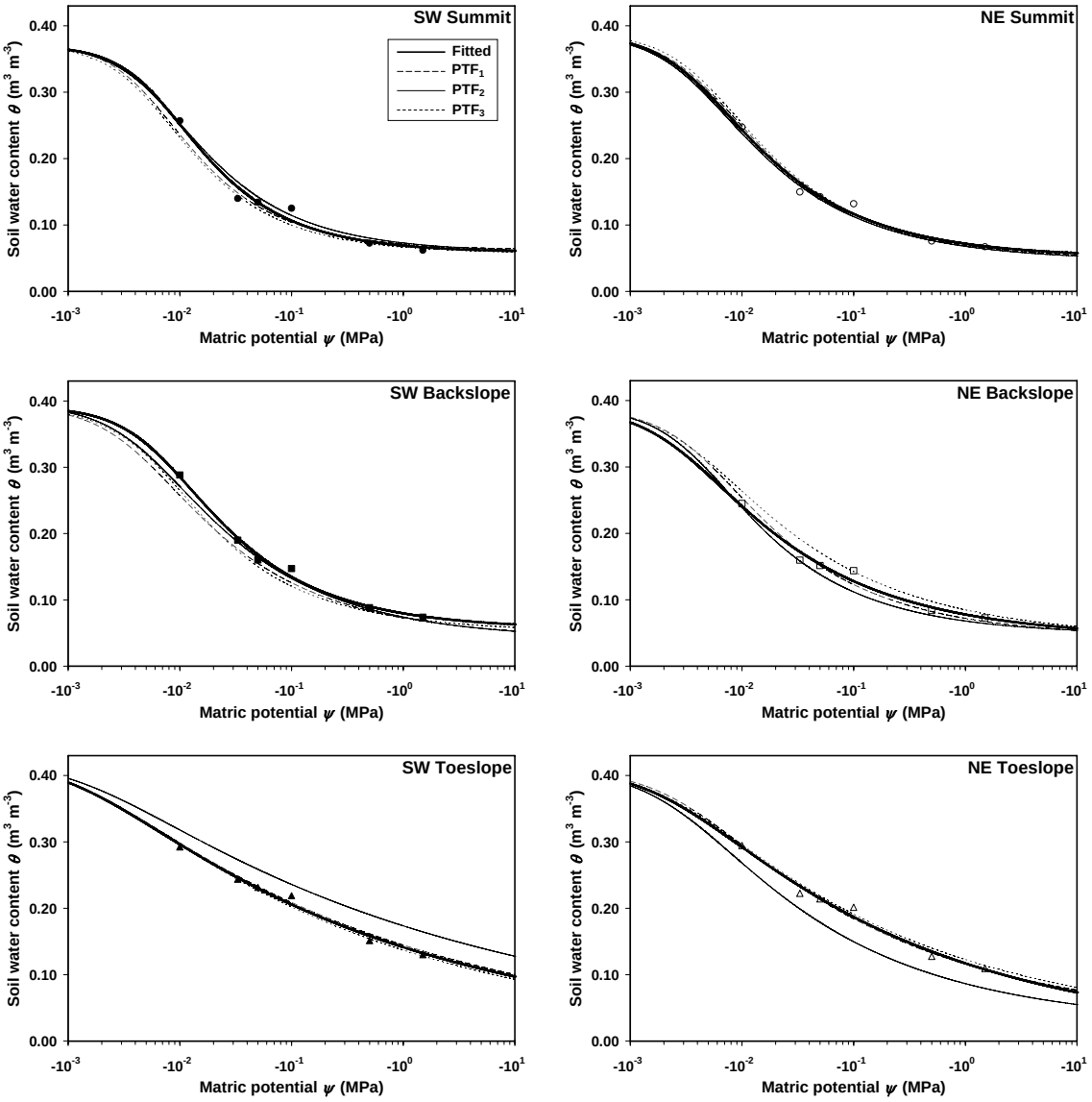

Fig. 5.4. Predicted SWRCs for PTF_1, PTF_2, and PTF_3 indicating soil water contents (θ) at soil matric potentials (ψ) among the hillslope positions using the van Genuchten (VG_2) model for soil depth increment of 25–50 mm. Fitted SWRCs are shown for the 25–50 mm soil depth increment.

Table 5.13. Validation indices comparing the predictive accuracy of the soil water retention models predicted by the pedotransfer functions and the models fitted to the measured soil water retention data.

Pedotransfer function	IME†			IRMSE‡			*r*§
Hillslope position	Mean (SD)	Min	Max	Mean (SD)	Min	Max	
	$m^3\ m^{-3}$						–
PTF_1							
SW summit	−0.0050 (0.0107)	−0.0165	0.0046	0.0103 (0.0091)	0.0045	0.0208	0.9978
SW backslope	−0.0143 (0.0172)	−0.0302	0.0039	0.0204 (0.0148)	0.0043	0.0334	0.9953
SW toeslope	0.0024 (0.0295)	−0.0256	0.0331	0.0204 (0.0166)	0.0017	0.0334	0.9994
NE summit	0.0013 (0.0045)	−0.0024	0.0062	0.0049 (0.0041)	0.0015	0.0095	0.9997
NE backslope	0.0033 (0.0088)	−0.0068	0.0090	0.0127 (0.0042)	0.0079	0.0158	0.9990
NE toeslope	0.0004 (0.0084)	−0.0093	0.0054	0.0085 (0.0021)	0.0063	0.0104	0.9998
Total dataset	−0.0020 (0.0145)	−0.0302	0.0331	0.0129 (0.0104)	0.0015	0.0334	0.9985
PTF_2							
SW summit	0.0037 (0.0023)	0.0014	0.0060	0.0058 (0.0038)	0.0029	0.0101	0.9995
SW backslope	−0.0070 (0.0040)	−0.0115	−0.0042	0.0108 (0.0081)	0.0059	0.0202	0.9979
SW toeslope	0.0245 (0.0180)	0.0090	0.0442	0.0259 (0.0187)	0.0102	0.0465	0.9995
NE summit	−0.0042 (0.0057)	−0.0076	0.0024	0.0065 (0.0025)	0.0036	0.0082	0.9998
NE backslope	−0.0061 (0.0116)	−0.0195	0.0015	0.0141 (0.0070)	0.0094	0.0221	0.9989
NE toeslope	−0.0269 (0.0260)	−0.0514	0.0005	0.0319 (0.0214)	0.0102	0.0529	0.9966
Total dataset	−0.0027 (0.0197)	−0.0514	0.0442	0.0158 (0.0146)	0.0029	0.0529	0.9987
PTF_3							
SW summit	−0.0093 (0.0148)	−0.0210	0.0073	0.0161 (0.0085)	0.0078	0.0248	0.9971
SW backslope	−0.0135 (0.0120)	−0.0270	−0.0041	0.0150 (0.0136)	0.0045	0.0303	0.9976
SW toeslope	−0.0024 (0.0239)	−0.0293	0.0163	0.0175 (0.0119)	0.0061	0.0299	0.9994
NE summit	0.0048 (0.0078)	−0.0034	0.0120	0.0088 (0.0046)	0.0053	0.0139	0.9994
NE backslope	0.0150 (0.0172)	−0.0048	0.0252	0.0193 (0.0124)	0.0050	0.0269	0.9979
NE toeslope	0.0036 (0.0141)	−0.0098	0.0183	0.0119 (0.0061)	0.0067	0.0186	0.9996
Total dataset	−0.0003 (0.0164)	−0.0293	0.0252	0.0148 (0.0092)	0.0045	0.0303	0.9985

† Integral mean error.
‡ Integral root mean square error.
§ Pearson correlation coefficient.

occurred in PTF_2 for the toeslope positions, thus limiting the accuracy of PTF_2 to the coarser soils of the upper hillslope positions. The IRMSE validation indicated that PTF_1 performed the best, followed by PTF_3 (Table 5.13). The mean of *r* values indicated similar correlation between predicted and fitted SWRCs for all the PTFs.

The soil water content at specific matric potentials in the 25–50 mm soil increment predicted by the PTFs was compared to the soil water content for the fitted equations for each hillslope position (Table 5.14; Fig. 5.4). PTF_3 which used parameters based on detailed particle-size distribution, predicted water contents more similar to the fitted model than PTF_2 which was based on the original soil variables. The ability of PTF_2 to accurately predict water content was limited to the coarser soils of the upper hillslope positions (Table 5.14). The advantage of using detailed particle-size distribution parameters improved prediction of water content most notably for the soils with greater clay content in the lower hillslope positions. Rajkai et al. (1996) found higher accuracy in the less negative matric pressures of the SWRC by including the d_g and σ_g parameters in the detailed particle-size distribution. Improvements in accuracy in our study with detailed particle-size distribution parameters occurred for almost all matric pressures and particularly for the lower hillslope positions. Overall, PTF_3 predicted the most water content estimations similar to the fitted model (Table 5.14). Despite common parameters occurring in only 50% of the SWRC models (Tables 5.11 and 5.12), water contents for predicted and fitted models were similar for virtually all PTFs across the hillslope positions, with the exception of toeslope positions for PTF_2 (Table 5.14). This may be indicative of flexibility in the range of the parameter values in deriving water content.

5.5.2.2 Prediction of SWRCs for Incremental Depths in the Seedling Recruitment Zone

The SWRC for the adjacent upper (0–25 mm) and lower (50–75 mm) incremental soil depths in the shallow seedling recruitment zone were estimated by PTF using soil physical properties from within each soil increment coupled with the SWRC information from the center (25–50 mm) soil increment. Soil texture varied in the seedling recruitment zone with clay generally increasing with depth (Table 5.1). Organic matter generally decreased with depth in the seedling recruitment zone, whereas BD increased

Table 5.14. Comparison of water content at specific matric potentials predicted by the pedotransfer functions and water content of the models fitted to the measured soil water retention data.

Hillslope position	Water content					
PTF model	−0.01 MPa	−0.033 MPa	−0.05 MPa	−0.1 MPa	−0.5 MPa	−1.5 MPa
	$m^3\ m^{-3}$					
SW summit						
Fitted	0.2514	0.1570	0.1341	0.1066	0.0751	0.0665
PTF_1	0.2363	0.1484	0.1282	0.1041	0.0767	0.0692
PTF_2	0.2532	0.1648	0.1424	0.1145	0.0803	0.0700
PTF_3	0.2318	0.1443	0.1240	0.0998	0.0721	0.0646
SW backslope						
Fitted	0.2866*a*	0.1924	0.1669	0.1344	0.0910	0.0758
PTF_1	0.2575*b*	0.1768	0.1550	0.1258	0.0836	0.0678
PTF_2	0.2710*ab*	0.1873	0.1639	0.1323	0.0861	0.0686
PTF_3	0.2650*ab*	0.1737	0.1501	0.1206	0.0824	0.0696
SW toeslope						
Fitted	0.2968	0.2463*b*	0.2303*b*	0.2058*b*	0.1581*b*	0.1320*b*
PTF_1	0.2985	0.2487*b*	0.2330*b*	0.2088*b*	0.1616*b*	0.1357*b*
PTF_2	0.3180	0.2732*a*	0.2587*a*	0.2360*a*	0.1905*a*	0.1645*a*
PTF_3	0.2951	0.2433*b*	0.2270*b*	0.2021*b*	0.1541*b*	0.1280*b*
NE summit						
Fitted	0.2433	0.1635	0.1431	0.1166	0.0805	0.0681
PTF_1	0.2489	0.1654	0.1438	0.1159	0.0783	0.0654
PTF_2	0.2379	0.1590	0.1389	0.1126	0.0766	0.0640
PTF_3	0.2535	0.1680	0.1461	0.1181	0.0812	0.0690
NE backslope						
Fitted	0.2410*ab*	0.1723*ab*	0.1536*ab*	0.1279*ab*	0.0887*ab*	0.0728*ab*
PTF_1	0.2537*ab*	0.1730*ab*	0.1515*ab*	0.1229*b*	0.0823*ab*	0.0673*ab*
PTF_2	0.2388*b*	0.1585*b*	0.1382*b*	0.1119*b*	0.0765*b*	0.0643*b*
PTF_3	0.2637*a*	0.1916*a*	0.1711*a*	0.1425*a*	0.0975*a*	0.0789*a*
NE toeslope						
Fitted	0.2928*ab*	0.2329*a*	0.2143*a*	0.1864*a*	0.1351*a*	0.1090*a*
PTF_1	0.2954*a*	0.2324*a*	0.2130*a*	0.1843*a*	0.1329*a*	0.1076*a*
PTF_2	0.2683*b*	0.1991*b*	0.1788*b*	0.1498*b*	0.1013*b*	0.0794*b*
PTF_3	0.2957*a*	0.2372*a*	0.2189*a*	0.1912*a*	0.1402*a*	0.1139*a*

a–b Within columns and hillslope position, water content means followed by different letters are significantly different at $p \leq 0.05$ according to Fisher's protected LSD.

with depth (Table 5.1). The greatest soil physical property differences with depth occurred in the toeslope positions, as indicated by differences in clay content, OM and BD (Table 5.1).

The estimated SWRCs for each of the soil incremental depths of the hillslope positions were derived with average parameters from the three PTFs as predictors (Fig. 5.5). Values of soil properties from the 0–25 mm and 50–75 mm soil increments were inserted into the equations containing transformed PCs in Table 5.9 to construct pedotransfer functions based on PTF_2 and PTF_3 to predict the VG_2 parameters for the upper and lower increments. Parameters from PTF_2 for the toeslope positions were excluded from the average due to lack of predictive accuracy (Tables 5.13 and 5.14).

Contrasts of model parameters for incremental soil depths and hillslope positions were based on mean-centered bootstrap resampling of parameter values predicted by all PTFs excluding predictions for the toeslope position by PTF_2 (Table 5.15). No differences for any of the model parameters were apparent for soil depth. Differences occurred for all parameters however, both within and between hillslopes for virtually all hillslope positions (Table 5.15). The NE summit and NE backslope were shown to have similar values of all parameters. This can be attributed to similar soil properties except for OM occurring on these two hillslope positions.

Despite differences in soil properties with incremental depth in the seedling recruitment zone, differences in water retention were generally not observed (Table 5.16). The increase in clay content with depth for several of the hillslope positions was insufficient to produce differences in water contents held at specific potentials. This may have been due to corresponding decreases in OM and increases in BD with depth, both effects that generally reduce water retention. Water content held at specific matric potentials increased downslope although differences across the hillslope had little effect on water retention at depth (Table 5.16). The only exception where water contents differed with depth was in the drier portion of the SWRC for SW toeslope position, although neither the upper nor lower soil increments had water contents held at specific potentials that differed from the middle increment. This was attributed to differences occurring in several soil properties with depth in the recruitment zone (Table 5.1). It is

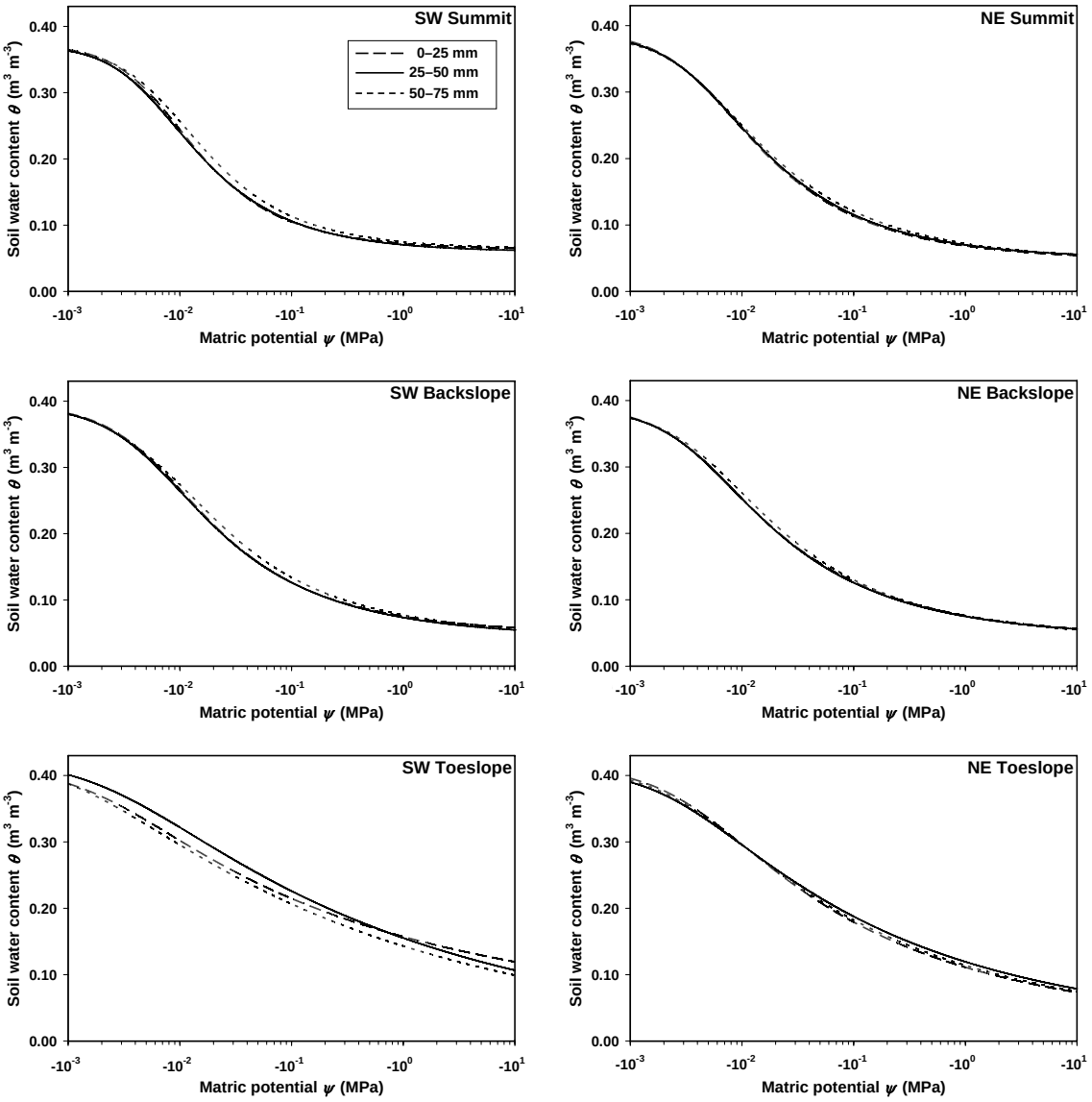

Fig. 5.5. Predicted SWRCs using the average of accurate PTFs indicating soil water contents (θ) at soil matric potentials (ψ) among the hillslope positions using the van Genuchten (VG_2) model for soil depth increments of 0–25 mm, 25–50 mm, and 50–75 mm.

Table 5.15. Contrasts of model parameters predicted by the pedotransfer functions comparing levels of soil depth and hillslope position.

Variable	Model parameter			
Contrast†	θ_r	θ_s	α^{-1}	n
	p value (SE)‡			
Soil depth (mm)				
0–25 vs. 25–50	0.9309 (0.0008)	0.9932 (0.0003)	0.9790 (0.0005)	0.9449 (0.0007)
0–25 vs. 50–75	0.9744 (0.0005)	0.5910 (0.0016)	0.9932 (0.0003)	0.9894 (0.0003)
25–50 vs. 50–75	0.9932 (0.0003)	0.8719 (0.0011)	0.8901 (0.0010)	0.9932 (0.0003)
Hillslope (within)				
SW summit vs. SW backslope	<.0001 (0.0000)	<.0001 (0.0000)	0.7054 (0.0014)	<.0001 (0.0000)
SW summit vs. SW toeslope	<.0001 (0.0000)	<.0001 (0.0000)	<.0001 (0.0000)	<.0001 (0.0000)
SW backslope vs. SW toeslope	<.0001 (0.0000)	<.0001 (0.0000)	<.0001 (0.0000)	<.0001 (0.0000)
NE summit vs. NE backslope	0.5646 (0.0016)	0.9932 (0.0003)	0.9932 (0.0003)	0.3409 (0.0015)
NE summit vs. NE toeslope	<.0001 (0.0000)	<.0001 (0.0000)	0.0003 (0.0001)	<.0001 (0.0000)
NE backslope vs. NE toeslope	<.0001 (0.0000)	<.0001 (0.0000)	0.0030 (0.0002)	<.0001 (0.0000)
Hillslope (between)				
SW summit vs. NE summit	<.0001 (0.0000)	<.0001 (0.0000)	0.3531 (0.0015)	<.0001 (0.0000)
SW backslope vs. NE backslope	0.9421 (0.0007)	0.0364 (0.0006)	0.9611 (0.0006)	0.4602 (0.0016)
SW toeslope vs. NE toeslope	<.0001 (0.0000)	<.0001 (0.0000)	<.0001 (0.0000)	0.0044 (0.0002)

† Contrasts of model parameters based on mean-centered bootstrap resampling of parameter values predicted by all PTFs excluding predictions for the toeslope position by PTF_2.

‡ Resampling-based adjusted p value and simulation standard error.

Table 5.16. Comparison of water content at specific matric potentials predicted by the average of the pedotransfer functions for the incremental depths in the seedling recruitment zone.

Hillslope position	Water content					
Soil depth	−0.01 MPa	−0.033 MPa	−0.05 MPa	−0.1 MPa	−0.5 MPa	−1.5 MPa
	$m^3\ m^{-3}$					
SW summit						
0–25 mm	0.2446*c*	0.1513*c*	0.1299*b*	0.1049*b*	0.0774*c*	0.0701*c*
25–50 mm	0.2404*c*	0.1525*c*	0.1315*b*	0.1061*b*	0.0764*b*	0.0679*b*
50–75 mm	0.2568*bc*	0.1645*b*	0.1412*b*	0.1133*b*	0.0811*b*	0.0724*b*
SW backslope						
0–25 mm	0.2673*b*	0.1802*b*	0.1568*b*	0.1265*b*	0.0853*c*	0.0708*c*
25–50 mm	0.2645*b*	0.1793*b*	0.1564*b*	0.1262*b*	0.0840*b*	0.0687*b*
50–75 mm	0.2740*ab*	0.1904*b*	0.1663*b*	0.1340*b*	0.0887*b*	0.0722*b*
SW toeslope						
0–25 mm	0.3013*a*	0.2509*a*	0.2354*a*	0.2122*a*	0.1691*a* (*a*)	0.1465*a* (*a*)
25–50 mm	0.2968*a*	0.2460*a*	0.2300*a*	0.2054*a*	0.1579*a* (*ab*)	0.1318*a* (*ab*)
50–75 mm	0.2918*a*	0.2371*a*	0.2201*a*	0.1945*a*	0.1460*a* (*b*)	0.1202*a* (*b*)
NE summit						
0–25 mm	0.2448*c*	0.1614*bc*	0.1403*b*	0.1132*b*	0.0770*c*	0.0647*c*
25–50 mm	0.2467*bc*	0.1641*bc*	0.1429*b*	0.1155*b*	0.0787*b*	0.0662*b*
50–75 mm	0.2500*c*	0.1696*b*	0.1485*b*	0.1206*b*	0.0817*b*	0.0678*b*
NE backslope						
0–25 mm	0.2528*bc*	0.1758*bc*	0.1551*b*	0.1273*b*	0.0867*c*	0.0712*c*
25–50 mm	0.2521*bc*	0.1744*bc*	0.1536*b*	0.1258*b*	0.0854*b*	0.0702*b*
50–75 mm	0.2609*bc*	0.1815*b*	0.1597*b*	0.1301*b*	0.0869*b*	0.0704*b*
NE toeslope						
0–25 mm	0.2976*a*	0.2327*a*	0.2130*a*	0.1840*a*	0.1327*b*	0.1076*b*
25–50 mm	0.2956*a*	0.2348*a*	0.2160*a*	0.1878*a*	0.1365*a*	0.1107*a*
50–75 mm	0.2970*a*	0.2349*a*	0.2158*a*	0.1873*a*	0.1359*a*	0.1103*a*

a–*c* Within columns and soil depth, soil property means followed by different letters are significantly different at $p \leq 0.05$ according to Fisher's protected LSD.

(*a*–*b*) Within columns and hillslope position, soil property means followed by different letters are significantly different at $p \leq 0.05$ according to Fisher's protected LSD.

reasonable from this analysis that the SWRC for the middle soil increment be used for the upper and lower incremental depths of the seedling recruitment zone as well.

5.6 CONCLUSIONS

Soils along the hillslopes in this study were variable with diverse physical properties that influence the SWRC within the shallow seedling recruitment zone. The SWRC for a given hillslope position were specific to estimate the soil water content at a given pressure. Although soil physical properties varied with incremental depth in the recruitment zone, this did not translate into differences in water retention, most likely the result of opposing effects of different soil properties on water retention.

Evaluation of analytical models to describe the SWRC of the shallow seedling recruitment zone indicated that the Brooks-Corey, van Genuchten, and Campbell models ranked similarly well in their ability to describe the water retention relationships. The four parameter van Genuchten model, however was considered to be superior for its ability to represent the water retention relationships at low pressures due to its continuous form. Parameters of the VG_2 model estimated using soil physical variables and detailed particle-size distribution information predicted models that were comparable to fitted models. Fitting the parameters of the VG_2 model using PCs as predictors where multicollinearity exists among the original soil predictor variables characterizes water retention relationships as well as a model based on the original soil variables. Greater information in PTF_3 having detailed particle-size distribution improved predictive fit of the parameters in the VG_2 model over that of PTF_2 which was based on the original soil variables. The SWRC for soil increments in the shallow seedling recruitment zone across hillslopes can be predicted with PTFs using the SWRC from the middle soil increment coupled with basic soil physical properties of the immediate soil increment.

Accuracy of the PTFs may have been improved by incorporating soil structural variables into the functions. The water retention curve is strongly affected by porosity changes due to soil structure particularly at high water potentials near saturation, therefore a variable to describe the soil structural component may have be beneficial (Ungaro et al., 2004). Furthermore, the predictive ability of the PTFs may have been restricted by the limited range of values in the soil properties used in this study.

The accuracy of the PTFs was generally indicated by low average deviation between predicted and fitted SWRCs. However, estimation of SWRCs by the PTFs may depend on local conditions as suggested by Schaap and Leij (1998b) in order to provide reasonable representation of the soil water status across field topography and recruitment depth for use in seedling recruitment modeling. Evaluation of the SWRC across incremental depths in the 75 mm recruitment zone indicates that a single SWRC is sufficient to describe the water content–potential relationship for the conditions of our study. The practical aspects of PTFs by effectively deriving information from readily available soil properties to predict SWRCs in the seedling recruitment zone can be used in predictive recruitment modeling.

5.7 REFERENCES

Ahuja, L.R., J.W. Naney, and R.D. Williams. 1985. Estimating soil water characteristics from simpler properties or limited data Soil Sci. Soc. Am. J. 49:1100–1105.

Akaike, H. 1974. A new look at the statistical model identification. IEEE Trans. Autom. Control. AC-19:716–723.

Akaike, H. 1978. A Bayesian analysis of the minimum AIC procedure. Ann. Inst. Stat. Math. 30:9–14.

Arya, L.M. and J.F. Paris. 1981. A physicoemperical model to predict the soil moisture characteristic from particle-size distribution and bulk density data. Soil Sci. Soc. Am. J. 45:1023–1030.

Bouma, J. 1989. Using soil survey data for quantitative land evaluation. Adv. Soil Sci. 9:177–213.

Brooks, R.H. and A.T. Corey. 1964. Hydraulic properties of porous media. Colorado State Univ. Hydrol. Paper 3:1–27.

Brubaker, S.C., A.J. Jones, D.T. Lewis, and K. Frank. 1993. Soil properties associated with landscape position. Soil Sci. Soc. Am. J. 57:235–239.

Bruce, R.R and R.J. Luxmoore. 1986. Water retention: Field methods. p. 663-686. In G.S. Campbell, R.D. Jackson, M.M. Mortland, D.R. Nielsen and A. Klute ed. Methods of soil analysis. Part 1. Physical and mineralogical methods. 2nd ed. Soil Sci. Soc. Am. Madison, WI.

Burden, D.S. and H.M. Selim. 1989. Correlation of spatially variable soil water retention for a surface soil. Soil Sci. 148:436–447.

Burnham K.P. and D.R. Anderson. 2002. Model selection and multimodel inference: A practical information-theoretic approach. 2nd ed. Springer-Verlag, New York.

Campbell, G.S. 1974. A simple method for determining unsaturated conductivity from moisture retention data. Soil Sci. 117:311–314.

Campbell, G.S. 1985. Water potential. p. 40–48. In G.S. Campbell ed. Soil physics with basic: Transport models for soil–plant systems. Dev. Soil Sci. 14. Elsevier, Amsterdam.

Campbell, G.S. and S. Shiozawa. 1992. Prediction of hydraulic properties of soils using particle-size distribution and bulk density data. p. 317–328. In M.Th. van Genuchten, R.J. Leij, and L.J. Lund ed. International workshop on indirect methods for estimating the hydraulic properties of unsaturated soils. University of California, Riverside, CA.

Carsel, R.F. and R.S. Parrish. 1988. Developing joint probability distributions of soil water retention characteristics. Water Resour. Res. 24:755–769.

Cassel, D.K. 1983. Spatial and temporal variability of soil physical properties following tillage of Norfolk loamy sand. Soil Sci. Soc. Am. J. 47:196–201.

Centner, V., D.L. Massart, O.E. de Noord, S. de Jong, B.M. Vandeginste and C. Sterna. 1996. Elimination of uninformative variables for mutivariate calibration. Anal. Chem. 68:3851–3858.

Chan, T.P. and R.S. Govindaraju. 2004. Estimating soil water retention curve from particle-size distribution data based on polydisperse sphere systems. Vadose Zone J. 3:1443–1454.

Chirico, G.B., H. Medina, and N. Romano. 2007. Uncertainty in predicting soil hydraulic properties at the hillslope scale with indirect methods. J. Hydrol. 334:405–422.

Cook, F.J. and H.P. Cresswell. 2008. Estimation of soil hydraulic properties. p. 1139–1161. In M.R. Carter and E.G. Gregorich ed. Soil sampling and methods of analysis. 2nd ed. Can. Soc. Soil Sci. CRC Press, Boca Raton, FL.

Cornelis, W.M., M. Khlosi, R. Hartmann, M. Van Meirvenne, and B. De Vos. 2005. Comparison of unimodal analytical expressions for the soil-water retention curve. Soil Sci. Soc. Am. J. 69:1902–1911.

Cornelis, W.M., J. Ronsyn, M. Van Meirvenne, and R. Hartmann. 2001. Evaluation of pedotransfer functions for predicting the soil moisture retention curve. Soil Sci. Soc. Am. J. 65:638–648.

Dane, J.H. and J.W. Hopmans. 2002. Water retention and storage. p. 671–690. In J.H. Dane and G.C. Topp ed. Methods of soil analysis. Part 4. Physical methods. Soil Sci. Soc. Am., Madison, WI.

De Jong, R., C.A. Campbell, and W. Nicholaichuk. 1983. Water retention equations and their relationship to soil organic matter and particle size distribution for disturbed samples. Can. J. Soil Sci. 63:291–302.

Dunteman, G.H. 1989. Principal components analysis. Sage university paper series on quantitative applications in the social sciences, series 07-064. Sage Publications, Newbury Park, CA.

Efron, B. and R.J. Tibshirani. 1993. An introduction to the bootstrap. Monographs on statistics and applied probability. Chapman and Hall, New York.

El-Sharkawi, H.M. and I. Springuel. 1977. Germination of some crop plant seeds under reduced water potential. Seed Sci. Technol. 5:677–688.

Fayer, M.J. and C.S. Simmons. 1995. Modified soil water retention functions for all matric functions. Water Resour. Res. 31:1233–1238.

Givi, J., S.O. Prasher, and R.M. Patel. 2004. Evaluation of pedotransfer functions in predicting the soil water contents at field capacity and wilting point. Agric. Water Manage. 70:83–96.

Greminger, P.J., Y.K. Sud, and D.R. Nielsen. 1985. Spatial variability of field-measured soil-water characteristics. Soil Sci. Soc. Am. J. 49:1075–1082.

Gupta, S.C. and W.E. Larson. 1979. Estimating soil water retention characteristics from particle size distribution, organic matter content and bulk density. Water Resour. Res. 15:1633–1635.

Hadi, A.S. and R.F. Ling. 1998. Some cautionary notes on the use of principal components regression. Am. Stat. 52:15–19.

Haverkamp, R. and J.Y. Parlange. 1986. Predicting the water retention curve from particle-size distribution: 1. Sandy soils without organic matter. Soil Sci. 142:325–339.

Hill, J.N.S. and M.E. Sumner. 1967. Effect of bulk density on moisture characteristics of soils. Soil Sci. 103:234–238.

Hillel, D. 1982. Soil water: Content and potential. p. 57–89. In D. Hillel ed. Introduction to soil physics. Academic Press Inc., San Diego, CA.

Irani, R.R. and C.F. Callis. 1963. Particle size: Measurement, interpretation, and application. John Wiley & Sons, Inc., New York.

Jauhiainen, M. 2002. Relationships of particle size distribution curve, soil water retention curve and unsaturated hydraulic conductivity and their implications on water balance of forested and agricultural hillslopes. PhD. Diss. Helsinki Univ. of Technol. Espoo, Finland.

Kern, J.S. 1995. Evaluation of soil water retention models based on basic soil physical properties. Soil Sci. Soc. Am. J. 59:1134–1141.

Kosugi, K. 1994. Three-parameter lognormal distribution model for soil water retention. Water Resour. Res. 30:891–901.

Kreznor, W.R., K.R. Olson, W.L. Banwart, and D.L. Johnson. 1989. Soil, landscape, and erosion relationships in a Northwestern Illinois watershed. Soil Sci. Soc. Am. J. 53:1763–1771.

Kvålseth, T.O. 1985. Cautionary note about R^2. Am. Stat. 39:279–285.

Lenhard, R.J., J.C. Parker, and S. Mishra. 1989. On the correspondence between Brooks-Corey and van Genuchten models. J. Irrig. Drain. Eng. 115:744–751.

Li, S., D.A. Lobb, and M.J. Lindstrom. 2007. Tillage translocation and tillage erosion in cereal-based production in Manitoba, Canada. Soil Tillage Res. 94:164–182.

Matula, S., M. Mojrová, and K. Špongrová. 2007. Estimation of the soil water retention curve (SWRC) using pedotransfer functions (PTFs). Soil Water Res. 2:113–122.

Milly, P.C.D. 1987. Estimation of Brooks-Corey parameters from water retention data. Water Resour. Res. 23:1085–1089.

Montgomery, D.C., E.A. Peck, and G.G. Vining. 2006. Multicollinearity. p. 323–368. In D.C. Montgomery et al. (ed.) Introduction to linear regression analysis. 4th ed. John Wiley & Sons, Hoboken, NJ.

Mualem, Y. 1976. A new model for predicting the hydraulic conductivity of unsaturated porous media. Water Resour. Res. 12:513–522.

Nemes, A. and W.J. Rawls. 2004. Soil texture and particle-size distribution as input to estimate soil hydraulic properties. p. 47–70. In Ya. Pachepsky and W.J. Rawls ed. Development of pedotransfer functions in soil hydrology. Elsevier, Amsterdam, Netherlands.

Nemes, A., M.G. Schaap, and J.H.M. Wösten. 2003. Functional evaluation of pedotransfer functions derived from different scales of data collection. Soil Sci. Soc. Am. J. 67:1093–1102.

Nielsen, D.R., J.W. Biggar, and K.T. Erb. 1973. Spatial variability of field-measured soil-water properties. Hilgardia. 42:215–259.

Ovalles, F.A., and M.E. Collins. 1986. Soil landscape relationships and soil variability in north central Florida. Soil Sci. Soc. Am. J. 50:401–408.

Pachepsky, Ya., W.J. Rawls, and D. Giménez. 2001a. Comparison of soil water retention at field and laboratory scales. Soil Sci. Soc. Am. J. 65:460–462.

Pachepsky, Ya., W.J. Rawls, and D.J. Timlin. 1999. The current status of pedotransfer functions: Their accuracy, reliability, and utility in field- and regional-scale modeling. p. 223–234. In D.L. Corwin, K. Loague, and T.R. Ellsworth ed. Assessment of non-point source pollution in the vadose zone. Geophys. Monograph 108. Am. Geophys. Union, Washington, DC.

Pachepsky, Ya., D.J. Timlin, and W.J. Rawls. 2001b. Soil water retention as related to topographic variables. Soil Sci. Soc. Am. J. 65:1787–1795.

Page, E.R., R.S. Gallagher, A.R. Kemanian, H. Zhang, and E.P. Fuerst. 2006. Modeling site-specific wild oat (Avena fatua) emergence across a variable landscape. Weed Sci. 54:838–846.

Penning de Vries, F.W.T., D.M. Jansen, H.F.M. ten Berge, and A. Bakema. 1989. Soil water balance. p. 147–190. In F.W.T. Penning de Vries, D.M. Jansen, H.F.M. ten Berge, and A. Bakema ed. Simulation of ecophysiological processes of growth in several annual crops. Pudoc, Wageningen, Netherlands.

Puckett, W.E., J.H. Dane, and B.F. Hajek. 1985. Physical and mineralogical data to determine soil hydraulic properties. Soil Sci. Soc. Am. J. 49:831–836.

Quinn, G.P. and M.J. Keough. 2002. Experimental design and data analysis for biologists. Cambridge University Press, New York.

Rajkai, K., S. Kabos, M.Th. van Genuchten, and P.E. Jansson. 1996. Estimation of water-retention characteristics from bulk density and particle-size distribution of Swedish soils. Soil Sci. 161:832–845.

Rajkai, K., S. Kabos, and M.Th. van Genuchten. 2004. Estimating the water retention curve from soil properties: Comparison of linear, nonlinear and concomitant variable methods. Soil Tillage Res. 79:145–152.

Rawls, W.J., 1983. Estimating soil bulk density from particle size analysis and organic matter content. Soil Sci. 135:123–125.

Rawls, W.J. and D.L. Brakensiek. 1982. Estimating soil water retention from soil properties. J. Irrig. Drain. Div. Am. Soc. Civ. Eng. 108:166–171.

Rawls, W.J. and Ya. Pachepsky. 2002. Using field topographic descriptors to estimate soil water retention. Soil Sci. 167:423–435.

Rawls, W.L., T.J. Gish, and D.L. Brakensiek. 1991. Estimating soil water retention from soil physical properties and characteristics. Adv. Soil Sci. 16:213–234.

Rawls, W.L., A. Nemes, and Ya. Pachepsky. 2004. Effect of soil organic carbon on soil hydraulic properties. p. 95–114. In Ya. Pachepsky and W.J. Rawls ed. Development of pedotransfer functions in soil hydrology. Elsevier, Amsterdam, Netherlands.

Rawls, W.L., Y.A. Pachepsky, J.C. Ritchie, T.M. Sobecki, and H. Bloodworth. 2003. Effect of soil organic carbon on soil water retention. Geoderma. 116:61– 76.

Roman, E.S., A.G. Thomas, S.D. Murphy, and C.J. Swanton. 1999. Modeling germination and seedling elongation of common lambsquarters (*Chenopodium album*). Weed Sci. 47:149–155.

Romano, N. and G.B. Chirico. 2004. The role of terrain analysis in using and developing pedotransfer functions. p. 273–294. In Ya. Pachepsky and W.J. Rawls ed. Development of pedotransfer functions in soil hydrology. Elsevier, Amsterdam.

Romano, N. and M. Palladino. 2002. Prediction of soil water retention using soil physical data and terrain attributes. J. Hydrol. 265:56–75.

Romano, N. and A. Santini. 1997. Effectiveness of using pedo-transfer functions to quantify the spatial variability of soil water retention characteristics. J. Hydrol. 202:137–157.

Russo, D. 1988. Determining soil hydraulic properties by parameter estimation: On the selection of a model for the hydraulic properties. Water Resour. Res. 24:453–459.

Saito, H., K. Seki, and J. Šimůnek. 2008. Geostatistical modeling of spatial variability of water retention curves. Hydrol. Earth Syst. Sci. Discuss. 5:2491–2522.

SAS Institute, Inc. 2004. SAS/STAT User's guide. Version 9. SAS Institute, Inc., Cary, NC.

Schaap, M.G. 2004. Accuracy and uncertainty in PTF predictions. p. 33–43. In Ya. Pachepsky and W.J. Rawls ed. Development of pedotransfer functions in soil hydrology. Elsevier, Amsterdam.

Schaap, M.G. and F.J. Leij. 1998a. A comparison of methods to predict unsaturated hydraulic conductivity. Soil Sci. Soc. Am. J. 60:1732– 1741.

Schaap, M.G., and F.J. Leij. 1998b. Database-related accuracy and uncertainty of pedotransfer functions. Soil Sci. 163:765–779.

Scheinost, A.C., W. Sinowski, and K. Auerswald. 1997. Regionalization of soil water retention curves in a highly variable soilscape, I. Developing a new pedotransfer function. Geoderma 78:129–143.

Shaykewich, C.F. and M.A. Zwarich. 1968. Relationships between soil physical constants and soil physical components of some Manitoba soils. Can. J. Soil Sci. 48:199–204.

Shein, E., A. Guber, and A. Dembovetsky. 2004. Key soil water contents. p. 241–249. In Ya. Pachepsky and W.J. Rawls ed. Development of pedotransfer functions in soil hydrology. Elsevier, Amsterdam.

Shiozawa, S. and G.S. Campbell. 1991. On the calculation of mean particle diameter and standard deviation from sand, silt, and clay fractions. Soil Sci. 152:427–431.

Shirazi, M.A. and L. Boersma. 1984. A unifying quantitative analysis of soil texture. Soil Sci. Soc. Am. J. 48:142–147.

Tani, M. 1982. The properties of water-table rise produced by a one-dimensional, vertical, unsaturated flow. J. Jpn. For. Soc. 64:409–418.

Tietje, O. and M. Tapkenhinrichs. 1993. Evaluation of pedo-transfer functions. Soil Sci. Soc. Am. J. 57:1088–1095.

Tomer, M.D., C.A. Cambardella, D.E. James, and T.B. Moorman. 2006. Surface-soil properties and water contents across two watersheds with contrasting tillage histories. Soil Sci. Soc. Am. J. 70:620–630.

Topp, G.C., Y.T. Galganov, B.C. Ball, and M.R. Carter. 1993. Soil water desorption curves. p. 569–579. In M.R. Carter ed. Soil sampling and methods of analysis. Can. Soc. Soil Sci. Lewis Publ., Boca Raton, FL.

Ungaro, F., C. Calzolari, and E. Busoni. 2005. Development of pedotransfer functions using a group method of data handling for the soil of the Pianura Padano–Veneta region of North Italy: water retention properties. Geoderma 124:293–317.

van Genuchten, M.Th. 1980. A closed-form equation for predicting the hydraulic conductivity of unsaturated soils. Soil Sci. Soc. Am. J. 44:892–898.

van Genuchten, M.Th. and D.R. Nielsen. 1985. On describing and predicting the hydraulic properties of unsaturated soils. Ann. Geophys. 3:615–628.

van Genuchten, M.Th., F.J. Leij, and S.R. Yates. 1991. The RETC code for quantifying the hydraulic functions of unsaturated soils. Report No. EPA/600/2–91/065, R.S. Kerr Environ. Res. Laboratory, US Environ. Prot. Agency, Ada, OK.

Vereecken, H. and M. Herbst. 2004. Statistical regression. p. 3–19. In Ya. Pachepsky and W.J. Rawls ed. Development of pedotransfer functions in soil hydrology. Elsevier, Amsterdam.

Vereecken, H., J. Maes, J. Feyen, and P. Darius. 1989. Estimating the soil moisture retention characteristics from texture, bulk density and carbon content. Soil Sci. 148:389–403.

Walczak, R.T., F. Moreno, C. Sławiński, E. Fernandez, and J.L. Arrue. 2006. Modeling of soil water retention curve using soil solid phase parameters. J. Hydrol. 329:527–533.

Williams, J., P. Ross, and K. Bristow. 1992a. Prediction of the Campbell water retention function from texture, structure, and organic matter. p. 427–441. In M.Th. van Genuchten et al. ed. Proc. Int. Workshop on Indirect Methods for Estimating the Hydraulic Properties of Unsaturated Soils. 11–13 Oct. 1989. Univ. California, Riverside.

Williams, R.D., L.R. Ahuja, and J.W. Naney. 1992b. Comparisons of methods to estimate soil water characteristics from soil particle size distribution, bulk density and limited data. Soil Sci. 153:172–184.

Wösten, J.M.H., and M.Th. van Genuchten. 1988. Using texture and other soil properties to predict the unsaturated soil hydraulic functions. Soil Sci. Soc. Am. J. 52:1762–1770.

Wösten, H., A. Nemes, and M. Acutis. 2004. Functional evaluation of pedotransfer functions. p. 390–394. In Ya. Pachepsky and W.J. Rawls ed. Development of pedotransfer functions in soil hydrology. Elsevier, Amsterdam.

Wösten, J.H.M., Ya.A. Pachepsky, and W.J. Rawls. 2001. Pedotransfer functions: Bridging the gap between available basic soil data and missing soil hydraulic characteristics. J. Hydrol. 251:123–150.

6.0 Modeling Temperature and Water Profiles in the Shallow Seedling Recruitment Zone across Field Topography

6.1 ABSTRACT

Process-based modeling can provide detailed spatial and temporal information of the microsite environment in the shallow seedling recruitment zone across field topography where field temperature and water measurements are not sufficient. Hourly temperature and water profiles for the shallow seedling recruitment zone across field topography for a period of 75 days after seeding were simulated from the process driven simultaneous heat and water (SHAW) model using on-site microclimate data. The SHAW model simulated heat and water transfer through surface residue, early vegetation and soil. The model was parameterized with hourly soil temperature and semi-weekly soil water measurements. A combination of measured and modeled parameters was used for plant growth and soil cover properties. Simulations were evaluated using model efficiency (ME), root mean square deviation (RMSD), and mean bias error (MBE). The greatest amount of error in simulated temperature was the lack of correlation in the pattern of the fluctuation across the measurements, followed by bias of the simulation from the measurement. Simulations of soil temperature generally tracked measurements well with the exception of overestimation prior to crop canopy closure. Soil temperature simulations were overestimated by about 2.1ºC across all topographical factors and soil depths. Simulations of soil water captured much of the essence of evaporation, precipitation and crop development events. Process-based modeling of soil temperature and water in the seedling recruitment zone depicts the microsite environment as very heterogeneous in which temperature and water was shown to fluctuate considerably, especially at the soil surface.

6.2 ABBREVIATIONS

DAE, days after emergence; DAP, days after planting; DOY, day of year; DTM, days to maturity; GDD, growing degree days; ME, model efficiency; MBE, mean bias error; RMSD, root mean square deviation; SHAW model, simultaneous heat and water model.

6.3 INTRODUCTION

The shallow seedling recruitment microsite is a dynamic temporal and spatial environment due to variable climatic influences on heterogeneous layers in the vertical soil profile across topographic irregularities at the soil surface (Stoller & Wax, 1973; Oke, 1987; Penning de Vries et al., 1989). To represent the vertical heterogeneity of the soil environment in the seedling recruitment zone, the soil profile is considered as a series of horizontal layers. The greatest exchange of energy and water occurs at the soil surface, subjecting the shallow seedling recruitment zone to frequent and intense environmental alterations (Oke, 1987). Detailed spatial and temporal representation of the seedling recruitment zone is necessary to predict seedling emergence. The spatial and temporal sources of variability in the soil environment may be the result of edaphic or climatic processes. Sources of variability in soil properties across the topography are important in modeling the shallow seedling recruitment zone because results may be biased if generalizations are made across heterogeneous soil and topographic conditions.

A seedling recruitment microsite is the soil environment that has a direct influence on weed recruitment (Harper, 1977; Pareja et al., 1985; Egley, 1986; Hurtt and Taylorson, 1986; Andreasen and Streibig, 1991). In general, the two most important predictors of weed seedling recruitment are the processes of soil heat and soil water transfer (Forcella et al., 2000; Bradford, 2002; Leguizamón et al., 2005).

Soil processes associated with weed seedling recruitment are quantified by either direct measurement or estimation of soil properties associated with each process. The condition of the recruitment microsite at a given time and location are represented by the state variables of soil heat and water content. The state variables result from one or more soil processes controlled by the soil properties associated with each process. Soil temperature and soil water content are often a result of interactions between the two soil properties that influence the processes of soil heat and water transfer (Moore, 1940; Gardner, 1955; Cary, 1966; Campbell and Gardner, 1971).

The seedling recruitment zone can be difficult to measure due to rapid changes in microclimate conditions acting on the shallow soil layer. Diurnal fluctuations of temperature and water within shallow seedling recruitment zone during the early growing season require frequent measurements to capture the status of the changing soil

environment. Many temperature sensors are required to accurately represent vertical and horizontal thermal gradients within the recruitment zone across heterogeneous field topography. Measuring soil water is more difficult since a reliable and low cost sensor that can frequently measure soil water near the soil surface is currently not available (Tsegaye et al., 2004).

Modeling continuous spatial and temporal soil temperature and soil water profiles derived from occasional measurements that are sparsely distributed can enable accurate representation of microsite properties. Simulations of the soil environment within the shallow seedling recruitment zone can be used to predict timing of weed seedling recruitment. The objectives of this study were to 1) simulate hourly soil temperature and soil water profiles for the 75 mm profile depth of the shallow seedling recruitment zone across field topography with the process driven simultaneous heat and water (SHAW) model using on-site hourly microclimate and soil temperature data, and semi-weekly soil water measurements, and 2) verify the predictive accuracy of the simulations by comparing the simulated data to the measurements using model performance indices.

6.4 MATERIALS AND METHODS

6.4.1 Field Site

Field plots were established in 2003 and 2004 across a field topography within an annually cropped field at the Orchard farm immediately west of Graysville, MB in south-central Manitoba, Canada (49º30´ N, 98º09´ W). The experiment consisted of two opposing aspects (southwest and northeast), each containing three hillslope positions (summit, backslope and toeslope). Each aspect covered an area of approximately one hectare. Soil texture of the hillslope positions ranged from silt loam to clay loam, with increasing clay content downslope (Table 6.1).

The experiment was organized as a split-plot design with the whole plot factor arranged in a randomized complete block design on each hillslope position. The experiment included five factors (hillslope aspect, hillslope position, year, soil residue, soil depth). Blocks of six replications were randomized within each hillslope position. The two years were randomized within replication, and soil residue levels (resident and added) were randomized within year. Soil depth was measured in three 25-mm

Table 6.1. Measured physical properties of the soil profile within the seedling recruitment zone.

Hillslope aspect	Hillslope position	Soil depth (mm)	Bulk density		Organic matter†		Soil texture		
			Resident‡	Added§	Resident	Added	Sand	Silt	Clay
			g cm^{-3}		%		%		
Southwest	Summit	0–25	1.1	1.0	3.2	3.5	20.2	74.8	5.0
		25–50	1.1	1.0	3.4	3.5	19.7	74.6	5.7
		50–75	1.2	1.2	3.1	3.3	19.5	74.7	5.8
	Backslope	0–25	1.0	0.9	3.7	3.9	27.8	62.4	9.8
		25–50	1.0	1.0	3.7	3.9	28.5	61.8	9.7
		50–75	1.1	1.1	3.5	3.8	27.7	61.1	11.2
	Toeslope	0–25	0.8	0.7	6.8	6.8	38.8	33.4	27.8
		25–50	0.8	0.8	6.8	6.6	39.5	32.7	27.8
		50–75	0.9	0.9	6.5	6.6	38.3	32.5	29.2
Northeast	Summit	0–25	1.0	1.0	4.2	4.1	22.5	68.8	8.7
		25–50	1.1	1.0	4.2	4.1	22.8	68.9	8.3
		50–75	1.2	1.1	3.9	3.9	22.7	68.3	9.0
	Backslope	0–25	1.1	1.0	3.2	3.2	25.0	65.0	10.0
		25–50	1.1	1.1	3.2	3.1	25.8	64.7	9.5
		50–75	1.2	1.2	3.0	3.0	25.0	64.2	10.8
	Toeslope	0–25	1.0	0.9	4.7	4.7	37.5	46.8	15.7
		25–50	1.0	0.9	4.6	4.6	38.2	46.1	15.7
		50–75	1.1	1.1	4.3	4.4	37.2	45.6	17.2

† Values shown averaged over years.
‡ Previous year soybean residue.
§ Spring applied oat straw residue (6000 kg ha^{-1}).

increments within each plot. Individual plot size was 2 m by 4 m. Blocks were arranged perpendicular to the gradient of the hillslope to maximize homogeneity within each hillslope position.

The experiment was established on previous soybean (*Glycine max* [L.] Merr.) residue. Plots were managed in a manner that mimics normal farming practices to facilitate the accompanying biotic portion of the experiment. Spring wheat (*Triticum aestivum* L., cv. AC Barrie) was metered evenly onto the soil surface at a rate of 500 viable seeds m^2 on 6 May (DOY 126) in 2003 and 6 May (DOY 127) in 2004 with a cone seeder mounted on a double disc press drill by removing the seed tubes from the discs. Residue treatments included the presence or absence of 6000 kg ha^{-1} finely chopped oat (*Avena sativa* L.) straw on a dry weight basis in addition to resident soybean residue. In treatments with high residue, the oat straw was manually spread evenly over the entire plot. Plots were rototilled to a depth of 75 mm to incorporate and distribute the oat straw and wheat seed throughout the depth of the recruitment zone. Incorporation of the wheat seed simulated a weed seedbank dispersed throughout the 75 mm vertical profile of the seedling recruitment zone. Flax (*Linum usitatissimum* L., cv. CDC Bethune) was then seeded with the double disc press drill at a rate of 675 viable seeds m^2. Soybeans (cv. OAC Prudence) were seeded at a rate of 40 viable seeds m^2 into the second-year plots in preparation for the second year.

6.4.2 Model Description

The Simultaneous Heat and Water (SHAW) model is a one-dimensional process-based model that simulates heat, water and solute transfer to a specified depth within a vertical soil column (Flerchinger, 2000). Selection of the model was based on its applicability to mechanistically simulate microsite environmental conditions within the shallow seedling recruitment zone using measured microclimate and soil data from the field. The SHAW model was developed on process-based theory and verified with field data to simulate heat, water and solute transfer through snow, crop residue, and soil (Flerchinger and Saxton, 1989a; Flerchinger and Saxton, 1989b). Provisions were later added to the SHAW model for vegetative cover to evaluate heat and water conditions for plant establishment through an air–plant–soil continuum (Flerchinger and Pierson, 1991).

The SHAW model uses microclimate, vegetative, and soil input data to simulate heat and water movement through the atmosphere–plant–residue–soil continuum (Pierson et al., 1992; Flerchinger and Pierson, 1997; Hardegree et al., 2003; Flerchinger and Hardegree, 2004). The environment in the soil profile of the SHAW model is represented as a series of layers.

To simulate the physical processes and interactions which control heat and water flow within the soil, the SHAW model requires microclimate conditions above the upper boundary as drivers of heat and water flow. Initial soil temperature and water content profile conditions are required. General site information required includes slope aspect, slope gradient, latitude, and surface roughness parameters. Input soil surface cover properties include vegetative cover, residue loading, residue layer thickness, percent cover, and albedo. Required soil properties are texture, bulk density, saturated hydraulic conductivity, organic matter, and soil water retention characteristic. Heat and water equations are solved iteratively until a simultaneous solution is derived. The model simulates daily average and diurnal changes in heat and water on an hourly basis.

6.4.3 Model Parameterization

6.4.3.1 Microclimate

Microclimate data was monitored at each hillslope position by a weather station with environmental sensors (Onset Computer Corporation, 536 MacArthur Boulevard, Pocassat, MA, 02559-3450). Air temperature was logged hourly at a height of 1.5 m above the soil surface with HOBO^{TM} temperature dataloggers fitted with a solar radiation shield beginning 9 May in 2003 and 2 May in 2004. Precipitation was measured with tipping bucket rain gauges at a height of 1.5 m above the soil surface beginning 9 May in 2003 and 2 May 2004. HOBO^{TM} weather station data loggers were installed 26 May in 2003 and 2 May in 2004 with hygrometers fitted with a solar radiation shield to monitor hourly relative humidity, silicon pyranometers to monitor hourly total incoming solar radiation (300–1100 nm), and 3 cup anemometers to monitor hourly wind speed. Relative humidity sensors and anemometers were mounted at 1.5 m above the soil surface. Pyranometers were mounted level on a base 15 cm above the soil surface.

Incoming solar radiation and albedo were instantaneously measured on all plots at intervals throughout the early season with a LI-COR model LI-200 pyranometer and model LI-1000 handheld logger (LI-COR Biosciences, 4421 Superior Street, Lincoln, NE, 68504-0425) as close as possible to solar noon. Incoming solar radiation was measured by placing the pyranometer on a base parallel to the soil surface, and albedo was measured by facing the pyranometer downwards 20 cm from the soil surface supported on a wire U-shaped frame. Shortwave surface albedo was expressed as a percentage of total incoming shortwave solar radiation.

Hourly environmental data from the beginning of the year until installation of the environment loggers in the field just after seeding in the experiment were obtained from other stations. Air temperature, relative humidity, and precipitation data were obtained from the University of Manitoba weather station at Carman MB, which was 10 km from the experiment site. Solar radiation and wind data were obtained from the North Dakota State University Agricultural Weather Network station at Walhalla (70 km distance). Wind data were equilibrated to the Graysville dataset to account for height of measurement (3 m at Walhalla), surface drag, and topographic differences (Oke, 1987).

6.4.3.2 Soil Surface

The field topography was mapped by utilizing global positioning system technology (GPS). A GPS coordinate was determined with a Trimble TSC1 Surveyor Controller™ (Trimble Navigation Ltd., 935 Stewart Drive, Sunnyvale, CA 94085) by averaging coordinates over a four hour period at a single location adjacent to the summit hillslope position at each hillslope aspect. A Sokkia SET4110 Total Station™ (Sokkia Co. Ltd., 260-63, Hase, Atsugi, Kanagawa, 243-0036, Japan) was positioned over the GPS coordinate at each aspect location, and used to map easting, northing and elevation coordinates for the corners of every plot, as well as areas between hillslope position blocks, and a buffer of 10 m surrounding each experimental area.

Slope gradient, slope aspect, and elevation for plot corners were derived from analyzing the GPS coordinates of plot corners with GPS points from areas between and around the hillslope position blocks using a Triangulated Irregular Network (TIN) model within ArcView Spatial Analyst™ (Environmental Systems Research Institute Inc.

(ESRI), 380 New York Street, Redlands, CA, 92373-8100). Single values of slope gradient, slope aspect, and elevation for each plot were derived by averaging values from the four corners of each plot. Values of all plots residing within a single hillslope position were then averaged to derive a common value for that hillslope position. Topographical properties of the site are shown in Table 6.2.

Table 6.2. Measured topographical properties of the site.

Hillslope aspect	Hillslope position	Slope aspect†	Slope gradient	Elevation
		°	%	m
Southwest	Summit	181.2	2.1	282.0
	Backslope	238.6	12.3	279.4
	Toeslope	253.2	1.9	277.8
Northeast	Summit	43.5	3.0	281.5
	Backslope	65.4	11.2	279.8
	Toeslope	123.7	2.2	277.8

† Degrees clockwise from due north.

Soil surface residue cover was determined after seeding and before any plant emergence by digital photography taken at an angle perpendicular to the ground surface. Gap Light Analyzer™ (Institute of Ecosystem Studies, Simon Fraser University, Burnaby, BC, V5A 1S6) was used to determine the percentage of residue cover by contrasting plant residue against the soil background in the digital images. Residue cover for each plot was expressed as a percentage of total ground area (Table 6.3). Soil surface cover was related to the biomass of soybean and oat residue on the soil surface by an exponential function (Gregory, 1982; Steiner et al., 2000). Residue biomass was then derived from the inverse of the exponential function to create the logarithmic equation

$$B_r = -\ln(1 - C_r) / k_c \qquad [1]$$

where B_r is residue biomass (g m^{-2}), C_r is the fraction of soil covered with residue, and k_c is the cover coefficient (m^2 g^{-1}).

Plant growth characteristics for the spring wheat were determined by a combination of measured and modeled input data (Fig. 6.1). The percentage of wheat vegetative cover to ground surface was obtained three times over the early growing season by analyzing digital photographs taken at an angle perpendicular to the ground

Table 6.3. Measured soil cover properties.

Year	Hillslope aspect	Hillslope position	Residue cover		Vegetative cover†						Vegetative biomass‡	
					M1		M2		M3			
			Resident§	Added¶	Resident	Added	Resident	Added	Resident	Added	Resident	Added
			%								g m^{-2}	
2003	Southwest	Summit	9.0	14.7	9.7	9.3	43.5	33.0	93.4	89.1	429.4	400.9
		Backslope	10.2	16.3	14.1	12.0	54.4	45.0	94.3	91.6	494.2	471.4
		Toeslope	13.8	20.3	10.8	5.3	52.9	32.6	97.5	96.4	536.5	376.8
	Northeast	Summit	8.7	13.9	11.5	8.5	50.2	33.8	96.9	91.9	532.3	414.5
		Backslope	7.6	14.6	10.8	6.1	47.9	37.1	88.8	84.0	412.1	352.0
		Toeslope	8.0	14.9	13.4	11.1	59.5	49.4	99.1	98.1	621.2	514.0
2004	Southwest	Summit	2.6	16.9	5.4#	5.4	24.9	24.9	84.3	84.3	309.3	292.0
		Backslope	4.0	16.2	5.4	5.4	24.9	24.9	84.3	84.3	342.8	320.7
		Toeslope	7.1	16.4	5.4	5.4	24.9	24.9	84.3	84.3	439.9	344.8
	Northeast	Summit	5.1	17.2	5.4	5.4	24.9	24.9	84.3	84.3	421.4	328.5
		Backslope	7.3	17.2	5.4	5.4	24.9	24.9	84.3	84.3	373.0	213.1
		Toeslope	6.9	17.5	5.4	5.4	24.9	24.9	84.3	84.3	433.0	310.0

† Vegetative cover measured DOY 141, 149, and 162 in 2003; DOY 144, 149, and 168 in 2004 for M1, M2 and M3, respectively.
‡ Vegetative biomass measured on a dry basis DOY 178 in 2003 and DOY 180 in 2004.
§ Previous year soybean residue.
¶ Spring applied oat straw residue (6000 kg ha^{-1}).
# Vegetative cover for hillslope positions and residue treatments were not measured individually in 2004.

201

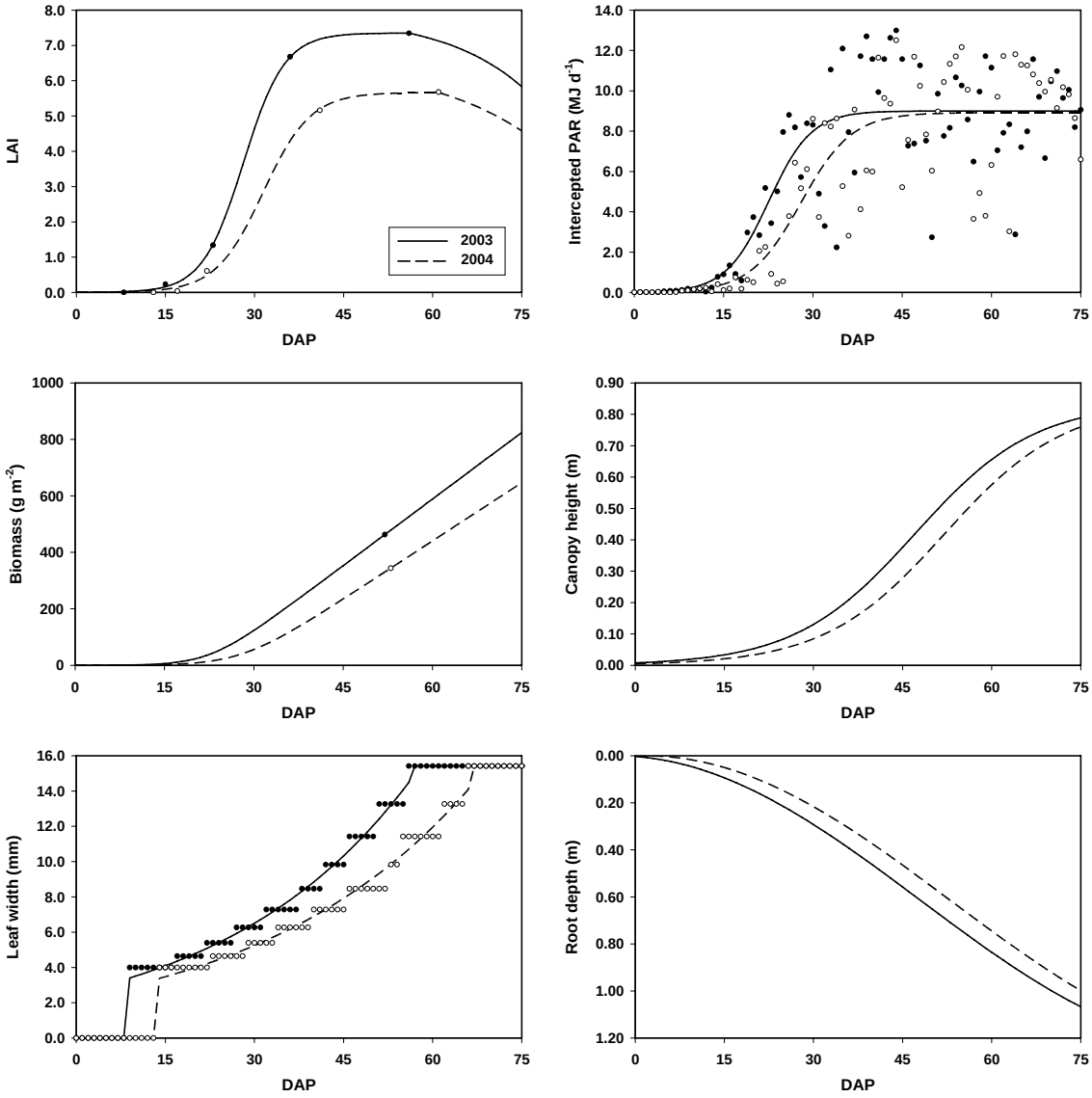

Fig. 6.1. Average functions for model parameterization of continuous wheat growth characteristics for the duration of the simulation period.

surface (Table 6.3). Green vegetative area was contrasted against the soil background in the digital images using Assess^{TM} (American Phytopathological Society, St. Paul, MN). Vegetative cover is related to leaf area index (LAI) and the solar extinction coefficient by an exponential function known as the Lambert-Beer Law (Evers et al., 2006). The exponential function was inverted to solve for LAI using a solar radiation extinction coefficient of 0.47 for spring wheat (Evers et al., 2006) and the measured vegetative cover with the following logarithmic equation

$$\mathrm{LAI} = -\ln(1 - C_v) / k \qquad [2]$$

where LAI is the total one-sided area of leaf tissue per unit ground surface area, C_v is the fraction of vegetative cover to ground surface, and *k* is the extinction coefficient. Values of LAI derived from green cover were fit with a logistic function to model continuous LAI over the simulation period for each individual treatment in 2003 and all treatments in 2004

$$\mathrm{LAI_i} = a/\left(1 + be^{-c\mathrm{DAP}}\right) \qquad [3]$$

where *a* is a parameter representing maximum LAI, *b*, and *c* are curve fitting parameters, and DAP is the number of days after planting. The fitting of the sigmoidal relationship was facilitated by adding a zero value in the lag phase accounting for the time of emergence of wheat along with a value at the late boot stage assuming a further increase in LAI of 10% beyond the third measurement for each year. The LAI peak occurs at the late boot stage for spring wheat after which LAI declines at an exponential rate (Bauer et al., 1987). Although the LAI peak is unknown, a LAI of 5.0 for wheat intercepts approximately 90% of the photosynthetically active radiation (PAR) (Hipps et al., 1983). Estimation of the LAI peak beyond 5.0 would have little effect on the fraction of PAR intercepted and biomass accumulation (Lawless et al., 2005). Increases of LAI beyond 5.0 would also not be expected to greatly influence evaporative loss from the underlying soil environment.

Above ground plant dry biomass $\left(B_i\right)$ for the wheat was derived from measured and modeled data. Biomass was measured 52 DAP at wheat stage Z47 (Zadoks et al., 1974) in 2003 and 53 DAP at stage Z37 in 2004. Biomass for any day was modeled as an integral function of daily growth rate (Monteith, 1977)

$$B_i = \int_{t_e}^{t} \varepsilon Q dt \quad [4]$$

where the integration interval is defined by the lower limit t_e as the day of emergence and the upper limit t as any day within the time period, ε is the radiation use efficiency in g MJ^{-1} PAR, and Q is the intercepted PAR in MJ d^{-1}. The value for ε was set at 2.2 g MJ^{-1} for wheat (Gallagher and Biscoe, 1978). The intercepted PAR for each day was derived by the Lambert-Beer Law

$$Q = Q_o\left(1 - e^{-k\mathrm{LAI}}\right) \quad [5]$$

where Q_o is the incident PAR (MJ d^{-1}), and k and LAI are as defined previously. Incident PAR was derived as 0.50 of solar radiation measured on the site (Szeicz, 1974). Daily values of Q were fitted with a logistic function for each year

$$Q_i = a/\left(1 + be^{-c\mathrm{DAP}}\right) \quad [6]$$

where a is a parameter representing maximum incident PAR, b, and c are curve fitting parameters, and DAP is the number of days after planting. Daily cumulative biomass for each year was adjusted to fit the measured biomass values from each treatment.

Canopy height (H_i) was modeled with a logistic growth equation in which plant height was expressed as a function of time (Christensen, 1995)

$$H_i = H_m/\left(1 + e^{a-b\mathrm{DAE}}\right) \quad [7]$$

where H_i is the canopy height (m) at a specific time after emergence, H_m is the maximum canopy height of 0.84 m for AC Barrie wheat (Manitoba Agriculture, Food and Rural Initiatives, 2009), a and b are constants representing the temporal displacement of stem elongation, and the rate of stem elongation, respectively, and DAE is the number of days after emergence. The time from planting to emergence was 9 d in 2003 and 14 d in 2004.

Leaf width was modeled from an exponential function describing the maximum blade width for each leaf for a duration of growth of one phyllochron

$$LW_m = 3.44e^{0.15n} \quad [8]$$

where LW_m is the maximum leaf blade width (mm), and n is the leaf number. The first leaf was modeled as 4 mm, and leaves after L10 had similar width to L10 (Rawson et al., 1983; McMaster et al., 1991). A constant phyllochron of 86 GDD from DAE for spring

wheat in southern Manitoba was used to determine leaf appearance (Gan and Stobbe, 1996). The phyllochron was based on air growing degree days measured on site over the simulation period. Leaf width values for each phyllochron period from L1 to L10 were fitted with an exponential function

$$LW_i = ae^{b\mathrm{DAP}} \quad [9]$$

where LW_i is the leaf width (cm) at a specific DAP, and *a* and *b* are curve fitting parameters.

Rooting depth (RD_i) for the wheat was derived from an equation expressing rooting depth as a sine function of time (Borg and Grimes, 1986). Estimates of rooting depth were derived by

$$RD_i = RD_m\{0.5 + 0.5\sin[3.03(\mathrm{DAP}/\mathrm{DTM}) - 1.47]\} \quad [10]$$

where RD_i is the rooting depth (m) at a specific time in DAP, RD_m is the maximum rooting depth of 1.23 m for spring wheat (Merrill et al., 2002), DAP is the number of days after planting, and DTM is the number of days to maturity which is 99 days for AC Barrie wheat in southern Manitoba (Manitoba Agriculture, Food and Rural Initiatives, 2009).

6.4.3.3 Soil Microsite

Soil temperature was logged hourly with Stowaway Tidbit™ temperature loggers (Onset Computer Corporation, 536 MacArthur Boulevard., Pocassat, MA, 02559-3450) beginning at the time of seeding in three replications across all factors. Four dataloggers were installed in each plot to measure the vertical temperature profile to a depth of 75 mm in the seedling recruitment zone. Dataloggers were placed at 1, 13, 38, and 63 mm depths to represent the soil surface and each of the three 25-mm depth increments.

Soil water content was measured twice weekly in six replications by excavating gravimetric soil samples of a known volume from three 25-mm increments to a depth of 75 mm in 2003. Soil water content was also simultaneously measured with a ThetaProbe™ ML2x impedance soil water sensor (Delta-T Devices Ltd., 128 Low Road, Burwell, Cambridge, CB5 0EJ, UK). In 2004, soil water was measured with the impedance soil water sensor only. Soil water content results from the impedance soil

water sensor were equilibrated with that from the volumetric soil water measurements. Soil water retention was determined for three replications in each hillslope position with a model 1600 5-bar pressure plate extractor with a 1-bar ceramic pressure plate, and a model 1500 15-bar pressure plate extractor with 5-bar and 15-bar ceramic pressure plates (Soil Moisture Equipment Corp., P.O. Box 30025, Santa Barbara, CA, 93130). Soil water retention was determined at 0.010, 0.033, 0.050, 0.100, 0.500, and 1.500 MPa (0.10, 0.33, 0.50, 1.0, 5.0, and 15.0 bar) pressures by determining the amount of volumetric water at each osmotic pressure (Dane and Hopmans, 2002). The soil water retention characteristic was determined for each hillslope position using a four parameter van Genuchten model

$$\theta = \theta_r + (\theta_s - \theta_r)\left[1 + (\alpha\psi)^n\right]^{-m} \qquad [11]$$

where θ is volumetric water content, ψ is matric potential, θ_r and θ_s are residual and saturated soil water contents, respectively, α is the capillary pressure related to ψ^{-1} and the slope of the curve at inflection, and n and m are dimensionless curve fitting parameters where $m = 1 - 1/n$ (van Genuchten, 1980). Volumetric soil water content was converted to water potential by expressing the van Genuchten water retention model in terms of water potential by

$$\psi = \left[\frac{\left(\frac{\theta_s - \theta_r}{\theta - \theta_r} \right)^{1/m} - 1}{\alpha^n} \right]^{1/n} \qquad [12]$$

where the model parameters are as previously described.

Saturated hydraulic conductivity (Table 6.4) was derived from the soil water retention characteristic of the van Genuchten model by

$$K_s = C(\theta_s - \theta_r)^{5/2}\alpha^2 \qquad [13]$$

where K_s is the predicted saturated hydraulic conductivity in cm s^{-1}, θ_s and θ_r are the saturated and residual water contents, respectively, α^{-1} is the van Genuchten retention parameter representing capillary pressure at the inflection point of the curve, and C is a constant in units of cm^3 s^{-1} (Mishra and Parker, 1990). The constant C is described as

$$C = \left(\frac{G}{\tau}\right)\left(\frac{2\gamma}{\rho_w g}\right)\left(\frac{\rho_w g}{\eta}\right) \quad [14]$$

where G is a geometric factor equal to 8 for cylindrical pores (Brutsaert, 1967), τ is flow path tortuosity equal to 2.5 (Corey, 1977), γ, ρ_w, and η are surface tension, density, and viscosity, respectively, of water at 20ºC, and g is acceleration due to gravity.

Table 6.4. Soil water retention characteristic and saturation parameters.

Hillslope aspect	Hillslope position	Water retention characteristic		Saturation parameters	
		λ †	ψ_e ‡	K_s §	θ_s
		–	m	cm h^{-1}	m^3 m^{-3}
Southwest	Summit	3.09	−0.278	0.80	0.370
	Backslope	3.36	−0.332	1.04	0.392
	Toeslope	6.26	−0.112	0.07	0.423
Northeast	Summit	3.49	−0.182	0.36	0.388
	Backslope	3.92	−0.147	0.19	0.389
	Toeslope	5.07	−0.186	0.19	0.411

† Campbell's pore-size distribution index.
‡ Campbell's air-entry potential.
§ Saturated hydraulic conductivity is modeled from the van Genuchten soil water retention characteristic.

Soil water retention characteristic input to the SHAW model were Campbell's pore-size distribution index and air-entry potential derived from a fitted Campbell soil water retention equation for each topographic position

$$\theta = \theta_s\left[\frac{\psi}{\psi_e}\right]^{\lambda} \quad [15]$$

where ψ_e is the air entry matric suction, and λ is a dimensionless curve fitting parameter representing pore size distribution (Campbell, 1974; Cory, 1977). Parameters for the soil water retention characteristic for the hillslope positions are shown in Table 6.4.

Soil physical properties were sampled in three replications after time of seeding on 14 May (DOY 134) in 2003 from three 25-mm increments to a depth of 75 mm. Particle size analysis was determined by the hydrometer method (Gee and Or, 2002). Bulk density was determined by averaging 17 time measurements of gravimetric soil water samples of a known volume in six replications from three 25-mm increments in

2003. Organic matter content was determined by the loss in weight resulting from igniting the soil in contact with air (McKeague, 1978).

The simulated soil temperature profile was extended to a depth of 4 m to create a lower boundary where soil temperature was assumed constant and approximated by the mean annual air temperature of 3ºC for Graysville (Environment Canada, 2009). Soil water flow was set at unit gradient for the lower boundary.

6.4.4 Model Evaluation

Simulations of hourly soil temperature and soil water potential from the SHAW model were compared with measured hourly soil temperature and semi-weekly soil water potential data in the seedling recruitment zone across field topography. Twenty-four simulations (2 years × 2 hillslope aspects × 3 hillslope positions × 2 residue levels) ran for duration of 75 DAP. The simulations were evaluated with model performance measures (Nash and Sutcliffe, 1970; Green and Stephenson, 1986). Model efficiency (ME) as proposed by Nash and Sutcliffe (1970) is a measure of likelihood analogous to the coefficient of determination of a regression analysis. ME considers goodness-of-fit by representing the fraction of variation in measured values explained by the model expressed as

$$ME = 1 - \left[\frac{\sum_{i=1}^{n} \left(Y_i - \hat{Y}_i \right)^2}{\sum_{i=1}^{n} \left(Y_i - \overline{Y} \right)^2} \right] \qquad [16]$$

where Y_i are measured values, $\hat{Y}_i$ are simulated values, $\overline{Y}$ is the mean of measured values, and n is the number of observations. ME ranges from negative infinity to 1. The closer ME approximates 1, the better the model will predict individual values. A model with ME close to 0 would not normally be considered a good model (Wallach, 2006). A negative ME value indicates that the simulation is a worse predictor than the mean observation over the time period (Wallach, 2006). Root mean square deviation (RMSD) is a measure of the squared difference between values predicted by the model and values measured in the field. RMSD is derived by

$$RMSD = \sqrt{\frac{1}{n}\sum_{i=1}^{n}\left(\hat{Y}_i - Y_i\right)^2} \quad [17]$$

where $\hat{Y}_i$ are simulated values, Y_i are measured values, and n is the number of observations. RMSD represents the mean distance between simulated and measured values. The interpretive advantage of RMSD is that it has the same units as Y_i. Mean bias error (MBE) is the amount by which the simulated values differ from the measured values. MBE is an indicator of the bias in modeled predictions compared to measured values by

$$MBE = \frac{1}{n}\sum_{i=1}^{n}\left(\hat{Y}_i - Y_i\right)^2 \quad [18]$$

where $\hat{Y}_i$ are simulated values, Y_i are measured values, and n is the number of observations. MBE is the square of RMSD. MBE assesses the quality of the simulated values in terms of their variation and bias. The lower the value of MBE, the closer the simulation is to the observation. The important advantage of MBE is that it can be decomposed into separate contributions that can be useful in identifying the sources of error (Wallach, 2006). The components contained in MBE are squared bias (SB), squared difference between standard deviations (SDS), and lack of correlation weighted by the standard deviations (LCS) (Kobayashi and Salam, 2000, Wallach, 2006). The components of MBE are indicated as

$$MBE = SB + SDS + LCS \quad [19]$$

where SB reflects the bias of the simulation from the measurement

$$SB = \left(\bar{\hat{Y}} - \bar{Y}\right)^2 \quad [20]$$

where $\bar{\hat{Y}}$ is the mean of simulated values and $\bar{Y}$ is the mean of measured values. SB is the square of model bias

$$Bias = \frac{1}{n}\sum_{i=1}^{n}\left(\hat{Y}_i - Y_i\right) \quad [21]$$

where bias represents the difference between means of simulation and measurement. Where SB is a large component of MBE, the importance of bias becomes apparent. A negative bias value indicates that on the average, the model under-predicts the measured

values by the simulation, and conversely, if the model over-predicts on the average, the bias is positive (Wallach, 2006). SDS is the difference between the simulation and the observation with respect to the deviation from the means in the equation

$$SDS = \left(\sigma_{\hat{Y}} - \sigma_Y\right)^2 \quad [22]$$

where $\sigma_{\hat{Y}}$ and σ_Y are standard deviations of the values in the simulation and measurement, respectively. SDS represents the difference in the magnitude of fluctuation between the simulation and measurement. A large SDS value indicates that the model failed to simulate the magnitude of fluctuation among the *n* measurements. The $\sigma_{\hat{Y}}$ and σ_Y measures are derived by the equations

$$\sigma_{\hat{Y}} = \sqrt{\frac{1}{n}\sum_{i=1}^{n}\left(\hat{Y}_i - \overline{\hat{Y}}\right)^2} \quad [23]$$

and

$$\sigma_Y = \sqrt{\frac{1}{n}\sum_{i=1}^{n}\left(Y_i - \overline{Y}\right)^2} \quad [24]$$

LCS indicates the lack of correlation weighted by the standard deviations that is derived by

$$LCS = 2\sigma_{\hat{Y}}\sigma_Y\left(1 - r\right) \quad [25]$$

where *r* is the correlation coefficient between the simulation and measurement models expressed as

$$r = \left[\frac{1}{n}\sum_{i=1}^{n}\left(\hat{Y}_i - \overline{\hat{Y}}\right)\left(Y_i - \overline{Y}\right)\right] / \left(\sigma_{\hat{Y}}\sigma_Y\right) \quad [26]$$

where a larger *r* value would reduce MBE and increase model accuracy. The *r* value is important where LCS is a major component of MBE. LCS is an indicator of a lack of positive correlation with a large LCS value indicating that the model failed to simulate the pattern of the fluctuation across the *n* measurements.

6.5 RESULTS AND DISCUSSION

6.5.1 Model Calibration

Initial calibration involved extending the simulated profile to a depth of 4 m. This moved uncertainty in the simulations away from the depth of interest. The simulation was started on DOY 90 which allowed over one month for the simulation to run accounting for temperature and water equilibration from the microclimate. The lower boundary at 4 m was set at 3ºC which reflects average annual air temperature for the site. Because water at the lower boundary could not be estimated, the simulation for water flow was set for unit gradient.

Calibrations to the model in an attempt to decrease simulated soil temperature included increasing albedo from 0.15 to 0.30 and increasing the wind roughness parameter from 1 to 2 cm. Although there were improvements in simulated soil temperature beyond these parameter values, the values were considered to be reflective of the site conditions.

6.5.2 Soil Temperature

Simulated hourly soil temperatures for the hillslope positions are shown in Figs. 6.2 to 6.4. Simulated temperatures tracked that of measurements reasonably well except for overestimation of temperature early in the season prior to crop canopy. Simulations of soil temperature were generally biased toward overestimation by an average of 2.1ºC across all treatments (Table 6.5). Calibration of parameters in an attempt to lower soil temperature early in the season improved performance measures only slightly. Installation of the on-site weather stations 20 DAP in 2003 may have contributed to overestimation of temperature by the simulation. Although remote microclimate data may have been less representative for the site for 2003, overestimation of temperature occurred in early 2004 as well.

Expected trends in simulated temperature fluctuation were tracked reasonably well. Temperature fluctuation progressively decreased as a result of crop canopy shading as the season progressed (Figs. 6.2 to 6.4). A decrease in fluctuation occurred with depth in the recruitment zone, presumably due to the increased time lag in daily maximum and minimum temperatures with depth (Oke and Hannell, 1966; Rosenberg et al., 1983). The

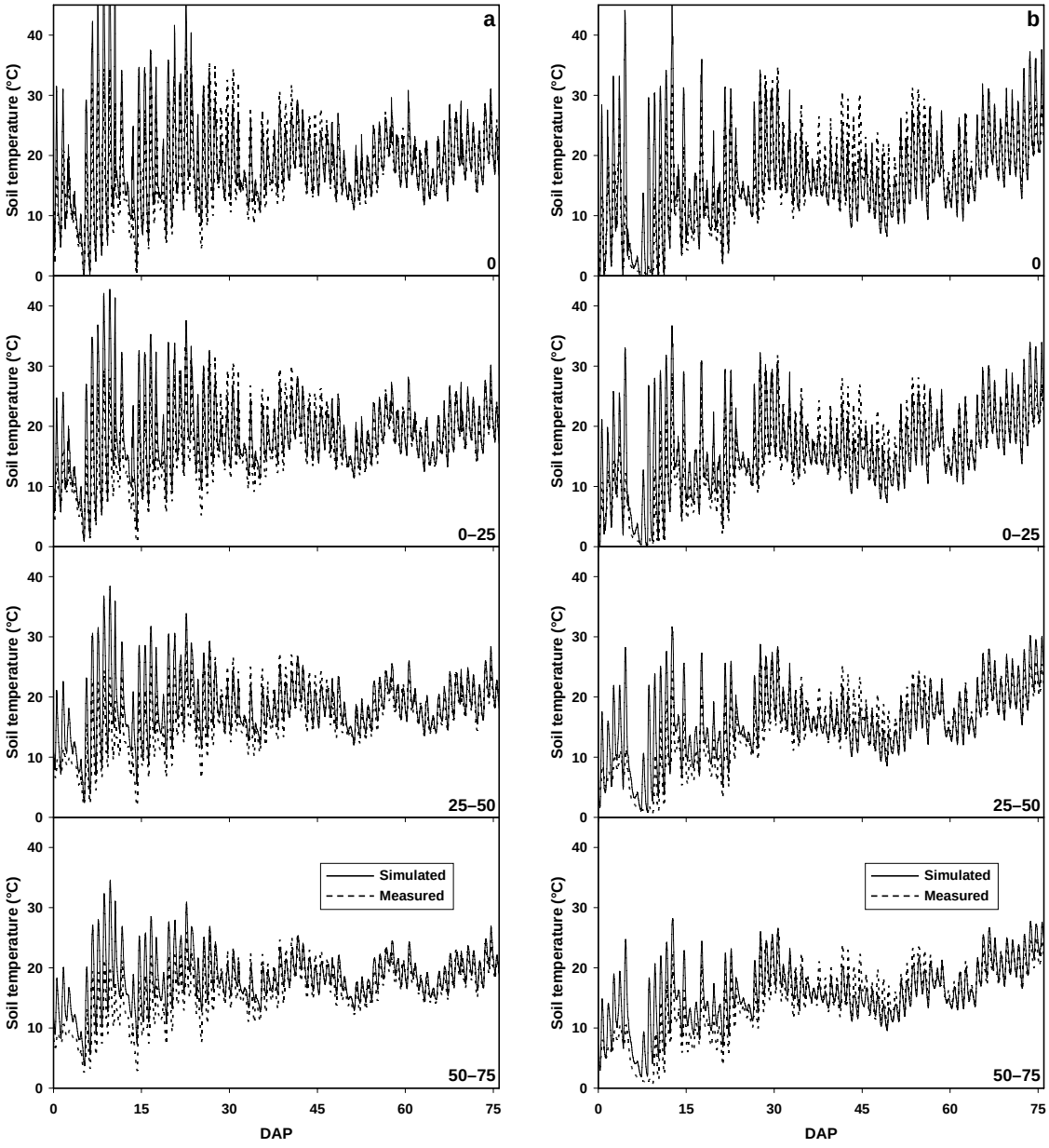

Fig. 6.2. Simulated and measured hourly soil temperature for profile increments of the 75 mm seedling recruitment zone for the summit hillslope position. Simulations for the experimental factors were averaged across topographical aspect and soil residue for a) 2003 and b) 2004.

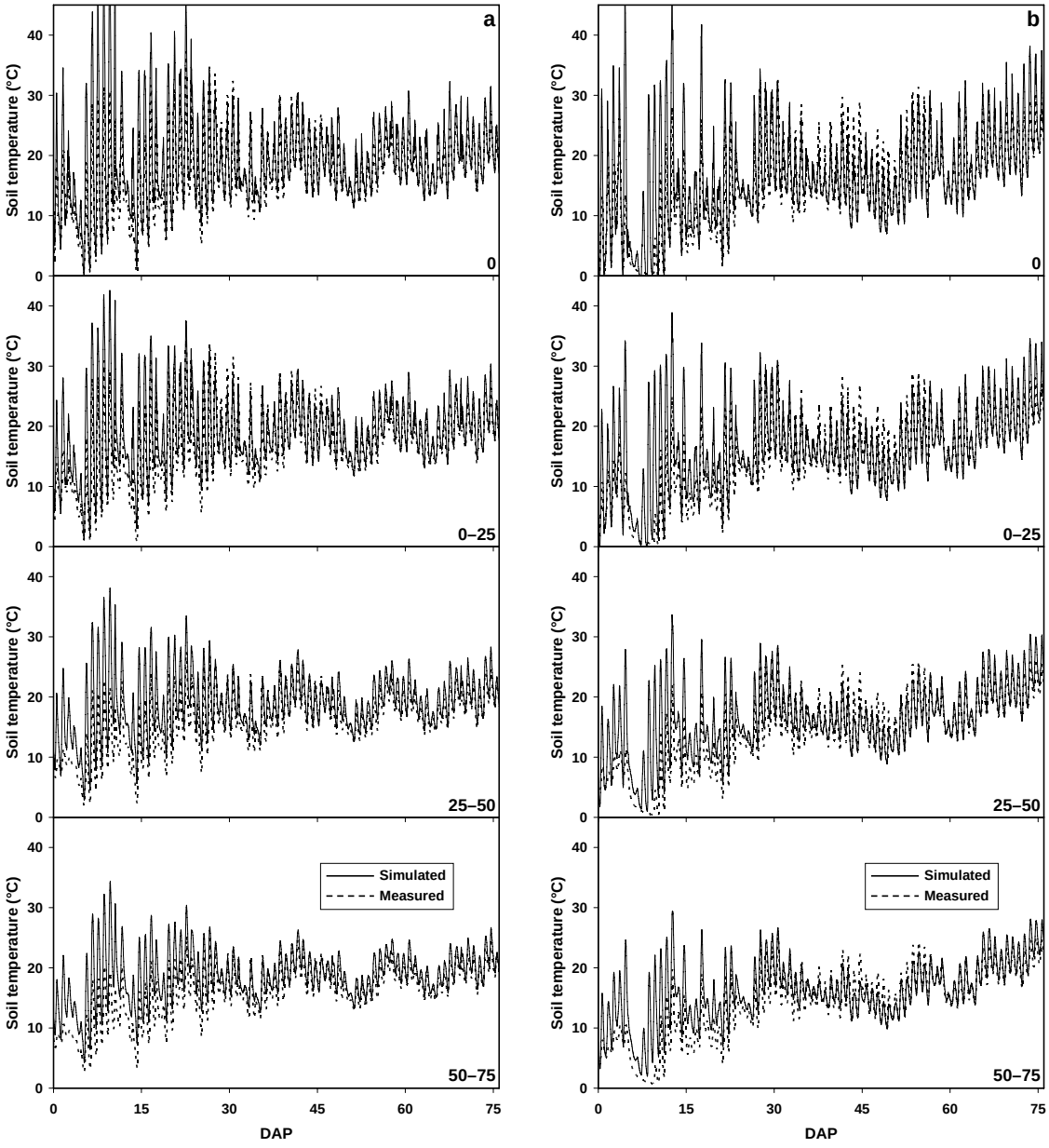

Fig. 6.3. Simulated and measured hourly soil temperature for profile increments of the 75 mm seedling recruitment zone for the backslope position on the hillslope. Simulations for the experimental factors were averaged across topographical aspect and soil residue for a) 2003 and b) 2004.

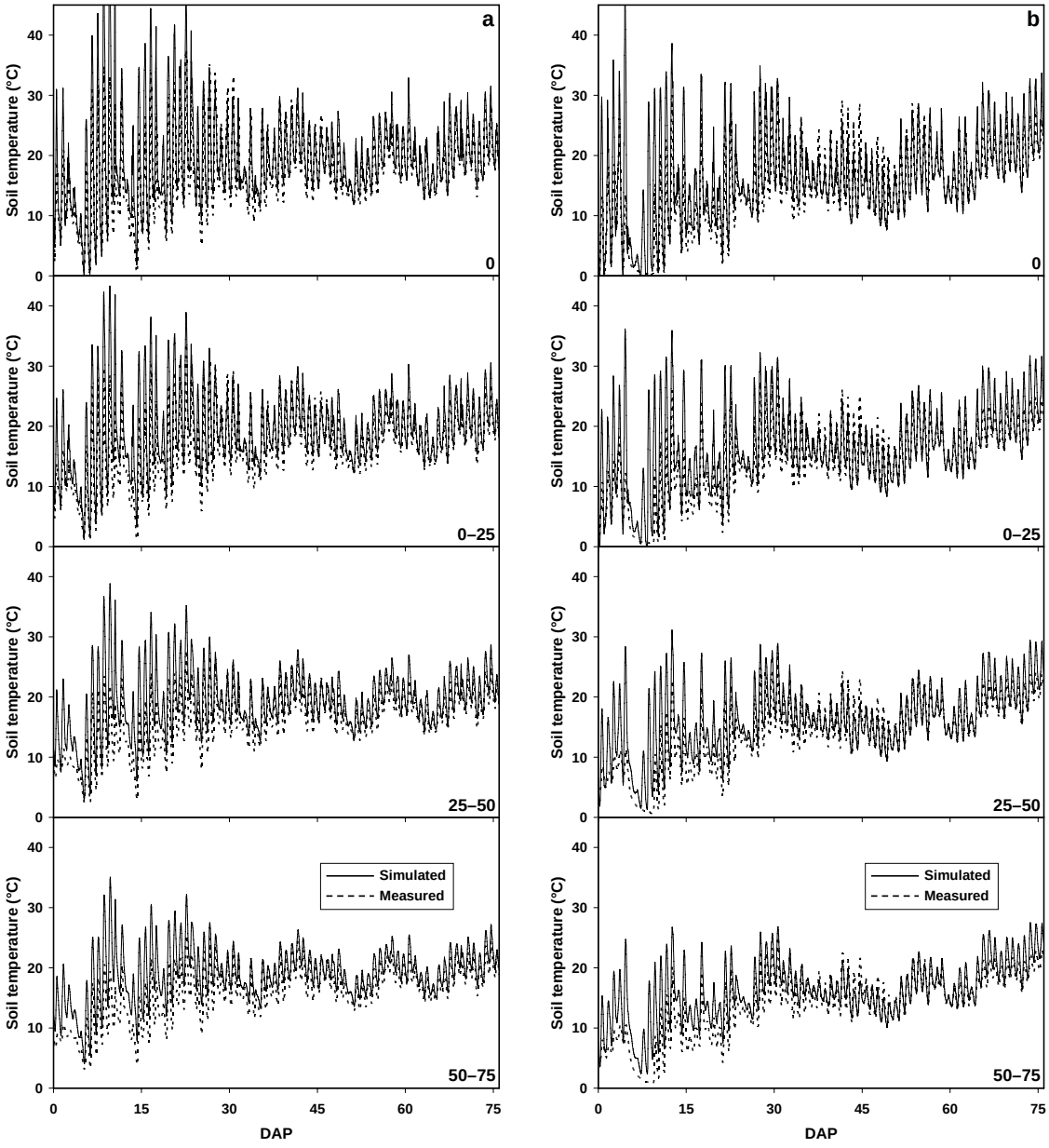

Fig. 6.4. Simulated and measured hourly soil temperature for profile increments of the 75 mm seedling recruitment zone for the toeslope position on the hillslope. Simulations for the experimental factors were averaged across topographical aspect and soil residue for a) 2003 and b) 2004.

Table 6.5. Average model performance measures for the hourly soil temperature simulations for the hillslope positions. Performance measures are averaged across simulations for topographical aspect and soil residue factors.

Year	Hillslope position	Soil depth	ME†	RMSD	MBE‡						Bias¶	*r*#
					SB		SDS		LCS			
				ºC	$(Bias)^2$	%§		%§		%§	ºC	
2003	Summit	0	0.72	3.5	2.2	0.17	0.4	0.03	9.9	0.79	1.5	0.90
		0–25	0.69	3.3	3.4	0.31	<0.1	<0.01	7.4	0.69	1.8	0.90
		25–50	0.55	3.4	4.7	0.40	<0.1	<0.01	7.0	0.60	2.2	0.86
		50–75	0.44	3.4	5.4	0.46	0.1	0.01	6.3	0.53	2.3	0.84
	Backslope	0	0.54	4.2	5.6	0.33	1.5	0.09	10.1	0.59	2.4	0.89
		0–25	0.69	3.4	4.8	0.42	<0.1	<0.01	6.5	0.58	2.2	0.91
		25–50	0.36	3.9	7.9	0.53	<0.1	<0.01	7.0	0.47	2.8	0.85
		50–75	0.29	3.8	7.7	0.54	<0.1	<0.01	6.4	0.45	2.8	0.83
	Toeslope	0	0.60	4.1	6.2	0.37	1.0	0.06	9.3	0.56	2.5	0.90
		0–25	0.59	3.7	7.1	0.53	0.2	0.01	6.2	0.46	2.7	0.91
		25–50	0.30	4.0	9.3	0.59	0.1	<0.01	6.4	0.41	3.0	0.87
		50–75	0.21	3.9	9.7	0.63	<0.1	<0.01	5.8	0.37	3.1	0.85
2004	Summit	0	0.67	4.2	0.6	0.04	0.1	<0.01	16.9	0.96	0.8	0.85
		0–25	0.70	3.7	1.2	0.09	<0.1	<0.01	12.2	0.91	1.1	0.87
		25–50	0.70	3.4	1.7	0.16	0.1	0.01	9.3	0.83	1.3	0.87
		50–75	0.72	3.1	1.8	0.19	0.6	0.06	7.1	0.75	1.3	0.88
	Backslope	0	0.55	4.8	2.9	0.12	0.6	0.03	20.0	0.85	1.7	0.83
		0–25	0.59	4.3	3.2	0.18	<0.1	<0.01	15.0	0.82	1.8	0.84
		25–50	0.59	3.9	4.2	0.27	0.2	0.01	11.1	0.72	2.1	0.84
		50–75	0.61	3.6	3.9	0.30	0.6	0.05	8.6	0.65	2.0	0.85
	Toeslope	0	0.57	4.4	3.5	0.18	0.4	0.03	15.8	0.80	1.9	0.84
		0–25	0.54	4.1	4.8	0.28	0.2	0.01	12.0	0.71	2.2	0.85
		25–50	0.58	3.7	4.9	0.36	<0.1	<0.01	8.5	0.63	2.2	0.86
		50–75	0.58	3.5	5.3	0.44	0.3	0.02	6.4	0.53	2.3	0.87

† A higher model efficiency value indicates a better simulation.
‡ A lower value of mean bias error (and the components of MBE) indicate a better simulation.
§ Fraction of error for each component of MBE.
¶ Negative and positive bias values indicate underestimation and overestimation by the simulation, respectively.
# Pearson correlation coefficient.

greatest fluctuations observed at the surface of the recruitment zone can be attributed to influences of incoming and outgoing radiation (Stoller and Wax, 1973). A depression in temperature and corresponding decrease in temperature fluctuation during 5–7 DAP in 2004 was the result of snow accumulation on the field. The effect on temperature in the recruitment zone was apparent as heat from the soil surface ceased downward movement in the soil profile.

Modeling efficiency for temperature was better for 2004 compared to 2003 (Table 6.5) which may have been attributed to remote early season weather data for 2003. The SB and LCS measures formed the predominant part of MBE (Table 6.5). Bias was exclusively overestimated, however the interpretation of SB alone is insufficient to interpret accuracy of the simulation because the model can have both under- and over-predicted values that approximately cancel each other (Wallach, 2006). For example, there was under-prediction in the simulation after DAP 30 across much of the hillslope positions and with soil depth. The high LCS values represent a lack of measurement pattern reflected by the simulation probably due to a number of parameters that require further optimization.

6.5.3 Soil Water Potential

The soil surface exhibited extreme and frequent dry periods early in the simulation of both years, presumably due to numerous small precipitation events and direct evaporation (Figs. 6.5 to 6.7). Ehlers and Goss (2003) noted that evaporation in moist soil is largely controlled by microclimatic conditions, whereas drying soil is controlled by soil hydraulic properties. The frequent dry periods seen at the soil surface between seeding and crop canopy development were not observed lower in the soil profile (Figs. 6.5 to 6.7).

Semi-weekly measurements of soil water were insufficient in capturing the detailed temporal trend of soil water potential (Figs. 6.5 to 6.7). The lack of temporal measurement data also precluded analysis. Several days between sampling dates produced large gaps of unaccounted information that must be simulated if the information is to be used for seedling recruitment studies. Many of the extremely dry events, especially in the lower two soil increments, are not reflected in the water measurements.

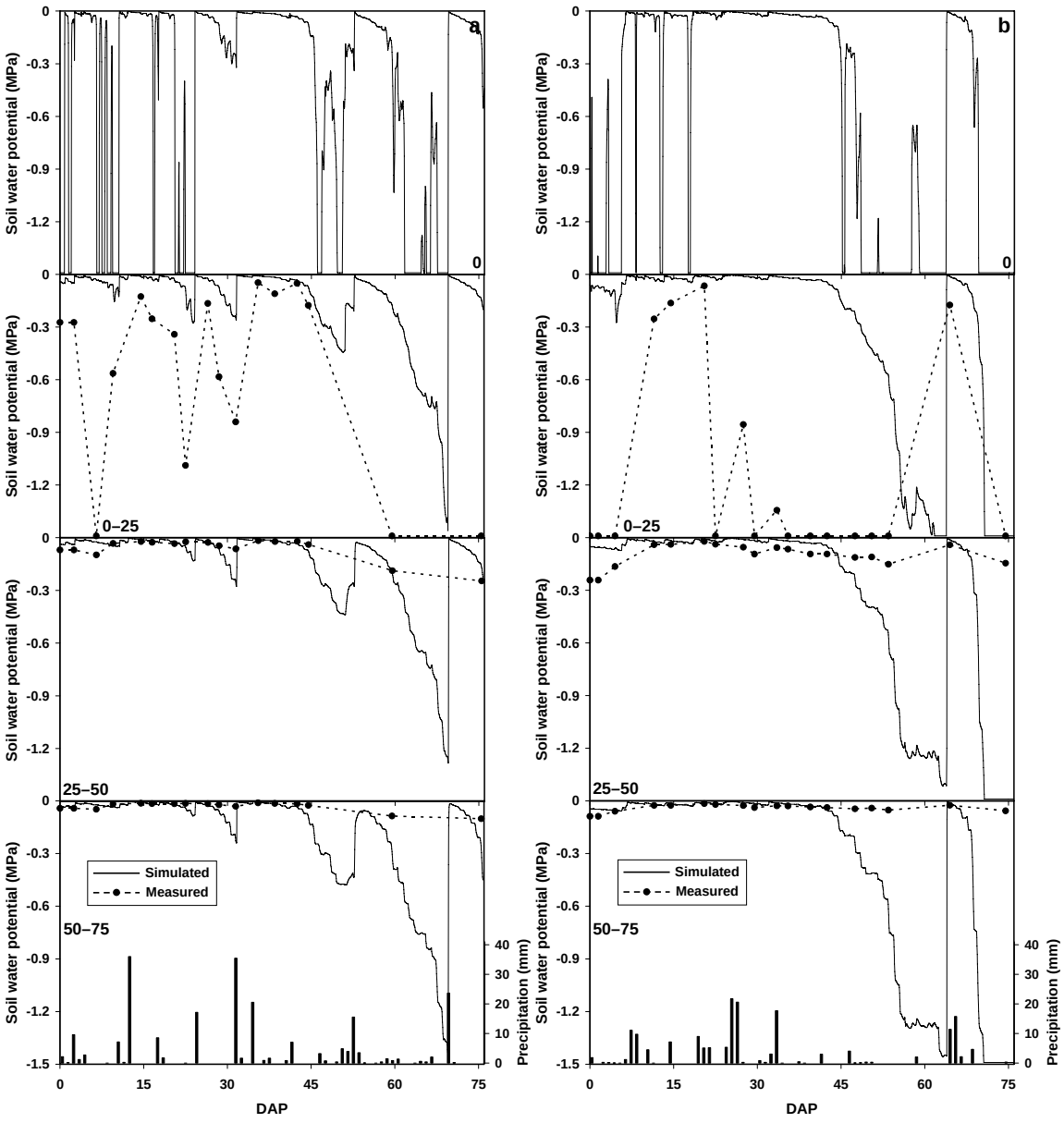

Fig. 6.5. Simulated hourly and measured semi-weekly soil water potential for profile increments of the 75 mm seedling recruitment zone for the summit hillslope position. Simulations for the experimental factors were averaged across topographical aspect and soil residue for a) 2003 and b) 2004.

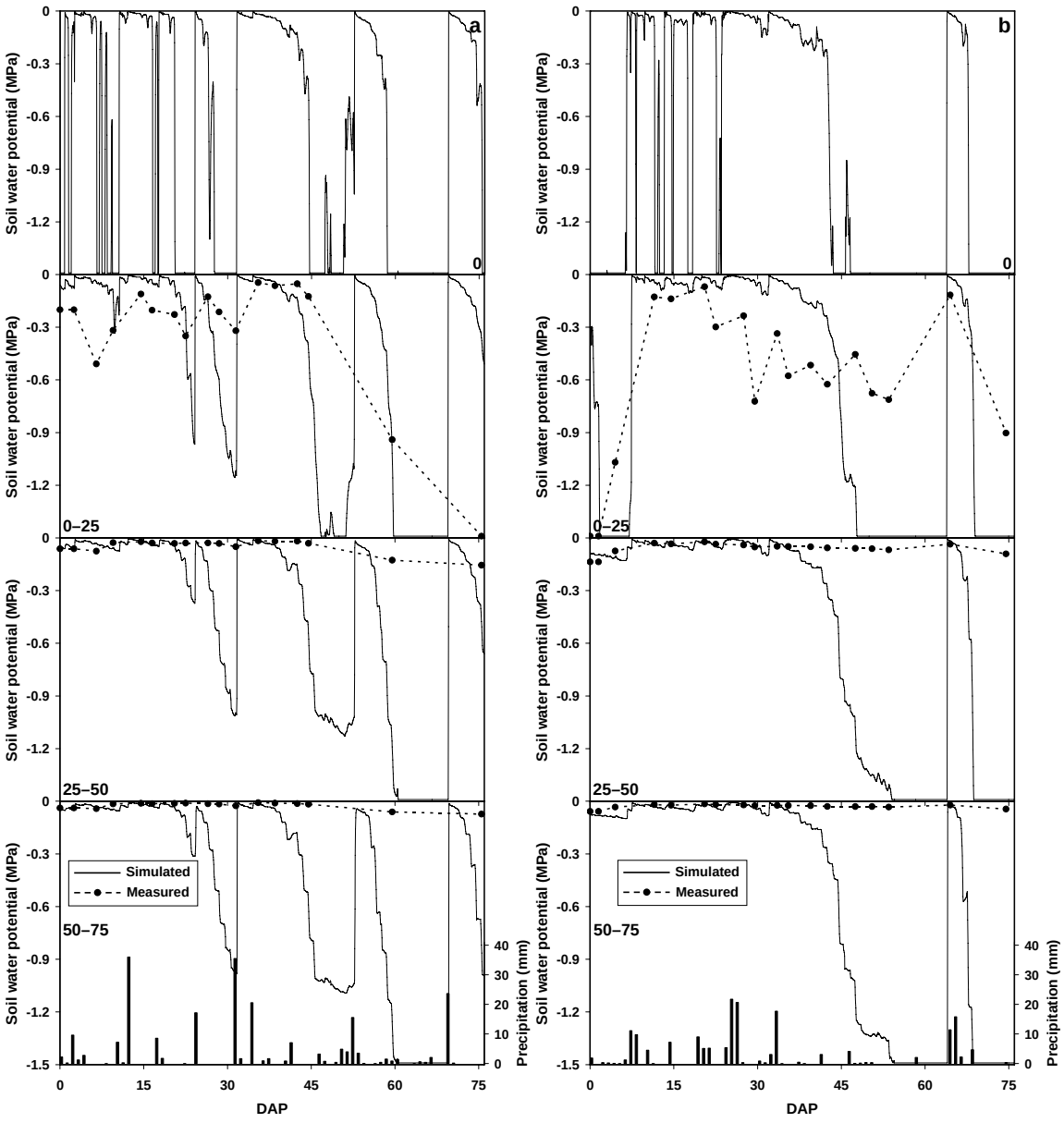

Fig. 6.6. Simulated hourly and measured semi-weekly soil water potential for profile increments of the 75 mm seedling recruitment zone for the backslope position on the hillslope. Simulations for the experimental factors were averaged across topographical aspect and soil residue for a) 2003 and b) 2004.

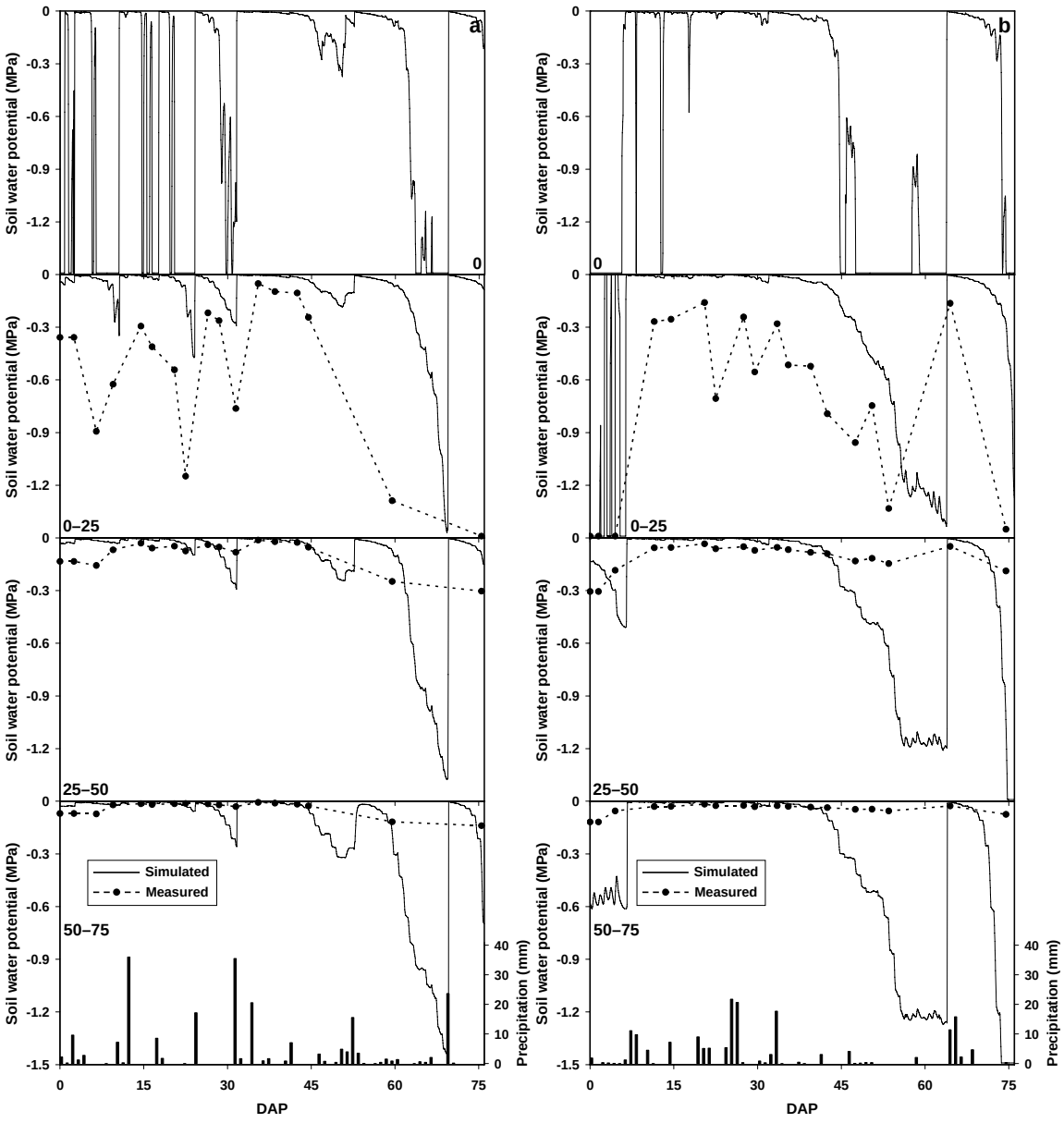

Fig. 6.7. Simulated hourly and measured semi-weekly soil water potential for profile increments of the 75 mm seedling recruitment zone for the toeslope position of the hillslope. Simulations for the experimental factors were averaged across topographical aspect and soil residue for a) 2003 and b) 2004.

Also, no water measurements were available for the soil surface, which contained the most variable water status. The surface was most variable prior to crop canopy closure with exposure to direct evaporation between precipitation events.

Continuous plant growth parameters over the simulation period enabled representative shading of the soil surface by the plant canopy providing a reduction in diurnal fluctuation of temperature and a reduction of water loss by direct evaporation from the soil surface. Water evaporation from the soil is directly related to the amount of solar radiation reaching the soil surface (Monteith, 1990). Under conditions of crop canopy, the ratio of soil evaporation to evapotranspiration is a function of crop LAI and decreases as LAI increases (Denmead, 1973; Denmead et al., 1997; Wang, 2007).

The soil water simulations closely reflected precipitation events (Figs. 6.5 to 6.7). Drying of the soil profile after DAP 45, especially at depth, was a result of crop usage of soil moisture. Overestimation of soil water in the 0–25 mm depth may have been a result of not enough moisture being evaporated from the surface, or slow movement of water through the soil profile.

6.6 CONCLUSIONS

The SHAW model simulates detailed heat and water movement in the shallow seedling recruitment zone across field topography by means of an atmosphere–plant–soil system with coupled heat and water movement. Hourly profiles of soil temperature and soil water potential were predicted for the seedling recruitment zone. Predictions were made using on-site hourly weather data and general site information by computing heat and water transfer through residue, early vegetation and soil.

Performance indices for soil temperature simulations indicated average modeling efficiencies. The greatest amount of error in temperature predictions was identified as the lack of simulation in the pattern of the fluctuation across the measurements, followed by bias of the simulation from the measurement. Soil temperature was over-predicted by 2.1ºC averaged across all factors and soil increments. Simulations of soil water captured much of the essence of evaporation, precipitation and crop development events. The lack of temporal measurements precluded performance measures for the soil water. Simulations of soil water potential were lower than −1.5 MPa for numerous periods of

time on the soil surface throughout the season, and later in the season for all soil increments as the crop developed. Although simulations reflected much of the trend in the measurements, additional calibration of the simulation may need to be explored to resolve the overestimation of soil temperature prior to canopy closure.

Process-based modeling of soil temperature and water in the seedling recruitment zone indicates a very heterogeneous environment in which temperature and water was shown to fluctuate considerably, especially at the soil surface. Large temperature and water fluctuations could have implications for dormancy or delayed germination of seeds located on or near the surface of the soil.

6.7 REFERENCES

Andreasen, C. and J.C. Streibig. 1991. Soil properties affecting the distribution of 37 weed species in Danish fields. Weed Res. 31:181–187.

Bauer, A., A.B. Frank, and A.L. Black. 1987. Aerial parts of hard red spring wheat. I. Dry matter distribution by plant development stage. Agron. J. 79:845–852.

Borg, H. and D.W. Grimes. 1986. Depth development of roots with time: An empirical description. Trans. ASAE. 29:194–197.

Bradford, K.J. 2002. Applications of hydrothermal time to quantifying and modeling seed germination and dormancy. Weed Sci. 50:248–260.

Brutsaert, W. 1967. Some methods of calculating unsaturated permeability. Trans. ASAE. 10:400–404.

Campbell, G.S. 1974. A simple method for determining unsaturated conductivity from moisture retention data. Soil Sci. 117:311–314.

Campbell, G.S. and W.H. Gardner. 1971. Psychrometric measurements of soil water potential: Temperature and bulk density effects. Soil Sci. Soc. Am. Proc. 35:8–12.

Cary, J.W. 1966. Soil moisture transport due to thermal gradients: Practical aspects. Soil Sci. Soc. Am. Proc. 30:428–433.

Christensen, S. 1995. Weed suppression ability of spring barley varieties. Weed Res. 35:241–247.

Cory, A.T. 1977. Mechanics of heterogeneous fluids in porous media. Water Resources Publications, Fort Collins, CO.

Dane, J.H. and J.W. Hopmans. 2002. Water retention and storage. p. 671–690. In J.H. Dane and G.C. Topp ed. Methods of soil analysis. Soil Sci. Soc. Am., Madison, WI.

Denmead, O.T. 1973. Relative significance of soil and plant evaporation in estimating evapotranspiration. p. 505–511. In Plant response to climatic factors. Proc. Uppsala Symposium, 1970, UNESCO, Paris.

Denmead, O.T., F.X. Dunin, R. Leuning, and M.R. Raupach. 1997. Measuring and modelling soil evaporation in wheat crops. Phys. Chem. Earth. 21:97–100.

Egley, G.H. 1986. Stimulation of weed seed germination in soil. Rev. Weed Sci. 2:67–89.

Ehlers, W. and M.J. Goss. 2003. Water dynamics in plant production. CABI Publ., Wallingford, UK.

Environment Canada National Climate Data and Information Archive. 2009. Climate normals and averages 1971–2000. [Online]. Available at http://www.climate.weatheroffice.ec.gc.ca/climate_normals/index_e.html (accessed 08 June 2009). Environment Canada, Ottawa, ON.

Evers, J.B., J. Vos, C. Fournier, B. Andrieu, M. Chelle, and P.C. Struik. 2006. An architectural model of spring wheat: Evaluation of the effects of population density and shading on model parameterization and performance. Ecol. Modell. 200:308–320.

Flerchinger, G.N. 2000. The Simultaneous Heat and Water (SHAW) model: technical documentation. USDA Technical Report NWRC 2000-09.

Flerchinger, G.N. and F.B. Pierson. 1991. Modeling plant canopy effects on variability of soil temperature and water. Agric. For. Meteorol. 56:227–246.

Flerchinger, G.N. and F.B. Pierson. 1997. Modelling plant canopy effects on variability of soil temperature and water: model calibration and validation. J. Arid Environ. 35:641–653.

Flerchinger, G.N. and K.E. Saxton. 1989a. Simultaneous heat and water model of a freezing snow-residue-soil system. I. Theory and development. Trans. ASAE. 32:565–571.

Flerchinger, G.N. and K.E. Saxton. 1989b. Simultaneous heat and water model of a freezing snow-residue-soil system. II. Field verification. Trans. ASAE. 32:573–578.

Flerchinger, G.N. and S.P. Hardegree. 2004. Modelling near-surface soil temperature and moisture for germination response predictions of post-wildfire seedbeds. J. Arid Environ. 59:369–385.

Forcella F., R.L. Benech-Arnold, R. Sanchez, and C.M. Ghersa. 2000. Modeling weed emergence. Field Crops Res. 67:123–139.

Gallagher, J.N. and P.V. Biscoe. 1978. Radiation absorption, growth and yield of cereals. J. Agric. Sci. 91:47–60.

Gan, Y. and E.H. Stobbe. 1996. Mainstem leaf stage and its relation to single plant grain yield in spring wheat. Crop Sci. 36:628–632.

Gardner, R. 1955. Relation of temperature to moisture tension of soil. Soil Sci. 79:257–265.

Gee, G.W. and D. Or. 2002. Particle size analysis. p. 255–293. In J.H. Dane and G.C. Topp ed. Methods of soil analysis. Soil Sci. Soc. Am., Madison, WI.

Green, I.R.A. and D. Stephenson. 1986. Criteria for comparison of single event models. Hydrol. Sci. 31:395–411.

Gregory, J.M. 1982. Soil cover prediction with various amounts and types of crop residue. Trans. ASAE. 25:1333–1337.

Hardegree, S.P., G.N. Flerchinger, and S.S. Van Vactor. 2003. Hydrothermal germination response and the development of probabilistic germination profiles. Ecol. Modell. 167:305–322.

Harper, J.L. 1977. The recruitment of seedling populations. p. 111–147. In J.L. Harper ed. Population biology of plants. Academic Press, London.

Hipps, L.E., G. Asrar, and E.T. Kanemasu. 1983. Assessing the interception of photosynthetically active radiation in winter wheat. Agric. Meteorol. 28:253–259.

Hurtt, W. and R.B. Taylorson. 1986. Chemical manipulation of weed emergence. Weed Res. 26:259–267.

Kobayashi, K. and M.U. Salam. 2000. Comparing simulated and measured values using mean squared deviation and its components. Agron. J. 92:345–352.

Lawless, C, M.A. Semenov, and P.D. Jamieson. 2005. A wheat canopy model linking leaf area and phenology. Europ. J. Agron. 22:19–32.

Leguizamón, E.S., C. Fernandez-Quintanilla, J. Barroso, and J.L. Gonzalez-Andujar. 2005. Using thermal and hydrothermal time to model seedling emergence of Avena sterilis ssp. ludoviciana in Spain. Weed Res. 45:149–156.

Manitoba Agriculture, Food and Rural Initiatives. 2009. Seed Manitoba: Variety selection and growers source guide. The Manitoba Co-operator, Winnipeg, Canada.

McKeague, J.A. 1978. Manual on soil sampling and methods of analysis. Method 3.8, loss on ignition. Canadian Society of Soil Science, Ottawa, ON, Canada.

McMaster, G.S., B. Klepper, R.B. Rickman, W. Wilhelm, and W.O. Willis. 1991. Simulation of shoot vegetative development and growth of unstressed winter wheat. Ecol. Modell. 53:189–204.

Merrill, S.D., D.L. Tanaka, and J.D. Hanson. 2002. Root length growth of eight crop species in Haplustoll soils. Soil Sci. Soc. Am. J. 66:913–923.

Mishra, S. and J.C. Parker. 1990. On the relation between saturated conductivity and capillary retention characteristics. Ground Water. 28:775–777.

Monteith, J.L. 1977. Climate and the efficiency of crop production in Britain. Philos. Trans. R. Soc. London, Ser. B. 281:277–294.

Monteith, J.L. 1990. Principles of environmental physics. 2nd ed. Edward Arnold, New York.

Moore, R.E. 1940. The relation of soil temperature to soil moisture: pressure potential, retention, and infiltration rate. Soil Sci. Soc. Proc. 5:61–64.

Nash, J.E. and J.V. Sutcliffe. 1970. River flow forecasting through conceptual models: Part I – a discussion of principles. J. Hydrol. 10:282–290.

Oke, T.R. 1987. Climates of non-uniform terrain. p. 158–189. In T.R. Oke ed. Boundary layer climates. 2nd ed. Routledge, New York.

Oke, T.R. and F.G. Hannell. 1966. Variations of temperature within a soil. Weather. 21:21–28.

Pareja, M.R., D.W. Staniforth, and G.P. Pareja. 1985. Distribution of weed seed among soil structural units. Weed Sci. 33:182–189.

Penning de Vries, F.W.T., D.M. Jansen, H.F.M. ten Berge, and A. Bakema. 1989. Soil water balance. p. 147–190. In F.W.T. Penning de Vries, D.M. Jansen, H.F.M. ten Berge, and A. Bakema ed. Simulation of ecophysiological processes of growth in several annual crops. Pudoc, Wageningen, Netherlands.

Pierson, F.B., G.N. Flerchinger, and J.R. Wight. 1992. Simulating near-surface soil temperature and water on sagebrush rangelands: a comparison of models. Trans. ASAE. 35:1449–1455.

Rawson, H.M., J.H. Hindmarsh, R.A. Fischer, and Y.M. Stockman. 1983. Changes in leaf photosynthesis with plant ontogeny and relationships with yield per ear in wheat cultivars and 120 progeny. Aust. J. Plant Physiol. 10:503–514.

Rosenberg, N.J., B.L. Blad, and S.B. Verma. 1983. Microclimate: The biological environment. 2nd ed. John Wiley and Sons. New York.

Steiner, J.L., H.H. Schomberg, P.W. Unger, and J. Cresap. 2000. Biomass and residue cover relationships of fresh and decomposing small grain residue. Soil Sci. Soc. Am. J. 64:2109–2114.

Stoller, E.W. and L.M. Wax. 1973. Temperature variations in the surface layers of an agricultural soil. Weed Res. 13:273–282.

Szeicz, G. 1974. Solar radiation for plant growth. J. Appl. Ecol. 11:617–636.

Tsegaye, T.D., W. Tadesse, T.L. Coleman, T.J. Jackson, and H. Tewolde. 2004. Calibration and modification of impedance probe for near surface soil moisture measurements. Can. J. Soil Sci. 84:237–243.

van Genuchten, M.Th. 1980. A closed-form equation for predicting the hydraulic conductivity of unsaturated soils. Soil Sci. Soc. Am. J. 44:892–898.

Wallach, D. 2006. Evaluating crop models. p. 11–54. In D. Wallach, D. Makowski, and J.W. Jones ed. Working with dynamic crop models: Evaluation, analysis, parameterization, and applications. Elsevier, Amsterdam.

Wang, H.X. and C.M. Liu. 2007. Soil evaporation and its affecting factors under crop canopy. Commun. Soil Sci. Plant Anal. 38:259–271.

Zadoks, J.C., T.T. Chang, and C.F. Konzak. 1974. A decimal code for the growth stages of cereals. Weed Res. 14:415–421.

7.0 General Discussion and Conclusions

7.1 General Discussion

The seedling recruitment microsite is the soil environment immediately surrounding the seed that has a direct influence on seedling recruitment. Microsite influences are most important for germination, emergence, and early seedling establishment. The primary environmental conditions within microsites that control seedling recruitment include temperature and water. The shallow seedling recruitment zone contains a diversity of spatial and temporal microsites that represent a heterogeneous environment influencing seedling germination and emergence.

The environment of microsites within the recruitment zone evolves and fluctuates due to above ground environmental conditions. Microsites are further modified by soil surface and topographical conditions. Heterogeneity of soil properties within the recruitment zone further create diversity of microsites due to the influence of soil physical properties on the movement and retention of heat and water.

The seedling recruitment zone represents a high degree of microtopographic diversity relative to the scale of seed size. A description of the spatiotemporal environment through both the vertical and horizontal soil profiles forms the basis for modeling weed seedling recruitment in the field. The spatial and temporal environment of a microsite controls the occurrence, timing, and proportion of seedling recruitment that influence the competitiveness and regeneration ability of a species. Knowledge of the soil environment is therefore principal to understanding and predicting recruitment of a species.

Microsites within the recruitment zone are highly heterogeneous across field topography offering widely diverse environments for seedling recruitment. The ability to model the recruitment of a species requires input of representative microsite properties accounting for hillslope scale complexity and heterogeneity. Detailed knowledge of the microsite environment across field topography can enable better prediction of occurrence of a species and thus better management of that species. Seedling recruitment knowledge is essential to effectively optimize agronomic practices.

Weeds generally recruit from a relatively shallow layer in the soil where the microsite environmental conditions can vary greatly with space and time. The shallow

recruitment layer is further variable across hillslopes in a field. The variability of the recruitment zone environment would be expected to have a diverse effect on weed recruitment from various microsites within the recruitment zone. Identifying weed recruitment across topography requires an understanding of the varying nature of the soil environment associated with a particular location and time in the topography. Clearly, models that do not account for the effect of small-scale heterogeneities in hillslope geometry on the recruitment microsite will be inadequate for predictive purposes.

The seedling recruitment microsite is influenced considerably by the above-ground environment. The temperature of the shallow seedling recruitment zone varies primarily due to changing intensity of diurnal and seasonal solar radiation intercepted at the soil surface. The temperature within layers of the seedling recruitment zone fluctuate diurnally due to alternating intervals of heat absorption and storage and heat release from the shallow soil layers. The recruitment zone is further diverse across field topography, where microclimate conditions act differentially across an uneven soil surface that contributes to form a variable environment within the recruitment zone.

Monitoring of the seedling recruitment zone requires numerous spatial and temporal recordings of temperature and water to accurately represent the heterogeneous soil environment. Although low cost temperature dataloggers are available, no such device currently exists to monitor the varying status of soil water. Because both temperature and water variables are required to describe the recruitment zone, simulation of the soil environment is an alternative to direct measurement. However, accurate and reliable measurement of soil environmental variables is still required for parameterization of recruitment zone modeling. Modeling needs to account for specific microclimate, soil surface, and soil differences. Interactions occur among microclimate, topography, and soil properties that influence the microsite. The status of soil water and soil temperature is often a result of interactions between soil properties that influence the processes of soil water and soil heat transfer. Because interactions between soil water and soil temperature are common in the recruitment zone, simultaneous modeling of both variables in this study is essential.

7.2 Conclusions

The manuscript in Chapter 3 describes the field calibration for an impedance soil water probe for the measurement of volumetric water content in seedbeds across field topography with variable soil properties. The objectives of this study were to identify the physical and chemical soil properties that influence the water probe readings, and to develop a calibration of the water probe by separating topographical and soil factors by factor level. It was identified that bulk density, electrical conductivity, and temperature positively increased volumetric water readings by the water probe. Because the identified soil physical properties varied across field topography and/or soil depth, individual calibrations were performed for hillslope units and soil profile increments. Hence, calibration of the probe was accomplished by separating individual levels of the experimental factors. Separating the soil water measurements by factor level produced significantly different calibrations due to the underlying influential soil properties. This study emphasized the requirement to consider calibrations across units of topography and soil depth to avoid misleading soil water content results due to underlying soil properties that can influence the water probe measurements.

The manuscript in Chapter 4 characterized microclimate and topographical influences on the seedling recruitment environment. The objectives of this study were to identify influences on the seedling recruitment zone environment by above-ground microclimate, field topography, soil residue, and soil depth. Mixed model analysis of two years of data measurements specified year as a random factor to enable the topographical and soil fixed factors of interest to be estimated. Results indicated that the amount of solar radiation received at the soil surface was greater at the southwest facing aspect compared to the northeast aspect. The greater amount of solar radiation received at the southwest aspect, however, did not result in higher soil temperatures or greater temperature fluctuation within the recruitment zone than the northwest aspect. Wind speed differed across topography, with higher wind speed and potentially greater evaporation from the seedling recruitment zone in upper hillslope regions. Soil temperature and soil temperature fluctuation were shown to decrease with depth in the seedling recruitment zone. Since solar radiation is received at the soil surface, thermal conductivity forms a downward gradient in the recruitment zone. Soil water generally

increased with soil depth and lower hillslope position. Hillslope position and recruitment zone depth were influential factors on the recruitment zone environment. Soil temperature and water in the recruitment zone varied primarily with hillslope position and soil depth.

The manuscript in Chapter 5 analyzes the spatial variability of the soil water retention characteristic (SWRC) for the shallow seedling recruitment zone across field topography. The SWRC is important in the study of water availability for seed germination. One objective of this study was to fit and compare six analytical models describing the SWRC for the middle increment for a three-layered recruitment zone. A second objective was to estimate and validate the accuracy of the SWRC for the middle increment with pedotransfer functions (PTFs) using basic soil properties. The best predicting PTFs were then used to estimate SWRCs for the upper and lower increments of the seedling recruitment zone by using basic soil property information in the upper and lower soil increments coupled with the PTF predicted SWRC from the middle soil increment. Soils along the hillslopes in this study had variable physical soil properties that influence the SWRC in the recruitment zone. As such, specific SWRCs for a given hillslope position are necessary to estimate soil water content at a given pressure. The SWRC did not differ with depth in the recruitment zone despite differences in soil physical properties, likely due to opposing effects of different soil properties on water retention. Although not statistically different, the four parameter van Genuchten model was considered superior to other models due to its continuous form that enabled better representation of the SWRC at low pressures. Estimating the residual soil water content parameter provided better model fit of the data. Parameters of the van Genuchten model were estimated with soil physical variables and detailed particle-size information to predict models that were comparable to fitted models. Greater information in the PTF having detailed particle-size distribution improved the predictive fit. Evaluation of the SWRC across incremental depths of the recruitment zone in this study indicated that a single SWRC is sufficient to describe the water content–potential relationship.

The manuscript in Chapter 6 parameterizes and evaluates simulations of detailed temperature and water profiles within the seedling recruitment zone across field topography. The objective of this study was to simulate hourly soil temperature and soil

water potential profiles for the seedling recruitment zone across field topography using a combination of measured and modeled parameterization. Performance measures were used to evaluate the accuracy of the simulations by comparing the simulations to the measurements. Soil temperature and soil water fluctuated considerably at the soil surface. Simulations of soil water captured much of the essence of evaporation, precipitation and crop development events. Soil temperature fluctuation decreased with depth in the profile. Soil temperature simulations were generally overestimated by an average of 2.5 ^{o}C across all treatments. Further calibration of parameters may be necessary to improve the model performance measures and better reflect the environment of the recruitment zone.

7.3 Summary of Contributions

The intention of the research in this thesis is to develop a better understanding of the physical environment of the seedling recruitment microsite. The role of modeling of the seedling recruitment microsite is to support research efforts of model development with the intent to facilitate decision making by crop managers. The methods employed in this study have provided detailed characterization of the recruitment zone and a means to interpret, quantify, and develop predictions for the seedling recruitment zone that can be used as input for seedling recruitment modeling. For this rationale, methods have been used in this study to model and evaluate environmental conditions of the recruitment zone. It is shown that soil temperature and soil water are most variable in the near-surface soil layers and therefore most difficult to predict for the recruitment zone. It is demonstrated in this thesis that models can represent the recruitment microsite environment with reasonable accuracy.

Contributions of this thesis are in the areas of instrument calibration, statistical evaluation of physical parameters of the seedling recruitment microsite, and parameterization and process-based modeling of the recruitment zone environment. The thesis is divided into several manuscripts excluding Chapter 1, introduction, and Chapter 2, literature review.

The manuscript contained in Chapter 3 describes the field calibration of a soil water probe used to measure volumetric water content within the recruitment zone. The

objectives of identifying soil properties that influence the soil water probe readings, and developing a field calibration for the water probe across the field topography of the study site was accomplished. Accurate measurement of water for recruitment purposes is extremely important to avoid misleading results. This study indicates that site-specific calibrations are required due to the variability of factors across field topography and soil depth. This study identified the soil properties that influence volumetric water content measured by the soil water probe. For field experimenters lacking measurements of the soil properties that were shown to influence the probe measurements, individual calibrations on hillslope positions and soil depth will provide more accurate water readings compared to a single calibration across topography.

The manuscript enclosed in Chapter 4 presents a characterization of the microclimate and physical soil environment of the recruitment zone across field topography and vertical soil profile depth. Identifying microclimate and topographical properties that influence the seedling recruitment zone is essential to establish a basic understanding of the variability of the recruitment zone environment in the field. The objectives of this study to identify microclimate and topographical influences on the recruitment zone environment were realized by the use of mixed-model analysis of two years of data. A mixed-model repeated measures analysis indicated the main trends in microclimate across field topography. A comprehensive description of the soil physical environment across field topography and soil depth was revealed to form a basis for subsequent investigations of the seedling recruitment zone across field topography.

The manuscript in Chapter 5 evaluates functions that describe the SWRC for the recruitment zone, and develops pedotransfer functions to predict the soil water retention characteristic within the seedling recruitment zone. The SWRC is an important soil property since soil pore-size distribution determines the water content that can be retained by a soil at a given matric potential. The first objective of this study was to fit analytical functions to the measured data and compare the models to best describe the SWRC for the middle of three increments in the recruitment zone. Analysis of the analytical functions indicted that the Campbell, Brooks–Corey, and van Genuchten models fitted the data equally well. However, the van Genuchten model with four parameters better represented the SWRC at low pressures due to its continuous form. The development and

application of PTFs in this study show the utility of such modeling as applied to the SWRC in the recruitment zone. The SWRC is a difficult to measure property whereas basic soil properties can be used via PTF to model the SWRC. Principal components analysis has been shown to be useful in application where multicollinearity exists among the original soil predictor variables. The SWRC for soil increments in the recruitment zone can be predicted with PTFs using the SWRC from the middle increment coupled with basic soil physical properties of the upper and lower increments. Evaluation of the SWRC across incremental depths of the recruitment zone in this study indicated that a single SWRC is sufficient to describe the water content–potential relationship. The practical feature of PTFs is that information can be derived from readily available soil properties to predict SWRCs for the seedling recruitment zone for use in predictive recruitment modeling.

The manuscript in Chapter 6 parameterizes and evaluates models of detailed temperature and water profiles within the seedling recruitment zone. The objective of this study was to simulate hourly soil temperature and soil water potential profiles for the seedling recruitment zone across field topography. Simulations were evaluated with performance measures reflecting model efficiency and bias. Simulations indicated that the seedling recruitment zone contains a very dynamic environment with implications for dormancy breaking and germination of seeds. The importance of this process based modeling will be realized in following studies that utilize the simulated temperature and water profiles for predicting species recruitment.

Successive recruitment work based on this study will involve emergence timing of spring wheat grown as a surrogate weed. Spring wheat seed was dispersed throughout the upper 75 mm in the recruitment zone in this study and its recruitment was monitored extensively. The following recruitment work will be based on temperature and water profiles generated from this study.

7.4 Future Directions

The spatiotemporal environment of the seedling recruitment microsite across topography and soil depth forms the basis for modeling and predicting weed seedling recruitment in the field. The practical application of modeling the seedling recruitment

zone is to provide producers and crop consultants with the ability to readily predict the time of emergence for weeds. Given specific microclimate, edaphic and management variables, a producer will then be able to predict the timing and duration of certain weeds within the field of interest. As a result, crop management decisions can become more efficient and reliable with the ability to predict weed emergence.

Detailed knowledge of the soil environment, recent and current microclimatic conditions, and management variables will enable site-specific prediction of weeds. Environmental and management variables for the recruitment microsite can be used in computer applications to generate readily available recruitment information for producers. The building of computer programs to predict seedling recruitment will require research modeling of the recruitment microsite environment and weed emergence timing.

7.4.1 Model Linkage

Modeling at a single process level or scale is not sufficient for recruitment studies. Modeling at a single scale provides information for further scientific research, and because the recruitment process is complex, multi-level parameterization is required for the complete process. Seedling germination is a result of the status of the seedling recruitment microsite, which in turn is controlled by the near-surface microclimate. Seedling germination models rely on adequate information about soil temperature and water conditions. Adequate parameterization for the seedling recruitment process requires a linkage of atmospheric, soil physical and biological models. Representative microclimate and soil microsite information needs to be available to adequately model seedling emergence of crops and weeds. Coupling germination models with models that describe the soil temperature and water status of the recruitment microsite would enable better understanding of interactions between germination processes and microclimate that would enhance the ability of crop managers to evaluate cropping decisions. With expected changes in climate leading to general temperature warming and shifts in precipitation patterns, anticipated alterations in species recruitment will likely influence crop production. An integrated approach to microclimate and crop modeling would

enhance projections of the effect of climate change on the recruitment process, thus enabling adaptation of cropping strategies to changing climate conditions.

The study of a single process is expanded to that of a cropping systems approach through linkage of sequential physical and biological models. Thus, numerous models are needed in combination to provide parameterization for subsequent models to fully explain the phenomenon of seedling recruitment. The linking or embedding of models related to the recruitment process provides a means to develop predictions about seedling recruitment based on the underlying mechanisms involved. The integration of different simulation models can be further developed into a systematic group of modules providing various soil and climate input parameters for an overall recruitment model. An integrated approach of models can provide a feedback mechanism for parameters such as climate change or land surface. Development of linkages to regional databases of climate, soil, and land surface information will provide additional development of a systems approach for recruitment studies.

The development of a systems approach to modeling the recruitment process is a necessary first step in model linkage. The application of such a system requires basic data describing climate and soil properties. Geographical information systems will integrate into the system to provide a means of linking basic climate and soil information to detailed topographical attributes. Geographical referencing of local site characteristics with environmental parameters will increase the accuracy to predict recruitment events for local conditions.

7.4.2 Model Parameterization

Modeling the seedling recruitment microsite is an iterative process of parameterization, evaluation of the simulation, and optimization of those parameters. The development of systematic methods of model calibration would expedite the process of model optimization. Evaluation indices indicative of calibration requirements are an essential component of model optimization. An evaluation feedback system that will expedite suitable calibration for the parameters will enhance the modeling process. As such, the optimization process is based primarily on knowledge of the processes involved. An approach that integrates the input parameters with sensitivity analysis to

provide convergence of a parameter value would be useful. On this basis, the development of a systematic approach for parameter optimization would expedite modeling efficiency.

The use of indices that reflect efficiency and bias of a simulation are useful in addition to visual representation of the simulation compared to the measured data. Calibrating model parameters is generally accomplished either by adjusting the parameter values through a feedback system such as sensitivity analysis, or by estimating parameter values based on empirical relationships for a local region. Suitable calibration of the parameters defining the recruitment microsite is very important for simulating temperature and water status on a topographical scale. Recruitment models could perform well if the model parameters defining the recruitment microsite are appropriately calibrated on the basis of calibration with measured data.

7.4.3 Model Georeferencing

Remote sensing of surface soil water can become feasible in the near future, providing near-surface detailed water measurements across topography of field units. This technology will provide large scale water measurements that could not otherwise be collected. Remote sensing will be especially valuable for fields with variable topography, for which coarse surface sampling would provide insufficient measurements to accurately specify emergence models.

Future recruitment microsite models need to comprise spatial elements including hillslope position and microsite depth that reflect local spatial and temporal dynamics of the recruitment zone environment that can be used to generate robust weed recruitment models. Observable characteristics based on regional properties of the microclimate, soil, and topography is required to refine model accuracy. Implications for predictions of weed recruitment across a field topography would therefore be reliant not only on site-specific properties of the topography, but also the vertical location of the microsite within the profile of the recruitment zone as they are affected by hillslope position and near-surface microclimate conditions.

Modeling of microsite conditions can be improved by inclusion of local management variables that influence properties that are difficult to define such as soil

structure. Soil structure is a physical soil property that generally differs on a regional basis. It is, however, a variable that is reflected in the physical environment of the recruitment microsite that needs to be quantified in some manner. For example, wider geographic application of pedotransfer functions may occur as a result of inclusion of a parameter describing soil structure in the equation.

The use of soil process-based models can reduce the need for actual measurements of soil water and temperature, expediting the modeling process by integrating local microclimate data with soil cover and seedbed conditions. Soil profile models that reflect temperature and water status of the recruitment zone in finer increments of time and space produce a more detailed description of the recruitment zone profile. Subsequently, this leads to increased accuracy of emergence models. Microclimate variables are a critical component of the modeling process, and expanded access to regional microclimate data is essential to increase accuracy of emergence models for topographical subunits.

Appendix A. Experimental Plot Georeferencing to Soil Type and Elevation

A.1 General Methodology

Field experimental plots were established at the Orchard farm west of Graysville, MB (49º30´ N, 98º09´ W). Topographic properties of the experimental plots were determined by utilizing global positioning system technology (GPS). A GPS coordinate was determined with a Trimble TSC1 Surveyor Controller™ (Trimble Navigation Ltd., 935 Stewart Drive, Sunnyvale, CA 94085) by averaging coordinates over a four hour period at a single location adjacent to the summit hillslope position at each hillslope aspect in the field. A Sokkia SET4110 Total Station™ (Sokkia Co. Ltd., 260-63, Hase, Atsugi, Kanagawa, 243-0036, Japan) was positioned over the GPS coordinate adjacent to the summit at each hillslope aspect. The Total Station™ was used to map easting, northing and elevation coordinates for the corners of every plot, areas between hillslope position blocks, and a buffer of 10 m surrounding each experimental area.

A.2 Experimental Plot Georeferencing To Soil Type

The experimental plots were georeferenced to soil types within the field by overlaying the plots and soil series onto an orthophoto of the quarter section (Fig. A.1). The three hillslope positions (summit, backslope, and toeslope) within each of the two aspects (southwest and northeast) in the experiment are indicated as dark rectangles (Fig. A.1). The locations of the experimental blocks are indicated at a scale of 1:20,000. Each hillslope position was 36 m by 10 m containing 36 plots arranged in two rows with a 2 m aisle (the toeslope on the northeast aspect was 24 m by 16 m containing 36 plots arranged in three rows with two 2 m aisles). The total area of each hillslope aspect including aisles and a 10 m buffer was approximately 0.5 ha.

The southwest aspect was situated on Gervais (GVS) and Willowbend (WWB) soil series. The northeast aspect was situated on Almissipi (ALS) soil series. The Gervais series is a Gleyed Cumulic Regosol of fluvial origin with silty clay surface texture and imperfect drainage. The Willowbend series is a Rego Humic Gleysol of fluvial origin with loam surface texture and poor drainage. The Almissipi series is a Gleyed Rego

Black Chernozem of lacustrine origin with loamy fine sand surface texture and imperfect drainage.

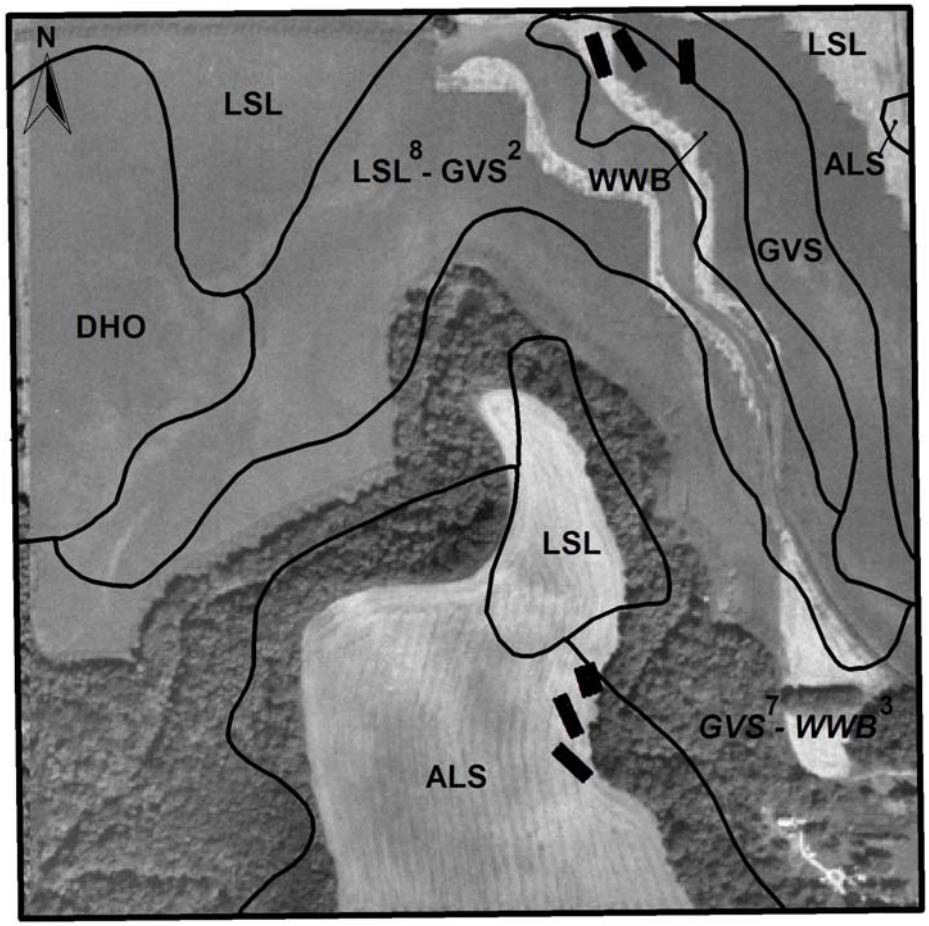

Fig. A.1. Experimental plots georeferenced to soil series and overlaid onto quarter section orthophoto.

A.3 Experimental Plot Digital Elevation Model

The plots for each hillslope position were georeferenced to a digital elevation model (DEM) and overlaid onto an orthophoto of the quarter section at a scale of 1:20,000 (Fig. A.2). The arrows indicate the direction of declining elevation in the hillslope (Fig. A.2). The gradient and aspect of the hillslope were derived from analyzing the GPS coordinates for plot corners and areas between and around hillslope position

blocks with ArcView Spatial Analyst™ (Environmental Systems Research Institute Inc. (ESRI), 380 New York Street, Redlands, CA, 92373-8100). Gradient and aspect for each plot were derived by averaging values of the four corners for each plot. The summit and toeslope hillslope positions had an average gradient of 1º, and the backslope positions had an average gradient of 7º. The average declines in elevation from summit to toeslope for the southwest and northeast aspects were 4.2 and 3.8 m, respectively. The southwest and northeast aspects were 239º and 65º, respectively, clockwise from due north.

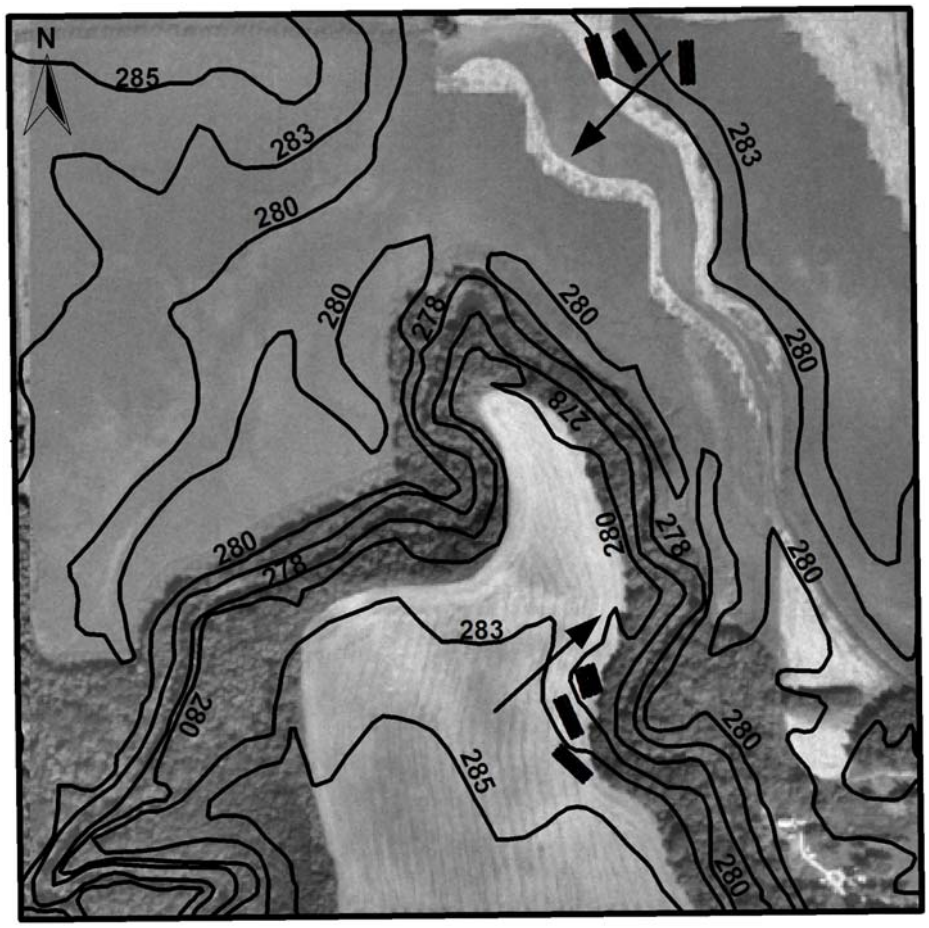

Fig. A.2. Experimental plots georeferenced to a digital elevation model and overlaid onto quarter section orthophoto.